UNIVERSITY OF SOUTHAMPTON

FACULTY OF MEDICINE

Clinical and Experimental Sciences Academic Unit

Host cellular and immune responses in models of inflammatory skin conditions

Daniel James Holbrook

Thesis for the Doctor of Philosophy

January 2019

UNIVERSITY OF SOUTHAMPTON

ABSTRACT

FACULTY OF MEDICINE

Clinical and Experimental Sciences

HOST CELLULAR AND IMMUNE RESPONSES IN MODELS OF INFLAMMATORY SKIN CONDITIONS

Daniel James Holbrook

Skin colonisation of varied communities of commensal microorganisms, such as *Staphylococcus aureus* (SA), *Staphylococcus epidermidis* (SE) and *Staphylococcus capitis* (SC) form the microbiome; a necessity for healthy skin. A number of inflammatory skin conditions, including atopic dermatitis (AD) and dandruff, are strongly associated with microbial dysbiosis of the skin. AD is a common skin disease affecting 30% of UK children, it has a complex and multifactorial aetiology that combines genetic, environmental and immune factors. The skin changes characteristic of AD have been shown to provide a favourable niche for SA colonisation. Indeed, dysbiosis and increased numbers of SA are strongly associated with AD lesions, and correlate with increased disease severity. However, whilst tissue invasion by SA in acute infection is understood to result in severe inflammation, whether SA colonisation has a role in maintaining chronic stable inflamed AD is not well established. This research aims to study interactions between staphylococci and the skin. The goal is to explore the differences in the epidermal response to different species, in an attempt to understand how such differential bacterial regulation may contribute to skin tolerance or inflammation.

Staphylococcal challenge of keratinocyte monolayers, showed similar growth curves for SA and SE, whereas when applied to a more realistic human epidermis in a reconstructed human epidermal (RHE) model, SA proliferation was significantly inhibited in contrast to that seen with SE at both high and low colonisation loads after 24 hours (CFU load 10^2 p=0.037; 10^6 p=0.0001). These data strongly suggest species specific regulation of staphylococcal growth, mediated by interaction with the epidermis. This finding was validated in human skin explant models.

Additionally, the different staphylococcal species induced a different outcome on dendritic cell activation by bacteria primed epidermal models. To explore the impact of various staphylococci and inoculum doses, multiplex bead array analysis of the soluble inflammatory mediators in culture media from epidermal models was undertaken and showed that although some differences were noted between SA strains, SA induced keratinocyte production of IL-1α, IL-1β, GM-CSF and TNFα after 24hrs of colonisation, whereas SE was less inflammatory.

To investigate the specific signalling within keratinocytes that might account for species specific responses, transcriptomic analysis was undertaken. Interestingly a strong IL-17/23 pathway signal was induced with SA colonisation, whereas SE induced strong upregulation of the negative regulator of inflammation NF-κB inhibitor A20 (TNFAIP3). Pathway analysis showed that a key regulator of response to SA/SE in keratinocytes was regulated through NF-κB and mediated by the IKK complex regulatory network.

This work provides strong evidence of the highly tuned nature of skin keratinocytes to different bacterial species and identifies the key regulatory mechanisms involved in induction of tolerance or inflammation induced by staphylococci.

Table of Contents

List of Tables

List of Figures

DECLARATION OF AUTHORSHIP

I, Daniel James Holbrook declare that this thesis entitled

Host cellular and immune responses in models of inflammatory skin conditions

and the work presented in it are my own and has been generated by me as the result of my own original research. I confirm that:

1. This work was done wholly or mainly while in candidature for a research degree at this University;
2. Where any part of this thesis has previously been submitted for a degree or any other qualification at this University or any other institution, this has been clearly stated;
3. Where I have consulted the published work of others, this is always clearly attributed;
4. Where I have quoted from the work of others, the source is always given. With the exception of such quotations, this thesis is entirely my own work;
5. I have acknowledged all main sources of help;
6. Where the thesis is based on work done by myself jointly with others, I have made clear exactly what was done by others and what I have contributed myself;
7. None of this work has been published before submission.

Signed: .....

Date: .....

Acknowledgements

This work would not have been possible without the help of my supervisors, Associate professor Michael Ardern-Jones, Professor Myron Christodoulides and Dr Rebecca Ginger. I would like to thank them for support, advice and inspiration throughout this research.

I would also like to thank from the bottom of my heart my parents; who without their constant love, encouragement, support and faith in me, I would not have succeeded.

I would like to thank my friends and fellow PhD students who I worked along side with, providing the support and motivation to get through the long nights in the lab.

I would like to acknowledge the help and advice of my colleagues, both in and out of the lab. At Southampton General Hospital; Associate Professor Marta Polak, Dr Tim Millar, Dr Carolann McGuire and Richard Jewell. Additionally at Unilever; Dr Fei-ling Lim, Dr Diana Cox, Dr Duncan Talbot, Dr Della Hyliands and Dr Jenny Pople.

I would also like to acknowledge and thank the donors of skin and blood throughout this research. As well as the surgeons and nurses at the spire hospital for the assistance in providing human skin tissue.

And finally, thanks to Gena, the one who got me over the finishing line.

Abbreviations

ABIN-1	A20-binding inhibitor of NF-kappa-B activation 1
AD	Atopic Dermatitis
ADAM8	A disintegrin and metalloproteinase domain-containing protein 8
ADPRT	Adenosine diphosphate-Ribosyltransferase
Agr	Accessory gene regulator
AhR	Aryl hydrocarbon receptor
ALI	Air liquid interface
AMP	Antimicrobial peptide
AP-1	Activator protein-1
APC	Antigen presentating cell
aps	antimicrobial peptide sensor
ATF4	Activating Transcription Factor 4
BMP	Bone morphogenetic protein
BSA	Bovine serum albumin
C3	Complement component 3
CCL	Chemokine (C-C motif) ligand
CCR	Chemokine (C-C motif) receptor
CD	Cluster of differentiation
cDC	Conventional dendritic cell
CFU	colony-forming unit
CLA	Cutaneous Lymphocyte-associated Antigen
Clf	Clumping factor
Cna	Collagen adhesin
CSF	Colony stimulating factor
CXCL	Chemokine (C-X-C motif) ligand
CXCR	Chemokine (C-X-C motif) receptor
DAMP	Damage-associated molecular pattern
DC	Dendritic Cell
DDC	Dermal dendritic cell
DEG	Differentially expressed gene
DMEM	Dulbecco's modified eagle medium
eap	Extracellular adherence protein
Ebps	Elastin binding protein
ECM	Extracellular matrix

efb	Extracellular fibrinogen binding protein
eIF	Eukaryotic initiation factor
EMMPRIN	Extracellular matrix metalloproteinase inducer
FBS	Fetal bovine serum
FC	Fold change
FDR	False discovery rate
FnBP	Fibronectin binding protein
FSC	Forward scatter
G-CSF	Granulocyte colony-stimulating factor
GDP	Guanosine diphosphate
GM-CSF	Granulocyte-macrophage colony-stimulating factor
GTP	Guanosine triphosphate
H&E	Hematoxylin and eosin
hBD	Human β-defensin
HDAC	Histone deacetylase
HLA-DR	Human leukocyte antigen – DR isotype
HSE	Human skin equivalent
ica	Intercellular adhesin
ICAM	Intercellular adhesion molecule
IFN	Interferon
Ig	Immunoglobulin
IKK	IκB kinase
IL	Interleukin
IPA	Ingenuity pathway analysis
IsdA	Iron-regulated surface determinant protein A
ISR	Integrated stress response
IκB	NF-κB inhibitor
KGM	Keratinocyte growth medium
LB	Lysogeny broth
LC	Langerhans cell
LPS	Lipopolysaccharide
LTA	Lipoteichoic acid
LXR/RXR	Liver X receptor / Retinoid X receptor
MEKK3	Mitogen-activated protein kinase kinase kinase 3
MHC	Major histocompatibility complex
MoDC	Monocyte derived dendritic cell
mRNA	messenger RNA
MSCRAMM	Microbial surface components recognising adhesive matrix molecule

MTC	Multiple test correction
MyD88	Myeloid differentiation primary response 88
NF-κB	Nuclear factor kappa-light-chain-enhancer of activated B cells
NGF	Nerve growth factor
NHEK	Neonatal Human Epidermal Keratinocyte
NKT cell	Natural killer T cell
NLR	Nod-like receptor
NLRP	Nucleotide-binding oligomerization domain, Leucine rich Repeat and Pyrin domain containing
NMF	Natural moisturizing factor
NOD	Nucleotide oligomerization domain
PAMP	Pathogen associated molecular pattern
PBMC	Peripheral blood mononuclear cell
PBS	Phosphate buffered saline
PCA	Principal component analysis
pDC	Plasmacytoid dendritic cell
PDGF	Platelet-derived growth factor
PGF	Placental growth factor
PPAR	Peroxisome proliferator-activated receptor
PRR	Pattern recognition receptor
PSM	Phenol-soluble modulin
PVL	Panton-Valentine leucocidin
RFU	Relative fluorescence units
RHE	Reconstructed human epidermis
RhoGDI	RHO protein GDP dissociation inhibitor
RIG-I	Retinoid acid-inducible gene-I
RIP1	Receptor-interacting serine/threonine-protein kinase 1
RLR	RIG-I like receptors
RNA	Ribonucleic acid
RPMI	Roswell Park Memorial Institute
RSI	Relative spot intensity
RTA	Ribitol teichoic acid
SA	*Staphylococcus aureus*
SA29	SA strain ATCC 29213
SA65	SA strain NCTC 6571
SA83	SA strain NCTC 8325-4
SAB	SA bacteremia

SC	*Staphylococcus capitis*
SC27	SC strain ATCC 27840
Sdr	Ser-Asp rich fibrinogen-binding protein
SE	*Staphylococcus epidermidis*
SE12	SE strain ATCC 12228
SE35	SE strain ATCC 35984
SEA	Staphylococcal enterotoxin A
SEB	Staphylococcal enterotoxin B
SEC	Staphylococcal enterotoxin C
SERAM	Secreted expanded repertoire adhesive molecule
siRNA	Silencing RNA
SIRT	Sirtuin
SNP	Single nucleotide polymorphism
SpA	Staphylococcal protein A
SSC	Side scatter
SSTI	Skin and soft tissue infection
TAB	TAK1-binding protein
Luk	Leukocidin
TAK1	TGFβ activated kinase 1
TCR	T cell receptor
TGF	Transforming growth factor
Th	T helper
TIR	Toll/IL-1 receptor
TLR	Toll-like receptor
TNF	Tumor necrosis factor
TNFAIP	TNF Alpha Induced Protein
TRADD	TNF receptor type 1-associated death domain protein
TRAF	TNF receptor-associated factor
TREM	Triggering receptor expressed on myeloid cells
TRIM	Tripartite Motif Containing
TSLP	Thymic stromal lymphopoietin
TSS	Toxic shock syndrome
TSST-1	Ttoxic shock syndrome toxin
TWEAK	TNF related weak inducer of apoptosis
Ubc	Ubiquitin-conjugating enzyme E2
uPAR	Urokinase receptor
VEGF	Vascular endothelial growth factor

Chapter 1: Introduction

1.1 The skin

The skin is a multifunctional organ fundamental for sensory input, thermoregulation and defence. It provides a barrier of protection and serves as the initial surface for interaction with the external environment. Thus, it is crucial in protecting against environmental challenges, which can manifest in a variety of forms; including UV radiation, mechanical stresses and pathogenic microorganisms. Although the skin as a physical barrier is the first line of defence against environmental challenges, other components are also necessary including the cutaneous immune system and the cutaneous microbiome.

1.1.1 Structure

The skin is comprised of two layers, epidermis and dermis, connected by the basement membrane. The outermost layer is the epidermis and thus acts as the defensive barrier of the skin. The dermis is the lower layer and is attached to subcutaneous tissue of the body. The dermis functions to support the epidermis in a multitude of ways, including in mechanistic strength and nutrient supply. The skin also incorporates other components such as hair follicles, sebaceous glands, lymphatic vessels and blood vessels (**Figure 1.1a**).

The epidermis is composed of four sublayers of stratified keratinocytes, known as strata (**Figure 1.1a**). Keratinocytes gradually and constantly differentiate through these layers resulting in cornification, the process of terminal differentiation to become corneocytes (Eckhart et al., 2013). Corneocytes are flattened dead cells that form the stratum corneum, which are eventually shed through desquamation. This results in the constant demand for proliferation and differentiation of keratinocytes (Eckhart et al., 2013). Balance between desquamation and proliferation is controlled to retain the epidermal thickness. Proliferation occurs in the stratum basale, the lowest epidermal strata, consisting of a single layer of highly proliferative keratinocytes, supplying the epidermis with keratinocytes to gradually differentiate through the strata. The stratum spinosum is composed of the daughter cells of the stratum basale and is the location in which differentiation is initiated. As differentiation continues, and the cells become non-viable, keratinocytes reach the stratum granulosum and finally the stratum corneum (Wickett and Visscher, 2006).

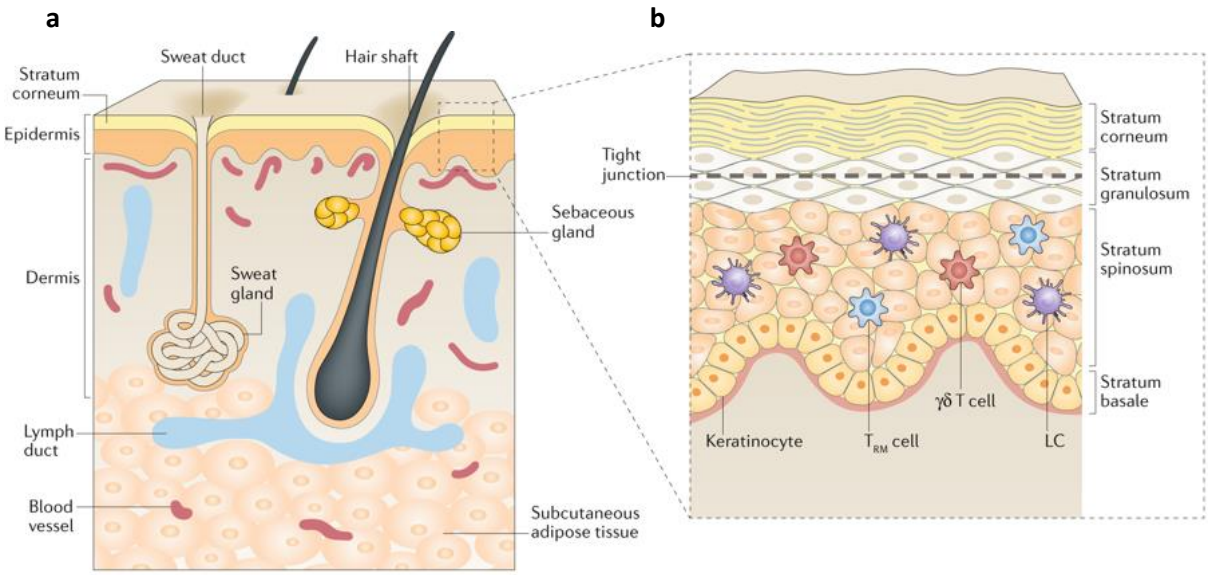

Figure 1:1: Diagram of the skin and epidermal structure
Structure of the skin (**a**) and epidermis (**b**) showing epidermal strata and incorporation of immune cells within it (Kabashima et al., 2019).

Keratinocytes are connected by cell to cell junctions that vary between strata, thus changes in the type of junction is a key aspect of differentiation. Desmosomes and adherens junctions are both common in the stratum basale granting mechanical strength and cell-cell regulatory mechanisms. Differentiation into the stratum granulosum results in the formation of tight junctions (Sumigray and Lechler, 2015) (as noted on **Figure 1.1b**), which regulate the intercellular movement of epidermal water to the stratum corneum. Stratum corneum regulation of epidermal water loss is discussed below.

The composition of the dermis enables it to support the epidermis as a mechanically strong foundation. The fibroblasts that largely comprise it provide mechanical and structural support through the generation of collagen and elastin fibres (Krieg and Aumailley, 2011). The complex vascular network in the dermis acts as provider of epidermal nourishment, including nutrient and oxygen supply. This network exists as two horizontal plexuses. The lower plexus, situated at the dermal-subcutaneous tissue interface supplies the upper plexus via connective arterioles/venules. Various capillary loops extend from the upper plexus into the papillary dermis (Braverman, 1989), the uppermost dermal layer consisting of loosely arranged collagen fibres. Although the dermis is primarily composed of fibroblasts, it also contains numerous leukocytes to act in both innate and adaptive immune responses, which provides the dermis with an important role in defence.

Connecting the epidermis to the papillary dermis is the basement membrane, a thin layer of extracellular matrix (ECM) identified on electron microscopy as comprised of a lamina lucida and lamina densa. The intracellular keratinocyte hemidesmosome adheres to the lamina densa by attachment of fibrils of connective tissue including collagen XVII (BP180), integrins, anchoring filaments and laminins in the lamina lucida. These connect between to the collagen IV, nidogen and perlecan of the lamina densa which in turn is bound to the dermal collagens (I, III and V) by anchoring filaments made up of collagen VII (Theocharis et al., 2016). The basement membrane enables secure attachment of basal keratinocytes to the loosely arranged fibres of the papillary dermis (Boyle, 2008).

1.1.2 Differentiation

Epidermal differentiation is a terminal transformative process resulting in cornification, during which keratinocytes become the corneocytes that constitute the stratum corneum. During the migration through strata of the epidermis the keratinocytes change both morphologically and biochemically to end up as dead cells that are both durable and flexible (Eckhart et al., 2013).

The unceasing process of differentiation is initiated in the stratum basale and supplied by keratinocytes, also known as epidermal stem cells. Proliferation is highly regulated to match desquamation, but in certain situations such as wound healing, it can be increased.

Calcium is pivotal in initiation and regulation of differentiation. Regulation stems from a calcium gradient across the epidermis, with low concentrations in the stratum basale that progressively increase towards the stratum corneum. Calcium along this gradient aid the morphological changes during differentiation. Intracellularly, calcium mediates changes in cell-cell adhesion, extracellularly it cross-links structural proteins that make up the cornified envelope (Bikle et al., 2012, Lee and Lee, 2018). However, high confluency has also been shown to be vital for the initiation of differentiation (Rinnerthaler et al., 2015).

During differentiation keratinocytes modify their structural proteins to change morphology, increasing their strength and gradually producing the proteins to compose the cornified envelope. Keratinocytes of the stratum basale contain an abundance of keratin filaments; a fibrous structural protein that constructs the cytoskeleton and provides mechanical strength. Initially large amounts of the keratin filaments K5 and K14 are manufactured, progression into the stratum spinosum causes a change in production to filaments of K1 and K10. Involucrin production is also initiated, which will be important for the cornified envelope formation. The

stratum granulosum is characterised by the keratohyalin granules contained within the keratinocytes, these granules are comprised of profillaggrin a precursor of fillaggrin or loricrin a component of the cornified envelope (Bikle et al., 2012, Wikramanayake et al., 2014, Menon et al., 2012). Eventually, calcium causes degranulation, releasing the profillaggrin for dephosphorylation and proteolysis. Fillaggrin aggregates the keratin filaments forming tight bundles collapsing the cell to form a flattened shape that make up the stratum corneum (Nishifuji and Yoon, 2013).

Cornification also induces degradation of the cellular organelles and nucleus to leave the corneocytes dead, but existing as component of the stratum corneum(Eckhart et al., 2013, Lippens et al., 2005). Furthermore, desmosomes develop into corneodesmosomes, with connections to the intracellular keratin filaments of the corneocytes as well as mediating the intercellular adhesion between them (Ishida-Yamamoto and Igawa, 2015, Serre et al., 1991). Additionally the Golgi complex of the stratum granulosum produce lamellar bodies that contain the lipid components of the lipid lamellae (Feingold, 2012, Feingold and Elias, 2014).

1.1.3 Stratum Corneum

As a product of epidermal differentiation, the stratum corneum makes up the outer surface of the skin, this barrier is therefore the initial interaction surface with environmental challenges. The extensive keratinization and organelle degradation provides the stratum corneum with mechanical and structural strength.

Corneocytes are the main structural component of the stratum corneum, acting as the ‘bricks’ in the ‘brick and mortar’ model. Thus, the cornified cellular envelope corresponds to the ‘mortar’ (Menon et al., 2012).

Surrounding each corneocyte is the cornified cell envelope (**Figure 1.2**), which consists of an internal protein envelope and an external lipid lamellae. The protein envelope is a layer of calcium dependent cross-linked proteins that includes loricrin, involucrin, envoplakin and periplakin. Formation of the envelope across the inner surface of the cell membrane provides a scaffold for the outer layer of lipids, known as the lipid lamellae (Lee and Lee, 2018). The lipids are aligned and coordinated by the proteins of the cellular envelope with covalent bonds to involucrin on the inner scaffold. The lipid lamellae consist of ceramides, fatty acids, cholesterol and its esters (Elias et al., 2014). The lipids of the lamellae and their structural organisation provide the stratum corneum with its permeability to water (Darlenski et al., 2011), but they have also been shown to

have a role in signalling and can regulate increased cornification upon distress (Feingold and Elias, 2014).

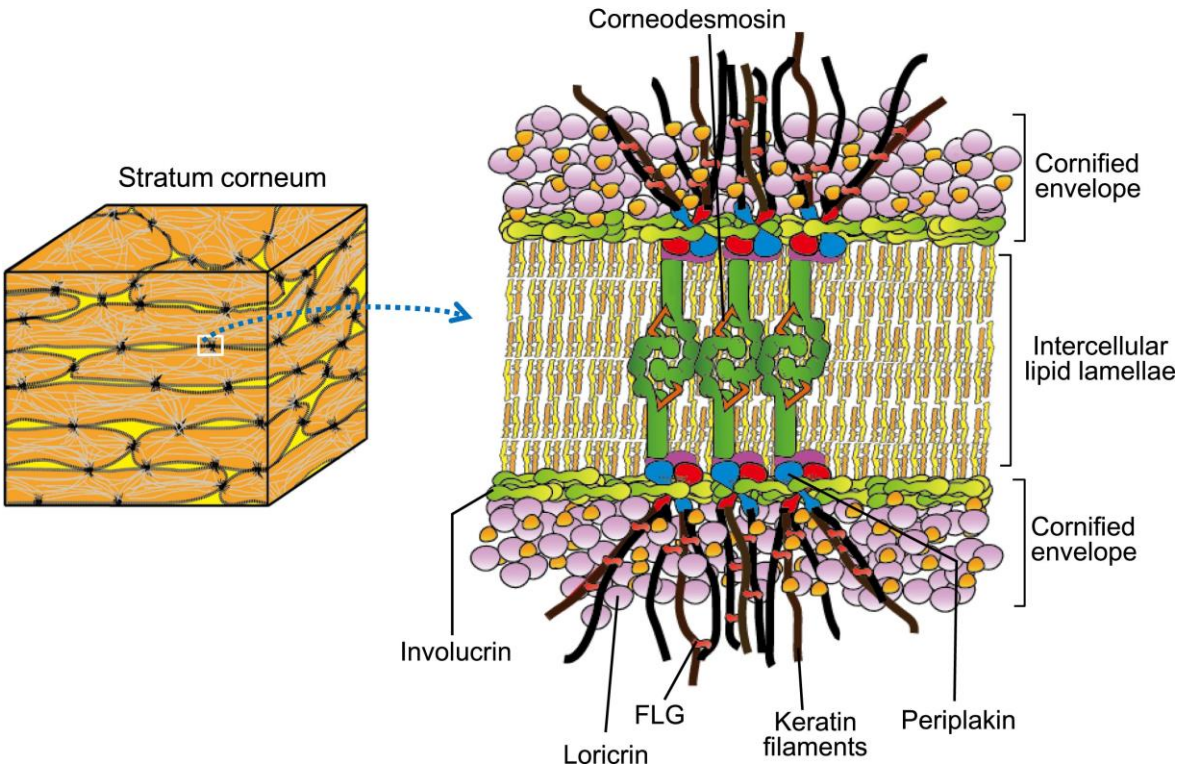

Figure 1:2: Diagram of the cornified envelope and corneodesmosomes
Structures of the cornified envelope and corneodesmosomes. Adapted from Egawa and Kabashima (2018)

Corneodesmosomes are the main adhesion junction in the stratum corneum. Transformed from desmosomes in the stratum granulosum during differentiation, they eventually become incorporated into the cornified envelope through cross-linking (Ishida-Yamamoto and Igawa, 2015). However the degradation of the extracellular component of the corneodesmosomes allows for the desquamation of the corneocytes.

Desquamation is an active process performed for defence. It produces a fresh intact surface for the epidermis, although it is still not completely clear why it is continuously active. However, its importance is evident from genetic defects in which abnormal desquamation presents as excess scale. This physiopathology can be caused by defects in proteins of structure, signalling or metabolism (Milstone, 2004).

The stratum corneum provides a physical barrier as protection from the external environment and helps to generate a surface inhospitable for microbial survival. The permeability barrier of the stratum corneum limits water and mineral residence and enables the stratum corneum to host the “acid mantle”, which is produced by sebaceous glands (Lee et al., 2006, Pappas, 2009).

Furthermore, free fatty acids that constitute the lipid lamellae of the stratum corneum have antimicrobial activity towards certain microbes including SA (Drake et al., 2008).

1.2 The skin as an immune organ

To aid in defence, the skin acts as an essential part of the immune system with both dermis and epidermis accommodating specialised immune cells, as well as keratinocytes functioning as immune sentinels and non-professional antigen-presenting cells (APCs). The dermis incorporates various leukocytes including macrophages, dendritic cells (DCs), mast cells and a variety of T lymphocytes. The specialised immune cells integrated into the strata of the epidermis are Langerhans cells (LCs), and two T cell subsets, γδ T cells and CD8+ resident memory T (TRM) cells (Nestle et al., 2009, Pasparakis et al., 2014, Kabashima et al., 2019).

1.2.1 Keratinocytes

Keratinocytes have multiple functions with regards to host immunity: acting to initiate both innate and adaptive immune responses. They act as sentinels of the skin, recognising bacterial structures and responding with the secretion of proinflammatory mediators. Keratinocytes also act to amplify the immune response, by responding to the inflammatory mediators and enhancing immune interactions (Klicznik et al., 2018). Additionally, the APC nature of keratinocytes enables them to display antigen and mediate an adaptive T cell response (Black et al., 2007).

1.2.1.1 Molecular pattern recognition

Keratinocytes initial sensing of harmful pathogens is performed through pattern recognition receptors (PRRs), which are stimulated by pathogen associated molecular patterns (PAMPs) (Miller, 2008); as well as damage associated molecular patterns (DAMPs). The main subsets of PRRs are Toll-like receptors (TLRs), nucleotide oligomerization domain (Nod) like receptors (NLRs) and retinoid acid-inducible gene-I (RIG-I) like receptors (RLRs). PRRs are constitutively expressed by immune cells and non-immune cells. PAMPs activation of PRRs induces a specific signalling pathway to a defined innate immune response, which can aid in priming an adaptive response (Ermertcan et al., 2011).

TLRs are the most studied family of PRRs, with a range of TLR1-10 expressed as transmembrane receptors in human cells. Keratinocytes specifically express TLR1-6 and TLR9, which includes extracellular (TLR1, 2, 4, 5 and 6) receptors that recognise the microbial surface antigen and intracellular (TLR3 and 9) receptors that detect bacterial or viral nucleic acids (Ermertcan et al., 2011, Nestle et al., 2009, Yazdi et al., 2016). TLRs induce specific responses depending on their stimulation defined signalling pathways. The subsequent and varied response can induce

increased production in a variety of proinflammatory mediators; such as cytokines, chemokines, adhesion molecules and antimicrobial peptides (AMPs). A notable example is the stimulation by Lipoteichoic acid (LTA), which causes heterodimerization of TLR2 and TLR6 (Kang et al., 2009, Niebuhr et al., 2010), which induces activation of the transcription factor NF-κB.

NLRs are intracellular cytosolic receptors that respond to both PAMPs and DAMPs. Functionally, they can be divided into four groups based on what activation induces: inflammasome formation, signal transduction, transcription activation, and autophagy. Similarly to TLRs, NLRs, specificially NOD1 and NOD2, can induce activation of NF-κB to mediate an inflammatory response by cytokine and chemokine release (Kim et al., 2016). For example, NOD2 mediates a cytokine response of TNFα, IL-6, CXCL1 and CXCL2 upon recognition of the pore-forming toxin α-hemolysin of *Staphylococcus aureus* (Hruz et al., 2009).

RLRs are also intracellular cytosolic receptors, but respond to viral replication by recognition of viral RNA and DNA. Correspondingly, RLR activation induces signal transduction to transcription factors that can generate an antiviral response, driven by interferon production. As with TLRs and NLRs, RLRs can induce activation of NF-κB to mediate the innate response towards their stimulation (Loo and Gale, 2011).

1.2.1.2 NF-κB

Nuclear factor-κB (NF-κB) describes a family of transcription factor subunits, that hetero- or homodimerise to transcribe numerous inflammatory genes. It is considered a paramount transcription factor for an immune response (Liu et al., 2017). The NF-κB subunits p50, p52, P65 (RelA), RelB and c-Rel; dimerise into different pairs to induce differential responses of specifically targeted genes based on the signal transduction (Siggers et al., 2011). The NF-κB subunits are constitutively expressed and therefore the dimerisation is highly regulated. Blocking the undesired dimerisation of NF-κB is a family of inhibitory proteins, known as the IκB family, comprised of IκBα, IκBβ, IκBε and IκBγ. Consequently NF-κB activation is induced by the phosphorylation and degradation of these inhibitors, enabling dimerisation (**Figure 1.3**). This phosphorylation is mediated by the the IκB kinase (IKK) complex, comprised of two kinase subunits, IKKα and IKKβ, as well a regulatory subunit IKKγ (NEMO) (Hinz and Scheidereit, 2014). This mechanism of NF-κB activation is part of the NF-κB canonical signalling pathway and can be induced by varied stimuli, to correspond to receptors of PRRs and TNF receptor (TNFR) superfamily members. Other receptors for NF-κB activation are expressed on specialised cells, such as leukocytes, this includes the T-cell receptor (TCR) and B-cell receptor (Liu et al., 2017).

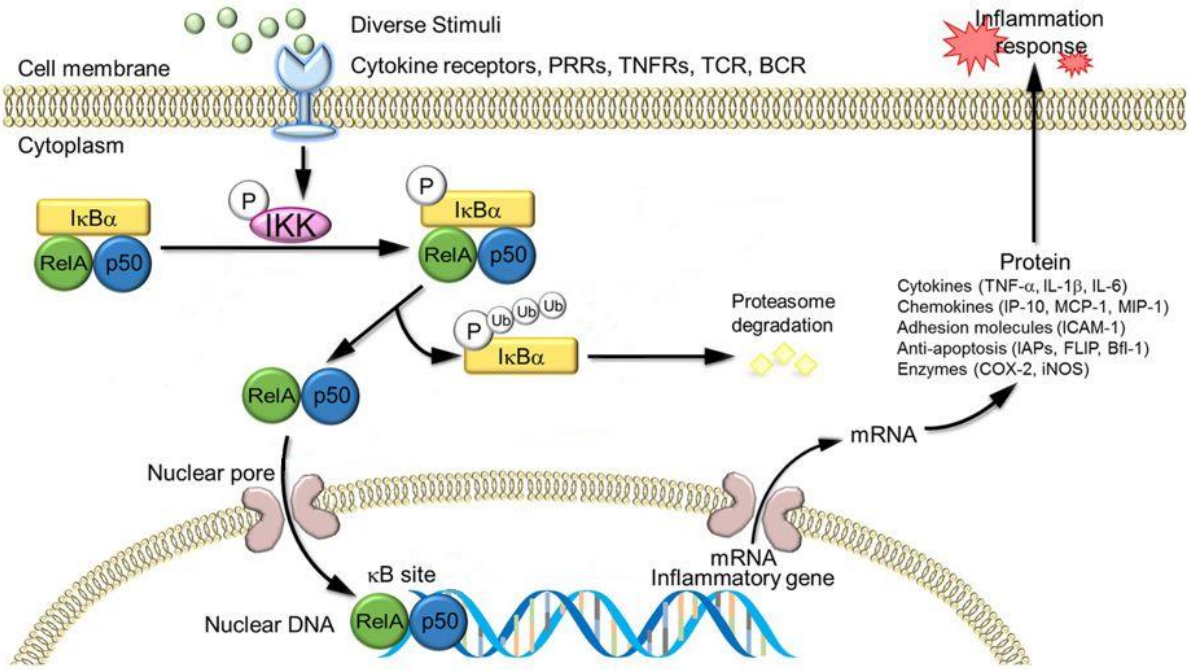

Figure 1:3: Diagram of NF-κB activation
Regulation of NF-κB activation by IKK complex and IκB. Adapted from Liu et al. (2017).

The induction of the canonical NF-κB signalling pathway can occur through a number of signal transduction pathways. This includes the stimulation of the TNF receptor I and the associated proteins TRADD and TRAF2/5, which recruits UbcH5 and cIAP1 that form an E2/E3 ligase complex. The resultant ubiquitination of RIP1 enables MEKK3 to phosphorylate and subsequently activated IKKβ (Shih et al., 2011, Blonska et al., 2005).

Alternatively, ligand stimulation of IL-1R and/or TLRs use the receptor-associated protein MyD88 to form a complex with IRAK4 and IRAK1. IRAK4 induces the autophosphorylation of IRAK1, which is released to associated with TRAF6 an E3 ligase and Ubc13 an unbiquitin-conjugation enzyme. TRAF6 K63-linked polyubiquitination of TAK1, along with its regulatory subunits TAK1, TAK2 and TAK3, enables phorsphorylation of IKKβ (Kawasaki and Kawai, 2014).

The non-canonical NF-κB signalling pathway operates as IKKγ-independent IKKα kinase complex that acts slowly and persistently, which opposes the rapid and temporary nature of the canonical pathway, but is less diverse in its response (Sun, 2011). Induced by members of the TNFR superfamily it relies on NF-κB-inducing kinase (NIK) to phosphorylate IKKα. This subsequently phosphorylates the IκB-like molecule p100 that can specifically inhibit RelB (Sun, 2017).

Activation of NF-κB, induces a wide array of inflammatory responses, including the production of cytokines, chemokines, adhesion molecules, and enzymes (as indicated in **Figure 1.3**). However, it

also regulates inflammasomes, either to induce activation or to negatively regulate them (Liu et al., 2017).

1.2.1.3 Inflammasome

Inflammasomes are multimeric complexes formed intracellularly in respond to PAMPs and DAMPs. Thus, their activation acts as part of the innate immune response to pathogens or damaged cells. Inflammsomes are grouped and characterised by their PRR, including NLRs, ALRs (absent in melanoma 2 (AIM)-like receptors) and pyrin (Broz and Dixit, 2016). Their activation is based on priming and stimulation, for example, the NLRP3 inflammasome is associated with NLRs for activation and TLRs or TNFR for priming (Jo et al., 2016). Priming is initiated by the transcription of NLRP3 by NF-κB, which acts as a scaffold to recruit inactive pro-caspase-1. Thus, activation via PAMPs or DAMPs induces autoproteolytic cleavage of pro-caspase-1 into capsase-1, an active form. The response generated by caspase-1 can be cytokine mediated, such as cleavage of pro-IL-1β and pro-IL-18 into active IL-1β and IL-18. However, caspase-1 can also induce pyroptosis, an inflammatory form of cell death (Broz and Dixit, 2016, Guo et al., 2015, Sharma and Kanneganti, 2016).

1.2.1.4 Cytokine, chemokine and antimicrobial response

In essence, the keratinocytes main role is as a sentinel during inflammation. Their production and release of cytokines, chemokines and antimicrobial peptides (AMPs) is a critical factor of any cutaneous immune response. Depending on the stimulation, keratinocytes produce cytokines to mediate the inflammatory response in a paracrine or autocrine manner. Therefore, communicating and stimulating surrounding or localised keratinocytes and leukocytes. Chemokines enhance inflammation by recruitment of other leukocytes. Whereas AMPs act in host defence directly, by inhibition of pathogen proliferation. The key inflammatory mediators regulating cutaneous inflammation are briefly discussed below:

Tumor necrosis factor α (TNFα): proinflammatory cytokine that can induce production of other proinflammtory mediators or apoptosis, functions through members of the TNFR superfamily and has a notable role in NF-κB activation (Hanel et al., 2013).

Interleukin-1 (IL-1) Family: Comprised of proinflammatory cytokines (IL-1α, IL-1β, IL-18, IL-33, IL-36α, IL-36β and IL-36γ) and antagonistic cytokines (IL-1Ra (Receptor agonist), IL-36Ra, IL-37 and IL-38) that induce an anti-inflammatory effect. All of which are expressed by keratinocytes, but most prominent are IL-1α, IL-1β and IL-1Ra (Jensen, 2010). IL-1α is constitutively expressed as a biologically active precursor and is a dual function cytokine, which acts in the nucleus and at the cell membrane. Nuclear localisation causes IL-1α to function as a transcription factor for other

cytokines (Dinarello, 2018). Alternatively IL-1α can mediate a proinflammatory response by signal transduction. Furthermore the precursor, pre-IL-1α, acts as a DAMP when released from the cell under necrotic conditions (Di Paolo and Shayakhmetov, 2016). IL-1β acts to enhance the proinflammatory response after cleavage from pre-IL-1β by caspase-1 after inflammasome activation, thus it is a key inflammatory mediator towards pathogenic stimulation (Dinarello, 2018). Opposingly is IL-1Ra, which competitively binds the IL-1 receptor I (IL-1RI) to inhibit activation by IL-1α and IL-1β, thus inducing an anti-inflammatory effect (Dinarello, 2018).

Th2 cytokines: As part of a Th2 immune response CD4+ T cells produce interleukin-4 (IL-4) and interleukin-13 (IL-13), which can stimulate keratinocytes via the IL-4 receptor and IL-13 receptor. Although during a Th2 response IL-4 and IL-13 are known for B cell class switching to an IgE mediated and therefore humoral response, in the skin these cytokines can alter barrier integrity (Hanel et al., 2013). Treatment of keratinocytes with IL-4 and IL-13 induces a downregulation of filaggrin (Howell et al., 2009), loricrin and involucrin (Kim et al., 2008); therefore reducing keratinocytes ability to differentiate. This is particularly of note due to the important role of IL-4 and IL-13 in the pathogenesis of atopic dermatitis.

Interleukin-17C (IL-17C): From the IL-17 cytokine family (IL-17A-F) keratinocytes express the IL-17C isotype. IL-17C is a proinflammatory cytokine inducing cytokine, chemokine and antimicrobial peptide expression. It is known for its important role in host defence against pathogens, but also in mediating the pathogenesis of inflammatory skins diseases such as psoriasis and atopic dermatitis (Ramirez-Carrozzi et al., 2011).

Interleukin-23 (IL-23): IL-23 is a heterodimeric cytokine of two subunits, IL-23A and IL-12B. IL-23 is known for its ability to polarise CD4+ T cells towards Th17, therefore amplifying the IL-17 response with the subsequent production of IL-17A of Th17 cells (Floss et al., 2015).

Granulocyte-macrophage colony stimulating factor (GM-CSF): A proinflammatory cytokine secreted by keratinocytes to modulate the adaptive immune system, but also acting in an autocrine manner to induce keratinocyte inflammation and proliferation. Consequently making it important in wound healing (Fang et al., 2007), but also contributing to pathogenesis of atopic dermatitis (Pastore et al., 1997). GM-CSFs modulation of the immune system occurs both in recruitment of immune cells and in activation of them, specifically inducing Dendritic cell (DC) maturation and T cell polarisation (Shi et al., 2006).

Chemokines: A superfamily of small cytokines functioning as chemoattractants to recruit leukocytes to the inflammatory site or regulate their migration during homeostatic conditions. Keratinocytes can produce a wide array of chemokines of the subgroups of CXC and CCL,

including: CXCL1, CXCL2 (Olaru and Jensen, 2010), CXCL3, CXCL5, CXCL8 (Nograles et al., 2008), CXCL9, CXCL10, CXCL11 (Marshall et al., 2017), CCL1, CCL2, CCL5, CCL11, CCL13, CCL17, CCL18, CCL20, CCL26 and CCL27 (Nedoszytko et al., 2014). Differing expression of receptors for these chemokines (CXCR for CXCL and CCR for CCL) are expressed on T lymphocytes, Langerhans cells (LCs), monocytes, immature DCs and Eosinophils (Nedoszytko et al., 2014). Therefore, mediating recruitment of leukocytes. However, some chemokines also have immunomodulatory effects.

Antimicrobial peptides (AMPs): AMPs act to directly kill pathogens, but can also indirectly mediate the inflammatory response. Keratinocytes produce AMPs, both constitutively and upon stimulation of PRRs. Therefore, PAMP stimulation induces the production of specific AMPs at different concentrations (Harder et al., 2013). For example, human β-defensin 3 (hBD3) can be produced in response to bacterial lipoprotein stimulation of TLR2 via NF-κB activation (Sumikawa et al., 2006). Within the epidermis, keratinocytes express human β-defensin 1 (hBD1) human β-defensin 2 (hBD2), human β-defensin 3 (hBD3), human β-defensin 4 (hBD4), LL-37 (cathelicidin), RNase 7, and S100 proteins most notably S100A7 (psoriasin) (Wang, 2014).

1.2.1.5 Keratinocyte antigen presentation

The non-professional APC nature of Keratinocytes is exposed by the expression of MHC class II that is upregulated upon stimulation by IFNγ (de Bueger et al., 1993, Banerjee et al., 2004, Nickoloff and Turka, 1994). The presentation of antigen by keratinocytes is often related to modulating T cell auto-reactivity and therefore tolerance (Meister et al., 2015), but it can also induce superantigen driven T cell activation (Ardern-Jones et al., 2007).

1.2.2 Langerhans cells (LC)

LCs are the most prominent epidermal immune cell located throughout all strata but most prevalent in the stratum spinosum. Although LCs were initially considered an epidermal specific DC subset, ontogenic analysis has recently indicated LCs are actually tissue-resident macrophages with a DC like phenotype (Hoeffel et al., 2012, Kabashima et al., 2019). This DC like phenotype makes them transcriptionally different from dermal DCs and macrophages (Polak et al., 2014). LCs are often distinguished by the extracellular receptor langerin and the cytoplasm organelles named Birbeck granules, in which langerin is also located. Although the precise role of the Birbeck granules is still under investigation they have been shown to play a role in endosomal sorting. Langerin is a C-type lectin receptor which has been demonstrated to induce the formation of Birbeck granules (Mc Dermott et al., 2002, Lenormand et al., 2013, Valladeau et al., 2000).

Despite extensive investigation of LCs, their key role remains unclear (Romani et al., 2010). It was originally thought that LCs acted as classical DCs of the epidermis that migrate to lymph nodes to prime T cells. More recently it has been suggested that they are critical to regulating epidermal tolerance (Strandt et al., 2017). However, recent understanding of the fundamental differences between murine and human Langerhans cells has required a re-assessment of the evidence and current concepts consider Langerhans cells to be important regulators of both immune response and tolerance in inflammatory skin disease (Eidsmo and Martini, 2018). In addition to their role in immunity, Langerhans cells act as tissue resident macrophages and have a role in mediating homeostasis through clearance of apoptotic debris, which has been shown to be important for maintaining immune tolerance to self-antigen (Cummings et al., 2016). Similarly, LCs have been shown to reduce UVB induced cutaneous inflammation by inducing clearance of apoptotic keratinocytes (Hatakeyama et al., 2017).

LCs are also considered to have a role in mediating adaptive immunity by influencing regulatory T cells (Tregs), effector T cells, and resident memory T cells (West and Bennett, 2017). For instance, LCs can induce Treg proliferation to mediate immune suppression (Seneschal et al., 2012). Alternatively, LCs can activate and induce differentiation of CD4+ T cells to polarise to a Th1, Th2 or Th17 phenotypes depending on the signal (Aliahmadi et al., 2009, Matsui et al., 2015).

1.2.3 Dermal Dendritic cell (DDC)

Dermal DCs is a collective term to include all dermis resident DCs, but does not imply homogeneous function. Within the cutaneous immune system various subgroups of DCs can be characterised by their phenotype and can be further divided into smaller subgroups by function. The main groups are plasmacytoid DCs (pDCs), conventional DCs (cDCs) and monocyte derived inflammatory DCs. cDCs can be further divided into two subsets, cDC1 (CD141+) and cDC2 (CD1c+) (Heath and Carbone, 2009, Haniffa et al., 2015).These DC groups have overlapping but distinct roles in communicating the immune response (Haniffa et al., 2015, Schlitzer et al., 2015).

Normally, pDCs are absent in the skin, but they been identified during inflammation in which they mediate a systemic proinflammatory response and promote wound healing (Malissen et al., 2014). Alternatively, cDCs are commonly found in the skin and upon pathogenic stimulation undergo maturation through PAMP stimulated TLRs or cytokine stimulation. Maturation causes upregulation of MHC class II and costimulatory molecules, as well as migration to the lymph nodes to promote clonal expansion of naïve T cells. The two cDC subsets also induce differing T cell responses. cDC1 promotes Th1 polarisation and is more equipped for an anti-viral response.

Whereas, cDC2 can induce Th2 or Th17 polarisation, as well as Treg activation (Schlitzer et al., 2015).

Monocyte-derived DCs are also activated by pathogen encounter in similar manner to cDCs, however they primarily act to activate effector memory T cells already recruited to the inflammatory site (Malissen et al., 2014, Heath and Carbone, 2009).

The process of DC maturation is important in preparation for the change in its function, changing its phenotype and equipping it with necessary surface proteins depending on the situation. Maturation can occur during the steady state as well as during inflammation. However, there are differences in phenotypic changes. During the steady state DCs upregulate MHC class II and the co-stimulatory molecule CD40 to promote the expansion of Tregs, aiding tolerance (Baratin et al., 2015). Conversely, during inflammation DCs upregulate MHC class II and the co-stimulatory molecules CD86, CD80 and CD40. This is combined with increases in inflammatory cytokine production to regulate the inflammatory response depending on the stimulation. CD86 and CD80 induce T cell activation through binding CD28 on the surface of T cells. This activation promotes T cell proliferation and increased survival, as well as production of IL-2. However, CD86 and CD80 also bind CTLA-4, but with higher affinity. CTLA-4 is a T cell surface protein expressed upon T cell activation that inhibits the T cell response initially induced by CD28, therefore generating a negative feedback loop (Hubo et al., 2013, Buchbinder and Desai, 2016).

1.2.4 Skin resident T cells

The main role of T cells in the skin is to undertake immunosurveillance, which is the induction of migration through the skin regulated by chemokine signals from inflammatory responses. T cell activation is based on the presentation of antigen by MHC class I or II. MHC class I activates cytotoxic CD8 T cells to release cytotoxins to kill the pathogen, conversely the MHC class II of APCs will activate helper CD4 T cells, which will assist in inflammation mediation through the secretion of cytokines and chemokines. Cytokine induced differentiation of the CD4 T cell will determine the profile of the T cell and thus its effect concerning the pro- or anti-inflammatory response.

It was originally thought that peripheral T cells were the main effectors of the skin's immune response. However it has been shown that healthy skin contains twice the number of T cells as compared to the numbers circulating in blood (Clark et al., 2006). A large proportion of these are long-lived in skin and known as a resident T cells. It has also been shown that the skin resident T cells are adequate at generating the inflammatory response, without the aid of circulating T cells

(Pasparakis et al., 2014). The majority of skin resident T cells are CD4 T cells, which express CLA (Cutaneous Lymphocyte-associated Antigen), CCR4 (chemokine receptor 4) and CCR6 (Chemokine receptor 6). They also have a large TCR repertoire (Clark et al., 2006), which is necessary for an effective immune system in order to recognise a large variety of MHC mounted antigen. Differentiation of CD4 T cells during inflammation, will induce phenotypes of the Th1, Th2, Th17 or Treg subgroups depending on the inflammatory conditions (Nestle et al., 2009). However approximately 95% of the CD4 resident T cells in normal skin were polarized to Th1 (Clark et al., 2006).

Skin resident CD8 memory T cells have been shown to act as rapid responders towards pathogens they already recognise, quickly migrating towards an infection and providing superior protection through immediate cytotoxic action (Ariotti et al., 2012).

There are also other subtypes of T cell in the skin, such as γδT cells and Natural Killer T (NKT) cells. Whilst these populations are smaller and less understood, they have been shown to play important functions in the skin. γδT cells act in homeostasis and tissue repair (Jameson and Havran, 2007), and NKT cells have been shown to act through cytokine secretion to aid inflammation or to suppress it depending on the situation (Bendelac et al., 2007).

1.2.5 Cutaneous Macrophages

Macrophages are a highly phagocytic cell type that perform a number of functionalities within the dermis. In steady state conditions dermal macrophages aid in maintenance of homeostasis. During wound repair macrophages help in return to homeostasis through wound clearance and stimulation of proliferation (Yanez et al., 2017). During bacterial infections macrophages have a specific role of killing microorganisms, through phagocytosis and the production of chemokines to allure neutrophils. Macrophages have a poor antigen presentation capacity in comparison to DCs and don't migrate to the lymph nodes, therefore macrophage antigen presentation to T cells it is performed at the inflammatory site (Malissen et al., 2014).

1.3 Microbiome

The microbiome describes the ecosystem of microorganisms that live on or in the human body. It consists of bacteria, fungi, viruses and mites that exist as commensal organisms sometimes with symbiotic relationships to the host. The skin acts as an interface with the external environment and thus provides a habitat for microbial colonisation. Moreover, the microbiome can provide symbiotic benefits in aiding cutaneous defence from other pathogen microorganisms. In order to colonise the skin surface and maintain homeostasis requires a tolerogenic relationship with the immune system to avoid an inflammatory response. Thus, dysfunction or imbalance within this relationship, known as dysbiosis, can result in infections or inflammatory responses.

The skin microbiome is a diverse and dynamic ecosystem, which varies depending on host factors and environmental factors, but also alters over time. Host factors include age, gender and location; these factors provide variation in the physiological characteristics of the skin. Environmental factors can include occupation, antibiotic usage, cosmetic/soap usage and environmental temperature/humidity. The topographic variability of different locations of the skin provide more specific habitats that offer different niches for colonisation. The topographic variability includes characteristics such as skin thickness and density of follicles or sebaceous glands, which will influence the population of the local microbiome (Grice and Segre, 2011).

The microbiome contributes to the defence of the skin, protecting it from more pathogenic bacteria. This protection stems from out competing other microbes in a niche they are more adapted to live in. To aid in this competition some commensals can secrete bacteriocins, inhibiting the growth of other bacteria (Otto, 2010).

Profiling the diversity of the skins microbiome has elucidated four main bacterial phyla: Actinobacteria (51.8%), Firmicutes (24.4%), Proteobacteria (16.5%) and Bacteroidetes (6.3 %). However, at the species level of bacterial identification a much larger diversity was observed (Grice et al., 2009). Microbial diversity within a specific habitat has been described as “the number and abundance distribution of distinct types of organism” (Human Microbiome Project, 2012) and has been demonstrated to be important for health of the host. In the gut low microbial diversity has been linked to Crohn’s disease (Manichanh et al., 2006). Whereas in the skin low bacterial diversity and high *S. aureus* colonisation is associated to atopic dermatitis (AD) (Kobayashi et al., 2015). Yet in contrast, high microbial diversity in the vagina is linked to vaginosis (Fredricks et al., 2005). Alternatively, although acne is considered to be related to *Cutibacterium acnes* colonisation, it may not be related to *P. acnes* abundance. Instead Barnard et al. (2016) suggested that disruption to the balance of the microbiome was responsible for the dysbiosis of acne.

With the constant colonisation of the skin from birth it is important to consider how the microbiome is regulated to maintain homeostasis in balance with the skin immune system. Control of the balance is complex and not fully understood, but diseases of dysbiosis demonstrate its importance. It is therefore important that the immune system can determine the difference between commensal and dysbiotic or pathogenic colonisation. Whilst this mechanism has not fully been elucidated, it has been proposed to be induced by tolerance of the immune system. Long term exposure to commensals may cause desensitization resulting in a decrease in TLR activity, either through inhibition or downregulation (Strober, 2004, Grice and Segre, 2011, Tlaskalova-Hogenova et al., 2004). Alternatively, it has shown that tolerance can be established in neonatal mice, but not adult mice, indicating timing is the dominant factor in establishing tolerance to commensal organisms (Scharschmidt, 2017). However, little is known about the differences between responses induced between potential commensals and pathogens, and how the immune system can differentiate between them.

1.4 Staphylococci

Staphylcocci are common colonisers of the skin with various different species in competition and therefore constitute an important component of the microbiome to study.

Staphylococcus was initially described in 1880 by Alexander Ogston due to its grape like appearance and was isolated in 1884 by Friedrich Julius Rosenbach. Rosenbach named the two species *S. aureus* (SA) and *S. albus* (later re-named *S. epidermidis* (SE)), for their golden and white colony colours (Sejvar, 2013). They are Gram-positive bacteria that appear as spherical cells, which can be alone, in pairs or in clusters. They optimally grow at 37°C under aerobic conditions, but are also facultatively anaerobic (Breed et al., 1957).

Taxonomically, the genus of Staphylococcus is of the Firmicute Phylum and Bacilli Class. The genus contains over 40 species, most of which are non-pathogenic. SA and SE are the two most well studied species, due to their prevalence of colonising human skin. SA and SE were originally distinguished by their appearance; both appearing circular and smooth on agar, but with differing colours. However, another key difference commonly used to distinguish them is their ability to coagulate blood, SA being coagulase positive and SE being coagulase negative (Breed et al., 1957). Coagulase positive or negative is often used to group species of staphylococci. Other coagulase negative species include *S. capitis* (SC), *S. hominis*, *S. Ludgunensis* and *S. Warneri*. However, more recent research has described coagulase negative strains of SA (Matthews et al., 1997). Additionally, SA can also be distinguished from SE by its ability to ferment mannitol, whereas SE cannot (Breed et al., 1957).

Structurally staphylococci are surrounded by a cell wall consisting of mainly peptidoglycan chains, which are composed of polysaccharide subunits. Peptidoglycan can act as an exotoxin for some strains including SA, furthermore variation in peptidoglycan structure alters its activity. Amidst the cross-linked peptidoglycan chains are lipoteichoic acid (LTA) and Ribitol teichoic acid (RTA, also known as wall teichoic acid), as shown in **Figure 1.4b**. LTA and RTA provide structural support to the cell wall via covalent bonds throughout the peptidoglycan layer, but LTA is also anchored to the cytoplasmic membrane. Additionally, the bacterial cell wall contains a variety of other surface proteins depending on the growth phase of the bacterium (**Figure 1.4a**). Many of these surface proteins share common features, such as a cell wall anchoring region and a ligand binding domain (**Figure 1.4c**). Generally surface proteins are adhesins, which are given function by their ligand binding domain.

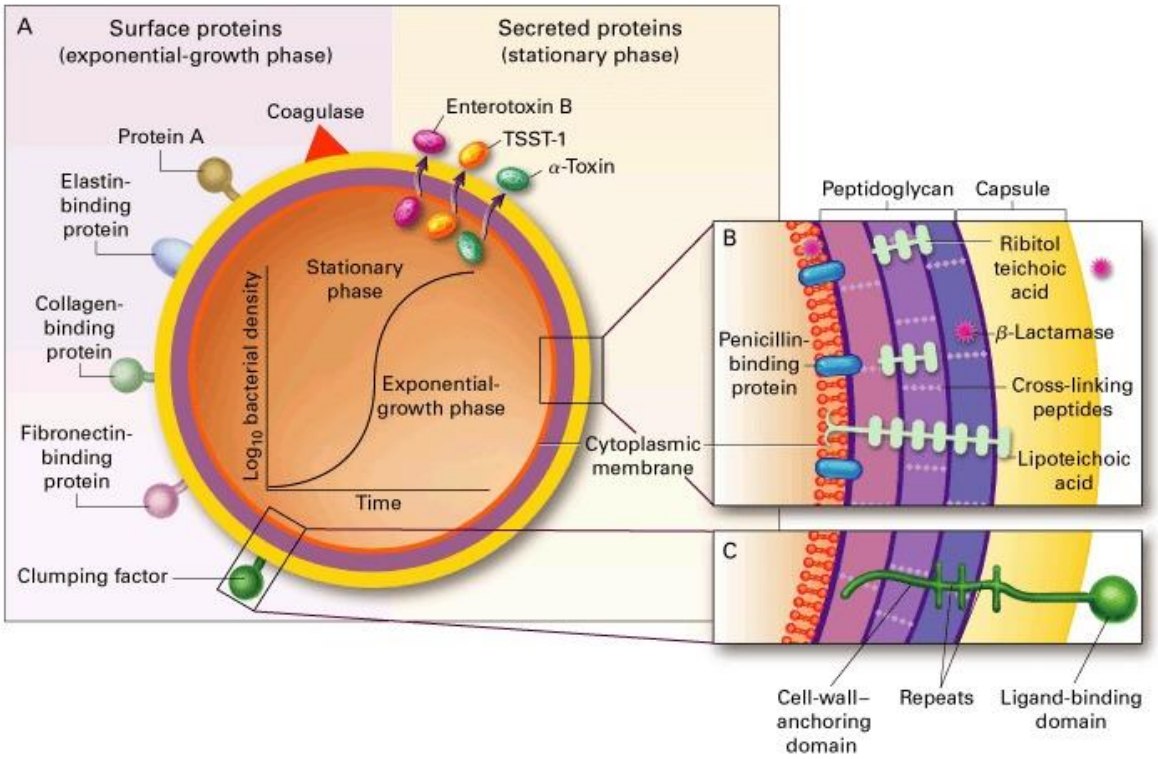

Figure 1:4: Structure of SA
Depiction of staphyloccal structure displaying surface and secreted proteins (**a**), cell wall composition (**b**) and surface protein structure (**c**) (Lowy 1998).

Adhesins assist bacterial adhesion, operating by binding specific ligands (**Table 1.1**), including components of extracellular matrix. These adhesins are thus classified as microbial surface components recognizing adhesive matrix molecules (MSCRAMMs). The function of MSCRAMMs dictates their importance in colonisation (Ghasemian et al., 2015). However, the carriage rate of adhesins differs between strains (Nowrouzian et al., 2011), granting strains differing virulence. Subsequently, adhesins are considered virulence factors.

Bacterial virulence factors are distinguished by their function and can assist in host invasion, host defence evasion or pathogenicity of a disease. Therefore classifying adherence factors, invasion factors, exotoxins, endotoxins and the bacterial capsule as virulence factors. Staphylococcal virulence factors vary between both species and strain and thus will be discussed in great detail later.

Table 1.1: Adherence factors of SA, SE and SC

Adherence factors	Related genes	
Autolysin	atl	Surface protein and peptidoglycan hydrolase for both SA (altA), SE (altE) and SC (altE). It adheres to polystyrene, but has binding activity to vitronectin and fibronectin. It is also important for biofilm development (Biswas et al., 2006).
Cell wall associated fibronectin binding protein	ebh	SA, SE and SC MSCRAMM that specifically binds fibronectin (Clarke et al., 2002).
Clumping factor A **Clumping factor B**	clfA clfB	Fibrinogen-binding MSCRAMM of SA. clfA and clfB are distinct genes and not allelic variants, thus are not closely linked and also bind different ligands of fibrinogen (McAleese et al., 2001). Additionally, ClfB also binds cytokeratin 10 (Xiang et al., 2012) and loricrin (Vitry et al., 2017). SE also expresses fbe, a fibrinogen binding MSCRAMM of similar homology to clfA (Nilsson et al., 1998).
Collagen binding protein	cna	SA MSCRAMM for adherence to collagen. Adherence to collagen also causes virulence in the pathogenesis of septic arthritis (Patti et al., 1994).
Elastin binding protein	ebps	Surface associated MSCRAMM of SA, SE and SC that binds soluble elastin products and tropoelastin precursor (Downer et al., 2002).
Extracellular adherence protein	eap	Secreted by SA and SE it binds numerous ECM proteins, including fibronectin, fibrinogen, vitronectin, bone sialoprotein and thrombospondin (Palma et al., 1999). Additionally it can bind ICAM-1, therefore inhibiting the host inflammatory response (Athanasopoulos et al., 2006).
Extracellular fibrinogen binding protein	efb	Secreted by SA, SE and SC it acts in immune evasion by binding fibrinogen and complement C3 (Ko et al., 2011).
Fibronectin binding proteins	fnbA fnbB	SA and SE MSCRAMM enabling attachment to host cells via binding of fibronectin, as well as fibrinogen and elastin (Burke et al., 2010). Fibronectin is a component of ECM that is bound to the α5β1 integrin on the host's cell surface. Fibronectin binding protein (FnBP) A and B have similar structure and are anchored to the bacterial cell wall by the LPXTG motif (Shinji et al., 2011).
Intercellular adhesin	icaR icaA icaD icaB icaC	SA, SE and SC adhesins that mediates bacterium cell-cell adhesion enabling biofilm formation (Cramton et al., 1999).
Iron-regulated surface determinant protein A	isdA	SA and SE MSCRAMM functioning in an iron regulated manner that strongly binds fibronectin and fibrinogen, as well as transferrin and hemin (Clarke et al., 2004).

Laminin binding protein	eno	MSCRAMM of SA that binds laminin (Carneiro et al., 2004).
Ser-Asp rich fibrinogen-binding proteins	sdrC sdrD sdrE sdrF sdrG sdrH sdrX sdrZL	Family of MSCRAMMs anchored to the cell wall by the LPXTG motif and characterized by repeated serine-aspartate dipeptides, but differing in their ligand binding domains. However, not all their ligands have been elucidated (Wang et al., 2013). SdrC/D/E are expressed by SA, whereas SdrG/FH are expressed by SE and SdrX/ZL are expressed by SC. • SdrC binds β-neurexin (Barbu et al., 2010) • SdrD binds Desmoglein 1 (Askarian et al., 2016) • SdrE binds complement regulatory protein factor H (Sharp et al., 2012) • SdrF binds keratin (Trivedi et al., 2017) and collagen (Arrecubieta et al., 2007) • SdrG binds to fibrinogen (Davis et al., 2001) • SdrX binds to collagen (Liu et al., 2004)
Staphylococcal protein A	spa	SA MSCRAMM anchored by the IPXTG motif that binds to the Fc domain of IgG, therefore inhibiting opsonophagocytosis. It also binds the B-cell receptor, thus acting as a B-cell superantigen that causes programmed cell death (Kobayashi and DeLeo, 2013).

SA and SE are the predominant staphylococci colonising the skin and due to the pathogenicity of SA it is often considered in contrast to the SE; this is particularly notable for investigating AD (Holland et al., 2009, Laborel-Preneron et al., 2015, Dotterud et al., 2016). SE colonises most areas of human skin including the nares, axillae, head, legs and arms (Kloos and Musselwhite, 1975). However, other staphylococcal species occupy more specific topographical niches. SA primarily colonises the anterior nares, which can act a reservoir to supply other areas (van Belkum et al., 2009). Whereas SC colonises the head and arms but is less prevalent than SE (Kloos and Musselwhite, 1975).

1.4.1 *Staphylococcus aureus* (SA)

SA is the most well studied species of staphylococci. It has an approximate carriage of 30% for persistent colonisation, 60% for intermittent colonisation and 20% are almost never colonised (den Heijer et al., 2013, Brown et al., 2014). The opportunistic pathogenic nature of SA does mean SA is infective, and persistent colonisation has been shown to increase the risk of infection (Wertheim et al., 2004). Comparatively to other staphylococci, SA is more infective with aggressive virulence factors not found in other species. The infection of SA can lead to a number of severe diseases (**Table 1.2**), however SA colonisation is usually non-pathogenic and asymptomatic. Yet AD has been strongly linked to SA colonisation (Totte et al., 2016), with

increased lesional severity associated with an increased abundance of SA colonisation (Gong et al., 2006).

Table 1.2: SA infections
(Reviewed by Tong et al. (2015))

SA infections
SA bacteremia (SAB): infection of the bloodstream
Infective endocarditis: infection of the heart valves and its inner chambers
SSTI (skin and soft tissue infection): SA causes a range of SSTIs that vary between benign and life-threatening. • Impetigo: infection of the epidermis • Necrotizing fasciitis: infection of the fascia (connective tissue) • Pyomyositis: muscle infection • Folliculitis: hair follicle infection • Furunculitis: hair follicle infection causing a furuncle • Cellulitis: infection of the dermis or subcutaneous fat • SSI (surgical site infection)
Osteoarticular infections: SA infection of bone results in inflammatory destruction and necrosis • osteomyelitis: bone infection • native joint septic arthritis: joint and synovial fluid infection • prosthetic joint infection: joint infection associated to joint replacement
Prosthetic device infections: SA is proficient at infecting prosthetic devices through biofilm formation • Prosthetic joint infection • Prosthetic valve endocarditis • Cardiac device infection • Intravascular catheter infection • Breast implant infection • Ventricular shunt infection • Penile implant infection
Pleuropulmonary infections: SA infection of lung and pleura that in severe cases results in pneumonia
Epidural absecess: SA intracranial or spinal infection
Meningitis: SA infection of the meninges
Toxic shock syndrome (TSS): SA toxin mediated illness caused by superantigen based T cell activation

SA predominantly colonises the stratum corneum, however it can be found at lower quantities throughout the lower strata down to the stratum basale (Hanssen et al., 2017). Numerous virulence factors enable and aid colonisation, their expression is situation dependent and therefore tightly regulated by the bacterium. The regulation of expression is controlled through several regulatory loci and is determined on quorum sensing and environmental signals; such as pH, osmolarity, temperature and nutrient availability (Bien et al., 2011). Quorum sensing is the ability to detect population density (quorum) and respond, this can be controlled through the accessory gene regulator (Agr). Agr is an important regulator for infection, upregulating genes of exoenzymes and toxins (Le and Otto, 2015). This includes pore-forming toxins such Panton-Valentine Leukocidin (PVL), γ-hemolysin and other leukocidins (Cheung et al., 2011). As well as peptide toxins such as Phenol-soluble modulins (PSMs) which are strong proinflammatory and can lyse numerous cell types including neutrophils and erythrocytes (Wang et al., 2007). Consequently, PSMs are notably involved in the pathogenesis of SA infections.

Agr is also involved in the degradation of biofilm matrix components enabling dispersal, such that Agr dysregulation leads to enhanced biofilm formation. Thus, Agr dysregulation has been associated with the infection of indwelling devices (Le and Otto, 2015). Furthermore, Agr has shown to be inactive during colonisation. This colonisation was characterised by expression of adhesive (clfB, fnbA and isdA) and immune-modulatory factors (Spa), but lacked toxins (α-hemolysin, PSM and a bi-component leukotoxin homologue (blhB)) (Burian et al., 2010).

Other regulators of SA virulence factors include sarA, sae, sigB and arl, which act in a network using “cross talk” of several regulators to provide the specific gene expression required for the environmental conditions (Bien et al., 2011).

SA’s ability to produce toxins is associated to its virulence and pathogenicity, there are a diverse range of toxins with various effects (**Table 1.3**). However, certain toxins are superantigens (SEA, SEB, SEC and TSST-1) that are able to activate T cell proliferation through non-specific bridging of TCRs to MHC class II of APCs, as well as enhancing costimulation of CD86 to CD27. This results in activation of APCs such as macrophages. Superantigen can stimulate up to 20-30% of T cells, whereas ordinary antigens may stimulate <1%. The consequent inflammatory response caused by activation of high numbers of T cells and macrophages is known as a cytokine storm (Spaulding et al., 2013, Kaempfer et al., 2017).

Table 1.3: Toxins of SA

SA toxins	
α-hemolysin γ-hemolysin Panton-valentine leucocidin (PVL) Leukocidins: • LukED • LukAB • LukMF	Cause membrane damage through pore-formation (Seilie and Bubeck Wardenburg, 2017).
Phenol soluble modulins (PSM): • PSMα1 • PSMα2 • PSMα3 • PSMα4 • PSMβ1 • PSMβ2 • δ-hemolysin	Cause a proinflammatory response and have differing cytolytic activity. PSMα3 is known for its notable potency, whereas PSMβs are non-cytolytic (Peschel and Otto, 2013).
β-hemolysin	Causes membrane damage by hydrolysing the plasma membrane lipid sphingomyelin (Vandenesch et al., 2012).
Staphylococcal enterotoxin A (SEA) Staphylococcal enterotoxin B (SEB) Staphylococcal enterotoxin C (SEC) Toxic shock syndrome toxin (TSST-1)	Superantigen that causes T cell activation (Spaulding et al., 2013).
Exofoliative toxin A (ETA) Exofoliative toxin B (ETB)	Serine protease that cleaves desmosomal cadherins, disrupting cell-cell adhesion of keratinocytes (Bukowski et al., 2010).

Adherence of SA to the stratum corneum is meditated through a number of adhesins, however different adhesins are expressed and used depending on the situation. For instance Jenkins et al. (2015) demonstrated a different expression of adhesins for colonisation and infection, further concluding that ClfB and SdrC are key to nasal colonisation. They also showed upregulation of ClfA, icaB, SdrD, and efb; suggesting nasal colonisation required a multifactorial process. Although SdrC is known for binding to the neuronal presynaptic protein β-neurexin (Barbu et al., 2010) more recently alternative interactions have been elucidated. SdrC has been shown to mediate strong attachment to hydrophobic surfaces, as well as weak cell-cell adhesion through homophillic bonds that may indicate a role in biofilm formation (Feuillie et al., 2017). ClfB can bind fibrinogen, cytokeratin 10 and loricrin, however the high affinity binding of ClfB to loricrin

(Vitry et al., 2017) is particularly important for nasal colonisation. Loricrin is a major component of the cornified envelope and its importance was indicated by reduced nasal colonisation in loricrin deficient mice (Mulcahy et al., 2012).

Interactions of MSCRAMMs are aided by SERAMs (Secreted expanded repertoire adhesive molecules), which are bacterially secreted molecules that have adhesive and immunoevasive activity. An important SERAM specific to SA is the Extracellular adherence protein (Eap), which can bind a number of ECM components such as fibrinogen and fibronectin, as well as the coagulation factor prothrombin and the proinflammatory adhesin ICAM1. Binding of Eap to ICAM1 prevents leukocyte adhesion, thus dampening an inflammatory response to an infection (Haggar et al., 2004, Chavakis et al., 2005).

Most virulence factors that aim to modulate the immune system through suppression or evasion are more important for infection than colonisation, however there are exceptions. It has been suggested that SA can be resistant to AMPs that have previously been demonstrated to be effective at killing them; including hBD3 (Kisich et al., 2007), LL-37 (Noore et al., 2013) and RNase 7 (Simanski et al., 2010). Certain strains of SA can produce proteases that cause degradation of LL-37 and inactivation of hBD3 (Peschel and Sahl, 2006). Midorikawa et al. (2003) demonstrated variable efficiency for hBD3 and LL-37 for different strains of SA. It has also been demonstrated that the susceptibility of clinical strains to AMPs is variable and strains collected from skin colonisation are more resistant than strains collected from bacteremia (Rieg et al., 2011). Alternatively, resistance could be a result of mutations in the bacterial surface membrane resulting in a reduced negative charge (Peschel et al., 2001). As β-defensins and LL-37 are cationic AMPs that use electrostatic forces to bind bacteria this would reduce their effectiveness. Despite the methods of resistance to AMPs Midorikawa et al. (2003) also proved that AMPs in coordination were considerably more effective at killing SA and especially for the combination of hBD3 and LL-37.

Furthermore, SA can secrete a serine protease known as V8, a virulence factor that induces damage to the barrier integrity. However, IL-1β induced production of hBD2 can protect against this damage (Wang et al., 2017), demonstrating the role of AMPs in barrier protection in conjunction with defensive.

1.4.2 *Staphylococcus epidermidis* (SE)

SE is a fundamental species of the skin microbiome that colonises 100% of people. It can colonise most skin surfaces including the nares, axillae, head, legs and arms. As the predominant staphylococcal skin commensal it is often used in comparison with SA. Although SE is an

opportunistic pathogen it primarily acts in a symbiotic relationship with the skin, providing a number of beneficial functions to protect the skin from other more pathogenic microorganisms. It has been suggested the SE inter strain competition selects for low virulence, favouring virulence factors of immunoevasion and persistence over aggressive factors or toxins (Otto, 2010, Nguyen et al., 2017, Otto, 2009).

The most prevalent infections of SE are nosocomial infections and in contrast to SA, SE does not typically infect non-compromised individuals. Therefore SE is considered a dominant infector of immune-compromised patients, with entry mediated by indwelling medical devices, such as intravascular catheters. Biofilm formation associated to these devices makes these infections difficult to eradicate, furthermore dispersal of the biofilm can lead to bacteremia, which has high mortality rate (Vuong and Otto, 2002, Otto, 2017).

The inferior pathogenicity of SE in comparison to SA is associated to a difference in affiliated toxins, specifically SE lacks severe tissue damaging toxins (**Table 1.4**), instead favouring virulence factors of immunoevasion (Otto, 2012). This includes virulence factors that enable biofilm formation. After attachment and profileration, SE can produce an extracellular matrix consisting of the polysaccharide intercellular adhesion (PIA) exopolysaccharide, accumulation-associated protein (Aap), extracellular matrix binding protein (Embp), teichoic acids, and extracellular DNA. This biofilm formation inhibits opsonisation, phagocytosis, AMPs and complement components (Le et al., 2018).

Table 1.4: Toxins of SE

SE toxins	
Staphylococcal enterotoxin C3 (SEC3) Staphylococcal enterotoxin-like toxin L (SEIL)	Superantigen of rare occurrence in SE isolates (Madhusoodanan et al., 2011)
Phenol-soluble modulins • PSMα • PSMδ • PSMε • δ-toxin • PSM-mec	Induce a proinflammatory response and have moderate non-specific cytolytic activity. Additionally, PSMδ and δ-toxin may also be antimicrobial (Otto, 2014).
• PSMβ1 • PSMβ2	Induce a proinflammatory response and have biofilm-structuring activity (Otto, 2014).

Attachment during colonisation is mediated by MSCRAMMs (**Table 1.1**). For instance SdrG binds fibrinogen, SdrF binds keratin and IV collagen, and Ebps binds elastin (Bowden et al., 2005).

Additionally, certain MSCRAMMs of SA and SE share similar mechanisms, such as SA's ClfB and SE's SdrG which use a mechanism known as 'dock, lock, and latch' (Foster et al., 2014). However, SE has less cell wall associated adhesins than SA.

SE's symbiotic relationship with the skin can be demonstrated through its relationship with SA, its staphylococcal competitor. SE exhibits numerous methods of inhibition towards SA, both directly through the production of antimicrobials and indirectly through the stimulation of the skin to boost SA clearance (Gallo and Nakatsuji, 2011). PSMγ and PSMδ of SE have been shown to cause membrane leakage of SA (Cogen et al., 2010). Furthermore, SE's beneficial relationship with the skin has been shown in a more physiologically relevant situation, during which SE inhibited nasal colonisation of SA through secretion of Esp, a serine protease (Iwase et al., 2010). Additionally, SE has been shown to inhibit *agr*, a gene regulator vital for SA infection (Otto et al., 1999). SE can also induce increased AMP production from keratinocytes, which indirectly affects SA colonisation. This is mediated by a small SE secreted molecule that increased expression of hBD2 and hBD3 via stimulation of TLR2 (Lai et al., 2010).

The beneficial relationship between the skin and SE is not just related to aiding in defence against other pathogenic microbes, but also directly affects the skins innate immunology. SE's LTA has been shown to stimulate TLR2 causing inhibition of TLR3, dampening inflammation to limit damage and promote wound healing (Lai et al., 2009).

1.4.3 *Staphylococcus capitis* (SC)

SC is another common skin commensal that commonly colonises the scalp, face, neck, and arms, but is less well studied than SA or SE (Kloos and Musselwhite, 1975, Otto, 2010).

Similarly to SE, SC can act as an opportunistic pathogen associated to nosocomial infections and biofilm formation, however less is known about its pathogenesis (Cameron et al., 2015). SC is a notable problem in certain situations, for instance SC is responsible for up to 20% of neonatal sepsis cases in neonatal care units (Van Der Zwet et al., 2002). SC can also cause prosthetic endocarditis (Cone et al., 2005) and prosthetic joint infections (Tevell et al., 2017).

However, SC also been suggested to be associated with inflammatory scalp disease (Wang et al., 2015), Therefore SC could provide a useful comparator to investigating SA's role in mediating AD, as well as SE's commensal colonisation.

SC and SE also have comparable virulence factors, this includes adhesins (**Table 1.1**) and toxins such as PSMα, PSMδ, PSMβ1, PSMβ2 and δ-hemolysin. However, a number of these virulence factors are only known due to their homology to the genes for SE (Cameron et al., 2015).

1.5 Atopic Dermatitis (AD)

AD is a chronic inflammatory skin disease, visibly characterised through itchy eczematous lesions. AD is highly prevalent, affecting between 5-10% adults and 20-30% children worldwide (Silverberg and Hanifin, 2013) and whilst not fatal it can severely impact a sufferer's quality of life.

AD has a complex and multifactorial aetiology that combines genetic, environmental, and immune factors. The pathogenesis of AD can be related to three topics: skin barrier dysfunction, inflammation, and dysbiosis of the microbiome (Peng and Novak, 2015).

One of the major genetic predispositions to AD is mutation in the filaggrin gene (FLG), which results in skin barrier dysfunction. Mutation of FLG has been shown by one study to triple the risk of eczema (Weidinger et al., 2008). During differentiation filaggrin aggregates keratin filaments in the stratum granulosum, however in the stratum corneum filaggrin is gradually degraded into metabolites and ions that constitute the natural moisturizing factor (NMF). The NMF aids in maintainance of hydration and pH of the stratum corneum (Peng and Novak, 2015, O'Regan et al., 2008). These changes also increase penetration of allergens into the epidermis, which can then be followed by an enhanced immune response (Kawasaki et al., 2012). Additionally, genome-wide association studies (GWAS) of AD have provided other genetic susceptibilities to the disease, which involve other gene loci associated to epidermal barrier function, as well as immune function (Ellinghaus et al., 2013).

The immune dysfunction of AD is complex and involves numerous cell types, including both resident and infiltrating cells. For example, keratinocytes, LCs, DCs, T cells, macrophages and mast cells all contribute to the inflammation. Immunologically AD is characterised by a biphasic inflammatory response, initially developing as a Th2 response during the acute phase that transitions into a Th1-like profile during the chronic phase (Egawa et al., 2015). However, other T cell subsets are involved. Although Th2 cells are predominant in the acute phase, Th22 and Th17 cells also mediate the response. Additionally, Th2, Th17 and Th22 cells are all present and mediate the chronic phase, despite the Th1-like profile (Brunner et al., 2017).

As immune sentinels, keratinocytes also aid AD's inflammatory response. Production of cytokines and immune mediators such as TSLP (thymic stromal lymphopoietin) (Kumagai et al., 2017), IL-1α and GM-CSF (Girolomoni and Pastore, 2001) exacerbate the inflammation, as well recruit and stimulate DC's and T cells.

IL-4 and IL-13 are key Th2 cytokines, critical for the pathogenesis of AD and are highly prominent at lesional sites (Brandt and Sivaprasad, 2011). They have been shown to structurally affect the epidermis by inhibiting filaggrin expression (Howell et al., 2007), reducing ceramides in the

stratum corneum (Sawada et al., 2012) and increasing fibrinogen and fibronectin in the stratum corneum (Cho et al., 2001). IL-4 and IL-13 have also been shown to reduce AMP expression (Nomura et al., 2003, Howell et al., 2006a, Howell et al., 2006b) and increase IgE production (Brandt and Sivaprasad, 2011).

The atopic nature of AD is often identified by increased levels of IgE, which enables an overactive response to an allergen. Although the mechanisms of acute AD transitioning into chronic AD are not fully understood it could involve repeated allergenic stimulation of the skins immune system (Kim et al., 2014). Furthermore, a study using mouse models demonstrated activation of DCs via TLR2 stimulation induced a chronic Th2 response (Kaesler et al., 2014). The study included TLR2 stimulation by SA's LTA and therefore implies SA's assistance in transitioning from acute to chronic AD.

Colonisation of SA is strongly associated with AD (Totte et al., 2016). Dysbiosis occurs at lesional sites, with heightened SA colonisation and low bacterial diversity (Kong et al., 2012). Furthermore SA density correlates with lesional severity (Gong et al., 2006). Individuals with AD have an increased SA carriage rate of 90% (as compared to 30% in the general population), but also an increased prevalence to skin infections particularly by SA (Baker, 2006).

AD lesions provide a niche for SA colonisation via numerous changes to the epidermal environment. For example barrier dysfunction caused by down regulated filaggrin expression and reduced ceramide levels. An increase in SA's preferential binding receptors by heightened fibronectin and fibrinogen. However most influential is the reduction in AMP production, such as hBD3, hBD2 and LL-37.

SA has been shown to exacerbate the inflammatory response of AD. This is mediated by superantigens such as SEA, SEB and TSST-1, which have been shown to initiate, increase and maintain AD associated inflammation (Baker, 2006). Superantigens are known for direct non-specific T cell activation, but are also able to inhibit the immune suppression of Tregs (Ou et al., 2004). Therefore SA toxins can drive the pathogenesis of AD (Ardern-Jones et al., 2007).

There is evidence that AD enables SA colonisation and that SA colonisation exacerbates inflammation of AD (Geoghegan et al., 2018). However, it is still unclear whether SA dysbiosis is a by-product of AD that intensifies the inflammation or whether SA is key to the initial development of AD's pathogenesis.

Keratinocytes role as both immune sentinel and defensive barrier implicates them in mediating the initial response to SA colonisation. Therefore, investigating the keratinocyte response to SA colonisation provides an interesting avenue of study regarding the role of SA in AD pathogenesis.

1.6 Models of the skin

Skin research uses a wide array of different models to provide different platforms of study. These models have different attributes with pros and cons and therefore are suitable for different purposes.

In vivo models allow for a more systemic approach of investigation, enabling the study of the skins influence on the overall body or the immune system. Mice are commonly used as an *in vivo* model and have previously provided insight into various areas of interest, including AD (Martel et al., 2017). Murine models of AD can be generated by the knockout of specific genes that may add increased susceptibility, such as filaggrin (Kawasaki et al., 2012). Alternatively, mice can be treated with haptens to induce immune dysfunction corresponding to AD (Kitamura et al., 2018). However *in vivo* models have limitations, including the physiological differences in the skins epidermis, its immune system, and its microbiome (Pasparakis et al., 2014). Additional issues arise in the application of *in vivo* models, since their use has been prohibited in the cosmetics industry in the EU since 2009 (Vogel, 2009). This has further increased the necessity for reliable and accurate *in vitro* models of the skin.

In vitro cellular models are commonly used in research for predictive cell based assays. They are convenient, easy to set up and give a specific cellular response to a treatment or stimulation (Mathes et al., 2014). 2D monolayers of keratinocytes are frequently used as *in vitro* models of the skin; these can be composed of Primary keratinocytes or a spontaneously transformed cell line of keratinocytes, such as HaCaTs. 2D monolayers have been extensively used to investigate infection of SA in order to understand the interaction of skin and SA's transition from commensal to infection (Bur et al., 2013, Edwards et al., 2011, Mempel et al., 2002). However, monolayers have limited use in studying the interaction of the skin with commensal organisms. Monolayers are composed of confluent keratinocytes that have started to differentiate, however they do not differentiate fully and therefore lack a stratum corneum. This is a key limitation when studying commensal organism interactions with the skin. Initial interactions of a commensal on the skin will be with the stratum corneum and as a defensive barrier the stratum corneum provides a different environment for colonisation.

Alternatively to monolayer models there are 3D models, also known as organotypic skin models or reconstructed human epidermal (RHE) models. RHE models are multilayer stratified models grown from primary keratinocytes. The keratinocytes differentiate into the different strata of the epidermis, with the eventual formation of a stratum corneum by the terminal differentiation of corneocytes on the models surface (Frankart et al., 2012, Rosdy and Clauss, 1990). The stratum

corneum formation of the RHE model enables it to be a suitable model for studying commensal organisms on the skin (Popov et al., 2014, Holland et al., 2008, Holland et al., 2009).

RHE models have been developed by numerous groups, but are also commercially available as EpiDerm™ and EpiSkin® (Netzlaff et al., 2005). These commercially available models have been validated by ECVAM (European Centre for the validation of Alternative Methods) in comparison to the rat skin transcutaneous electrical resistance assay that was traditionally used as a predictor of skin corrosion (Fentem and Botham, 2002, El Ghalbzouri et al., 2008). However, research performed by Summerfield (2015) suggested these models were not reproducible enough and implied issues may have arisen during the lengthy transport from the supplier. Explaining why other groups cultivate their own models and justifying the necessity to develop an in-house RHE model.

Despite the validations of the RHE models there are shortcomings in comparison to human tissue. For example, it has been demonstrated that RHE models have a different packing structure of lipids in the stratum corneum, which results in increased permeability and reduced barrier function in comparison to human skin (Thakoersing et al., 2013). Another limitation of using RHE models is the restricted time period of use after growth. The models have a 2-3 day period during which tests can take place, therefore they cannot be used for prolonged or sustained testing. There are also reservations about the physiological relevance of the RHE models, as certain aspects of the normal skin function is missing, including desquamation. Stark et al. (2006) demonstrated that when RHE models are allowed to grow for longer than 14 days the thickness of the stratum corenum increases without the degradation of the corneodesmosomes.

3D *in vitro* skin models are not limited to models of the epidermis. Full thickness human skin equivalent (HSE) models incorporate the dermis by differentiating the keratinocyte monolayer into an epidermis on top of a layer of dermal fibroblasts. This provides a more physiological relevant model of the skin, but adds another layer of complexity to the model, meaning increased costs and variability (Mathes et al., 2014). The use of the dermal layer in the HSE models has the benefit of stabilising keratinocyte growth and differentiation, as the fibroblasts act as a feeder layer for keratinocytes. This principle has been further developed by seeding fibroblasts into a biocompatible scaffold, which provides a geometric configuration for tissue formation, resulting in a model more closely related to an *in vivo* situation (Stark et al., 2006). This model also allows for prolonged culture time giving the opportunity to study the proliferation and differentiation of keratinocytes. However, despite the stabilised growth and differentiation, the keratinocytes in this model still lack desquamation. Consequently, the stratum corneum continuously expands during the culture period.

HSE models can be further enhanced by incorporation of other cell types and structures into the epidermal or dermal layers, including LCs, melanocytes and hair follicles (Mathes et al., 2014). This increases their physiological relevance, but only in a specific manner. It does however enable investigation of specific areas of skin research. For example, the addition of melanocytes enables the study of how keratinocytes and fibroblasts influence melanocyte pigmentation (Hedley et al., 2002). As well as the inclusion of LCs in a HSE skin model can be used to study allergen induced LC maturation (Ouwehand et al., 2011).

Alternatively, *in vitro* skin models can be modified to investigate diseases of the skin, such as AD, psoriasis, vitiligo and melanoma (Bergers et al., 2016). AD-like *in vitro* skin models can be generated in three ways: Immune stimulation by cytokines, Genetic knockdown, and Models grown from cells of AD patients (De Vuyst et al., 2017). The AD-like models generated by cytokine treatment have been generated using a number of cytokine cocktails, most notably the Th2 cytokines IL-4 and IL-13. When used on day 10 of 13 during culture IL-4 and IL-13 induce epidermal spongiosis and keratinocyte apoptosis in HSE models (Kamsteeg et al., 2011). Furthermore, treatment of IL-4, IL-13, TNFα and IL-31 on day 7 of 18 during culture induces spongiosis, increased keratinocyte TSLP secretion and changes the lipid composition of the stratum corneum (Danso et al., 2014). Alternatively, siRNA has been used to knockdown filaggrin in HSE models, resulting in increased permeability and a loss of keratohyalin granules (Mildner et al., 2010). Berroth et al. (2013) used keratinocytes and fibroblasts from AD patients in combination with heathy keratinocytes and fibroblasts to culture different HSE variants. The models of healthy Keratinocytes and AD fibroblasts demonstrated the role of fibroblasts in mediating the pathogenesis of AD. However, the models of AD keratinocytes and AD fibroblasts failed to grow, suggesting a full *in vitro* model constructed from AD skin has yet to be developed.

However, these enhancements and modifications increase the complexity of the models. As models increase in complexity so does their maintenance requirements, cost, and period of growth culture. Furthermore, more complex models are less reproducible and are produced in a low throughput manner (Mathes et al., 2014).

Regarding the model to use in this research, it is important to note that use of a model is a balance between complexity and physiological relevance. To investigate the keratinocyte response to staphylococcal colonisation, the RHE model is ideal. It is complex enough to provide a defensive barrier of the stratum corneum, but is still reproducible and can be produced in a high-throughput manner.

1.7 Aims

SE is a normal and crucial aspect of the skins healthy microbiome, its colonisation can aid in immune regulation and tolerance, thus it provides a useful comparator to investigating staphylococcal induced immune responses. Contrastingly, dysbiotic colonisation of SA induces immune dysregulation as part of a lesional exacerbation of AD, with colonisation abundance associated with the lesional disease severity. By investigating the epidermal responses induced by SA or SE colonisation I hope to elucidate the communication and mechanisms involved in the relationship between the skin and colonising staphylococcal species. This research will also extend to include SC to draw upon links with scalp inflammation (dermatitis, dandruff). Thus I aim to explore shared mechanisms that result in immune dysregulation during staphylococcal dysbiosis.

Hypothesis:

Interactions between staphylococci and the skin are distinct between different species and differences may contribute to bacterial regulation of skin tolerance or inflammation.

Questions to address in this thesis:

1. How do staphylococci differ in their ability to colonise skin?
2. What are the differences in induction of inflammatory mediators by keratinocytes in response to different staphylococci?
3. What signalling pathways are activated similarly and differently between staphylococcal species?

Aims:

1) Development of an in house RHE model of epidermis which can tolerate microbial colonisation.
2) Characterise the relative efficiency of staphylococcal colonisation of the RHE model.
3) Investigate and characterise the outcome of staphylococcal colonisation through measurement of epidermal inflammatory mediator induction.
4) Utilise transcriptomic analysis of epidermis compared with and without colonisation to characterise the gene signalling pathways activated by staphylococci.

Chapter 2: Materials and Methods

2.1 Cell Culture

The cell culture media employed in this work is described in Table 2.1.

Table 2.1: Cell culture media

Medium	Recipe
KGM2	Keratinocyte Growth Medium 2 kit (PromoCell) supplemented with: • 0.004 ml/ml bovine pituitary extract • 0.125 ng/ml epidermal growth factor • 5 µg/ml insulin • 0.33 µg/ml hydrocortisone • 0.39 µg/ml epinephrine • 10 µg/ml transferrin • 0.06mM $CaCl_2$ Supplements are at pre-measured concentrations of the KGM2 kit and added prior to use.
KGM2-d	KGM2 with additional supplements: • 2% heat treated foetal bovine serum (FBS) (Gibco) • 100U/ml penicillin and 100µg/ml streptomycin (Gibco) • 1.8mM $CaCl_2$ (Sigma)
KGM2-i	KGM2 with modification: • Additional 2% heat treated FBS (Gibco) • Additional 1.8mM $CaCl_2$ (Sigma) • Without supplementation of hydrocortisone.
DMEM+s	Dulbecco's Modified Eagle Medium, high glucose (25mM), no glutamine, no calcium (Gibco) supplemented with: • 2mM L-glutamine(Gibco) • 1% heat treated FBS (Gibco) • 100 U/ml penicillin and 100µg/ml streptomycin (Gibco) • 10µM sodium pyruvate (Sigma) • 70µM $CaCl_2$ (Sigma)
DMEM-i	DMEM+s without penicillin and streptomycin.
R10	RPMI-1640 (Gibco) with supplements: • 10% FBS (Gibco) • 100U/ml penicillin and 100µg/ml streptomycin (Gibco).

2.1.1 Primary keratinocyte culture

Neonatal Human Epithelial Keratinocytes (NHEKs) from neo-natal foreskin (pooled donor) (Lonza) were cultured in 15ml KGM2 on the large surface of T-75's, which were maintained at 37˚C with 5% CO_2. Media was changed 3 times weekly and cells were passaged at 70-90% confluency. The initial 3 Passages were used for cell expansion and cryopreservation, later passages used for experiments up to passage 10.

Lifting and sub-culture: NHEK's were rinsed with phosphate buffered saline (PBS), dissociated with 5ml TrypLE Express (Gibco) and incubated (37˚C, 5% CO_2) for approximately 7 minutes. Cellular detachment was regularly monitored with microscopy and aided by gentle tapping of the flask. 5ml KGM2 was used to dilute the TrypLE Express and cells were harvested into a Centrifuge tube. A pellet was formed using centrifugation (310 x g, 5 mins) and was re-suspended in fresh KGM2. Quantification of the viable cells in suspension was performed using trypan blue and a haemocytometer. Cells were seeded at between $2x10^5$ and $2.5x10^5$ in T-75 flasks.

Cryopreservation: NHEKs were banked at $5x10^5$ in 250µl of CELLBANKER 2 (Clontech), frozen at -80 ˚C overnight in a Nalgene Mr Frosty surrounded by isopropanol and transferred into the air phase of liquid nitrogen for long term storage.

Thawing: Frozen NHEKs ($5x10^5$ cells) were thawed by hand rolling and transferred into 14ml prewarmed KGM2 in a T-75 flask. The remaining cells were rinsed from the cyrovial with KGM2. Media was changed after overnight incubation, removing unviable cells and the highly diluted CELLBANKER 2. Subculture was continued for one further passage before use in experiments, allowing for correct proliferation and further expansion.

2.1.2 HaCaT Cell Culture

HaCaTs were donated by Unilever and with appreciation towards Professor N. Fusenig. HaCaTs were cultured in 15ml of DMEM+s within T-75 flasks and were cultivated at 37˚C with 5% CO_2. Media was changed 3 times weekly and flasks were passaged at 70-90% confluency.

Lifting and Subculture: HaCaT's were rinsed with PBS, dissociated with 3.75ml Trypsin-EDTA solution (Sigma) and incubated (37˚C, 5% CO_2) for approximately 7 minutes. Cellular detachment was regularly monitored with microscopy and aided by gentle tapping of the flask. FBS (3.75ml) was used to neutralise the Trypsin-EDTA and cells were harvested into a Centrifuge tube. A pellet was formed with centrifugation (310 x g, 5 mins) and was re-suspended in fresh DMEM+s. Trypan

blue and a haemocytometer was used to quantify the viable cells in the suspension. Cells were seeded at between $3x10^5$ and $5x10^5$ in T-75 flasks.

Cryopreservation: HaCaT's banked in cryovials containing $5x10^5$ cells in 500µl. HaCaT's were centrifuged and re-suspended at $2x10^6$cells/ml in FBS. The cell suspension was slowly diluted to $1x10^6$cells/ml with a freezing buffer of 50% DMEM+s, 20% FBS and 30% DSMO. Cryovials were frozen at -80 ˚C overnight in a Nalgene Mr Frosty surrounded by isopropanol and were transferred into the air phase of liquid nitrogen for long term storage.

Thawing: Frozen HaCaT's ($5x10^5$ cells) were thawed by hand rolling and transferred into 14ml prewarmed DMEM+s in a T-75 flask. The remaining cells were rinsed from the cyrovial with DMEM+s and the media was changed after overnight incubation. Subculture was continued for one further passage before use in experiments, allowing for correct proliferation and further expansion.

2.1.3 Monocyte derived dendritic cells (MoDCs)

MoDCs are a frequently used model of dendritic cells (DCs) and within this study were used to investigate DC maturation following exposure to keratinocyte media following various bacterial exposures. Differentiation and culture of MoDCs was consistent throughout this research and concluded with the stimulation experiment performed on day 5 of differentiation (see below). MoDCs were differentiated from CD14+ PBMCs, which were initially separated from whole blood.

Peripheral blood mononuclear cell (PBMC) Separation: PBMCs were separated from whole blood donated by healthy individuals consented under ethical approval (LREC Number: 07/Q1704/46). Blood was collected into 10ml Vacutainer's (BD Vacutainer® with K_2EDTA from BD biosciences) and used immediately or kept on a roller and used within an hour. Blood was diluted with equal volumes of PBS and gently layered on 15ml Lymphoprep (Stemcell Technologies) in a 50ml centrifuge tube. Separate centrifuge tubes were used for each 10ml of blood. Centrifugation (600 x g, 30mins, 4˚C, performed with minimal acceleration/deceleration) generated layers through differential centrifugation allowing for separation of PBMCs by harvesting the buffy coat. The buffy coat was diluted with cold (4˚C) PBS and centrifuged (400 x g, 5mins, 4˚C). The supernatant was discarded and the remaining pelleted PBMCs were washed twice; by means of dislodging the pellet, re-suspension in cold PBS (20ml) and centrifugation (400 x g, 5mins, 4˚C). PBMCs were then re-suspended in cold PBS for quantification of the viable cells using trypan blue and a haemocytometer.

CD14+ isolation: The PBMC suspension was centrifuged (400 x g, 5mins, 4˚C) and after removal of the supernatant, the pellet was dislodged and re-suspended in PBS + 1% BSA (Bovine serum albumin) (90µl per 10^7 cells) and CD14 MicroBeads (Miltenyi Biotec) (10µl per 10^7 cells), both at 4˚C. Incubation (15mins, 4˚C) of the suspension allowed for magnetic bead attachment to CD14+ cells. The suspension was washed with PBS + 1% BSA (1ml per 10^7 cells), centrifuged (400 x g, 5mins, 4˚C) and re-suspended in 500µl of PBS + 1% BSA. To Isolate the CD14+ cells, the suspension was run through a MS column (Miltenyi Biotec) whilst magnetised. The column was rinsed 3 times (500µl PBS + 1% BSA), before eluting the CD14+ cells with 1ml PBS + 1% BSA from the un-magnetised column via its plunger. Trypan blue and a haemocytometer was used to count the viable cells.

MoDC differentiation: The CD14+ cell suspension was centrifuged (400 x g, 5mins, 4˚C) and resulting pellet was re-suspended in R10 at $1x10^6$ cells/ml. The suspension was supplemented with 250U/ml IL-4 and 500U/ml GM-CSF, seeded into a 24 well plate (1ml per well) and incubated (37˚C, 5% CO_2) for 5 days. The differentiating MoDCs were fed on day 3 through the addition of 1ml of R10 supplemented with 500U/ml IL-4 and 1000U/ml GM-CSF to each well.

2.2 3D Reconstructed human epidermal model

The 3D reconstructed human epidermal (RHE) model was originally adapted from the Cell n Tec protocol for establishment of 3D epidermal cultures. The RHE model protocol was developed and optimised (Chapter 3) to establish a standard protocol that could be used consistently throughout this research. The following describes the standardised protocol that was generated, which is also summarised in **Figure 2.2**.

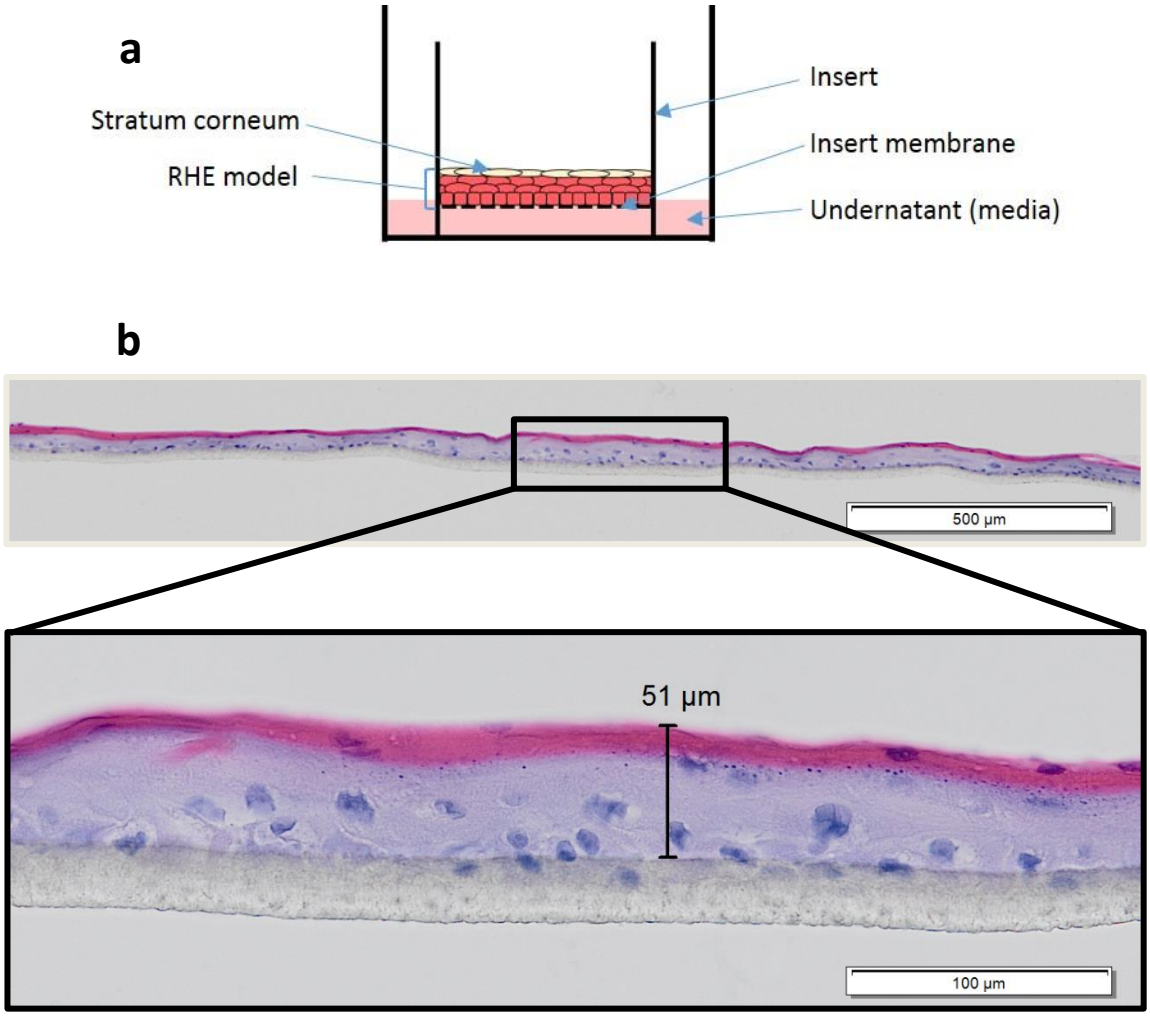

Figure 2:1: RHE model culture
Diagram of the RHE model (**a**) and morphology of the RHE model after 14 days of growth (**b**) histology displayed using H&E staining.

2.2.1 Model production

Seeding: NHEKs were seeded into Millicell Culture plate inserts (Polycarbonate, 0.4µm pore size, 12mm diameter) (Merck Millipore) at $2x10^5$ per insert in 400µl of KGM2. Inserts were grown in batches of 13 within a 10cm petri dish. The petri dish contained KGM2 levelled to the media inside the inserts. The petri dish was incubated in an unsealed humid box within an incubator at 37˚C with 5% CO_2. Inserts were cultured for 2 days, allowing monolayer formation.

Staining for confluency: After 2 days of growth, one insert was removed to test the monolayers confluency. Full confluency was confirmed with staining, using the CnT-ST-100 stain kit (Cell n Tec) and utilizing its associated standard protocol. If a confluent monolayer was observed, initiation of differentiation was performed on the remaining inserts. If incomplete monolayer formation is observed, the remaining inserts were incubated for another day before a fresh insert was stained. If confluency was still not achieved the remaining models were discarded due to inadequate proliferation to form a sufficient RHE model.

Initiation of differentiation: After confirming confluency differentiation was initiated. Media from the petri dish and the inserts were removed and replaced with KGM2-d. Inserts were incubated for 24hrs further (within the humid box, at 37˚C, 5% CO_2).

Lifting to ALI: A day after initiating differentiation the inserts were lifted to the Air-liquid interface (ALI). This was performed by removal of media from petri dish and inserts, KGM2-d was then added to level with the insert membrane, approximately 6ml.

Model Growth: ALI culture was maintained for 14 days (+/-1 day) of incubation (within the humid box, at 37˚C, 5% CO_2) to grow the RHE model. During which, models were fed 3 times weekly by removal of media and replacement with KGM2-d to level with the insert membrane. Models were regularly inspected to ensure the cell surface was dry and visually developing from shiny to matt; this surface texture alteration provided a rudimentary display of differentiation.

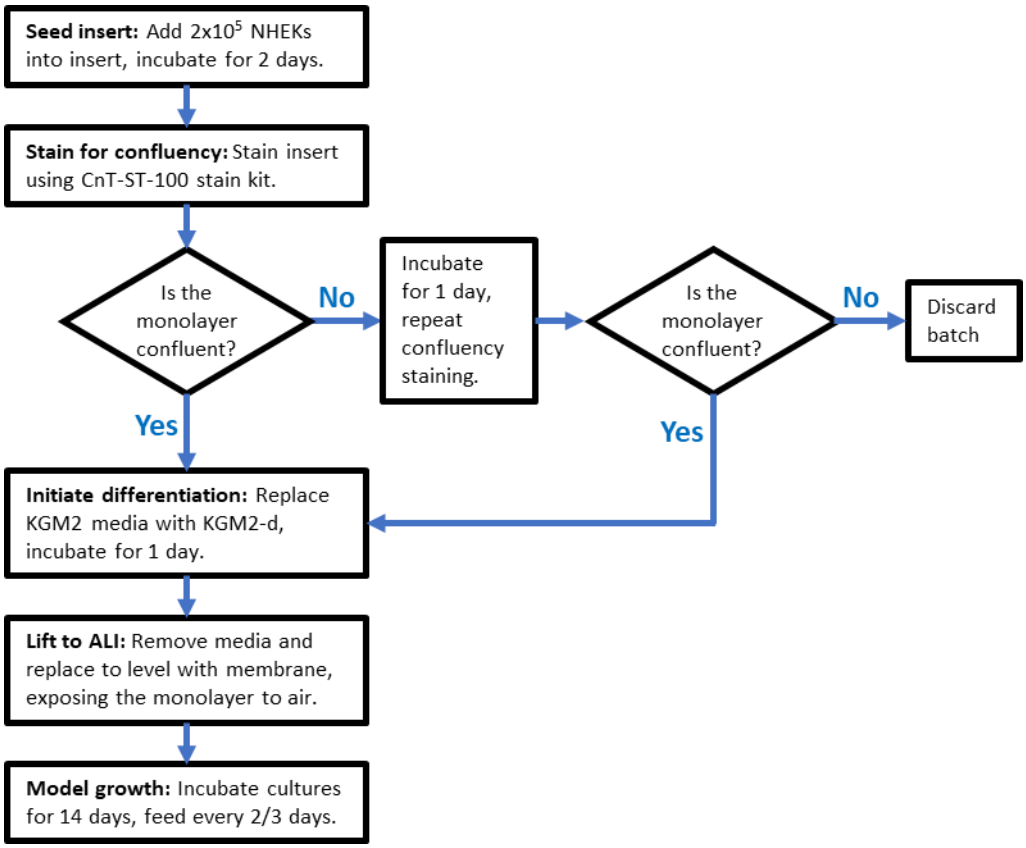

Figure 2:2: Flow diagram of RHE model production
Summary flow diagram of the RHE model production as previously described.

2.2.2 Haematoxylin and eosin staining of RHE Model

Haematoxylin and eosin (H&E) staining was used to demonstrate growth and differentiation of the RHE model. It visually presents a cross section of the model with colour contrast between the stratum corneum and the lower layers of the epidermis. Therefore enabling analysis of growth by its thickness and differentiation by its colour layers.

RHE Model Fixation and processing: After 14 days of growth the RHE models were transferred into a 24 well plate and fixed by submersion in 10% neutral buffered formalin (600µl in the well, 400µl in the insert). After overnight incubation at room temperature the models were removed and delicately cut from the insert along with their attached membrane. The thin cylinder of model was cut along its diameter, placed in a tissue embedding cassette surrounded by foam and submerged in 70% ethanol. The model could be safety stored in 70% ethanol until embedding could be performed. Models were embedded in paraffin wax with the cut diameter exposed to edge of the wax for sectioning. Embedding was performed by staff of the Histochemistry Research Unit of University of Southampton.

Model Sectioning: Paraffin embedded models were sectioned with a microtome at 4μm, with sections flattened by floating on warm water and were then transferred on to microscope slides. Slides were incubated overnight at 37˚C.

H&E staining: Staining was performed at Histochemistry Research Unit of University of Southampton, with their premade reagents. Slides were placed into a rack for the following process of dewax, rehydrate, stain and dehydrate. This was accomplished with submersion in each reagent described in **Table 2.2** for 5 minutes. Slides were air dried and mounted in pertex with a coverslip.

Table 2.2: H&E staining reagents and order of submersion

Protocol stage	Reagent
Dewax slide and hydration of tissue	Clearene
	Clearene
	100% IMS
	100% IMS
	70% IMS
	dH_20
H&E staining	Mayer's haematoxylin
	Running tap water
	2% Eosin in 2% Calcium chloride
	Running tap water
Dehydrate stained tissue	100% IMS
	100% IMS
	Clearene
	Clearene
	Clearene

2.3 Bacterial Culture

Bacterial suspensions were used to perform colonisation and infection experiments. Suspensions were generated throughout using the same protocol. This protocol used a frozen suspension of bacteria streaked on an agar plate to grow overnight to the stationary phase. The bacteria were then mixed into PBS and its optical density was measured, enabling the calculation of its approximate concentration. The suspension was then diluted to the required concentration for use, and a viable count of the 10^4CFU was also taken to later confirm the CFU.

2.3.1 Bacterial Subculture and suspension production

Bacteria were grown from frozen (-80°C) stocks by streaking on agar plates and incubating (37˚C, 5% CO_2) overnight to generate a bacterial lawn. Bacteria were scraped from half of the agar plate, mixed into PBS (1ml) and centrifuged (1000rpm, 1min) to remove any large bacterial aggregate. The suspension was then further diluted 100µl into 900µl PBS to make a master stock, to be quantified and further diluted for use.

Quantification was performed by spectrophotometer to measure the optical density (UV 260nm) of the bacterial lysate, which was composed of 100µl master stock and 900µl lysis buffer (1% SDS, 0.1% NaOH in PBS). The optical density was mathematically divided by the standard optical density for that specific staphylococcal strain (**Table 2.3**), generating a ratio. The ratio was multiplied by the known concentration of the standard of each strain to calculate the approximate concentration of the master stock. The master stock was then diluted to usable concentration that can be serially diluted to the concentration required for the inoculation.

Table 2.3: Strain standards for concentration calculations with optical density

Strain	Optical density	Concentration (CFU/ml)
SA 8325-4	1.67	$1.43x10^9$
SA 29213	1.85	$2.93x10^{10}$
SA 6571	2.10	$2.06x10^{10}$
SE 12228	1.83	$8x10^8$
SE 35984	1.72	$8.27x10^9$
SC 27840	1.08	$5.35x10^8$

The quantification of the suspension was validated through dilution into 10^4CFU/ml. 15µl of the 10^4CFU/ml suspension spread onto 2 agar plates, which are incubated (37˚C, 5% CO_2) overnight. The plates CFU counted and divided by 0.015 (15µl ÷ 1000µl = 0.015) to calculate the CFU within the 10^4CFU/ml stock.

2.3.2 Bacterial enumeration

In order to quantify a bacteria load from an experiment the suspension or lysate from the experiment was diluted serially at 1 in 10, within a 96 well plate (20µl suspension into 180µl PBS). 15µl of various dilutions across the series were spread onto half an agar plate; performed twice per plate to give duplicate results. The agar plates were incubated (37˚C, 5% CO_2) overnight and CFU was counted. The highest CFU of distinct colonies was used for further quantification. The average CFU of the plate (counted per half) was divided by 0.015 (15µl ÷ 1000µl = 0.015) to calculate the CFU/ml of the dilution, which would then be multiplied by the corresponding dilution factor to generate the CFU/ml of the original experiment suspension.

2.3.3 Staphylococcal strains

2.3.3.1 SA 8325-4 (SA83)

The primary strain of SA used in this research was NCTC 8325-4, a derivative of NCTC 8325 that was originally isolated from a sepsis patient in 1960. NCTC 8325 was initially used for research in antibiotic resistance transfer and was selected due to it susceptibility to the antibiotics of the time (Herbert et al., 2010). Since then it has been used extensively in research for decades (Bæk et al., 2013).

8325-4 is one of many derivatives of 8325 and was obtained through two cycles of UV irradiation used to cure the strain of three prophages. Comparative analysis of genetic variation by Bæk et al. (2013) demonstrated a difference of only 20 SNPs between 8325 and 8325-4. This included 13 SNPs causing non-synonymous substitutions or frameshifts, three SNPs considered synonymous substitutions and four SNPs located in intergenic regions. From these SNPs the most prominent mutation is caused by two changes to PSMα3, a toxin and important staphylococcal virulence factor. The SNPs cause a substitution and a frameshift that result in a premature end codon.

Bæk et al. (2013) also identified five large deletions in comparison to NCTC 8325, three of these correspond to the prophages that 8325-4 was cured of. However one of the deletions was in the

intergenic coding region between Spa and sarS, which caused a reduction in transcripts of sarS during the post-exponential steady state.

Furthermore, 8325-4 contains a small deletion in rsbU, a postitive regulator of sigB (Herbert et al., 2010) that upregulates virulence factors such as α-hemolysin and is important for mediating chronic SA infections (Tuchscherr et al., 2015)

Therefore 8325-4 is an SA strain of reduced virulence that may provide a good model of SA colonisation rather infection.

2.3.3.2 SA 29213 (SA29)

The strain ATCC 29213 (also known as NCTC 12973) is another SA strain commonly used as a reference strain. It is a MSSA (methicillin-sensitive SA) strain that has regularly been used as a control for investigating MRSA (methicillin-resistant SA) (Soge et al., 2009, Carson et al., 2007). Furthermore it has been used as a control for examining virulence of other isolates (Park et al., 2007, Iqbal et al., 2016) and as a cytotoxic strain for infecting mouse keratinocytes and fibroblasts (Krut et al., 2003). Therefore providing a more virulent strain of SA to investigate SA colonisation.

2.3.3.3 SE 12228 (SE12)

The strain ATCC 12228 is well characterised strain of SE that is nonpathogenic and non-biofilm-forming (MacLea and M Trachtenberg, 2017). It therefore provides a model of a SE skin commensal.

2.3.3.4 SC 27840 (SC27)

The reference strain ATCC 27840 is a more well-known SC strain initially studied by Kloos and Schleifer (1975).

2.3.4 Staphylococcal growth curves

Growth curves were used to assess how the main strains used in this research would proliferate over 24hrs. The growth curve experiments correspond to the standard RHE model inoculation of 10^2 and 10^6 CFU in 100µl of PBS, but was also repeated in LB (Lysogeny broth) as a high nutrient growth medium.

For each strain of SA83, SA29, SE12 and SC27 a 24 well plate was seeded with 10^3CFU/ml and 10^7CFU/ml in 1ml PBS or LB. After 3, 6, 9 and 24hrs of incubation (37˚C, 5% CO_2) a sample (20µl)

of each bacterial suspension was taken and used in a serial dilution for bacterial enumeration (described previously).

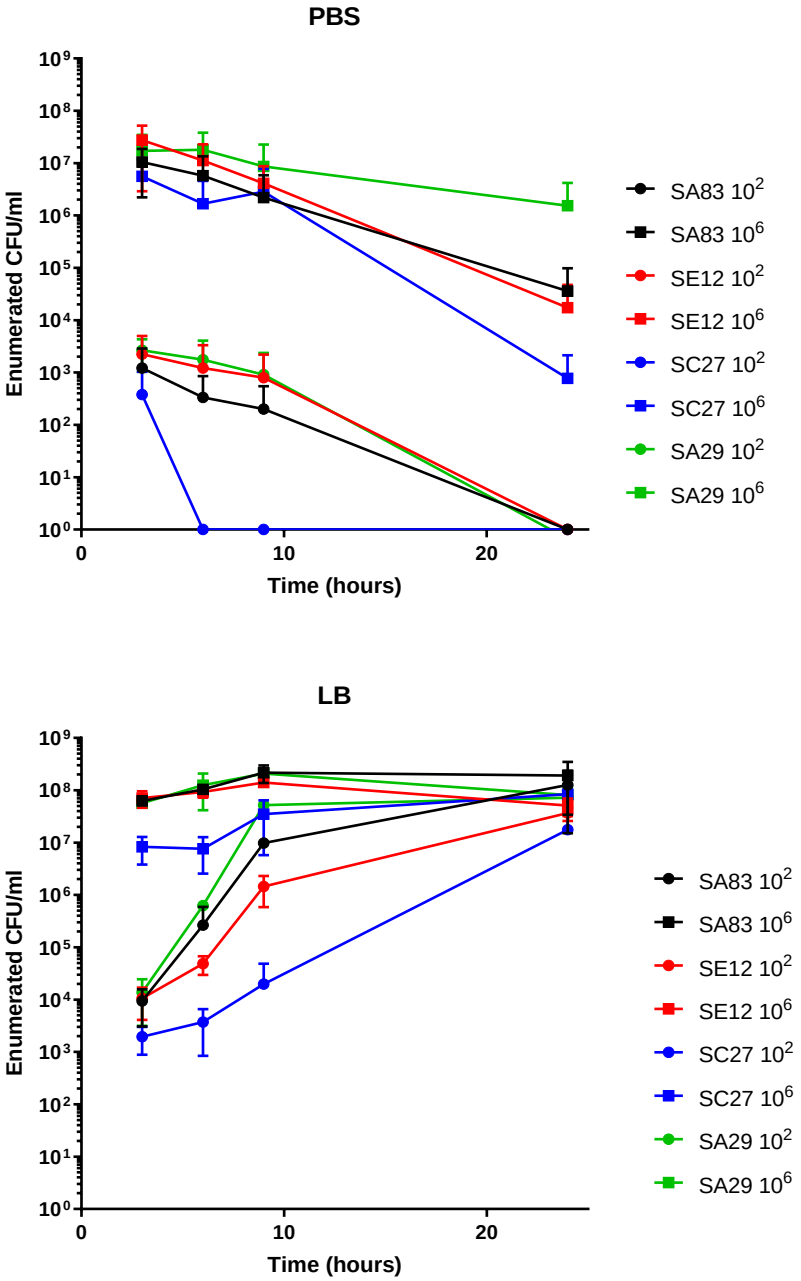

Figure 2:3: Staphylococcal growth curves
Growth of SA83 (8325-4), SE12 (12228), SC27 (27840) and SA29 (29213) in suspension of PBS or LB for 3, 6, 9 or 24hrs. Performed using initial concentrations of 10^3 and 10^7 CFU/ml in 1ml. Bacteria enumerated using serial dilutions on agar plates. Data expressed is CFU calculated by multiplication of serial dilution, shown as mean ± SD (n=3).

2.4 Explant inhibition Model

To examine the effect of human skin on microbial growth human skin explants were placed on agar plates spread with bacteria. After overnight incubation bacterial growth or inhibition was assessed.

Explant skin tissue was donated by volunteers undergoing plastic surgery and consented under ethical approval (LREC Number: 07/Q1704/46). The explant skin tissue was submerged in PBS and kept cold (4 ˚C) until use. A biopsy punch was used to cut 8mm biopsies from the explant tissue, which were kept in fresh cold PBS until use. Agar plates were spread with 10^6CFU, using 100µl of bacterial suspension at 10^7CFU/ml, produced as previously described. Biopsies were placed epidermis down onto the agar plate as shown in **Figure 2.4**, 3 biopsies per plate, 2 plates per bacterial strain and thus 6 replicates per donor.

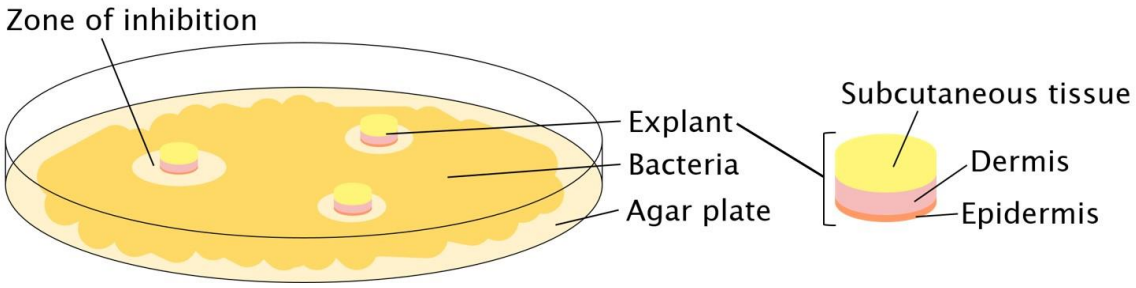

Figure 2:4: Diagram of the explant inhibition model .

Plates were incubated (37˚C, 5% CO_2) overnight, to allow bacterial growth. The area surrounding the biopsies devoid of bacterial growth were measured as zones of inhibition. Pictures taken alongside a ruler to enable quantification of the area using ImageJ.

The Inhibition zone was calculated by measuring the area of inhibition and subtracting the area displaced by the biopsy.

Antiseptic free explant was obtained by removal of a small sample from the middle of the explant tissue prior to its antiseptic wipe during surgery. The antiseptic free tissue was compared to normal explanted tissue of the same donor subsequently removed during the surgery. However due to the small size of the antiseptic free sample it was divided into 4 equal parts with a scalpel in lieu of a biopsy punch. Thus providing duplicate measurements for each donor.

2.5 Monolayer Infections

HaCaTs monolayers were seeded in DMEM+s into 24 well plates at $6x10^4$Cells/ml in 1ml. The monolayers were incubated (37˚C, 5% CO_2) for 4 days to become confluent. On day 2, monolayers were washed with PBS (1ml) and media changed to DMEM-i.

Primary keratinocytes (NHEKs) monolayers were seeded in KGM2 into 24 well plates at $8x10^4$Cells/ml (1ml). Confluency was achieved after 3 days of incubation (37˚C, 5% CO_2), with a PBS (1ml) wash and media change (KGM2-i) on day 2.

Suspensions of 10^2CFU/ml and 10^6CFU/ml were generated as previously described, however dilution of the master stock to the correct bacterial concentration was performed with either DMEM-i or KGM2-i depending on the monolayer.

Infections were performed with 1ml suspension added to triplicate monolayers for incubation periods of 3, 6, 9 and 24hrs. After which monolayers were washed 4 times with PBS (1ml) and lysed. Lysis was performed with 250µl saponin lysis buffer (1% saponin, 1% FBS in PBS and sterile filtered) that was added to monolayers for 15mins of incubation (37˚C, 5% CO_2), which lysed the HaCaTs without affecting the bacteria. Monolayers were further lysed with mechanical disaggregation via scraping with a pipette tip. The triplicate lysates were combined to produce an experimental average of the infection, which was quantified through bacterial enumeration as previously described.

2.6 RHE model colonisations

Colonisations were performed using RHE models grown for between 13 and 15 days. Models were only used if they demonstrated barrier formation through a change in surface texture and were absent of surface moisture.

2.6.1 RHE model wash

A wash procedure was performed 1 day prior to each colonisation experiment. The inserts containing models were washed internally and externally with KGM2-i. A fresh petri dish with KGM2-i was then used for the remaining day of ALI culture growth.

2.6.2 Colonisation experiments

The RHE models were placed into individual wells of a 24 well plate containing 300µl KGM2-i, which is suitable to maintain ALI culture in each well.

Bacterial suspensions of 10^3CFU/ml and 10^7CFU/ml in PBS were generated using the previously described methodology. 100µl of suspension was added to the surface of the models to colonise them with 10^2CFU and 10^6CFU and incubate (37˚C, 5% CO_2) depending on the colonisation.

2.6.2.1 Preliminary colonisations

RHE models were incubated for 3hrs before suspension removal, washed three times with PBS (400 µl) and incubated for 21hrs further. The RHE models were then washed with PBS three more times, retaining the PBS from the first of these of second washes for enumeration using agar plates as previously described. Models were trypsinated and lysed as described below. This colonisation protocol was only used for **Figure 3.6**.

2.6.2.2 Timecourse colonisations

RHE models were incubated for 3, 6, 9 and 24hrs. The RHE models were then washed 3 times with PBS (400µl), and then typsinated and lysed as described below.

2.6.3 Model trypsination and lysis

Inserts were transferred into a fresh 24 well plate containing 400µl trypsin (external), subsequently 200µl trypsin was added to the surface of the model (internal). After 15min of incubation (37˚C, 5% CO_2) the model was further disaggregated by thorough mixing of the internal trypsin, which was then added to an Eppendorf containing FBS (600µl). The external trypsin was used to rinse the remaining model from the insert and added to the Eppendorf, which was centrifuged (8000rpm, 5mins). The supernatant was removed and pellet was dislodged before 200µl saponin lysis buffer was added for eukaryotic cell lysis, therefore unaffecting the bacteria. The lysate was incubated (37˚C, 5% CO_2) for 15 min and quantified through enumeration as previously described.

2.6.4 Model RNA extraction

Following colonisation, models were washed 3 times and separated into separate wells of a 24 well plate. 400µl of RLT lysis buffer (QIAGEN) was added to the surface for a 1hr incubation at room temperature. The model lysate was mixed with a pipette and transferred to an Eppendorf (1.2ml). The lysate was homogenised with a 20G needle and syringe by repeated uptake, passing through the need 25 times.

The RNA was subsequently purified using the RNeasy plus mini kit (QIAGEN) as per the manufactures instructions using provided reagents:

The lysate was transferred to the gDNA Eliminator spin column within a 2ml collection tube. It was centrifuged (13,000rpm) for 30 seconds and the column was discarded. The flow-through was added to 350µl of 70% ethanol in a 1.5ml Eppendorf, which was subsequently mixed well by pipetting. The sample was transferred to the RNeasy spin column within a 2ml collection tube and centrifuged for 30 seconds (13,000rpm). After which, the flow-through was discarded.

700µl of RW1 Buffer was added to the RNeasy spin column, which was followed by centrifugation (13,000rpm) for 1 min and flow-through disposal.

500µl of RPE Buffer was added to the RNeasy spin column, which was followed by centrifugation (13,000rpm) for 1 min and flow-through disposal. This wash with RPE buffer was repeated, but with an extended centrifugation (13,000rpm) of 2 mins to dry the column.

The RNeasy spin column was transferred to a fresh 2ml collection tube and the old collection tube and flow-through was disposed of. The dry column was further centrifuged (13,000rpm) for 1 min to ensure no liquid was carried over.

The RNeasy spin column was transferred into a 1.5ml Eppendorf and 40µl RNase-free water was pipetted directly atop the column's membrane. The RNA was then eluted by centrifugation (13,000rpm) for 1 min.

The RNA was stored at -80˚C.

2.6.5 Undernatant Harvest

After colonisation and removal of the RHE model for further analysis the undernatant was harvested for future experiments. The undernatant was aliquoted into 2 Eppendorfs (600µl) of approximately 130µl each and stored at -80˚C.

Additionally, 15µl of undernatant was spread on an agar plate and incubated (37˚C, 5% CO_2) overnight to verify no bacterial presence.

2.6.6 IL-4 Colonisations

Bacterial Colonisations with IL-4 stimulated models were performed akin to the timecourse colonisation. However the IL-4 stimulated models were pretreated during the model wash. KGM2-i with 20ng/ml IL-4 was used for the wash and final day of model growth. Fresh KGM2-i with IL-4 was then used as undernatant in the colonisation experiment.

2.7 MoDC stimulation and flow cytometry

MoDC stimulations were performed to analyse the effect of bacterially colonised model secretions on DCs, which was analysed through changes in phenotype to be measured using flow cytometry.

MoDCs were harvested from culture, centrifuged (400 x g, 4˚C, 5min) and resuspended in RPMI. After counting with trypan blue, MoDCs were seeded into a 96 well U plate at $5x10^6$ Cells/ml in 10µl ($5x10^4$). Stimulation of MoDCs was performed with 90µl of undernatant from bacterial colonisations or media from HaCaT infections. The stimulation was performed overnight at 37˚C and 5% CO_2, the MoDC were then stained and analysed with flow cytometry.

Flow cytometry is widely used technique in immunology to analyse cell phenotype with the ability to measure multiple markers simultaneously. Cell incubation with fluorescently labelled antibodies targeting specific cell surface markers are enumerated in a single cell flow by laser induced fluorescence in a flow cytometer. Cell size and granularity are also captured by laser scatter. Computer analysis enables selection of specific cell populations based on measured aspects through gating, populations can then be examined for changes in specific cell markers.

2.7.1 MoDC surface staining

MoDCs were harvested from overnight stimulation and diluted with 1ml cold (4°C) PBS in individual FAC tubes (Falcon). The MoDCs were centrifuged (400 x g, 5min, 4°C), supernatant was removed and the cell pellet was dislodged.

Live/Dead staining: 100µl of cold PBS with Live/Dead stain (1µl/ml) was added to the MoDCs, which were then incubated on ice for 30 min in the dark. Subsequently, 1ml FACs buffer (PBS +1%BSA) was added, the MoDCs were then vortexed and centrifuged (400 x g, 5min, 4°C). The supernatant was then removed and the cells were either stained further or fixed.

HLA-DR and CD86 staining: MoDCs were resuspended in 50µl of antibody cocktail, which was comprised of PBS, 10µl/ml of HLA-DR and 50µl/ml of CD86. The MoDCs were then incubated on ice in the dark for 45 min. After which 1ml FACs buffer was added, the MoDCs were then vortexed and centrifuged (400 x g, 5min, 4°C). After supernatant removal MoDCs were fixed.

Cell fixation: MoDCs were resuspended in 100µl fixing buffer and vortexed. Following a 30 min incubation on ice in the dark the MoDCs were washed with 1ml permabilisation buffer, vortexed

and centrifuged (400 x g, 5min, 4°C). After supernatant removal the MoDCs were resuspended in 200µl of FAC buffer for storage and use in the flow cytometer.

Table 2.4: Antibodies used to stain MoDCs

Marker	Fluorophore	Host	Isotype	Supplier
Live/Dead	Violet1	N/A	N/A	Life technologies
HLA-DR	PerCP-Cy5.5	Mouse	IgG2a, κ	BD Pharmingen
CD86	FITC	Mouse	IgG1, κ	BD Pharmingen
HLA-ABC	FITC	Mouse	IgG1, κ	BD Pharmingen

2.7.2 Compensation controls

Compensation controls used unstimulated MoDCs stained with individual fluorophores that acted as postitive controls to compensation for overlapping fluorescence. The controls for each flurophore were:

Live/Dead: MoDCs were killed by incubation at 65°C for 20 min and then immediate transferred onto ice. Staining was performed as previously described with the Live/Dead stain.

PerCP-Cy5.5: MoDCs were stained with HLA-DR at 10µl/ml in 50µl PBS.

Fitc: MoDCs were stained with HLA-ABC at 100µl/ml in 50µl PBS.

2.7.3 Analysis

Flow cytometry was performed with the FACSaria™ (BD Biosciences) and analysed using FlowJo Version 10 (FlowJo, LLC; Oregon US).

2.8 Cell Viability Assay

The RealTime-Glo MT cell viability assay (Promega) was used to measure keratinocytes viability after 48hrs of growth in different media. The protocol was performed as per the manufacturer's instructions. The assay functions by the addition of the NanoLuc® Substrate to the cultures at 24hrs. Viable cells reduce the substrate over the following 24hrs of incubation. After which NanoLuc® Luciferase is added to generate a measurable luminescence, which is relative to the amount of the reduced substrate.

Primary keratinocytes were unbanked from long term storage in liquid nitrogen, rinsed with PBS and centrifuged (310 x g, 5 mins). After supernatant removal, the pellet was resuspended in PBS and counted with trypan blue. The cell suspension was divided into five and treated identically. Each suspension was centrifuged (310 x g, 5 mins) and after supernatant removal each pellet was resuspended at $6x10^4$ Cells/ml in various media. Suspensions were seeded (200µl) into a 96 well plate in triplicate, lower concentrations of the cells were generated through a two fold serial dilution within the plate. After 24hrs of incubation (37˚C, 5% CO_2) the media was replaced with 100µl fresh media, which includes the MT cell viability substrate and the Nanoluc® enzyme. The kit provided stocks of the substrate and enzyme at 1000X, which was diluted (1.5µl) in 1.5ml of each media used (See **Table 3.1**). After a further 24hr incubation (37˚C, 5% CO_2) the luminescence was measured using a Top count luminometer.

2.9 Proteome profiler

The Proteome Profiler™ Human XL Cytokine Array Kit (R&D systems) was used to semi-quantitatively measure RHE model undernatant media from the staphylococcal colonisations.

Colonisations of SA and SE at 10^6 CFU, and a control of PBS (100µl) were performed for 24hrs using triplicate models. The undernatants were collated for experimental averages for each treatment.

The protocol was performed as per the manufacturer's instructions:

2ml of buffer 6 (acting as a blocking buffer) and a membrane was added to each well of the 4 well multi-dish (provided with the kit). This was incubated for 1 hr on a rocking platform shaker. After the incubation, buffer 6 was aspirated and 750µl of undernatant (collated from 3 colonisations) diluted 1:2 with fresh buffer 6 was added to different wells of the 4 well multi-dish. This was then incubated overnight at 4°C on a rocking platform shaker. Each membrane was removed and washed with 20ml wash buffer in separate petri-dishes. The 4 well multi-dish was rinsed with deionised water and dried. Each membrane was then washed with wash buffer for 10 mins on a rocking platform shaker. This wash was repeated 2 more times.

120µl of detection antibody cocktail was added to 6ml of buffer 4/6, which was then added (1.5ml) to each well of the 4 well multi-dish. The membranes were removed from the wash dishes, allowing the wash buffer to drain off them and the edges were carefully dabbed dry on paper towel. The membranes where then added to the multi-dish, which was incubated for 1 hr on a rocking platform shaker. This was followed by 3 more membrane washes as previously described.

2ml of Streptavidin-HRP was added to each well of the multi-dish, after which the membranes were added after draining and dabbing. The multi-dish was incubated for 30 mins on a rocking platform shaker, which was followed by 3 more membrane washes. After draining and dabbing the membranes were placed on the bottom sheet of the plastic sheet protector. 1ml of chemi reagent mix was added evenly atop each membrane and the top sheet of the plastic sheet protector was lowered and smoothed out, removing any air bubbles. This was incubated for 1 min and then the excess chemi reagent mix was carefully squeezed out.

The membranes were placed in an autoradiography film cassette and X-ray film (CL-XPosure™) was exposed to them for 3 mins. This was repeated for 6 min and 9 min exposure times.

The X-ray film was developed and scanned for analysis in ImageJ. The film selected for analysis from the different exposure times, was the one showing largest variation between positive and negative controls.

ImageJ was used to measure the relative spot intensity (RSI), which was then averaged for the duplicate spots of each analyte on each membrane. The membrane's reference spots show the maximum intensity of each membrane. Results of 10% or below the maximum intensity were omitted as negligible signalling in comparison to the background.

2.10 Bead based analyte assay

The Luminex (R&D systems) platform was used to measure concentrations of specific analytes in the RHE model undernatant media.

RHE Model colonisations of 10^2 and 10^6 CFU were performed for 3 and 24hrs. Additional control colonisations of 100µl PBS and no PBS were performed in parallel. The undernatant media samples were harvest and stored (described previously) until use.

The assay used the Luminex 200IS platform (R&D systems) with two custom panels of the Luminex human magnetic assay kit (**Table 2.5**), which provided all necessary reagents.

Table 2.5: Custom Luminex panels of a 27-Plex and an 11-Plex

27-Plex	11-Plex
Angiogenin	Groα (CXCL1)
Angiopoietin-2	IL-1α
CCL1	sIL-4Rα
CCL2	IL-23
CCL5	IL-27
CCL11	Pentraxin-3
CCL13	Relaxin-2
CCL17	SHBG
CCL18	ST2
CCL27	TNFα
sCD14	VEGF
sCD30	
EMMPRIN	
ENA-78 (CXCL5)	
GM-CSF	
Groβ (CXCL2)	
IL-1β	
IL-1Ra	
IL-6	
IL-8	
IL-10	
IL-22	
IL-33	
Osteopontin	
PDGF-AA	
Resistin	
uPAR	

Standards were provided in each custom kit as a pre-prepared cocktail that was serially diluted (1:3) with assay diluent.

The 96 well plate (provided with the kit) was hydrated with wash buffer and removed with a vacuum manifold. The diluted bead solution was added to each well (25µl), along with wash buffer (200µl) for 30 seconds in the dark, by covering in foil. After which the wash buffer was removed with the vacuum manifold. This wash step was then repeated.

50µl of undernatant or standard was added to each well, along with 50µl of assay diluent. The plate was incubated in the dark at room temperature for 2hrs on an orbital shaker (500rpm) to keep the beads in suspension.

After 2hrs the liquid was removed by the vacuum manifold, which was followed by replicating the wash step twice with the wash buffer.

100µl of the diluted biotinylated detector antibody was added to each well and the plate was incubated in the dark at room temperature for 1hr on an orbital shaker (500rpm). After which, the liquid was removed and the wells were washed twice.

100µl of the diluted Streptavidin-RPE was added to each well and the plate was incubated in the dark at room temperature for 30mins on an orbital shaker (500rpm). Subsequently, the liquid was removed and the wells were washed three times.

The beads were then resuspended by adding 100µl wash buffer and then shaking on the orbital shaker (500rpm) for 2-3 minutes. The Luminex 200IS platform was then used to analyse the plate.

The software was set to read 100 events per bead region with a doublet discriminator gate set at 8000-16500. Data were collected as median relative fluorescence units (RFU) and the concentration of each cytokine was determined using the standard curves.

2.11 Transciptomics

The Aligent one-colour microarray system with the SurePrint G3 Human Gene Expression v3 8x60K Microarray Kit (Agilent) was used to examine transcriptomic changes of the RHE model, which were induced by staphylococcal colonisation.

RHE models were colonised with 10^6 CFU of SA83, SA29, SE12 and SC27 for 3 and 24hrs. After colonisation the RNA was extracted from the models as described previously.

2.11.1 Quantification and quality control

The Agilent 2100 Bioanalyser was used to assess the purity and concentration of the RNA extraction samples. This was performed using the RNA 6000 Nano kit (Agilent), according to the manufacturer's instructions with the provided reagents.

To prepare the gel-dye mix the RNA 6000 Nano gel matrix was added to the spin filter and was centrifuged (4000rpm) for 10 mins at room temperature. 65μl of the filtered gel-matrix was then transferred to an Eppendorf (600μl) and 1μl of Nano dye concentrate was added. This was followed by mixing by vortex, and centrifugation (14,000rpm) for 10 mins at room temperature.

This gel-dye mix (9μl) was loaded by pipette onto the RNA 6000 Nano chip, the syringe was then used to force the gel-dye throughout the chip. 9μl of gel-dye mix was then loaded into 2 further wells of the chip. The remaining wells were then loaded with 5μl RNA 6000 Nano marker, followed by 1μl of sample RNA or 1μl RNA ladder. For loading locations of the gel-dye and RNA ladder refer to the manufacturer's instructions.

The chip was vortexed for 1 min and analysed using the Agilent 2100 Bioanalyser. The sample purity was used to determine which samples would be used for transcriptomic analysis. The sample concentration was used to calculate how much RNA sample would be needed for generation of the cRNA.

2.11.2 Labelling and amplifying cRNA

This was performed using reagents provided with the SurePrint G3 Human Gene Expression v3 8x60K Microarray Kit (Agilent).

RNA samples were diluted based on quantification with the bioanalyser, resulting in 200ng of RNA in 8.3µl of nuclease free water. The T7 promoter primer (1.2µl) and one-colour spike mix (2µl of a diluted stock at 1:2500 in dilution buffer) (Agilent RNA spike-in kit) were added to each sample, which was then heated to 65˚C for 10 mins using a thermocycler. This denatured the sample and spike-in RNA, enabling the binding of the promoter primer. After heating, the samples were immediately cooled on ice for 5 mins.

During the sample heating and cooling the cDNA master mix was prepared. It contained first strand buffer (prewarmed to 80˚C for 3 mins) (4µl per sample), dithiothreitol (DTT) (2µl per sample), deoxynucleotide (dNTP) mix (1µl per sample), moloney murine leukemia virus (MMLV) reverse transcriptase (1µl per sample) and RNaseOut (0.5µl per sample).

8.5µl of cDNA master mix was added to each sample of primed RNA. Samples were subsequently incubated at 40˚C for 2 hrs, followed by 65˚C for 15 mins and then 5 mins on ice.

During the sample heating and cooling, the transcription master mix was prepared. It contained nuclease free water (13µl per sample), transcription buffer (20µl per sample), DTT (6µl per sample), NTP mix (8µl per sample), polyethylene glycol (PEG; pre-warmed to 40oC for 1 minute) (6.4µl per sample), RNaseOut (0.5µl per sample), Inorganic pyrophosphatase (0.6µl per sample), T7 RNA polymerase (0.8µl per sample) and Cyanine-3 CTP (2.4µl per sample).

60µl of transcription master mix was added to the cDNA samples, which were then incubated at 40˚C for 2 hrs.

The resultant labelled cRNA was purified.

2.11.3 Purification of cRNA

The cRNA was purified using the RNeasy mini kit (QIAGEN) using provided reagents.

20µl RNase-free water was added to each sample, for a total of 100µl. This was followed by adding 350µl RLT buffer, vortexing and adding 250µl ethanol. The sample was then mixed well and transferred to the RNeasy spin column within a 2ml collection tube. It was centrifuged (13,000rpm) for 30 seconds and the flow-through was discarded.

The RNeasy spin column was transferred to a fresh collection tube and 500µl of RPE Buffer was added. This was followed by centrifugation (13,000rpm) for 30 seconds and flow-through disposal. This wash with RPE buffer was repeated, with centrifugation (13,000rpm) of 30 seconds.

The RNeasy spin column was transferred to a fresh 2ml collection tube and the old collection tube and flow-through was disposed of. The dry column was further centrifuged (13,000rpm) for 1 min to ensure no liquid was carried over.

The RNeasy spin column was transferred into a 1.5ml Eppendorf and 40µl RNase-free water was pipetted directly atop the column's membrane. The RNA was then eluted by centrifugation (13,000rpm) for 1 min.

The purified cRNA could then be stored in the dark at -80˚C

2.11.4 Quantification of cRNA

The cRNA was quantified using a Nanodrop 1000 UV-visible spectrophotometer (Thermo Scientific) measuring at 260nm and 550 nm.

- 260nm measured RNA absorbance equating to cRNA concentration (ng/µl)
- 550nm measured cyanine-3 dye absorbance equating to Cyanine-3 dye concentration (pmol/µl)

The spectrophotometer was blanked with nuclease free water and 1µl of cRNA was used to measure each sample.
These measurements were used to calculate yield and specific activity to determine if the cRNA samples could be used in the hybridisation reactions.

- Yield (µg cRNA) = (ng/µl of cRNA) x 40µl (elution volume) / 1000
- Specific activity (pmol Cy3 per µg of cRNA) = (pmol/µl of Cy3) / (ng/µl of cRNA) x 1000

A yield below 1.65 µg and specific activity below 9.0 pmol Cy3 per µg of cRNA were considered insufficient.

2.11.5 Hybridisation preparation

Labelled cRNA samples (2µg) were bought to a volume of 19µl in nuclease free water. A master mix composed of blocking agent (5µl per sample) and fragmentation buffer (1µl per sample) was added to each sample, which was then incubated at 60˚C for 30 mins. This was immediately followed by cooling on ice for 1 min and then adding GEx hybridisation buffer HI-RPM to stop the

fragmentation process. The samples remained on ice until loading, which occurred as soon as possible.

2.11.6 Loading and hybridization

Hybridisation occurred in an Agilent SureHyb chamber loaded with the gasket slide into the chamber base. Sample (40µl) was slowly dispensed onto the slide within the gasket rings without letting it touch the gasket ring. The array slide was lowered down onto the gasket slide and the chamber was assembled with cover and side clamps.

The chamber was inserted into a rotisserie that continuously rotated for 17 hrs of incubation at 65˚C.

2.11.7 Microarray slide wash

After incubation the chamber was submerged in wash buffer 1 (Agilent) for disassembly and separation of the array slide from the gasket slide. Each array slide was then placed in a rack for further washing.

The rack was transferred into fresh wash buffer 1 for 1 min at room temperature, followed by wash buffer 2 (Agilent) for 1 min at 37˚C. This was followed by a wash of acetonitrile for 10 seconds exactly. The slides were allowed to dry and immediately covered with an Agilent Ozone protection cover. The arrays were scanned immediately afterwards.

2.11.8 Mircoarray scanning and analysis

The arrays were scanned with the Agilent microarray scanner.

Images of the arrays were visually examined for artefacts and the data was checked using the software's quality control readouts. The numerical expression data of each array was acquired by the feature extraction software and further analysis was performed in GeneSpring 14.9 (Agilent) and Ingenuity Pathway Analysis software (QIAGEN) as described in chapters 6 and 7.

2.12 Statistical Analysis

Statistical significance was determined by analysis in prism GraphPad version 7 (GraphPad Software Inc.; La Jolla, US) using a statistical test appropriate to the data.

Excluding transcriptomic data, which was statistically analysed using GeneSpring (Chapter 6) and IPA (Chapter 7).

Chapter 3: RHE model development and experiment optimisation

3.1 Introduction

Investigation of the epidermal response to colonisation depends upon utilisation of a reliable epidermal model. Previously, members of the lab have used the protocol and media supplies of CELLnTEC (Bern, Switzerland) to growth RHE models from NHEKs. However, CELLnTEC discontinued the specific keratinocyte differentiation media and their replacement media failed to generate a satisfactory differentiated model of the epidermis. Thus it was deemed necessary to develop an in house variation of the RHE model.

Development of an in house model was based upon the CELLnTEC protocol with optimisations made to the media. Various different lab groups use in house RHE model variations, but most use similar protocols in their generation. More specifically, they use the same time periods for monolayer growth, differentiation and ALI culture growth. The main differences in protocol are growth media, differentiation media, inserts and initial cell seeding number. The use of cell culture inserts suggested in the CELLnTEC protocol was continued, as they previously demonstrated successful model growth by other lab members. The inserts provide a porous base membrane, with an impervious surrounding wall for colonisation of the model, the insert is also on raised feet to enable a suspended model at ALI culture as displayed in **Figure 2.1**. The cell number for seeding was also maintained. However, variation in other protocols is based on the insert's surface area, aiming to provide enough cells to generate a fully confluent monolayer within 2 days. Therefore, development and optimisations focused on the growth media and differentiation media, as well as the growth conditions of ALI culture. This chapter also set out to optimise the inoculation protocol that would be implemented throughout this research. Additionally, it aimed to test the developed model in preliminary experiments to test functionality as model of the epidermis, thus enabling its continued use in future experiments.

Using MoDCs as a model of dendritic cells (DCs) is well established. In this research they are used to examine the soluble molecules signalling between the skin and DCs, which would relay the communication to the immune system. The effect of epidermal signalling to MoDCs will be studied in more detail in later chapters, however it is important to establish their use as a model in order to validate the study of this response.

3.2 Results

3.2.1 Choice of media for optimal keratinocyte proliferation

A critical aspect of growing RHE models from keratinocytes is maintaining high proliferation, not just for model growth but also in the routine keratinocyte tissue culture used for population expansion. To ensure optimal proliferation during tissue culture, five sources of keratinocyte growth media were compared (**Figure 3.1**) using the RealTime-Glo MT Cell viability assay (Promega). The assay was used to indirectly measure proliferation by measuring cell viability after 48hrs of growth.

KGM2 (PromoCell) was shown consistently to best support the proliferation of NHEKs at various different seeding densities. Furthermore, in comparison to the other evaluated media, it facilitated the greatest proliferation across the seeding densities tested. Thus, KGM2 was used for future keratinocyte culture.

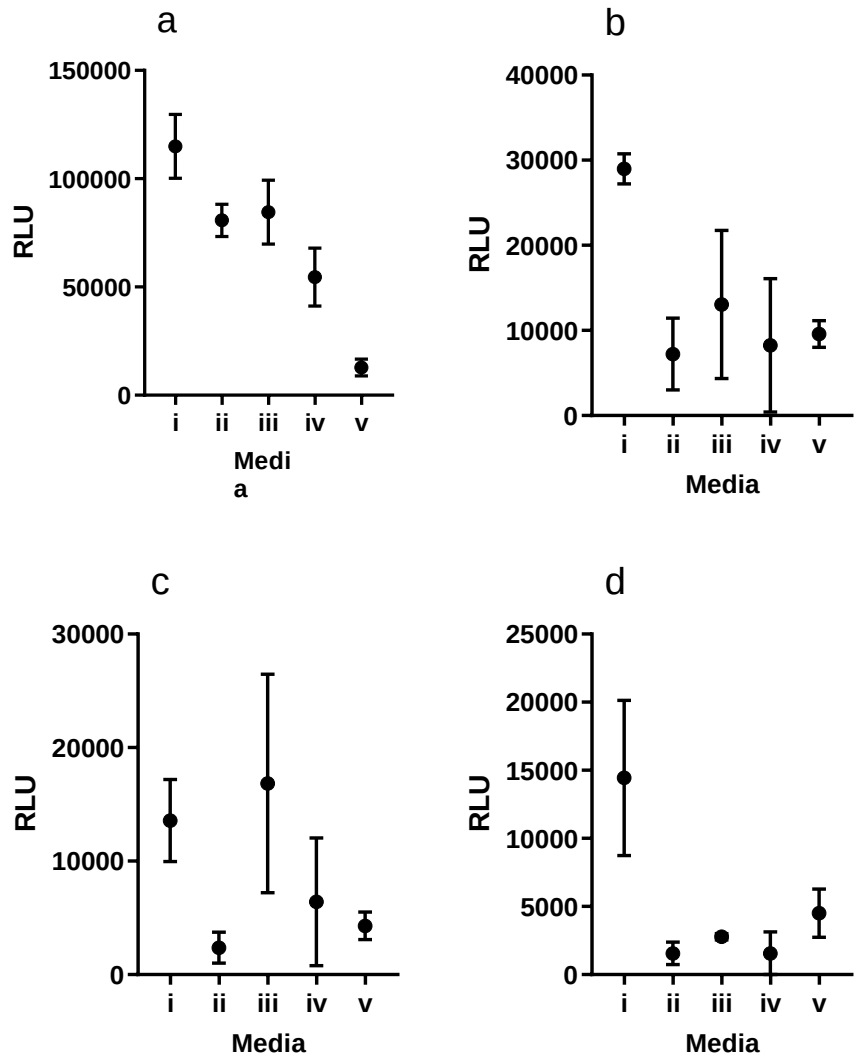

Figure 3:1: Keratinocyte proliferation in different media
NHEK growth in different media (i-v according to **Table 3.1**), seeded in a 96 well plate in 200µl at densities of $6x10^4$Cells/ml (**a**), $3x10^4$Cells/ml (**b**), $1.5x10^4$Cells/ml (**c**) and $7.5x10^3$Cells/ml (**d**). NHEKs incubated for 48hrs, with a feeding at 24hrs. RealTime-Glo MT Cell viability Assay used to measure proliferation. Data expressed is relative light units mean ± SD of triplicate wells (n=1).

Table 3.1: Media tested in Figure 3.1

Media i	KGM2 (PromoCell)
Media ii	CnT-57 (CELLnTEC)
Media iii	CnT-Prime (CELLnTEC)
Media iv	KGM Gold (Lonza)
Media v	DMEM+s (Gibco)

3.2.2 RHE model differentiation

Once a monolayer has formed differentiation of keratinocytes to form a 3D epidermal model is dependent upon calcium signalling (and other factors). Insufficiently differentiated models will lack a stratum corneum, conversely models suffering from limited proliferation may encompass a stratum corneum without adequate strata. Thus optimisation of the choice of differentiation media, which would support proliferation was undertaken.

As discussed previously, KGM2 was superior in comparison to other tested media for keratinocyte culture (**Figure 3.1**). Therefore, supplemented KGM2 variants were tested for initiation and maintenance of differentiation for 14 days of ALI culture growth. The variants of KGM2 tested were supplementations of Calcium (1.8mM), or both Calcium (1.8mM) and FBS (2%). CnT-Prime-3D was used as a control.

The media were compared by analysing the model differentiation as assessed by measurement of the resulting epidermal strata and stratum corneum thickness on H&E stained cross sections.

All three differentiation media variants induced good cellular proliferation, evident from the multiple strata above the insert membrane (**Figure 3.2**). Furthermore, both KGM2 variants (**Figure 3.2a** and **Figure 3.2b**) induced differentiation adequately to form a sufficient stratum corneum. The model differentiated with KGM2 + Calcium (1.8mM) displays a thicker stratum, whereas the model differentiated with KGM2 + Calcium (1.8mM) + FBS (2%) (KGM2-d) displays a thicker epidermis in regards to the other strata.

The control model cultured and seeded in KGM2 and differentiated in CnT-Prime-3D (**Figure 3.2c**) shows good cellular growth, but lacks the formation of a stratum corneum.

These results suggest that KGM2-d supported the optimal differentiation of the epidermal model, producing the most morphologically accurate representation of the epidermis. Therefore KGM2-d was selected for future experiments.

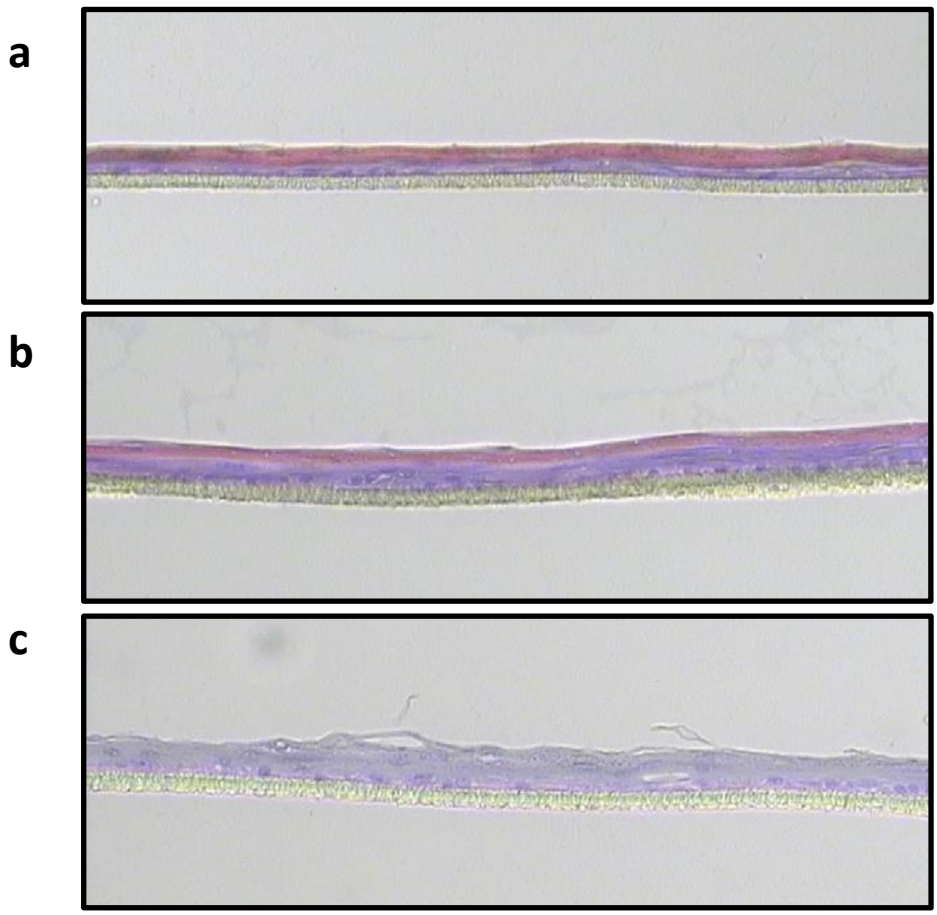

Figure 3:2: Keratinocyte differentiation with supplemented KGM2
Differentiation of NHEKs cultured and seeded in KGM2, then differentiated and grown in ALI culture for 14 days using KGM2 +1.8mM $CaCl_2$(**a**), KGM2 +1.8mM $CaCl_2$+2% FBS (**b**) and CnT-Prime-3D (**c**). Done according the standard model generation protocol. Pictures display H&E stains of microtomed sections of the fixed models.

3.2.3 Variation in environmental conditions of ALI culture growth.

Having established the preferred protocol for epidermal differentiation, it was important to examine the inter-model variability. Initial experiments suggested that on different occasions model outcomes could be variable. It seemed possible that variation in environmental factors during culture were likely to impact reproducibility of the model. These factors may derive from different exposures to the culture media, arising from changes in culture dish sizes. During ALI culture media volume is limited by membrane height, therefore alteration in culture dish size affects media supply. To assess the impact of using different culture dishes and therefore media volumes models were separate upon transfer to ALI culture into differently sized dishes. This included a 6 well plate (1.2ml), a 12 well plate (600µl) and a 24 well plate (300µl).

The various model set ups did modify morphology and growth as demonstrated in **Figure 3.3**. The 6 well plate (1.2ml) model (**Figure 3.3a**) showed a good amount of cellular growth and a well formed stratum corneum. Histology of the 12 well plate (0.6ml) model (**Figure 3.3b**) shows epidermal disorganisation, but this is a processing artefact. Detailed analysis actually suggests that this model showed a good growth and stratum corneum formation. However the growth is less than the 6 well plate model. Similarly, the 24 well plate (0.3ml) model (**Figure 3.3c**), showed inferior cell growth and stratum corneum formation to the 6 well plate model.

The results suggest altering the environmental growth conditions for each model modifies keratinocyte differentiation. Therefore, it is vital to maintain consistent growth conditions between batches to reduce variation.

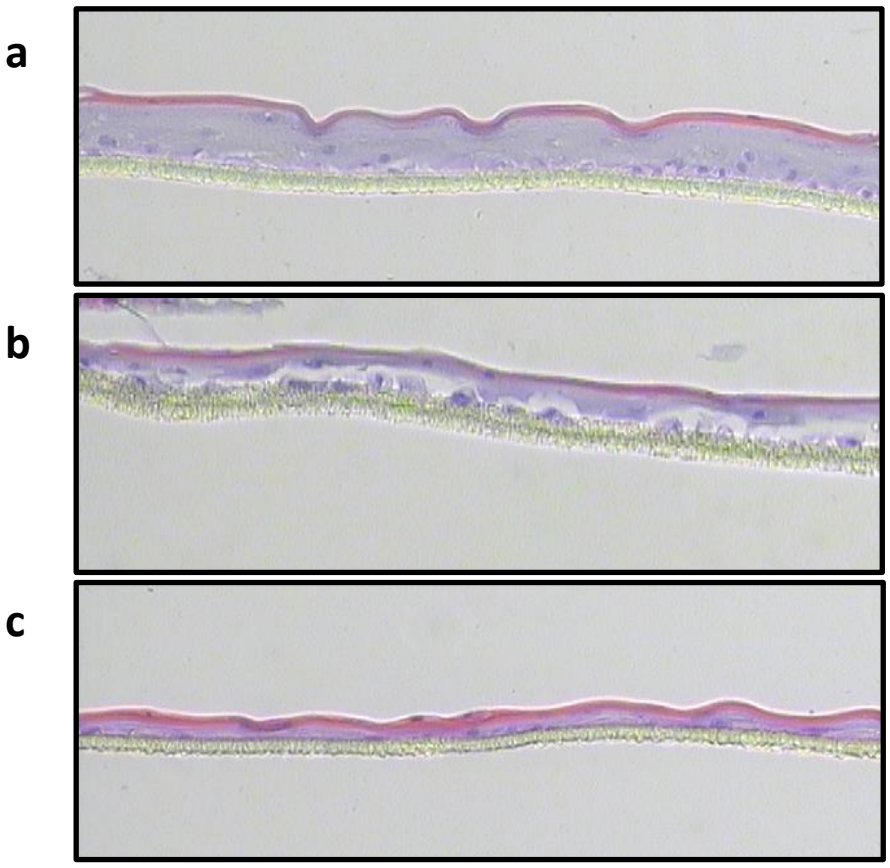

Figure 3:3: Keratinocyte differentiation in different culture conditions
Differentiation of NHEKs cultured and seeded in KGM2, differentiated with KGM2-d as per the normal model generation protocol in a 60mm petri dish. ALI culture performed in separate culture vessels of a 6 well plate (1.2ml) (**a**), a 12 well plate (600µl) (**b**) and a 24 well plate (300µl) (**c**) for 14 days. Image shows H&E stains of microtomed sections of the fixed models.

3.2.4 HaCaTs inability to differentiate

After demonstrating NHEKs ability to differentiate via supplementation and growth in ALI culture it was of interest to investigate whether HaCaT cells were capable of epidermal differentiation in the model system.

HaCaTs were cultured in DMEM+s for seeding and supplemented with 1.8mM Calcium for differentiation and ALI culture as describe above.

As expected, results showed that HaCaTs were unable to differentiate from a monolayer into a 3Depidermal model (**Figure 3.4**). No stratum corneum formation was identifed.

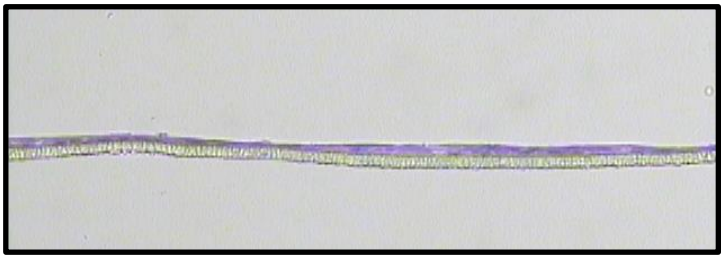

Figure 3:4: HaCaT differentiation with supplemented DMEM
HaCaTs cultured and seeded in DMEM+S corresponding to normal model generation protocol in a 6 well plate (1.2ml). Model differentiation performed with DMEM+s supplemented with additional 1.8mM $CaCl_2$. Image shows H&E stain of a microtomed section from the fixed model.

3.2.5 Optimisation of SA and SE inoculations

The primary objective of this research was to investigate the epidermal response to staphylococci. Therefore, it was necessary to assess the bacterial viability on the skin models to assess the optimal inoculation of different quantities of SA and SE.

Firstly the effect of exposure of different bacterial densities in solution on a keratinocyte monolayer (HaCaT) was tested (**Figure 3.5**). As expected, inoculation with lower densities of bacteria (10^2 – 10^6) showed inverse exponential (natural logarithm) expansion of SA, which reached a plateau density ~10^7 CFU at 24 hours. Whilst the proliferation of SE was similar to SA at the lower concentrations, the expansion appeared to be more linear. At the highest inoculum (10^8), a higher plateau was reached for both SA and SE. However, microscopy of the monolayer of the 10^8 SA inoculum showed significant keratinocyte disorganisation, suggesting loss of viability of the monolayer. Thus, 10^2 and 10^6 CFU inoculations were adopted as low and high colonising loads throughout this project.

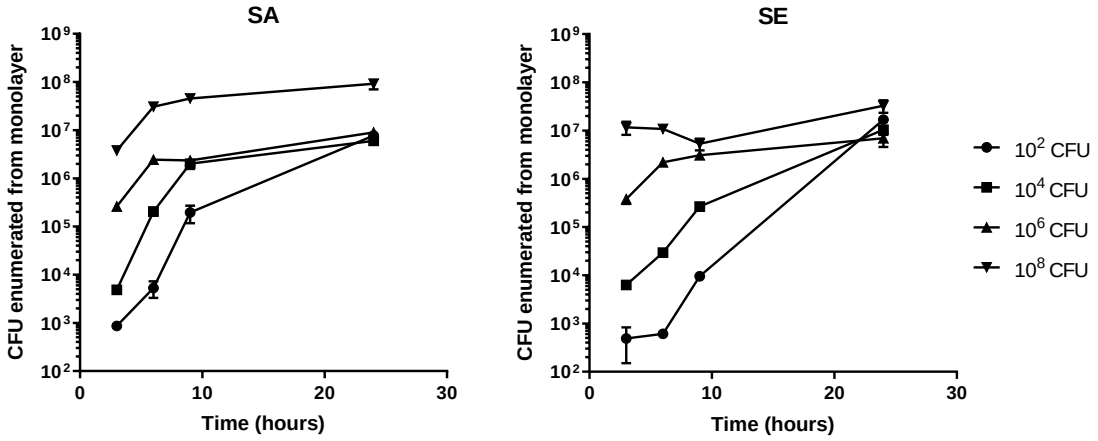

Figure 3:5: Staphylococcal proliferation and adherence to HaCaT monolayers
Staphylococcal growth on HaCaT monolayers after incubation of 3, 6, 9 or 24hrs. Inoculants of SA (8325-4) and SE (12228) added at concentrations of 10^2, 10^4, 10^6 and 10^8 CFU/ml in 1ml DMEM-i. Enumeration performed after wash procedure to remove non-adherent bacteria. Monolayers were lysed and bacteria enumerated using serial dilutions on agar plates. Data expressed is CFU calculated by multiplication of serial dilution, shown as mean ± SD (n=4).

3.2.6 Preliminary model colonisation with SA and SE

After demonstrating similar growth of SA and SE on HaCaTs, it was important to assess staphylococcal growth on the RHE model.

Bacterial suspensions of 10^2 and 10^6 CFU were used to colonise the model surface for 3hrs, which was previously shown to be enough time to adhere to a monolayer surface (**Figure 3.5**). At 3hrs, the model surface was washed removing non-adherent bacteria, leaving adherent bacteria. Colonisation was continued until 24hrs before quantification of non-adherent staphylococci (by wash analysis), and adherent/intracellular staphylococci (by trypsination and lysis).

SE was better able to proliferate at both 10^2 and 10^6 inoculants for both time points as compared to SA (**Figure 3.6**). Thus, implying a difference in the ability of SA to either proliferate or adhere to the model in comparison to SE.

However, this method of colonising the RHE model for 3 hours before and removing the non-adherent staphylococci, added extra handling of the inoculated models which increased the risk of model infection of the media. This problem resulted in the discontinuation of this methodology for model colonisation and refinement of model development and usage to minimise handling. Subsequent experimentation of staphylococcal colonisation was based on a protocol in which staphylococcal inoculation occurred and models were left with no interaction until the designated timepoint for analysis.

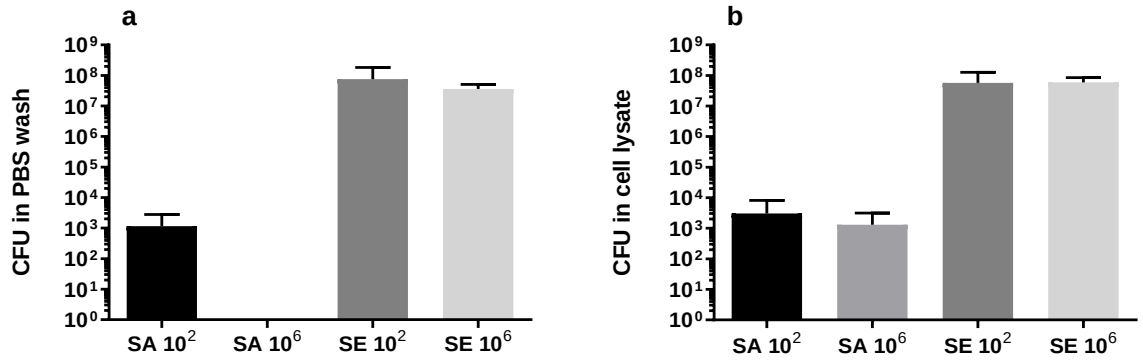

Figure 3:6: Adherent and non-adherent bacteria enumerated from RHE models. Quantification of staphylococci on RHE models after 24hrs, with removal at 3hrs. Inoculation of SA (8325-4) or SE (12228) as indicated in CFU in 100µl PBS. Non-adherent bacteria (**a**) and adherent / intracellular bacteria (**b**) were quantified with enumeration performed using serial dilution on agar plates. Data expressed as mean ± SD (n=2/3).

3.2.7 Optimisation of MoDC stimulations

To explore the cross-talk between epidermal exposure to pathogens and subsequent immune responses in the skin, monocyte derived dendritic cells (MoDCs) were employed to model tissue DCs (Lutz et al., 2017). Initially the outcome of bacterial contamination of the supernatant on MoDC viability was tested

Following SA or SE inoculation of the monolayer keratinocyte models, flow cytometric analysis of MoDCs viability was undertaken by analysis of forward scatter (FSC) side scatter (SSC) parameters and Live/Dead stain analysis (**Figure 3.7a-g**).

The results show SA infected supernatant induced cell death in MoDCs at both concentrations of inoculation. Contrastingly, SE infected supernatant induced negligible MoDC cell death at both concentrations of inoculation.

During the experiment centrifugation was used in attempt to remove bacteria from the supernatant, however it is unlikely to efficiently remove all the bacteria and thus induce MoDC cell death directly. Interestingly, SE did not have this effect on the MoDCs.

Consequently, the protocol was modified to centrifuged and filter (0.22µM) the supernatant prior to MoDC culture. Viability assessments demonstrate minimal loss of MoDC viability using this approach (**Figure 3.8**).

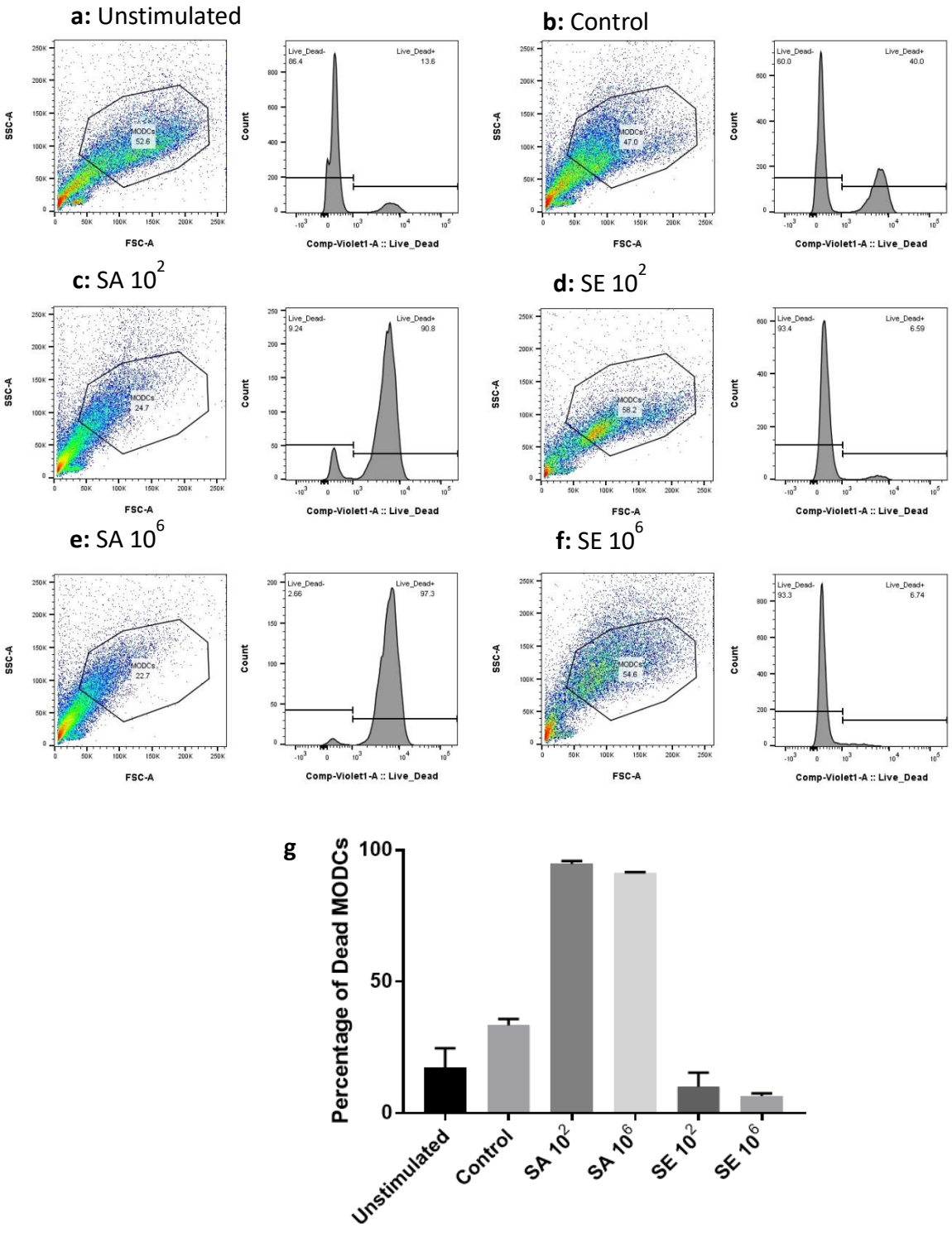

Figure 3:7: Supernatant from SA infected HaCaTs kills MoDCs

Flow cytometric analysis of MoDCs incubated with supernatant from HaCaT monolayers exposed to SA (8325-4) or SE (12228). Monolayers inoculated with staphylococci at 10^2 and 10^6 CFU/ml for 24hrs before harvesting supernatant for overnight MoDC stimulation. Graphs **a-f** (Unstimulated/control vs inoculation with SA or SE at 10^2 and 10^6 CFU) show gating strategy (left panels) and histogram analysis of Live/Dead stain (right panels) with summary data **g** showing percentage of the non-viable cells in the MoDC gate. Shown as mean ± SD (n=2).

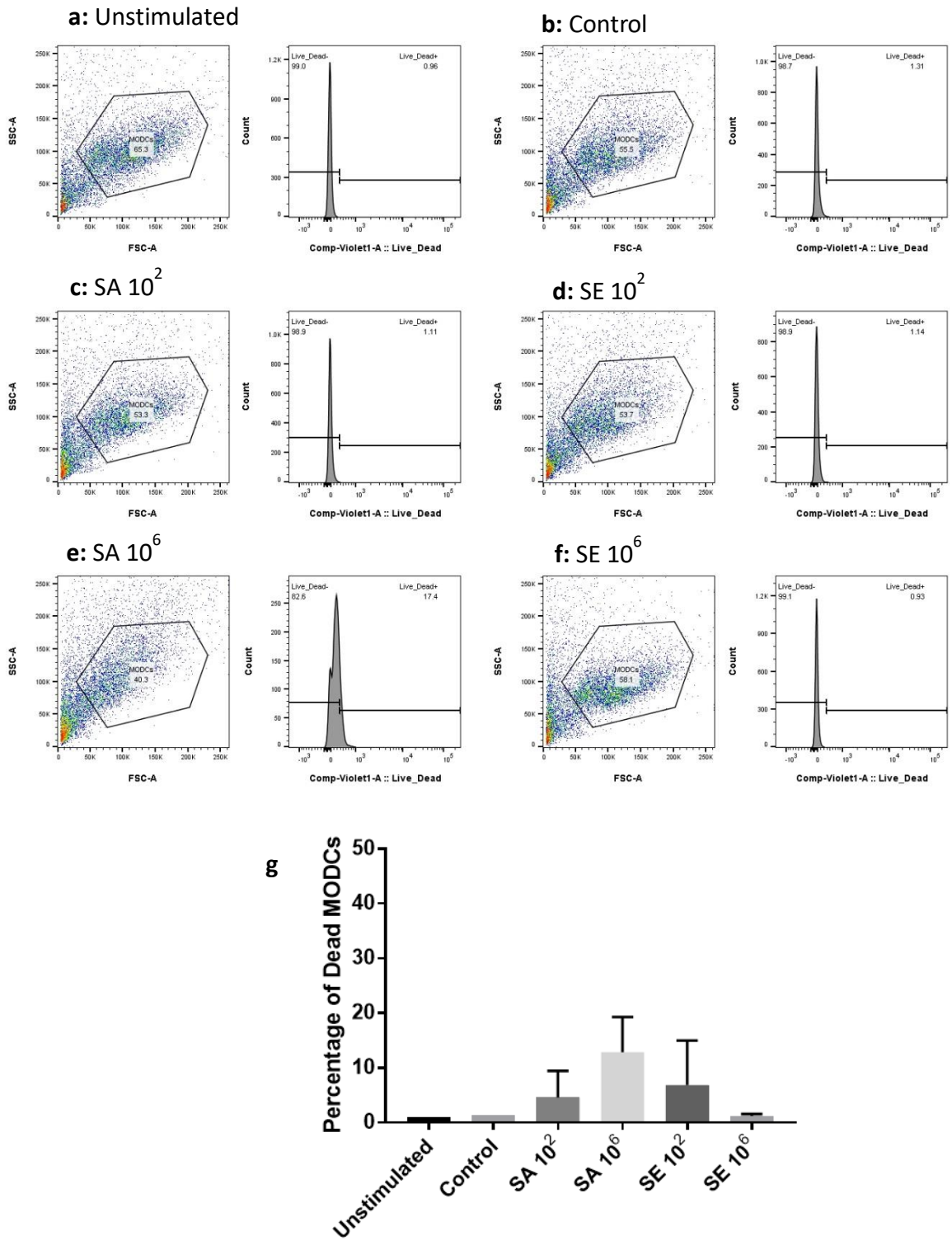

Figure 3:8: Filtering HaCaT Supernatant reduces SA induced MoDC death
Flow cytometric analysis of MoDCs incubated with supernatant from HaCaT monolayers exposed to SA (8325-4) or SE (12228). Monolayers inoculated with staphylococci at 10^2 and 10^6 CFU/ml for 24hrs before harvesting supernatant (debris spun down and filtered) for overnight MoDC stimulation. Graphs **a-f** (Unstimulated/control vs inoculation with SA or SE at 10^2 and 10^6 CFU) show gating strategy (left panels) and histogram analysis of Live/Dead stain (right panels) with summary data **g** showing percentage of the non-viable cells in the MoDC gate. Shown as mean ± SD (n=2).

3.2.8 Change in MoDC CD86 expression from stimulation with RHE undernatant

To enable investigation of the communication between the skin and immune system, MoDC cross-talk from colonised RHE models was assessed. After staphylococcal culture of RHE model the undernatant was harvested and employed in stimulation of MoDCs, which were subsequently stained for Live/Dead, HLA-DR and CD86.

Consequent to data described earlier, it was firstly confirmed that bacteria could not migrate from the outer surface of the RHE model to the undernatant by testing each undernatant sample for bacteria (not shown). Additionally, MoDCs stimulated with colonisation primed undernatant demonstrated no cell death (**Figure 3.9**), with either SA or SE.

MoDC were analysed for expression of CD86 (**Figure 3.10a-f**), a marker of MoDC activation.

Upregulation of CD86 expression was observed following PBS exposure of the RHE surface (control; **Fig 3.10b**). Whilst SA 10^2 showed little effect on MoDC activation, 10^6 CFU induced significant MoDC activation. Interestingly, SE induced significant MoDC activation at all CFU inoculums.

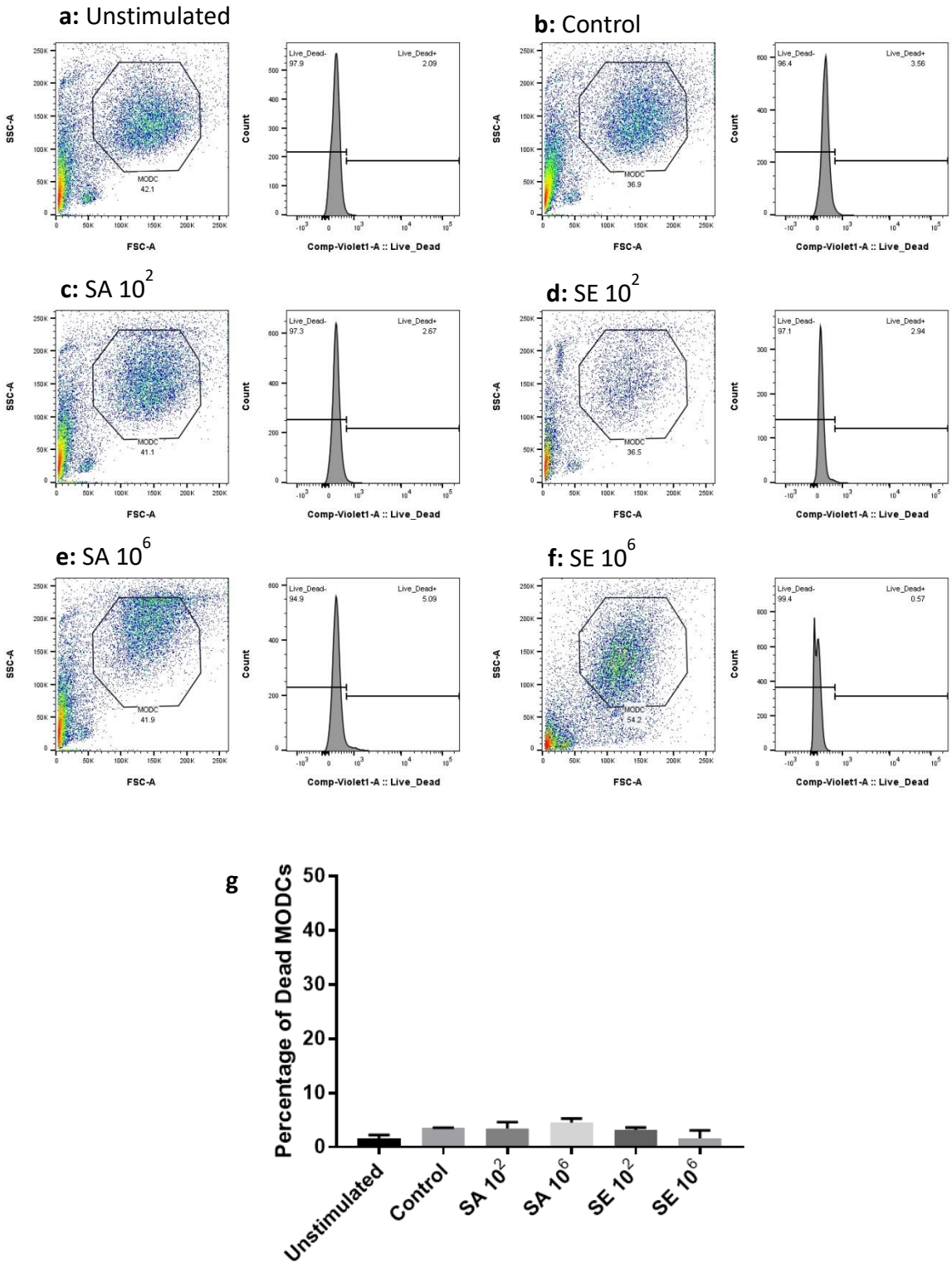

Figure 3:9: Undernatant from colonised RHE model does not induce MoDC death
Flow cytometric analysis of MoDCs incubated with undernatant from RHE models exposed to SA (8325-4) or SE (12228). Models inoculated with staphylococci at 10^2 and 10^6 CFU in 100µl PBS for 24hrs before harvesting undernatant for overnight MoDC stimulation. Graphs **a-f** (Unstimulated/control vs inoculation with SA or SE at 10^2 and 10^6 CFU) show gating strategy (left panels) and histogram analysis of Live/Dead stain (right panels) with summary data **g** showing percentage of the non-viable cells in the MoDC gate. Shown as mean ± SD (n=2).

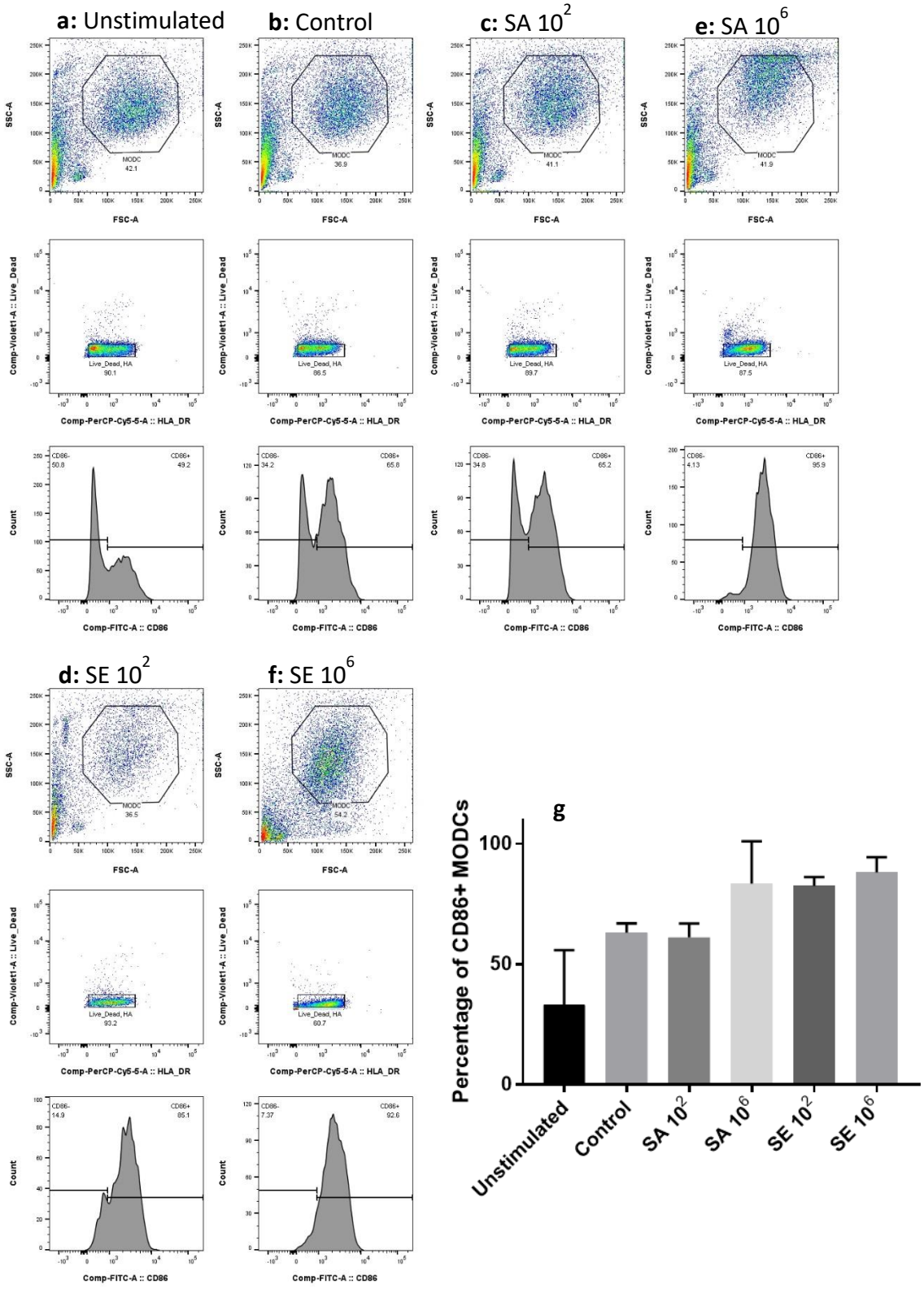

Figure 3:10: CD86 expression of MoDCs stimulated with RHE undernatant
Flow cytometric analysis of MoDCs incubated with undernatant from RHE models exposed to SA (8325-4) or SE (12228). Models inoculated with staphylococci at 10^2 and 10^6 CFU in 100µl PBS for 24hrs before harvesting supernatant for overnight MoDC stimulation. Graphs **a-f** show gating strategy of SSC vs FSC (top panels) and Live/Dead vs HLA-DR (middle panels); as well as histogram analysis of population of CD86+ cells (bottom panels). Summary data **g** shows percentage of the CD86+ population. Shown as mean ± SD (n=2).

3.3 Discussion

The main objective of this phase of work aimed to develop a functional RHE model that would be appropriate to address the research questions of this project. The aim was to study the epidermal response to staphylococcal colonisation and it was therefore necessary to validate and optimise model systems in which we knew the outcome of interaction of different pathogens at varying inoculations over time.

There are a wide variety of skin models used in dermatology research with varying levels of relevance to human skin, but as models increase in relevance to *in vivo*, their complexity increases correspondingly. Other groups have increased model complexity by seeding the primary keratinocytes onto fibroblasts to generate a full thickness model of the skin (Bell et al., 1981). Further, others have included other skin cells such as Langerhans cells, melanocytes or endothelial to increase the complexity and biological relevance (Mathes et al., 2014). Additionally, complex *in vitro* skin models based on this premise with further augmentation have been use to model skin diseases including psoriasis, vitiligo and melanoma (Bergers et al., 2016). There are disadvantages to all these improvements such as more demanding maintenance, increased costs and prolonged differentiation growth periods (Mathes et al., 2014). Furthermore, the resultant models can be less reproducible. The critical factor when deciding which model to use in an experiment is: will it answer the question being asked by the research? Therefore, it was decided that the basic epidermal model, as described here, is appropriate. This model generates the differentiation of keratinocytes and a stratum corneum. The model used also has the benefits of being relatively quick to grow and reproducible.

RHE model generation relies on highly proliferative and healthy keratinocytes, these properties are essential for both differentiation and morphology during experimental use (Carlson et al., 2008). Thus it was important to determine in which media keratinocytes would be most proliferative. Basal keratinocytes by their nature are highly proliferative. This aspect of their physiology is pivotal to their functional role, during both the constant replenishment necessary for desquamation as well as re-epithelialisation in wound healing (Pastar et al., 2014). Therefore high proliferation demonstrates the keratinocytes viability and normal functioning, as well as aiding in the supply of cells for future cultures and models. Indeed proliferation was used to assess primary keratinocyte viability for model generation and one model from each batch was stained to assess confluence. Failure to attain confluency within two or three days would result in their discontinuation, as the keratinocytes were thought to be inadequately viable to form and act as a representative model of the epidermis. Therefore, by minimising variables in epidermal

model set up it is possible to develop a reproducible RHE model with an appropriate stratum corneum to allow testing of skin exposures to SA and SE pathogens.

Different research groups use similar protocols for RHE model generation, but with various modifications. Formulations and volumes of growth media and differentiation media are examples of variation in protocol. This research tested five media sources to discover which would provide the highest proliferation. However models grown in KGM2 and differentiated in CnT-Prime-3D were unsuccessful for a model of the epidermis as no stratum corneum was formed. KGM2 showed full differentiation through stratum corneum formation. Therefore KGM2 was found to be superior and thus was used in model generation.

However differentiation of keratinocytes within a RHE model requires a careful balance, ensuring the highly proliferative nature of the keratinocytes is maintained throughout. If proliferation is hindered the model will form with insufficient cell layers and a thick stratum corneum, as displayed in **Figure 3.2a**. Keratinocytes on the path to terminal differentiation transition through different cell types that exist within the multiple strata of the epidermis. Without a high level of proliferation within the differentiating model the cells will mostly become corneocytes without seeding cells to differentiate into the lower strata. Alternatively inadequate differentiation would result in an insufficient barrier being formed on the surface of the model. If the correct balance of proliferation and differentiation is not maintained during ALI culture, the model will not grow to be an accurate representation of the skin.

Initially the differentiation media was supplemented with a large increase in calcium. *In vivo* a calcium increase is the principal stimulation causing differentiation. Extracellular calcium stimulates the intracellular release of calcium maintaining a constant supply that generates a concentration gradient across the epidermis with its peak concentration in the stratum granulosum. This change of calcium concentration from low to high is known as the “calcium switch” and is known to occur when the concentration changes from around 0.03mM to above 0.1mM (Bikle et al., 2012). Calcium is commonly used to differentiate keratinocytes in a variety of cellular models, including RHE models. On the other hand it has been shown that whilst high concentrations of calcium induce terminal differentiation it also reduces proliferation (Boyce and Ham, 1983).

The calcium supplemented model was grown in parallel with a model differentiated in increased calcium and a further supplementation of serum, in the form of FBS. The model grown with additional calcium (1.8mM) displayed increased levels of differentiation through a thicker stratum corneum formation. However, the model cultured with additional 1.8mM calcium and 2% FBS appeared to have an increase in proliferation as well as a sufficient level of differentiation. This

protocol induced an appropriately distinctive morphological difference between the stratum corneum and the basal layer, with a suitable stratum corneum. Despite our results showing an increase in growth due to the addition of FBS it has previously been shown that the addition of whole serum to keratinocyte cultures can inhibit growth and aid differentiation (Bertolero et al., 1986). However, Bertolero et al. also report that fractionated components of FBS show contrasting effects upon keratinocytes growth (Bertolero et al., 1986). Therefore the overall effect of FBS may be a result of the constitution of the specific serum.

One of the main considerations to maintaining consistency across different batches of models to ensure reproducibility was how the environmental growth conditions during ALI culture affected model growth and differentiation. Different sizes of culture dish were used to maintain growth at ALI culture, this changed multiple environmental growth conditions. Importantly it altered the volume of media used to achieve ALI culture, therefore altering the nutrient supply available. This factor was most likely the principal aspect causing the increase in growth for the larger culture dishes. However the large culture dishes provide a larger surface area from which evaporation can occur, altering the surrounding humidity within the culture dish. It has been shown that growth at a lower humidity enhances the barrier properties of the stratum corneum, it therefore has a direct effect on its formation (Sun et al., 2015). It is therefore important to maintain its consistency across various model batches, reducing possible variation. This brought about the necessity of a standardised protocol for growth conditions that could be utilized throughout this research. This standardised protocol required 12 models within a 10cm petri dish. This scaling of the model culture to include many models with a single dish generates a batch with minimized inter-batch variation due to shared growth conditions. Environmental growth conditions were further controlled for using a box in which culture dishes were placed within the incubator to maintain a stable environment outside the culture dish. This reduce environmental fluctuations caused by opening and closing the incubator and may reduce variation in the models.

HaCaTs have been used for a long time as a readily available substitute for primary keratinocytes. HaCaT differentiation was initially demonstrated (Boukamp et al., 1988) through production of differentiation protein markers, such as involucrin and filaggrin. Furthermore, improvements to the method of HaCaT differentiation, including the involvement of co-culture with fibroblasts, enabled the cornification and appropriate keratin changes (Schoop et al., 1999). However, these models had lipid deficiencies resulting in reduced lamellar bodies and lipids in comparison to normal keratinocytes. Contrastingly, experiments performed in this research showed no morphological evidence of differentiation or growth of a HaCat monolayer under appropriate conditions **(Figure 3.4)**. Therefore, further optimisation would be required for production of HaCaT based RHE models. Further limitations are noted regarding the disparity between primary

keratinocyte and HaCaT models in induction of immune responses. For example, comparison of primary keratinocytes and HaCaT models grown with Th2 cytokines shows differential expression of protein markers of differentiation (Seo et al., 2012). Additionally variation has been reported in TLR expression and IL-8 responses (Kollisch et al., 2005). However, most importantly HaCaTs show low expression of the NF-κB complex subunits (Qin et al., 1999), which results in a defective synthesis of proinflammatory cytokines. NF-κB is prominent transcription factor and notably involved in the TLR mediated response to PAMPs (Schwandner et al., 1999). Thus a HaCaT based RHE model is inadequate for use in this research.

Later experiments assessed the outcome of cross-talk between the epidermis and dendritic cells mediated by epidermal exposure to different pathogens. Testing MoDCs as model readouts for tissue based dendritic cells, the results showed that model optimisation was critical. SA was highly effective at inducing MoDC cell death (whereas SE did not) and SA leukocidin AB, a cytotoxin has been previously shown to directly kill MoDCs (Dumont et al., 2011). It was therefore necessary to optimise the model system to ensure that bacterial contamination of MoDC culture did not arise. After a carefully deduced protocol, the results demonstrated that in the absence of exposure to bacteria, SE was highly efficient at inducing epidermal signalling to MoDC driving activation. However, although similar changes were seen at higher inoculations with SA (10^6), no effect on MoDC activation was identified at lower density inoculums (10^2).

Taken together, these findings underscore the unique environmental niche of the surface of the skin. Whereas SA on the epidermal surface has a low propensity to proliferate and as such induces low level epidermal signalling, on damage to the epidermal barrier (as modelled in the monolayer experiments) SA shows superior proliferative capacity and causes keratinocyte and dendritic cell death. However, SE proliferates more readily on intact epidermis, but a lesser proliferative capacity and minimal induction of cell death in situations of loss of the epidermal barrier. Interestingly, in intact skin, SE was better able to induce keratinocyte signalling to immune cells resulting in cellular activation. Whilst the functional outcome of this observation is difficult to be certain of, it could be postulated that activation of the adaptive immune response via dendritic cells could be to mediate the establishment of tolerance to SE colonisation.

Chapter 4: Differential regulation of SA and SE by the epidermis

4.1 Introduction

SA and SE both colonise human epithelial surfaces and although they can act as opportunistic pathogens, their normal interaction with the skin is as a commensal. SE colonisation is an important part of the normal microbiome in non-inflamed skin, acting in defence and immune tolerance (Nguyen et al., 2017). However, SA is more complex, and whilst the presence of SA on the skin is strongly associated with inflammatory skin disease including AD (Geoghegan et al., 2018), it is also recognised that SA exists as a commensal in 30% of healthy individuals and has no association with inflamed skin (Eriksen et al., 1995, van Belkum et al., 2009). SE is essentially a 'non-pathogen' in skin and invasive infections are rare. However, SA can act in an aggressive manner and be associated with a wide variety of cutaneous infections including impetigo, folliculitis, furunculitis, cellulitis and deep tissue infections (Tong et al., 2015, Creech et al., 2015). Further evidence for the role of SA in mediating inflammatory skin disease derives from observations showing that skin lesion density correlates with AD disease severity (Gong et al., 2006). The precise mechanisms whereby SA and SE induce such disparate states in epidermal response is not well understood. In this thesis I aim to investigate the different ways the two organisms interact with skin, to elucidate differences in the skin response to these pathogens and key pathways in the skin sensing of staphylococci.

In order to study the epidermal response to the staphylococcal colonisation it is first important to examine the ability of the microbe to colonise the epidermis. Previous results (**Figure 3.6**) showed different viability thresholds of SA and SE on the RHE model. To explore this further, I set out to explore in detail, the kinetics of SA and SE colonisation of RHE models (as optimised in Chapter 3).

4.2 Results

4.2.1 Comparable infection rates of keratinocytes by SA and SE

Monolayer models of keratinocytes were used to study the differential growth of the two lab strains chosen for this project: SA83 (8325-4) and SE12 (12228). HaCaT monolayer skin models showed that both SA and SE were able to proliferate in a similar manner (**Figure 4.2**). Additionally, this was also observed with primary keratinocytes (NHEKs).

Similar growth curves of SA and SE were observed on NHEKs and HaCaTs. These data suggest that undifferentiated keratinocytes do not inhibit staphylococcal growth.

However, the lack of a stratum corneum formation in these model systems suggested that further investigation in an epidermal model would be of value to confirm these data.

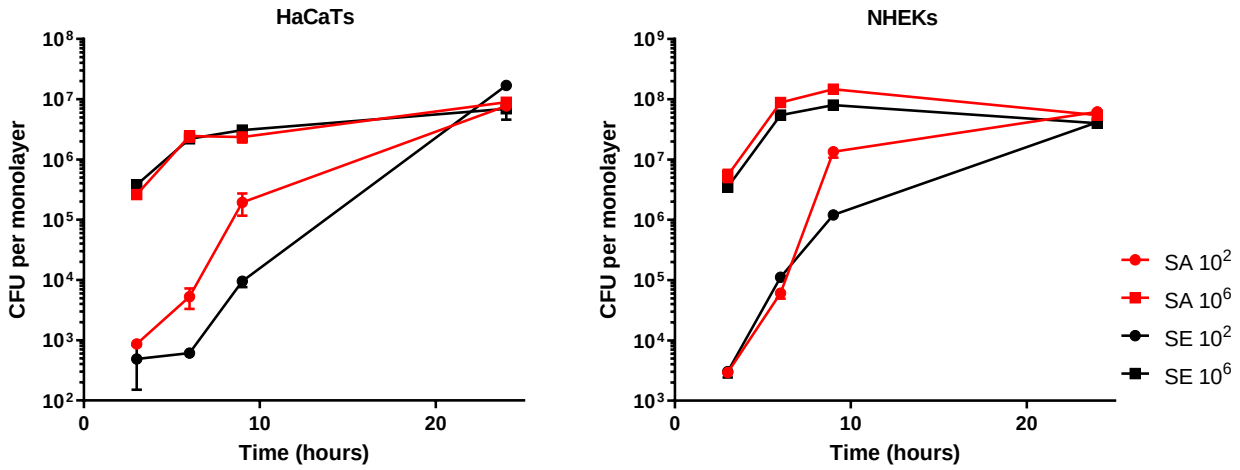

Figure 4:1: Adherent and infective bacteria enumerated from keratinocyte monolayers
Quantification of staphylococcal growth on HaCaT and NHEK monolayers inoculated with SA (8325-4) and SE (12228) at 10^2 and 10^6 CFU/ml. Data expressed is CFU and shown as mean ± SD (HaCaTs n=4; NHEKs n=1).

4.2.2 Differential regulation of SA and SE proliferation by the RHE model

The main role of the RHE model is to enable the characterisation of the epidermal response to staphylococcal colonisation. Therefore, it was important to understand how this colonisation occurred. Preliminary experiments demonstrated a differential ability of the two test strains SA83

and SE12 to colonise the surface of the RHE model. To further investigate this finding, the colonisation was studied over the course of 24 hours.

Inoculation of the RHE model with SE showed similar growth curves to that seen in the monolayer model as discussed above (**Figure 4.1**). As on the monolayer, on the RHE, SE growth increased exponentially to a plateau phase where density stabilisation was achieved (**Figure 4.2**). However, in contrast to the monolayer model, where similar growth curves for SE and SA were observed, inoculation with 10^6CFU SA showed direct inhibition by the epidermal model over 24 hours. This inhibition occurs after an initial phase of colonisation within 3 hours. Interestingly, inoculums at 10^2CFU of SA, showed no evidence of loss of viability, but also no significant proliferation was detected and bacterial density appeared to be stable over 24 hours.

The comparison between SA and SE growth clearly suggests a difference in staphylococcal regulation by the epidermal model which was specific to differentiated epidermis.

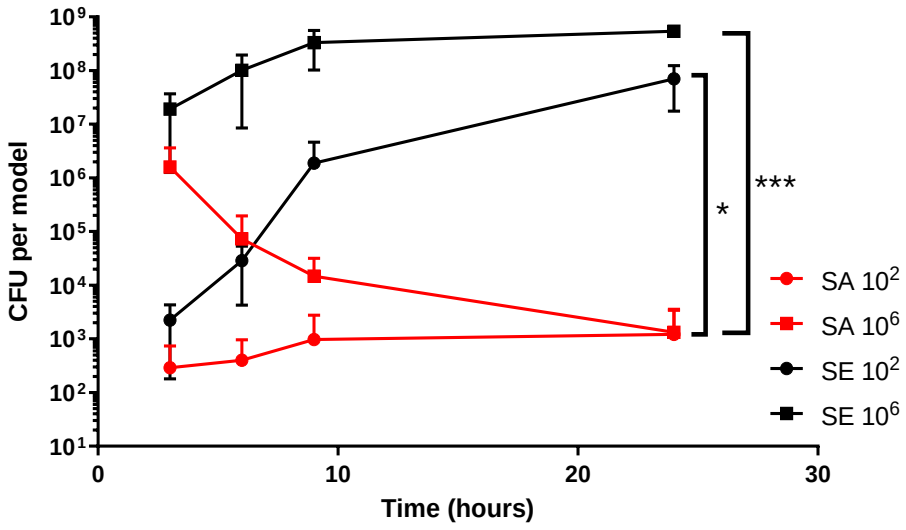

Figure 4:2: Colonisation of RHE models by SA and SE
Quantification of staphylococcal growth on RHE models inoculated with SA (red; 8325-4) and SE (black; 12228) at 10^2 and 10^6 CFU at time points as indicated. Data shown as mean ± SD. Unpaired T-tests were conducted between corresponding inoculation loads of different species at 24hrs; ***P<0.001, *P<0.05 (n=4).

4.2.3 Inhibition of SA growth by explant skin

To investigate the differential regulation of staphylococcal growth on the epidermis, another skin model was employed, the explant inhibition model. *Ex vivo* skin tissue from surgery was tested for functional influence on staphylococcal growth on agar plates.

The *ex vivo* skin tissue generated rings of inhibition within the field of bacteria grown on the agar plate (**Figure 4.3**). However, the inhibitory effect appears variable with large variation in the inhibited area. As expected SE12 was not inhibited. The quantification of the zones of inhibition (**Figure 4.4**) suggests differential regulation of staphylococcal growth by the skin, but also demonstrates large variation in the inhibitory effect by different donors of skin tissue.

The inhibition rings demonstrated by this model suggests that the inhibition is caused by a soluble factor, which diffuses around the explant skin during the incubation, stopping the proliferation of SA.

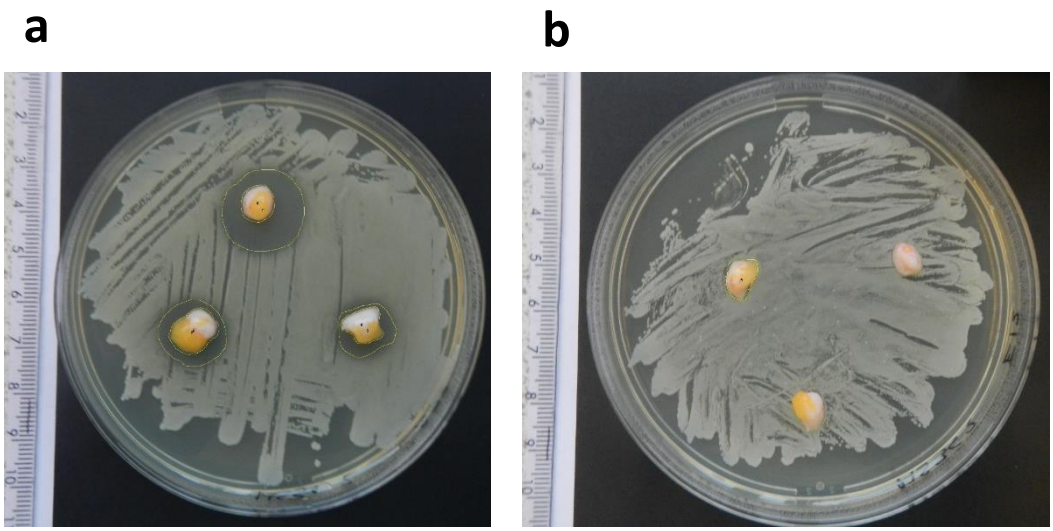

Figure 4:3: Inhibition of SA and SE growth induced by *ex vivo* skin
Representative pictures of the explant inhibition model. Agar plates were spread with SA (8325-4)(**a**) and SE (12228)(**b**) at 10^6 CFU in 100µl PBS. 8mm skin biopsies from explant tissue was washed and placed on agar plates for overnight incubation. Pictures analysed in ImageJ to measure the area displaced by the biopsy and the area of inhibition.

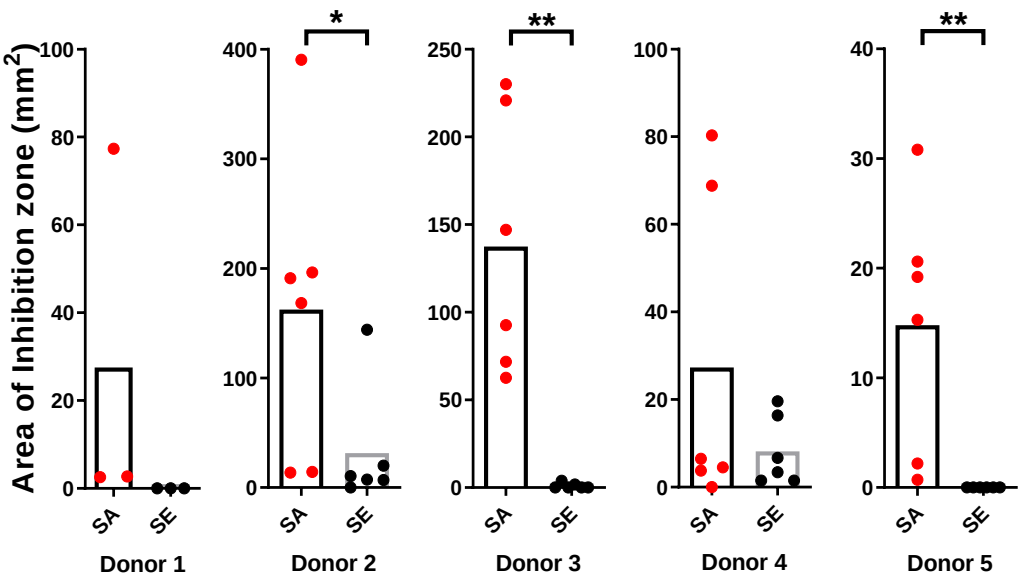

Figure 4:4: Area of inhibition of SA and SE growth induced by *ex vivo* skin
Calculated area of inhibition from the explant inhibition model for five donors. Agar plates spread with SA (8325-4) and SE (12228) at 10^6 CFU in 100µl PBS. 8mm skin biopsies from explant tissue washed and placed on agar plates for overnight incubation. Graphs display means and data points representing individual biopsies, calculated by inhibited area minus biopsy area. Mann-Whitney tests were conducted; *P<0.05, **P<0.01

4.2.4 Variation of inhibition by multiple strains of SA and SE

To expand this research into SA and SE the explant inhibition model was used to evaluate multiple staphylococcal strains, examining if the inhibitory effect is prevalent across the staphylococcal species or if it was strain specific.

Five strains were analysed: SA83 (8325-4), SA29 (29213), SA65 (6571), SE12 (12228) and SE35 (35984). A similar inhibitory effect to SA83 was demonstrated by SA65, however SA29 was not inhibited (**Figure 4.5**). As expected the additional SE strain of SE35 also showed no inhibition. This suggests a strain specific nature of the inhibition by the skin, which varies across multiple strains. Similarly to previous results there is large variation between the donors, supressing any statistical significance. However, inspecting results from individual donors, represented by different colours, suggests similar trends of inhibition for individual donors.

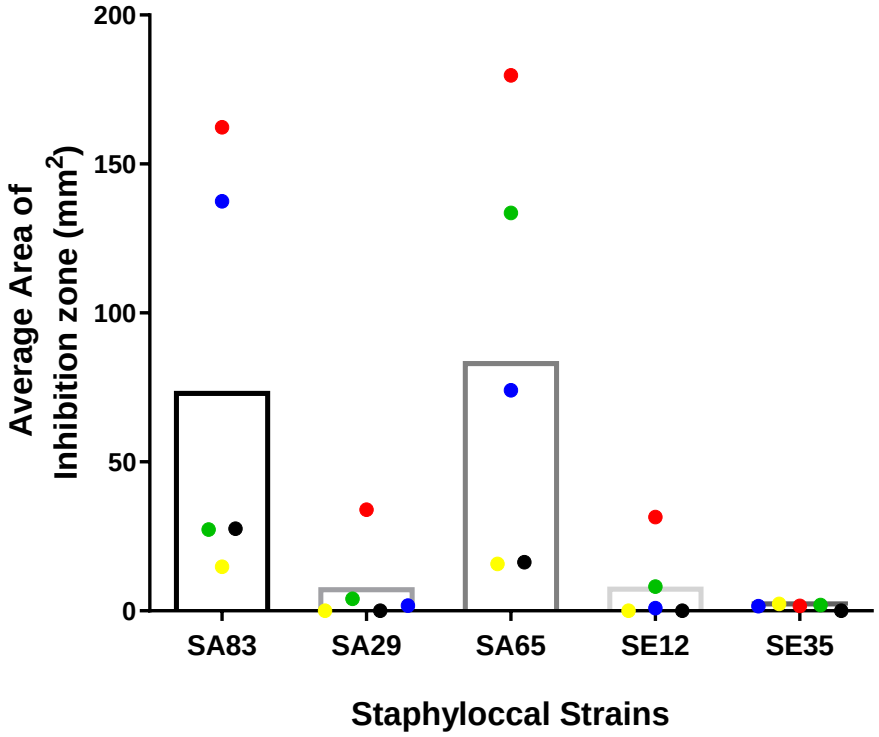

Figure 4:5: Area of inhibition of staphylococcal strains growth induced by *ex vivo* skin
Average area of inhibition from the explant inhibition model. Agar plates spread with SA83 (8325-4) SA29 (29213), SA65 (6571), SE12 (12228) and SE35 (35984) at 10^6 CFU in 100µl PBS. 8mm skin biopsies from explant tissue washed and placed on agar plates for overnight incubation. Graph displays the mean of each strain and data points for individual donors (n=5), represented by different colours. Data points represent mean area of inhibition of 6 skin biopsies.

4.2.5 Staphylococcal infection of skin explants

Due to concern about residual surgical antiseptic on the explant skin causing an inhibitory effect, the explant inhibition model was repeated with antiseptic free explant tissue. During surgery a small sample of explant was removed from the middle of the excised skin prior to the antiseptic wash. The antiseptic free tissue was used in conjunction with regular explant tissue, which was washed in antiseptic and then PBS.

Inhibition of SA83 was demonstrated by both explant with and without antiseptics (**Figure 4.6**). Despite the data lacking significance, SA growth was inhibited by the skin in a strain specific manner, which was also demonstrated in the RHE model.

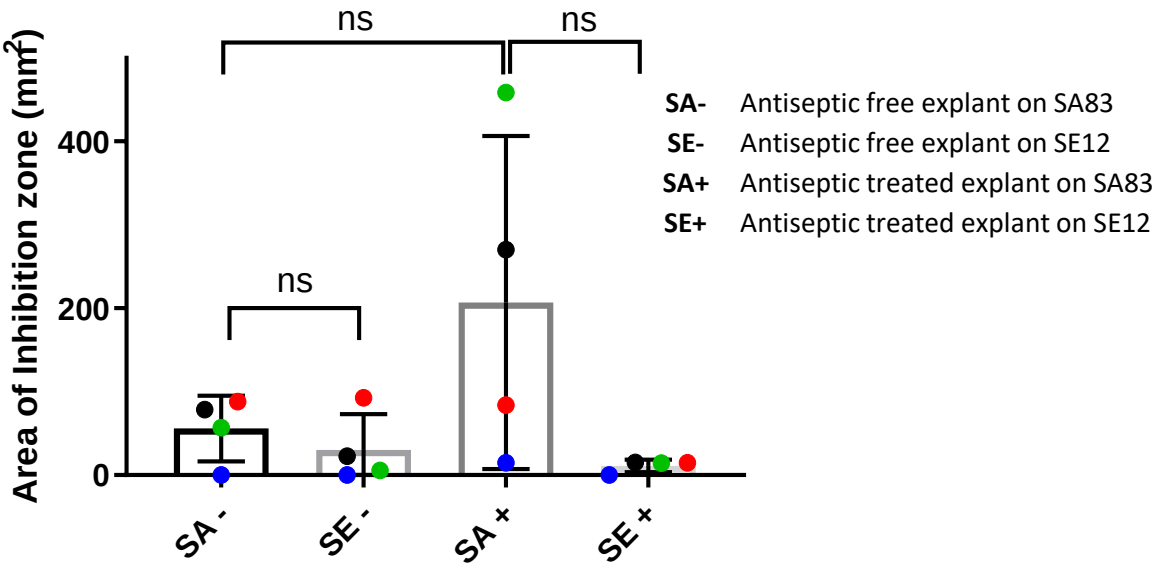

Figure 4:6: Area of inhibition of SA and SE growth induced by *ex vivo* skin with and without antiseptics
Average area of inhibition from the explant inhibition model. Agar plates spread with SA (8325-4) and SE (12228) at 10^6 CFU in 100µl PBS. 8mm skin biopsies from explant tissue treated with (+) antiseptic or without antiseptic (-), washed and placed on agar plates for overnight incubation. Graph displays the mean of each treatment and data points for individual donors (n=4), represented by different colours. Data points represent mean area of inhibition of 2 skin biopsies. Mann-Whitney tests were conducted.

4.2.6 Colonisation of the RHE model by SA 29213

Previous results using the RHE model and explant inhibition model have demonstrated inhibition of SA growth caused by the skin, however expanding the research to other strains has suggested this inhibition to be species specific. SA29 (29213) was shown not to be inhibited in the explant inhibition model, therefore the RHE model was used to further study SA29 and verify its non-inhibition and colonisation.

A 24hr timecourse of colonisation showed SA29 to colonise and proliferate on the RHE model (**Figure 4.7**). For both inoculant amounts the colonisation and proliferation parallels that of SE12, which was shown previously (**Figure 4.2**). This validates the strain selective manner of the skins inhibition of SA and also implies the association of the inhibition demonstrated by the two different models in which it was examined. Furthermore, it shows that different staphylococcal strains could induce different responses on the skin.

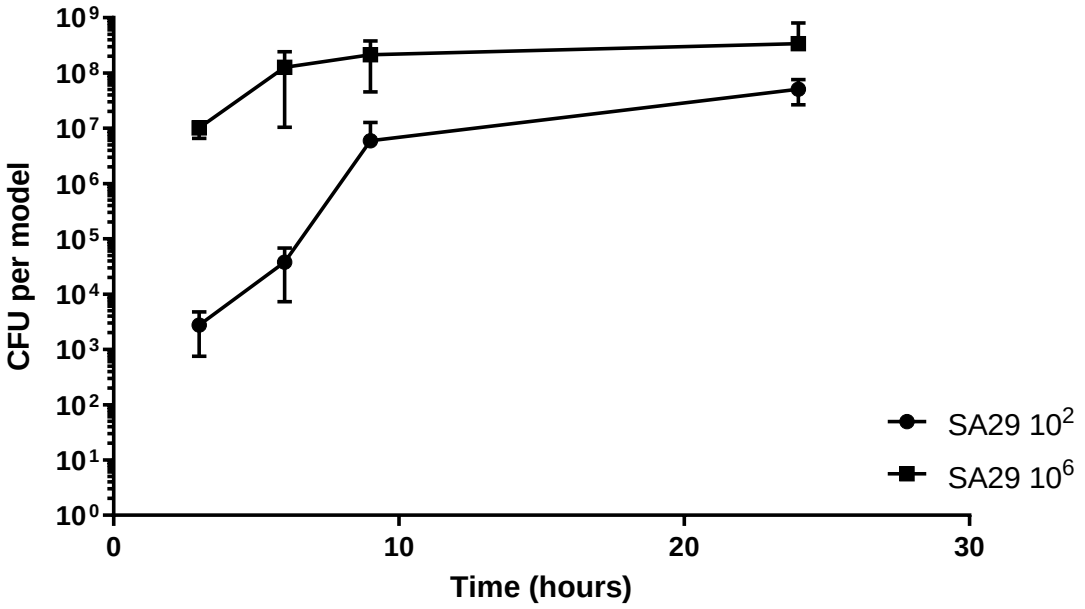

Figure 4:7: Colonisation of RHE models by SA 29213
Quantification of staphylococcal growth on RHE models inoculated with SA29 (29213) of 10^2 and 10^6 CFU in 100µl PBS. Data expressed is CFU as mean ± SD (n=3).

4.2.7 Colonisation of the RHE model by *S. capitis*

Staphylococcus capitis (SC) is another opportunistic pathogen that ordinarily acts as a commensal. However, its colonisation has been shown to be associated with inflammatory scalp disease (Wang et al., 2015).

SC colonisation of the RHE model is maintained at a steady state over the 24hr period measured. This differs from both SA and SE, which were either proliferative or inhibited by the model.

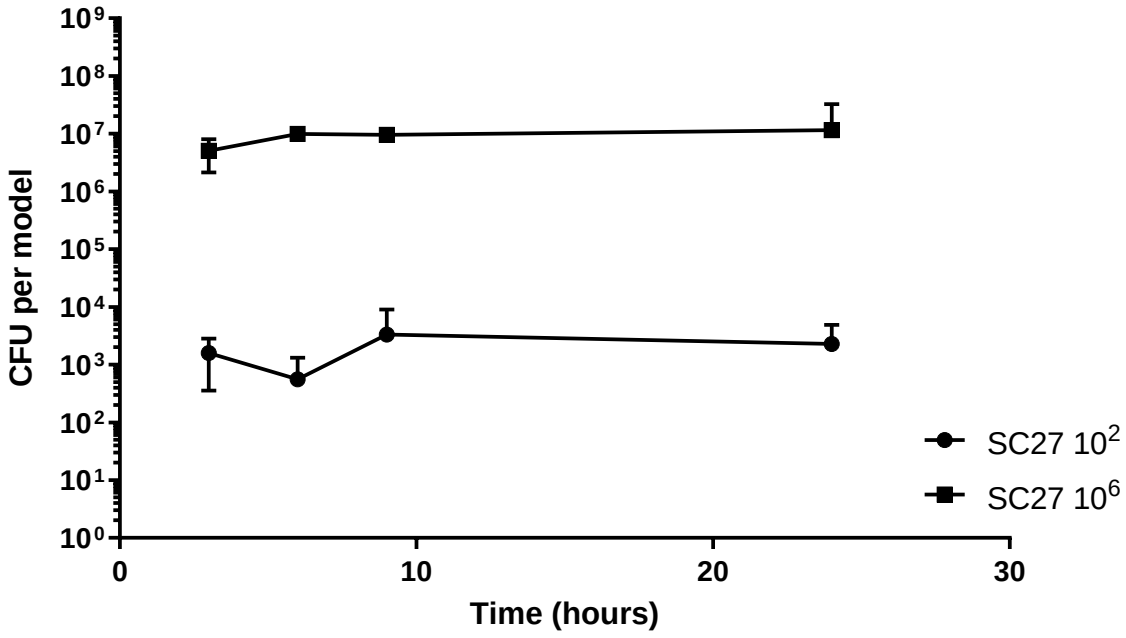

Figure 4:8: Colonisation of RHE models by SC 27840
Quantification of staphylococcal growth on RHE models inoculated with SC27 (27840) of 10^2 and 10^6 CFU in 100µl PBS. Data expressed is CFU and shown as mean ± SD (n=3).

4.2.8 IL-4 effects on SA colonisation

IL-4 is a pivotal cytokine in the Th2 immune response associated with AD and has been shown to modify epidermal AMP expression and alter the stratum corneum constitution. It has been proposed that IL-4 induces a favourable epidermal environment for SA colonisation (Nomura et al., 2003). Therefore IL-4 treated RHE models were used to assess if IL-4 could alter SA colonisation through the induction of an AD like phenotype.

Initial results from models colonised with 10^2 and 10^6 CFU of SA83 showed that treatment with IL-4 enabled effective SA83 colonisation at 3 and 24hrs for both inoculant amounts (**Figure 4.9**). However, these data were not reproducible (**Figure 4.10**).

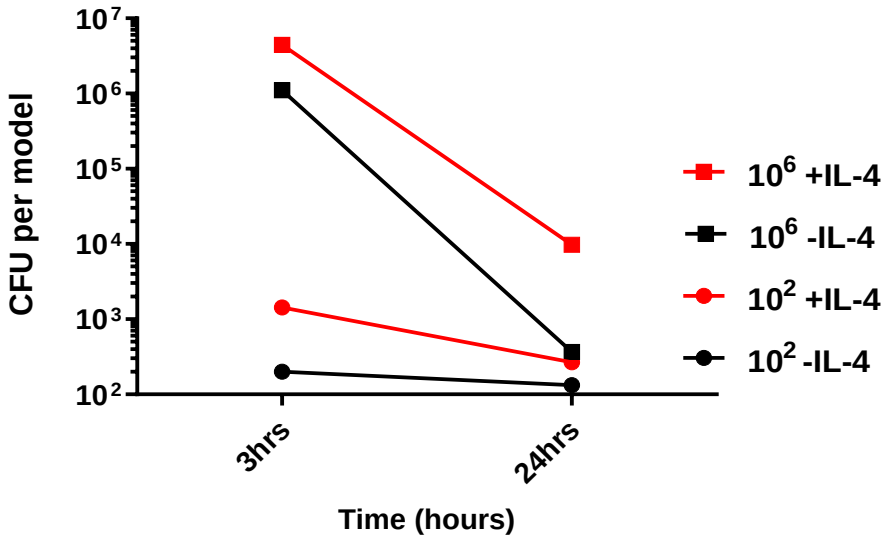

Figure 4:9: Effects of IL-4 stimulation on SA colonisation of RHE model
Quantification of staphylococcal growth on IL-4 treated (+IL-4) and non-treated (-IL-4) RHE models inoculated with SA (8325-4) of 10^2 and 10^6 CFU in 100µl PBS. Data expressed as CFU (n=1)

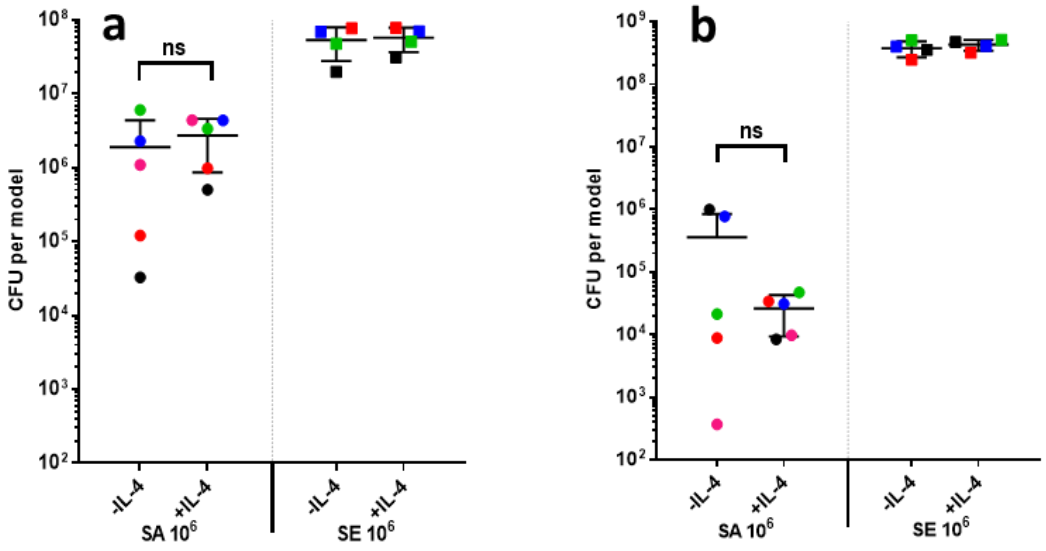

Figure 4:10: Effects of IL-4 stimulation on SA and SE colonisation of RHE model
Quantification of staphylococcal growth on IL-4 treated (+IL-4) and non-treated (-IL-4) RHE models inoculated with SA (8325-4) and SE (12228) of 10^6 CFU in 100µl PBS. Cultures incubated for 3hrs (**a**) or 24hrs (**b**) before washing. Data expressed is CFU. Mean ± SD (n=4/5). Unpaired T tests were conducted.

4.3 Discussion

Regulation of bacterial colonisation of the skin is of huge importance in health. Abnormal regulation resulting in dybiosis of the microbiome can induce a variety of microbially mediated inflammatory diseases of the skin.

Here, I aimed to investigate how different staphylococci colonise skin. SA and SE were found to have contrasting kinetics as skin colonisers. Whilst SE applied to the surface of an RHE model showed logarithmic proliferation and rapid plateau phase, SA proliferation was directly inhibited after an initial phase of colonisation. The differences observed between the RHE model and the monolayer data, suggest that the inhibition is associated with keratinocyte differentiation, which may include the presence of a stratum corneum.

Staphylococcal colonisation of human skin relies on niches of different environments to generate favourability of different strains. For example, SC is most commonly found on the scalp or forehead predominantly during puberty (Kloos and Schleifer, 1975, Becker et al., 2014), whereas SE colonises most epidermal surfaces but is more common in moist areas such as the axillae and nares (Kloos and Musselwhite, 1975).

To further validate the regulation of SA by epidermis, an explant model was employed. Here skin explants showed distinct inhibition of SA (but not SE) by the upturned skin sample. These data suggest that the inhibition is secondary to a soluble factor expressed by the skin. However, it also showed that there may be differences between biological strains in susceptibility to epidermal regulation. Indeed the species selective nature of the inhibition was observed with a non-inhibited SA strain. SA29 showed proliferative colonisation of the model, in a similar manner to that of SE. Alternatively, SC colonisation was neither proliferative nor inhibitory as observed with other staphylococcal strains.

The differential regulation between SA and SE as shown here suggests that there is species level specific interaction between keratinocytes and pathogens. Facilitation of proliferation of SE could be proposed as skin tolerance of the organism. However, it is possible that an evolutionary symbiosis exists whereby SE acts as an important modifier of epidermal function and therefore is integrated fully in the epidermal niche. It has also been postulated that inter strain competition of SE has led to strains favouring virulence factors of immune evasion, immune modulation and persistence over aggressive factors or toxins (Otto, 2010, Nguyen et al., 2017, Otto, 2009). However, the mixed response to SA suggests that epidermal regulation of SA is required in some settings, as suggested by the presence of invasive disease with this organism.

Indeed, recurrent SA colonisation seems to arise from SA presence in the anterior nares (Williams, 1963, Creech et al., 2009). The nose seems to act as a reservoir to repopulate other areas of the skin (Wertheim et al., 2005). Therefore, in addition to species level regulation, there may be differential tolerance or otherwise of different pathogens at different body sites (Iwase et al., 2010).

The inhibition demonstrated by the *ex vivo* skin and the RHE model is most likely produced by antimicrobial peptides (AMPs). Epidermal AMPs are both released in response to stimulation and also constitutively present on the epidermis. Human β-defensin 3 (hBD3) is the most probable candidate. It has been shown to be effective at killing SA (Kisich et al., 2007) and produced by keratinocytes in response to SA (Midorikawa et al., 2003). Furthermore, low hBD3 expression is associated to increased severity of SA infections (Zanger et al., 2010). However, other epidermal AMPs could be responsible as they have been shown to kill SA, this includes LL-37 (Noore et al., 2013) and RNase 7 (Simanski et al., 2010). Alternatively, combinations of AMPs have been shown to work synergistically with increased effect (Midorikawa et al., 2003).

Keratinocyte AMP expression is dependent on differentiation, with different AMPs secreted from different strata. For example, hBD3 is primarily localised to the lamellar bodies of the upper stratum spinosum and stratum granulosum, but is also present in the intracellular spaces of the stratum corneum (Sawamura et al., 2005). This arrangement provides a reservoir primed for stimulation or disruption, as well as low levels of constitutive expression. The constitutive expression is supplied by the natural release of the lamellar bodies into the intracellular space of the stratum corneum. Formation of lamellar bodies occurs during differentiation and they contain various molecules, including the lipids that make up the lipid lamellae (Feingold, 2012). hBD2 and LL-37 also show similar localisation (Oren et al., 2003, Braff et al., 2005). Alternatively, RNase 7 is spread throughout the epidermis, with increased intensity in the upper strata and further elevated levels in the stratum corneum (Koten et al., 2009).

The species selective nature of the inhibitory effect (SA83 was inhibited, whereas SA29 was not) suggests that either SA29 is resistant to AMP expression or does not induced the same response to generate the AMP expression. SA has a number of mechanisms generating resistance to AMPs, for example the dlt operon causes D-alanylation of teichoic acids on SA's surface. The D-alanylation reduces the negative charge of the bacterial surface, decreasing the chance of AMPs binding via their catonic charge (Peschel et al., 1999). Another example is the mprF gene, which is involved in the modification of membrane lipids with L-Lysine to reduce the negative change of the bacterial surface (Peschel et al., 2001). Such processes have been shown to be effective against hBD3 (Li et al., 2007a). Control of these AMP inhibition systems is regulated by the aps

AMP sensing system that determines variable resistance to AMPs (Li et al., 2007a). Furthermore, similar regulatory systems also exist in SE (Li et al., 2007b), but structural differences in the aps component apsS generate a differential induction of self-protective pathways (Li et al., 2007a). Therefore, these data suggest that variable control of AMP inhibition in SA and SE may explain the observed difference between SA83 and SA29.

The strain SA83 is renowned for its mutations, which include a deletion of the virulence factor PSMα3 and also result in low expression of the sarS regulator (Bæk et al., 2013). PSMs (Phenol-soluble modulins) are aggressive virulence factors involved in inflammatory stimulation, neutrophil lysis and biofilm formation (Peschel and Otto, 2013). PSMα3 has been shown to be particularly potent at inducing inflammation and neutrophil lysis (Wang et al., 2007), which suggests SA83 is a less virulent strain of SA.

It is possible that inhibition of SA reflects a healthy or normal response to colonisation, whereas the non-inhibition is more similar to dysbiotic colonisation. Dysbiosis can be characterised by a high abundance of colonisation of a single strain.

Recent meta-analysis of SA prevalence in AD exposed a carriage rate of 70% on lesional skin, as compared to 39% for non-lesional skin; this study further indicated an increase prevalence associated to increased AD severity (Totte et al., 2016). Therefore, there seems to be a disease specific effect which modifies skin homeostasis to facilitate SA colonisation above that in non-lesional skin. It has been well established that AD is characterised by a Th2 immune profile in the skin (Brunner et al., 2017) which is thought to induce favourable conditions for SA colonisation. Such effects in AD include reducing AMP expression, specifically hBD3 (Nomura et al., 2003) and LL-37 (Howell et al., 2006b), as well as disrupting the integrity of the epidermal barrier. IL-4 and IL-13 where shown to reduce expression of filaggrin (Howell et al., 2009), involucrin and loricrin therby damaging the epidermal barrier (Kim et al., 2008). IL-4 has also been shown to reduced ceramide synthesis in the stratum corneum (Hatano et al., 2005, Sawada et al., 2012). These effects concurrently reduce the effectiveness of SA clearance, whist generating a niche more suited for SA colonisation.

RHE models were incubated in IL-4 to reflect a Th2 skewed epidermis as might be expected in AD, before incubating with SA or SE. No significant difference between SA and SE colonisation was noted. The lack of effect may have been due to a technical limitation of the protocol adopted. It seems likely that *in vivo* disease there is an ongoing synthesis of Th2 cytokines in the skin, however, in the present study we only exposed the RHE models prior to inoculation. Continued IL-4 treatments throughout differentiation may generate RHE models with barrier disruption that would enable increased colonisation.

SC is a coagulase negative staphylococci and a common skin commensal, thus it is often compared to SE. However is was been shown to have increased colonisation of the scalp during bouts of dandruff (Wang et al., 2015). Therefore, SC colonisation induced epidermal inflammation may be of interest to study in comparison to both SA and SE. Whilst colonisation was shown to be moderately stable over the 24 hour time period, there was little evidence of direct modification of the bacteria in our model . Such a stable colonisation may suggest SC colonisation is not as effective on the RHE model, either through regulation by the model, or lack of adhesion molecules in glabrous models.

Each species evaluated here demonstrated differences in the kinetics of colonisation of the epidermal model. This is likely to reflect variations in the epidermal sensing of the pathogen. Therefore, further work was directed at exploring differences in the epidermal response induced by differential sensing of these pathogen

Chapter 5: Epidermal response to staphylococcal colonisation

5.1 Introduction

The skin immune system is vital in defending against pathogens. The epidermis is directly exposed to bacteria which comprise part of the skin microbiome. Therefore, the interaction between epidermis and skin commensals is a complex interrelationship which at the same time tolerates pathogen exposure and also prevents pathogen invasion. Understanding how the skin immune system responds to modulate immune defence or tolerance of colonisation is a critical part of understanding skin immunity. Within the epidermis, classical immune cells such as Langerhans cells and resident memory T cells are well known to play an important role in skin immunity. However, keratinocytes also perform a crucial role as part of the cutaneous immune system by working in coordination with surrounding immune cells. Keratinocytes are able to sense danger through expression of pattern recognition receptors as overviewed in Chapter 1, and can communicate with immune cells through the release many different mediators, including cytokines and chemokines that generate the appropriate response as dictated by the stimulation. The release of mediators by keratinocytes can initiate, regulate or resolve inflammation. Keratinocytes therefore act as sentinels of the skin, alerting the immune system as well as other cells in its surrounding (Nestle et al., 2009, Pasparakis et al., 2014, Klicznik et al., 2018).. Therefore, this chapter aims to characterise the synthesis of soluble mediators as a response by keratinocytes to various commensal exposures in the context of the epidermis.

Whilst measuring the induction of individual cytokines or chemokines following pathogen exposure can expose a specific effect of a stimulation, there is known redundancy in human cytokine signalling systems. Therefore, it is preferable to study a large number of inflammatory mediators so the whole 'signature' of keratinocytes induced by bacteria can be measured. The comparison of the profiles generated for different microbes may divulge the key mediators responsible for mediating the pathogen-specific effects on the cutaneous immune system.

Chapter 3 showed that staphylococcal colonisation induced different epidermal responses dependent upon whether the exposure was SA or SE and showed that these effects resulted in pathogen-specific signalling to dendritic cells, in a system which was dependent upon soluble factor signalling rather than cell contact. Therefore, characterisation of the soluble factors produced and released by the epidermal model in response to staphylococcal colonisation is

central to understanding how the skin regulates the adaptive immune system. This chapter aims to investigate the epidermal response that modifies dendritic cell activation, studying how this changes overtime as well as the key mediators.

5.2 Results

5.2.1 Bacterial colonisation of the RHE model induces dendritic cell maturation

Within the skin DCs act as immune sentinels to the adaptive immune system. To model this system, MoDCs were utilised as a read out for the communication from the epidermis relayed to the immune system by skin exposure to pathogens. As described earlier, cultured RHE epidermal models were exposed to various staphylococcal species and the media below the epidermal models sampled (undernatant). MoDCs were then cultured with undernatant overnight.

As discussed earlier, initial results (**Figure 3.10**) demonstrated that both SA and SE induced activation of DCs. To further explore the regulation of DC activation by SA or SE, experiments were conducted over a time course akin to the quantification analysis (Chapter 4) to assess how this response develops over time. Additionally, to test whether differences in staphylococci were genuinely species specific, SC exposure was included as a further experimental system.

MoDC phenotype was assessed with flow cytometric analysis of CD86 expression. The gating system selected the MoDC population based on FSC and SSC and then selected only the viable, HLA-DR+ MoDCs to examine the expression of CD86 (**Figure 5.1**).

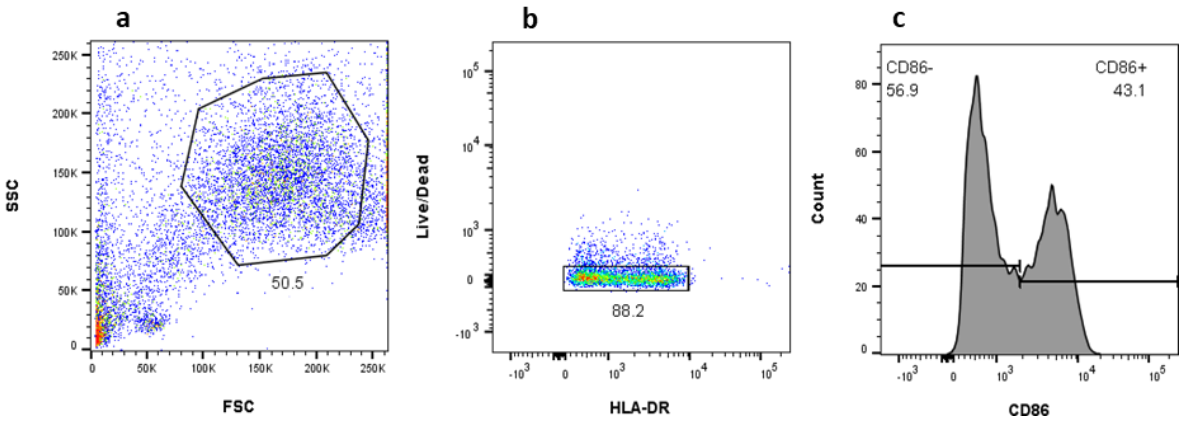

Figure 5:1: Gating strategy of CD86 expression
MoDC gating strategy used to analyse CD86 expression. The example displayed uses unstimulated MoDCs. Gating used SSC vs FSC (**a**) and Live/Dead vs HLA-DR (**b**) to select MoDC population, which were used to analyse CD86 expression (**c**).

Staphylococcal colonisation of RHE models induced synthesis of soluble mediators which induced activation of MoDCs as compared to RHE models which had no pathogen exposure (controls) (**Figure 5.2**). Time course analysis demonstrated that at initial inoculums of 10^6CFU, MoDC activation was greatest at 24 hours. However, SE and SC showed earlier responses than SA, as demonstrated by greater induction of MoDC activation at 9 hours. Furthermore, interspecies differences were observed and whilst both maximal SA and SE induced MoDC activation was similar, SC activated DCs to a lesser extent. Additionally, only SE was able to induce DC activation at low inoculum CFUs.

These results show a specific response is induced by model colonisation with each staphylococcal species. 10^6CFU inoculation for 24 hours was the best experimental setup for further analysis of the epidermal response to staphylococcal colonisation.

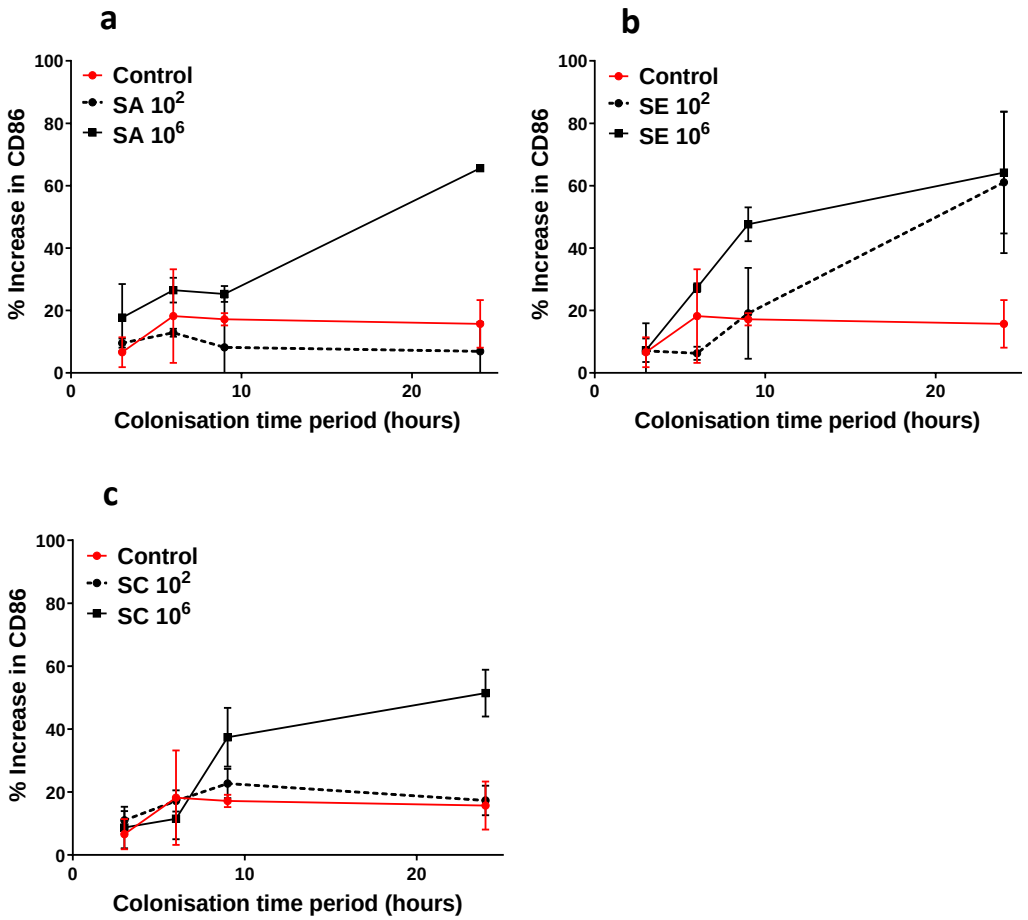

Figure 5:2: MoDC CD86 expression induced by staphylococcal colonisation
MoDCs CD86 expression after incubation with undernatant from RHE model colonisations inoculated with SA (8325-4)(**a**), SE (12228)(**b**) and SC (27840)(**c**) of 10^2 and 10^6 CFU for 3, 6, 9 or 24hrs. Undernatant harvested and used for overnight MoDC stimulation. MoDCs stained for Live/Dead, HLA-DR and CD86 and gated for as shown in **Figure 5.1**. Graph show % percentage increase in CD86 expression from unstimulated control and comparison to control colonisation (100µl PBS). Shown as mean ± SD (n=2).

5.2.2 Differential epidermal response to Staphylococcal colonisation

The staphylococcal induced epidermal response was previously shown to differentially activate MoDCs. To understand how the epidermis signals to DCs multi-analyte analyses of the undernatant were performed.

5.2.2.1 Membrane based analyte array

The Proteome profiler Human XL assay is a cytokine array kit utilising a membrane based sandwich immunoassay approach. It semi-quantitatively measures 102 specific analytes. This approach was undertaken to screen for key molecules or pathways that would be appropriate for further detailed study.

Undernatants combined from triplicate SA83, SE12, or PBS control inoculated RHE models at 10^6CFU (24hrs) were tested with the cytokine array analysis system. Due to the semi-quantitative nature of the assay analyte expression is only comparable between samples. Therefore data is expressed as fold change from the control (RHE model inoculated with PBS) (**Figure 5.3**).

Macroscopic analysis of the heatmap overall shows that SA83 colonisation induces more expression of the cytokines tested than SE. However, the experimental replicates demonstrated significant variability making further interpretation challenging. Nevertheless, some key analytes appeared to be more robustly modified and were included in the detailed analysis with a bead based assay.

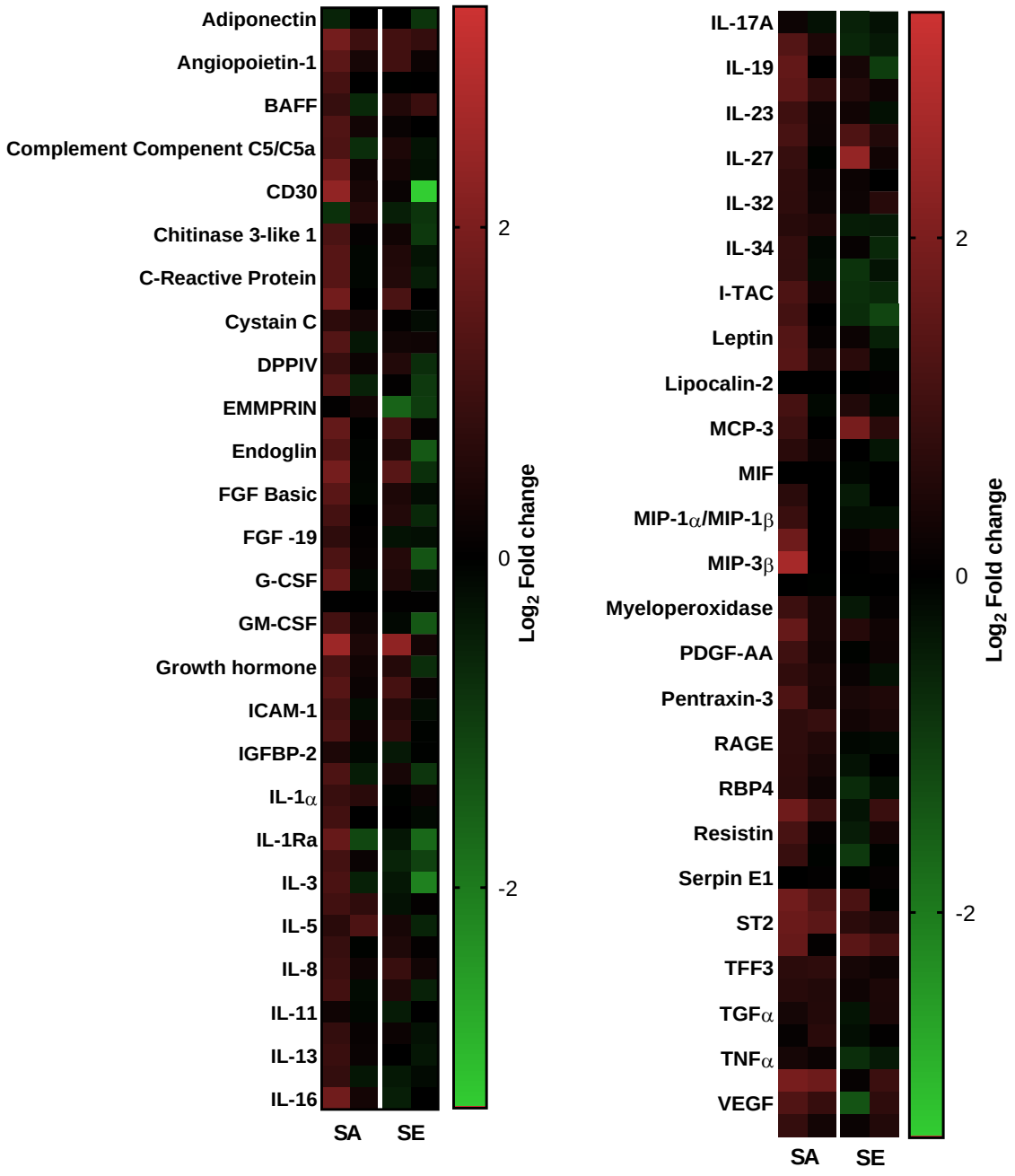

Figure 5:3: Analyte expression induced by SA and SE colonisation
Heatmap of analyte expression secreted in response to staphylococcal colonisation of the RHE model. The Proteome Profiler Human XL Cytokine Array kit used to analyse analyte expression in undernatant harvested from colonisations of 10^6CFU of SA (8325-4), SE (12228) and PBS control after 24hrs. Colonisations occurred in triplicate with collated undernatant used in the assay for an experimental average. Expression measured using ImageJ to determine relative spot intensity averaged between two spots per analyte, which was compared against the control sample. Data shown as Log_2 Fold change from control. Two experimental replicates shown in adjacent columns.

5.2.2.2 Bead based analyte assay

A custom Luminex panel (R&D systems) was consequently used to investigate the epidermal response to staphylococcal colonisation providing a more targeted analysis of specific mediators released from the RHE model. It also enabled expansion of the experimental parameters to also include more strains (SA29 and SC27), both inoculation amounts (10^2 and 10^6 CFU) and multiple timepoints of colonisation (3hrs and 24hrs). Resulting in a more comprehensive investigation of the epidermal response to staphylococcal colonisation.

The panel used in the Luminex system (**Table 5.1**) quantified a number of cytokines, chemokines and growth factors. The analyte selection for the panel was based on preliminary results of the proteome profiler, as well some performed by other researchers at Unilever. However, a large number of the selected analytes measured in the undernatant system were shown to be below the lower limit of quantification of the Luminex system. IL-1Ra and IL-8 expression were found to be above the upper limit of quantification of the luminex system after 24hrs of colonisation (**Table 5.1**). Therefore data is presented from the in range analytes.

Table 5.1: Luminex panel
Selected analytes used in the Luminex system to study epidermal cytokines, chemokines and growth factors. Table indicates analytes measured but were outside the range of quantification of the system at 3hrs and 24hrs.

Analyte	3hr	24hr
Angiogenin		
Angiopoietin-2		
CCL1		
CCL11		
CCL13		
CCL17		
CCL18		
CCL2		
CCL27		
CCL5		
sCD14		
sCD30		
EMMPRIN		
ENA-78 (CXCL5)		
GM-CSF		
Groα (CXCL1)		
Groβ (CXCL2)		
IL-10		
IL-1α		

Analyte	3hr	24hr
IL-1β		
IL-1Ra		
IL-22		
IL-23		
IL-27		
IL-33		
sIL-4Rα		
IL-6		
IL-8		
Osteopontin		
PDGF-AA		
Pentraxin-3		
Relaxin-2		
Resistin		
SHBG		
ST2		
TNFα		
uPAR		
VEGF		

: Below lower limit of quantification

: Above upper limit of quantification

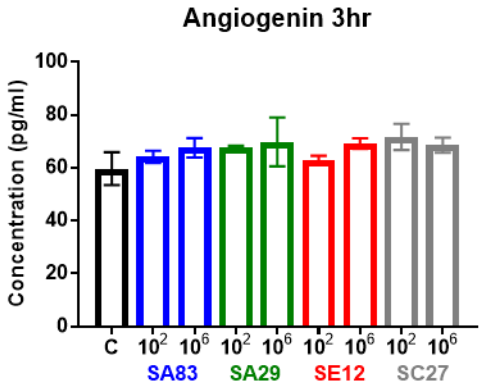
Angiogenin 3hr
Concentration (pg/ml)
100
80
60
40
20
0
C
10^2 10^6 10^2 10^6 10^2 10^6 10^2 10^6
SA83 SA29 SE12 SC27

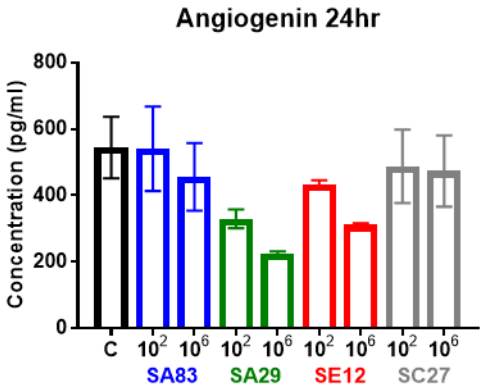
Angiogenin 24hr
Concentration (pg/ml)
800
600
400
200
0
C
10^2 10^6 10^2 10^6 10^2 10^6 10^2 10^6
SA83 SA29 SE12 SC27

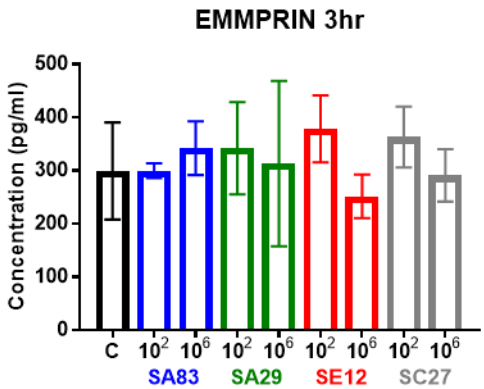
EMMPRIN 3hr
Concentration (pg/ml)
500
400
300
200
100
0
C
10^2 10^6 10^2 10^6 10^2 10^6 10^2 10^6
SA83 SA29 SE12 SC27

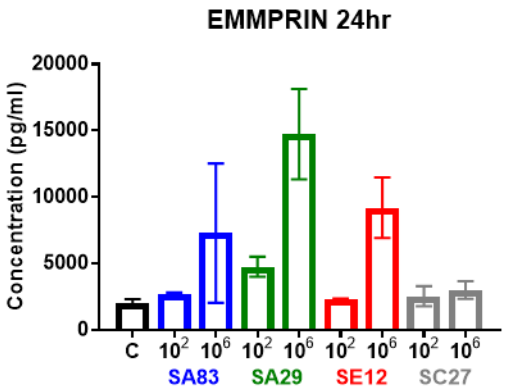
EMMPRIN 24hr
Concentration (pg/ml)
20000
15000
10000
5000
0
C
10^2 10^6 10^2 10^6 10^2 10^6 10^2 10^6
SA83 SA29 SE12 SC27

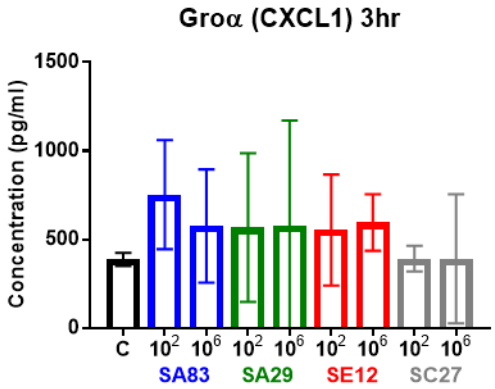
Groα (CXCL1) 3hr
Concentration (pg/ml)
1500
1000
500
0
C
10^2 10^6 10^2 10^6 10^2 10^6 10^2 10^6
SA83 SA29 SE12 SC27

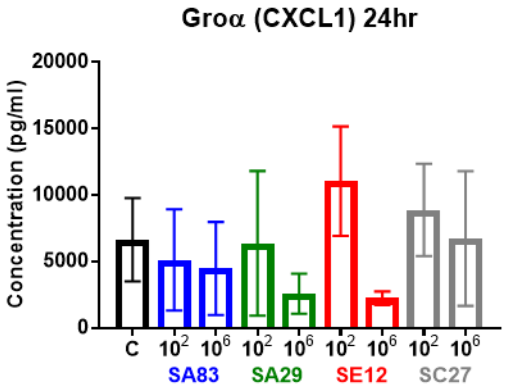
Groα (CXCL1) 24hr
Concentration (pg/ml)
20000
15000
10000
5000
0
C
10^2 10^6 10^2 10^6 10^2 10^6 10^2 10^6
SA83 SA29 SE12 SC27

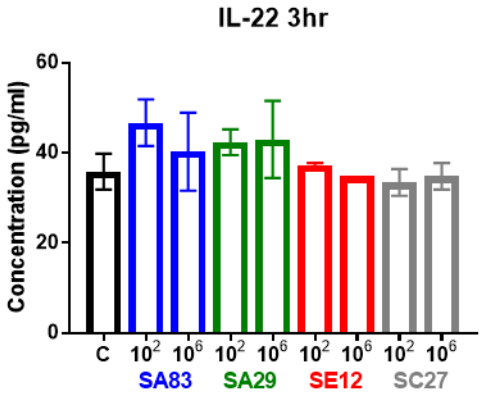
IL-22 3hr
Concentration (pg/ml)
60
40
20
0
C
10^2 10^6 10^2 10^6 10^2 10^6 10^2 10^6
SA83 SA29 SE12 SC27

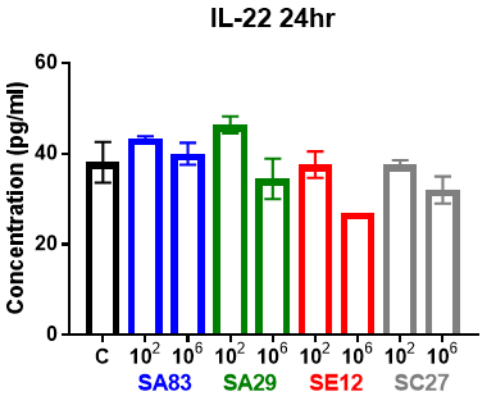
IL-22 24hr
Concentration (pg/ml)
60
40
20
0
C
10^2 10^6 10^2 10^6 10^2 10^6 10^2 10^6
SA83 SA29 SE12 SC27

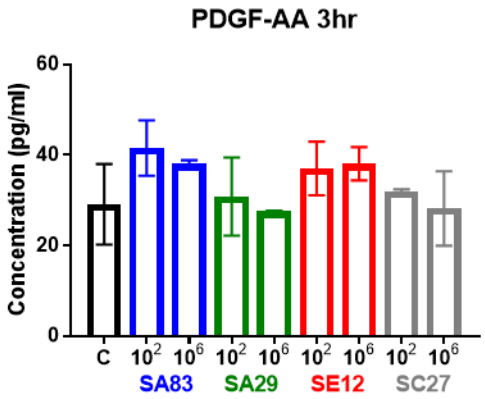
PDGF-AA 3hr
Concentration (pg/ml)
60
40
20
0
C
10^2 10^6 10^2 10^6 10^2 10^6 10^2 10^6
SA83 SA29 SE12 SC27

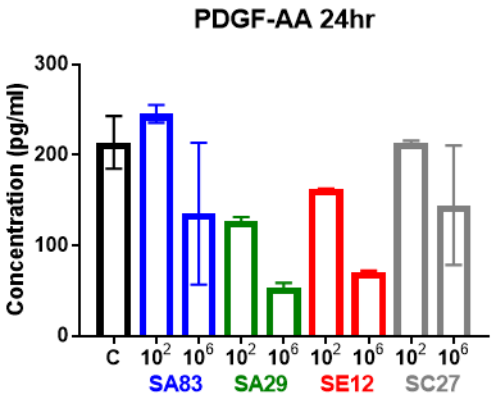
PDGF-AA 24hr
Concentration (pg/ml)
300
200
100
0
C
10^2 10^6 10^2 10^6 10^2 10^6 10^2 10^6
SA83 SA29 SE12 SC27

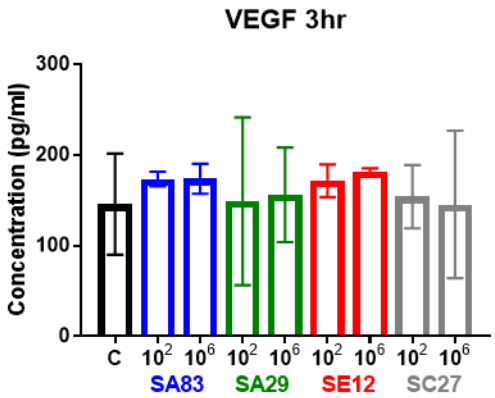
VEGF 3hr
Concentration (pg/ml)
300
200
100
0
C
10^2 10^6 10^2 10^6 10^2 10^6 10^2 10^6
SA83 SA29 SE12 SC27

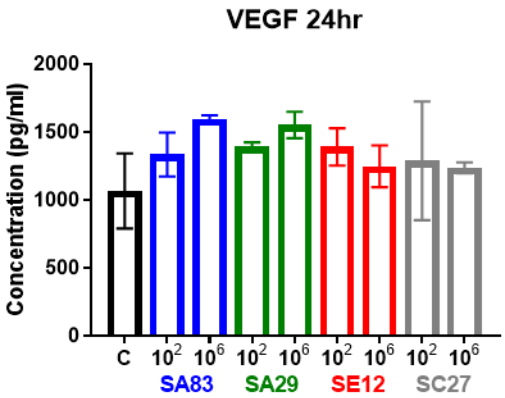
VEGF 24hr
Concentration (pg/ml)
2000
1500
1000
500
0
C
10^2 10^6 10^2 10^6 10^2 10^6 10^2 10^6
SA83 SA29 SE12 SC27

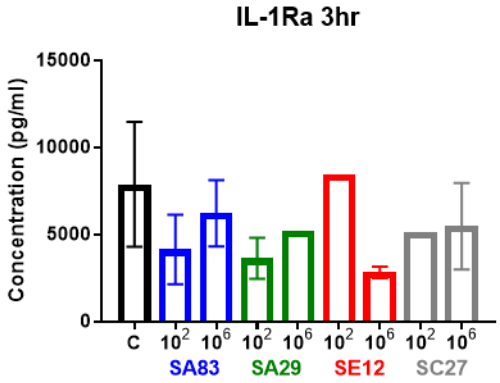
IL-1Ra 3hr
Concentration (pg/ml)
15000
10000
5000
0
C
10^2 10^6 10^2 10^6 10^2 10^6 10^2 10^6
SA83 SA29 SE12 SC27

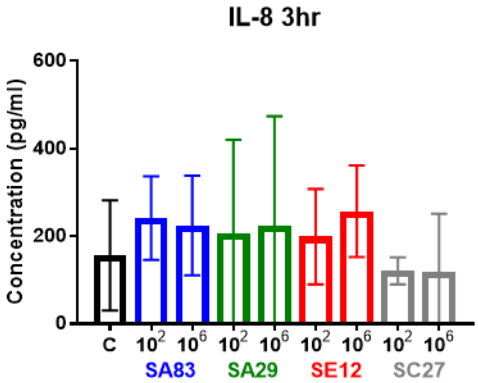
IL-8 3hr
Concentration (pg/ml)
600
400
200
0
C
10^2 10^6 10^2 10^6 10^2 10^6 10^2 10^6
SA83 SA29 SE12 SC27

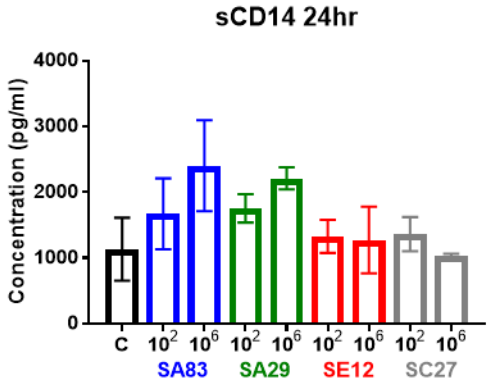
sCD14 24hr
Concentration (pg/ml)
4000
3000
2000
1000
0
C
10^2 10^6 10^2 10^6 10^2 10^6 10^2 10^6
SA83 SA29 SE12 SC27

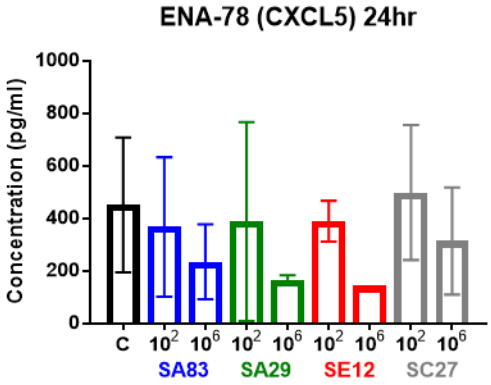
ENA-78 (CXCL5) 24hr
Concentration (pg/ml)
1000
800
600
400
200
0
C
10^2 10^6 10^2 10^6 10^2 10^6 10^2 10^6
SA83 SA29 SE12 SC27

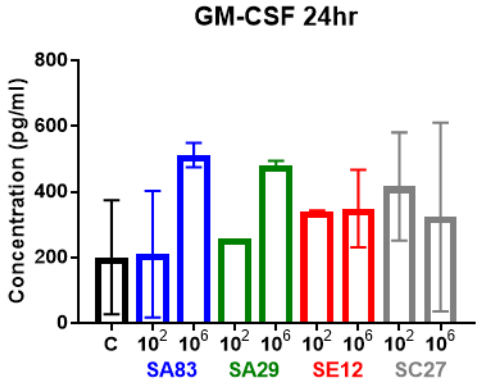
GM-CSF 24hr
Concentration (pg/ml)
800
600
400
200
0
C
10^2 10^6 10^2 10^6 10^2 10^6 10^2 10^6
SA83 SA29 SE12 SC27

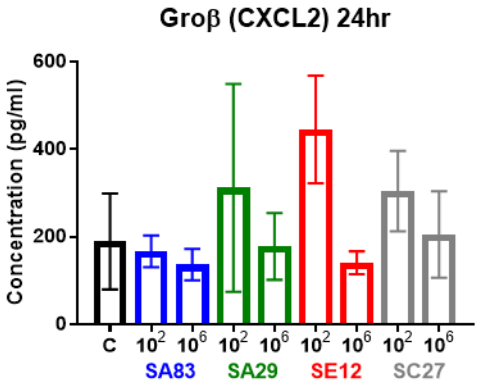
Groβ (CXCL2) 24hr
Concentration (pg/ml)
600
400
200
0
C
10^2 10^6 10^2 10^6 10^2 10^6 10^2 10^6
SA83 SA29 SE12 SC27

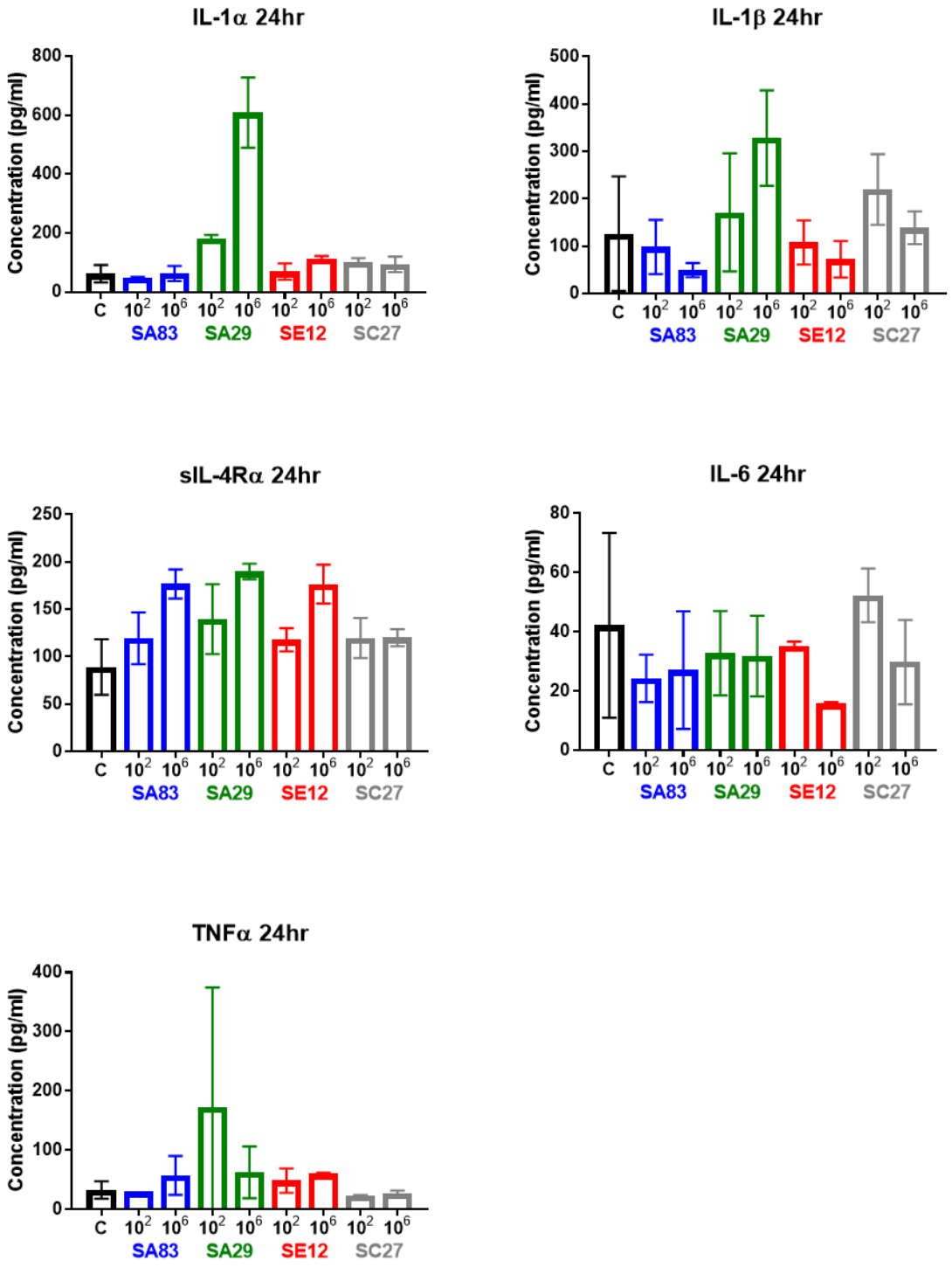

Figure 5:4: Quantification of Analyte expression induced by Staphylococcal colonisation
Quantification of individual analytes secreted by the RHE model in response to staphylococcal colonisation. Luminex system analysed harvested undernatant from RHE models inoculated with SA83 (8325-4), SA29 (29213), SE12 (12228) and SC27 (27840) at 10^2 and 10^6 CFU in 100µl PBS for 3hrs and 24hrs of colonisation; performed in parallel with PBS control RHE model (C) (n=4). Experiments performed in duplicate using separate model batches, shown as mean ± SD (n=2).

The expression of cytokines, chemokines and growth factors is differentially modified by staphylococcal colonisation dependent upon species. Additionally, the model system shows that different bacterial loads and the length of exposure are likely to modify epidermal responses (**Figure 5.4**).

At 24 hours, all SA and SE both inhibited synthesis of angiogenin (more so with higher inoculums), whereas this did not occur with SC. Similarly, although in reverse, SA and SE (but not SC) were both able to upregulate synthesis of EMMPRIN. CXCL1 showed a distinct differential response to inoculums with low or high loads of SE, low inducing increased expression, and high the reverse. Whilst high loads of SA were also able to inhibit CXCL1, but SC was not. Modification of IL-22 expression was minimal in all settings, but interestingly, SE did show inhibition of this cytokine at higher pathogen loads. All staphylococci inhibited PDGF and ENA-78, and this was most prominent at high pathogen loads, suggesting that these molecules may be regulated by a species level effect. Expression of VEGF and IL-8 were generally enhanced by all staphylococci (SC did not induce IL-8), although the effect size was small. All pathogens enhanced CXCL2 expression at low inoculums whereas at higher CFU, expression was generally reduced. SA29 prominently induced IL-1α, especially at higher inoculums whereas SA83, SE and SC did not. Similarly, SA also induced IL-1β, whereas the effect with SA83 and SE was inhibitory. SA and SE both induced soluble IL-4Rα, more at higher inoculums. IL-6 responses were generally reduced by all pathogens although the effect size was small. TNFα is a key epidermal cytokine and was induced by low inoculums of SA29, but not other pathogens.

Table 5.2: Overview of change in epidermal synthesis of soluble mediators following 24hrs of staphylococcal colonisation

SA minimal & SE minimal	SA up & SE minimal	SA down & SE minimal	SA up & SE up	SA down & SE down	Innoculum divergent response
IL-22	sCD14,		EMMPRIN	Angiogenin	CXCL1 (SE)
	IL-1α (SA29)		VEGF	PDGF	CXCL2 (SA and SE)
	IL-1β (SA29)		GM-CSF	IL-6	
	TNFα (SA29)		sIL-4Rα		

To facilitate further comparison, the 24hr results were also summarised in a heatmap (**Figure 5.5)**.

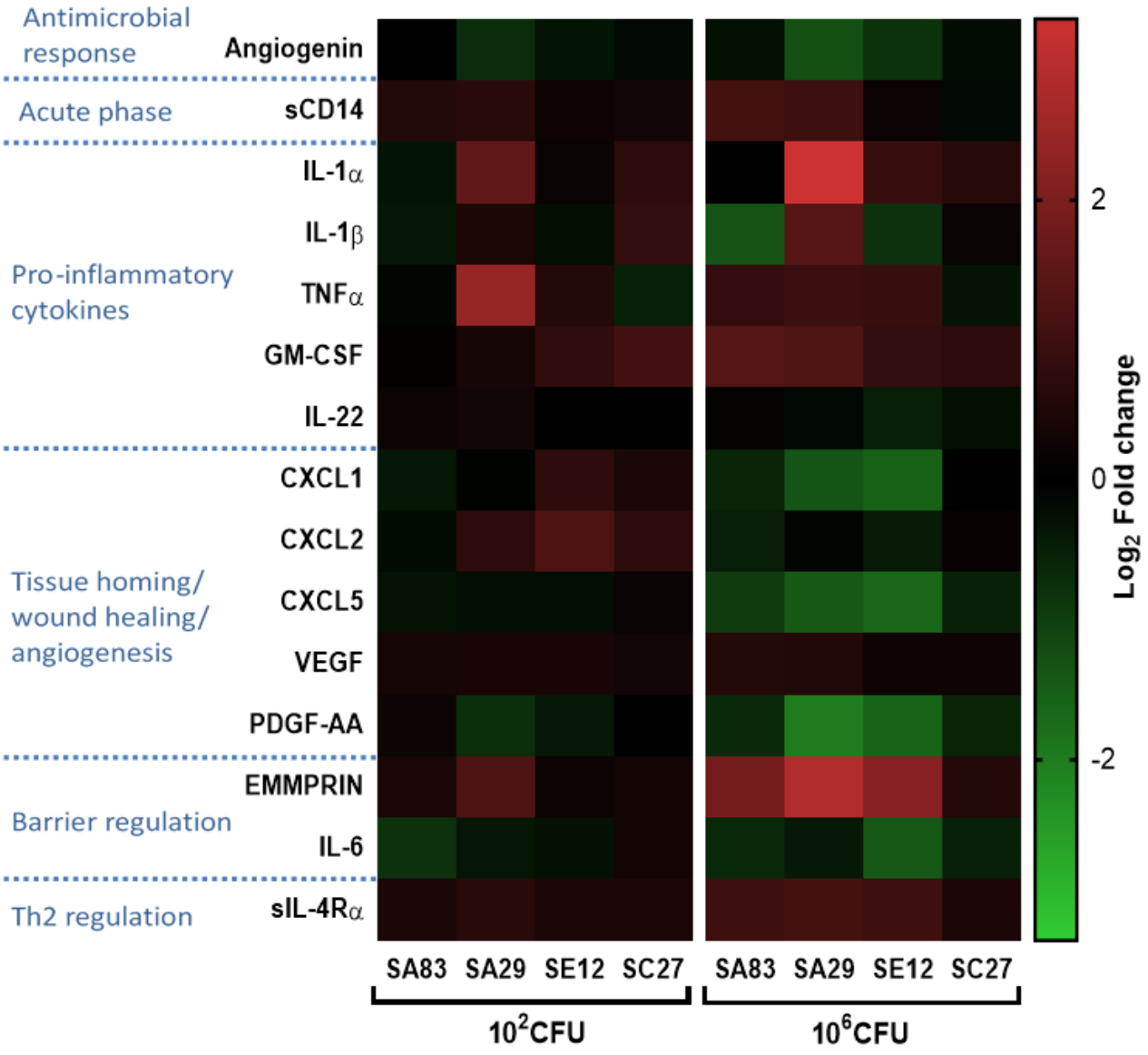

Figure 5:5: Summary of Analyte expression induced by 24hr Staphylococcal colonisation
Heatmap of fold change of individual analytes secreted by the RHE model in response to 24hrs of staphylococcal colonisation. Luminex system analysed harvested undernatant from RHE models inoculated with SA83 (8325-4), SA29 (29213), SE12 (12228) and SC27 (27840) at 10^2 and 10^6 CFU in 100µl PBS for 3hrs and 24hrs of colonisation; shown as Log_2 fold change from PBS control RHE model (n=4). Experiments performed in duplicate using separate model batches, shown as mean ± SD (n=2).

Between the different staphylococcal strains SA29 exhibits the strongest inflammatory profile with large increases in IL-1α, IL-1β, GM-CSF and TNFα after 24hrs of colonisation. SA83 and SE12 also demonstrate pro-inflammatory profiles after 24hrs, with increased in TNFα and GM-CSF. However, the colonisation of SC27 appears the least inflammatory, showing minimal change across all measured cytokines, chemokines and growth factors, especially in comparison to the other staphylococcal colonisations.

The staphylococcal induced reduction of angiogenin suggests a reduction in the antimicrobial response, which could explain the largest reduction by SA29, which was the pathogenic SA strain able to colonise the RHE model. Alternatively, angiogenin can act in an anti-inflammatory role that includes TNFα suppression (Lee et al., 2014), therefore its reduction would add to the evidence of SA29 inducing a more inflammatory response.

The increased production of sCD14 enhanced more by colonisation of SA29 as well as SA83, particularly for 10^6CFU. sCD14 performs a role in acute phase of inflammation and is critical in sensing bacterial presence (Lloyd-Jones et al., 2008). Its increase specific to SA could therefore be due to the skin predisposition to recognise SA as a pathogen and SE or SC as commensals. However, sCD14 has also has a role in the allergic inflammation of AD, with an increased concentration collated with increased severity (Kusunoki et al., 1998). Therefore, the differential increase between SA and SE could be an important aspect of the differential response.

A large number of chemokines were analysed using the luminex platform, however most were undetectable (**Table 5.1**). Only CXCL1 (Groα), CXCL2 (Groβ) and CXCL5 (ENA-78) were at measurable concentrations within the RHE models undernatant after 24hrs of colonisation. The staphylococcal induced effects on these three chemokines at 24hrs were variable for both concentrations of inoculation, but were similar between SA29 and SE12. 10^6CFU of SA29 and SE12 induced decreases of CXCL1 and CXCL5, whereas 10^2CFU induced increases of CXCL2. Alternatively, SA83 induces minimal change in chemokine expression, except for a reduction of CXCL5 by 10^6CFU.

PDGF-AA is also decreased by both SA29 and SE12 after 24hrs of colonisation, which could suggest a suppression of angiogenesis and remodelling. However, its suppression is also caused by pro-inflammatory cytokines, such as IL-1β and TNFα (Kose et al., 1996).

High production of EMMPRIN (Extracellular matrix metalloproteinase inducer) was induced by the colonisation of 10^6CFU SA83, SA29 and SE12. EMMRIN, also known as CD147, is generally considered important for matrix remodelling and thus regulation of the epidermal barrier.

However, it also performs other functions, acting as a pro-inflammatory mediator and suppressor of NOD2 signalling that operates in bacterial recognition (Till et al., 2008).

IL-6 also mediates the epidermal barrier in homeostasis (Wang et al., 2004), but was reduced by the staphylococcal colonisation of SA83, SA29 and SE12, most notably by 10^6CFU SE12. This suggests a suppression of homeostasis and barrier repair that would act in contrast to the pro-inflammatory response.

Soluble IL-4Rα (sIL-4Rα) was similarly increased by SA83, SE12 and SA29, with larger increases produced by 10^6CFU than 10^2CFU. The inhibiting effect of IL-4Rα on IL-4 suggests a dampening of Th2 mediated response further induced by higher colonising loads of staphylococci.

The expression of IL-1Ra (IL-1 receptor antagonist) was also shown to be reduced by 3hrs of staphylococcal colonisation. This occurred for all staphylococcal strains and inoculations except SE12 10^2CFU, however this opposed by 10^6CFU SE12 inducing the largest decrease. IL-1Ra is central to the role of an IL-1 based response.

The results of these individual cytokines, chemokines and growth factors show a differential response to the colonisation of different staphylococcal strains. Generally, showing SA29 to be more inflammatory, but also showing SE12 and SA83 to be inducing differing amounts of the examined inflammatory mediators.

5.3 Discussion

Keratinocytes act as sentinels of the epidermis, responding to a large range of different stimuli in order to regulate the epidermal immune response. Depending on the stimulus, they can act to initiate, escalate, mediate or resolve the corresponding inflammatory response. Keratinocytes communicate to surrounding cells through the production and release of inflammatory mediators, including cytokines, chemokines and growth factors.

To investigate the role of staphylococcal colonisation of the epidermis with regulation of cutaneous immunity, this chapter aimed to characterise the inflammatory mediators produced and released by the epidermal model.

Initially, the epidermal regulation of dendritic cell responses was confirmed with a MoDC model. CD86 is a marker of early DC maturation, the stimulation of its expression can be incurred by a variety of inflammatory mediators. CD86 acts as a co-stimulatory molecule required for T cell activation and polarisation (Dilioglou et al., 2003, Li et al., 2016). However, it does not indicate the functionality of the activated DC in regards to the direction of the T cell polarisation and consequent immune response.

Analysis of the immune mediators produced by the epidermal model here, provides insight into the response mediated by the staphylococcal colonisation of the skin. When studied using the membrane based proteome profiler colonisation with SA83 appears to induce a broader response that is inflammatory as compared to SE12 which is less inflammatory. These data seem to support previous work which has suggested that dysbiosis of the skin microbiome, with resulting loss of diversity and increased quantity of SA is strongly linked to the exacerbation and severity of AD (Higaki et al., 1999, Totte et al., 2016), which is characterised by skin inflammation (Werfel et al., 2016). Whereas, SE colonises the skin as part of the homeostatic microbiome (Otto, 2010). It also corresponds to microarray analysis of SA and SE colonisation of skin models by Holland et al. (2009) that demonstrated increased gene expression of TNFα, IL-1α, IL-1β and IL-17C specifically for SA.

Further analysis using a more targeted approach also demonstrated variation between SA83 and SE12. In all approaches, colonisation with SC27, a scalp commensal, which maintains a stable colonisation of the model system without any proliferation, showed minimal effects on the assayed proteins expressed by epidermal model.

Many similarities were identified between SA and SE. Colonisation induced a reduction in PDGF-AA and angiogenin, which can both be supressed by TNFα (Lee et al., 2014, Kose et al., 1996)

demonstrating the leading response. Additionally, IL-6 was reduced by both pathogens. Whereas EMMPRIN, VEGF, GM-CSF and sIL4-Rα were up regulated.

sIL-4Rα functions as an immune modulator important to the Th2 response, having specific effects on the Th2 cytokines IL-4 and IL-13. sIL-4Rα antagonistically binds IL-4 inhibiting the response, whereas it stabilises the binding of IL-13 and IL-13Rα1 (Andrews et al., 2006). The differential regulation of the Th2 cytokine balance could induce specific effects on the Th2 response. For example, both IL-4 and IL-13 are required to induce an IgE response (Punnonen et al., 1997), which is important for allergic inflammatory diseases such as AD. Furthermore, sIL-4R has been shown to inhibit allergic induced airway inflammation (Henderson et al., 2000). Suggesting that high colonisation may be inducing an inflammatory phenotype limiting the Th2 based allergic response through IL-4Rα production.

However, this work primarily aims to capture the differences between SA and SE to better understand how one pathogen can be ubiquitously found on the skin (SE) and almost never causes inflammatory disease, whereas the other (SA) is strongly associated with inflammatory skin disease.

Those inflammatory mediators which were differentially modulated by SA and SE included: sCD14 (upregulated by both SA strains), and IL-1α, IL-1β, and TNFα (up regulated by SA29).

Interestingly, increases in sCD14 specific to SA were demonstrated during studies of early intestinal colonisation (Lundell et al., 2006). CD14 functions as a receptor for a number of PAMPs including LPS and peptidoglycan, therefore acts to initiate an inflammatory response to bacterial presence during the acute phase of inflammation (Bas et al., 2004). However, it also performs a role in a number of inflammatory diseases. Increased levels of sCD14 in serum have been demonstrated during atopic dermatitis (Kusunoki et al., 1998), rheumatoid arthritis (Yu et al., 1998) and systemic lupus erythematosus (Nockher et al., 1994). The role of sCD14 in these disease states has not fully been elucidated, but could involve its action as an immune modulator. sCD14 has been shown to inhibit proliferation, activation and cytokine production of T cells (Nores et al., 1999), and IgE production of B cells; however, it simultaneously enhances B cell IgG1 production (Arias et al., 2000). These immune effects suggest sCD14 could be modifying the response to SA colonisation, but further understanding of the differential effect requires examination of the signalling instigating it.

IL-1α and IL-1β can both stimulate proinflammatory responses through activation of IL-1RI, where IL-1α acts as a DAMP to initiate inflammation (Kim et al., 2013), IL-1β acts to amplify it (Dinarello, 2018). Both these IL-1 cytokines are released from keratinocytes in response to SA infection as

part of NLRP3 mediate defence (Simanski et al., 2016), which could suggest SA29s greater virulence causes infection not demonstrated by other strains. However, IL-1α and IL-1β have been implicated in the inflammatory initiation of AD (Nambu and Nakae, 2010), despite recent failed attempts to treat AD with an IL-1 competitive inhibitor (Anakira)(Montes-Torres et al., 2015).

Within the skin, dermal DCs (DDCs) and Langerhans cells (LCs) regulate inflammation and tolerance by modifying T cell differentiation into various subsets of effector cells (Toebak et al., 2009). Upon stimulation and consequent activation in the skin, DCs mature and migrate to secondary lymphoid tissue to communicate the immune response to naive T cells (Th0). Resulting in the polarisation of T helper cells into differentiated subsets, which mediate the appropriate inflammatory response through the release of cytokines. The most well defined subsets are Th1 and Th2, which both produce inflammatory responses with non-overlapping functions and are therefore often considered opposing. Th1 cells produce IFNγ and TNFα, whereas Th2 cells produce IL-4, IL-5, and IL-13 (Swain, 1995, Wan and Flavell, 2009). Alternatively, regulatory T cells (Tregs) can also be differentiated from Th0 cells to induce suppression of an inflammatory response or regulate tolerance. The response of Tregs is generated by the release of TGFβ and IL-10 and causes the inhibition of effector T cell function, including T helper cells and cytotoxic T cells (Corthay, 2009). Th17 and Th22 are also helper T cell subsets that induce inflammatory responses, and have been shown to be important in the pathogenesis of inflammatory diseases. Th17 is characterised by the production of IL-17, IL-21 and IL-22, whereas Th22 produces IL-22 and TNFα (Wan and Flavell, 2009, Akdis et al., 2012).

The process regulating T cell polarisation is controlled by the priming antigen presenting cell (APC) including the production of cytokines by the DCs to induce the T cell differentiation into different effector T cell subsets that will direct the adaptive response (Lutz, 2016, Schmidt et al., 2012). Therefore, to extend the understanding from this work it would be important to investigate the cytokine production of the MoDCs and the regulatory effect on Th differentiation and this will be the subject of future work.

Investigation of the epidermal response to different staphylococci has demonstrated species specific epidermal immune responses. Most interestingly, whilst inflammatory responses to SC were modest, differential responses to SA and SE were noted with sCD14, IL1α (SA29), IL-1β (SA29), TNFα (SA29). These data suggest that epidermal induction of these molecules may be important in regulating a 'hospitable' skin environment, as seen with the commensal SE, or a less hospitable environment with SA that results in inflammation and inhibits bacterial proliferation (as seen in Chapter 4). To further characterise the molecular signalling pathways in keratinocytes

critical to induction of such species specific responses, the following chapter will use a transcriptomic approach to analyse the response to various pathogen exposures.

Chapter 6: Chapter 6: Staphylococcal colonisation induced differential gene expression

6.1 Introduction

The previous chapter demonstrated different staphylococcal species interacted with the epidermis to regulate inflammatory mediators at a species specific level, and that the consequence of such interaction regulated immune cell activation. However, to better understand the signalling pathways critical to such a finely honed species specific interaction, it is necessary to look at intracellular signalling process. To address this, a transcriptomic analysis of pathogen interaction with keratinocytes was undertaken and is the subject of this chapter. In addition to facilitating the analysis of key pathways involved in pathogen sensing, a transcriptomic approach would also allow a non-hypothesis driven assessment of other potential soluble mediators which could have been missed on the protein based assessment from Chapter 5.

The transcriptome describes the total RNA transcripts of a cell or cell population. Study of the transcriptome, known as transcriptomics, has only been developed within the last two decades, due to technological advances (Lowe et al., 2017). Transcriptomic analysis examines genome-wide gene expression at the RNA level, thus enabling a comprehensive study of the current cellular processes. Therefore it is a powerful technique for comparison of cells under different conditions or in disease states.

Consequently, transcriptomics has been used in various different areas of study, including AD. For instance, transcriptomic analysis comparing moderate-severe AD lesional skin to nonlesional skin and revealed novel increases in expression of TREM1 (Triggering receptor expressed on myeloid cells 1) and IL-36 (Suarez-Farinas et al., 2015). Alternatively, transcriptomic analysis of AD lesional skin was used to identify patients with filaggrin null mutations, which were then compared against AD patients without filaggrin mutations. Differences were found in 7 genes encoding proteins in the extracellular space, with correlation between gene regulation and filaggrin expression (Cole et al., 2014). Furthermore, transcriptomic analysis has been used to compare six different AD murine models against a meta-analysis–derived AD (MADAD) transcriptome. They found significant differences in the phenotype of each murine model, but suggested an IL-23 injected murine model best replicated human AD (Ewald et al., 2017).

Transcriptomics is predominantly performed with two techniques microarray and RNA-seq (a form of high-throughput sequencing). Fundamentally, microarrays work by the hybridisation of

RNA transcripts to an array of nucleotide oligomers, known as probes. Prior to this hybridisation, RNA is fluorescently labelled, which enables a microarray scanner to measure the intensity of the laser induced fluorescence of each probe. Probes in the array are specifically arranged so the scanner will know which probe corresponds to which transcript, thus providing a relative measure of each transcript (Bumgarner, 2013, Lowe et al., 2017).

RNA-seq is based on the high throughput sequencing of each transcript within an RNA sample. The RNA is first fragmented and transcribed in to ds-cDNA with adaptors attached to one or both ends. Following sequencing, the reads of the fragments are aligned *in silico* using a reference genome or reference transcript. However, assembly can be performed without a reference to generate a genome-scale transcription map (Wang et al., 2009b). This provides the advantage of detecting unknown genomic sequences, as well as revealing sequence variations such as SNPs. Another advantage of RNA-seq is the high sensitivity, measuring much smaller changes in expression than a microarray. Furthermore, RNA-seq requires much less RNA and can sequence the transcriptome of individual cells (scRNA-seq). However, RNA-seq is also more labour intensive in both sample preparation and data analysis. As well as being highly costly, particularly for a large number of samples (Wang et al., 2009b, Lowe et al., 2017).

This research aims to investigate the transcriptome of keratinocytes responding to staphylococcal colonisation. Therefore, detection of novel genomics, such as unannotated genes or sequence level alterations, is not necessary. Therefore, microarray analysis will be used. Additionally, using microarrays enables the study of a large number of samples, which would cost an exorbitant amount if RNA-seq was used.

Microarray transcriptomic analysis refers to a high throughput screening system for expression of mRNA. It uses an array chip of microscopic spots of DNA probes reflecting genes to be tested. Specifically, the SurePrint G3 Human Gene Expression v3 8x60K Microarray Kit (Agilent). This array incorporates approximately 60,000 genes, with eight arrays printed onto a glass slide. Thus allowing eight samples to be analysed and compared simultaneously. Samples of mRNA are reverse transcribed into cDNA, which is then used to transcribe fluorescently tagged cRNA, both labelling and amplifying the mRNA sample. Hybridisation allows the cRNA to hybridise to the corresponding probe of the microarray, which is then scanned. The Agilent microarray scanner (Agilent) measures the fluorescent signal of each spot in the specific array layout, generating a measurement of relative abundance for each mRNA transcript, which can be compared between samples.

Microarrays have also been used to compare transcriptomes of various skin models of different complexities. A study comparing keratinocyte monolayers and RHE models to *ex vivo* skin showed

comparable transcriptomes, with similar gene expression between all three sample types. They also showed the RHE model to be more similar to the *ex vivo* skin than the keratinocytes monolayers. The largest difference in keratinocyte monolayers was lower expression for proteins associated to epidermal differentiation, such filaggrin, loricrin, involucrin and differentiation-specific keratins (K1, K10) (Gazel et al., 2003). Overall this demonstrates the viability of using RHE models to study the transcriptome.

Microarray analysis examination of changes in the transcriptome and have commonly been used to compare the profiles of diseased and normal states. Both AD and Psoriasis have been extensively studied using microarrays, by comparing skin biopsies from diseased skin and normal skin (Bowcock et al., 2001, Gudjonsson et al., 2010, Sugiura et al., 2005, Choy et al., 2012). Furthermore, some of these studies have been used for meta-analysis of the diseases pathogenesis (Tian et al., 2012).

Additionally, microarrays have been used to investigate the response of RHE models and keratinocytes to cytokines associated to AD or psoriasis. For instance, keratinocytes stimulated with IFNγ or IL-1α were compared with psoriatic skin. Results showed a stronger correlation between the psoriatic profile and stimulation by IL-1α rather than IFNγ, suggesting a bias towards the innate immune response (Mee et al., 2007). Another study used microarrays to show IL-17 to induce similar gene expression as psoriasis on full thickness skin models (Chiricozzi et al., 2014). Furthermore, several cytokines have been used in combination to stimulate a disease-like state that can be assessed by microarray. For example, Rouaud-Tinguely et al. (2015) induced an AD-like phenotype by stimulating a RHE model with Poly I:C, TNFα, IL-4 and IL-13.

Staphylococcal colonisation has also been studied using microarray technology to assess differential gene expression in full thickness skin models (Holland et al., 2009). This study assessed both SA and SE colonisation, showing SA to induce expression of pro-inflammatory cytokines and AMPs. This included IL-23, IL-17C, IL-1α, IL-1β, TNFα and hBD4. Conversely, SE colonisation induced only expression of pentraxin-3 in regards to immune response and also induced downregulation of AMPs such as hBD3, hBD4, psoriasin and S100A15.

The aim of this chapter is to explore the differential gene expression in the epidermis, induced by the colonisation of different strains. The intent is to identify key differentially expressed genes (DEGs) altered by the each microbe to help interpret the effect of the colonisation on the skin.

6.2 Results

6.2.1 Microarray data analysis

6.2.1.1 Staphylococcal colonisation treatment selection

Microarray technology was used to analyse the transcriptome of RNA lysates generated from RHE models colonised with staphylococcal species. Experiment and array batches were performed with single species colonisations and mixed species colonisations, enabling future comparison. Although this chapter will focus entirely on single species colonisations, the initial data analysis and filtering was performed on all arrayed treatments (**Table 6.1**). Colonisation inoculums of 10^6CFU were used for all experiments, as optimised in previous chapters.

The experimental RHE colonisations employed are outlined in **Table 6.1**, with replicate inclusion displayed in **Table 6.2**. **Table 6.2** also shows array groupings, which are limited by eight samples per group and are indicated by colour. Importantly each array group contains a time relevant control for later normalisation. Sample exclusion was decided based on Nanodrop analysis used to measure both yield and specific activity of the labelling dye. **Table 6.3** briefly explains the exclusion criteria for each unused sample.

Table 6.1: Microarray treatment description
Description of the treatment names used in the microarray and its data analysis

Treatment name	Description of colonisation
Control	100µl PBS
SA83	10^6 SA83 (8325-4) in 100µl PBS
SE12	10^6 SE12 (12228) in 100µl PBS
SA29	10^6 SA29 (29213) in 100µl PBS
SC27	10^6 SC27 (27480) in 100µl PBS
A/E 1:1	10^6 SA83 and SE12 at a ratio of 1:1 in 100µl PBS
A/E 3:1	10^6 SA83 and SE12 at a ratio of 3:1 in 100µl PBS
C/E 1:1	10^6 SC27 and SE12 at a ratio of 1:1 in 100µl PBS
C/E 3:1	10^6 SC27 and SE12 at a ratio of 3:1 in 100µl PBS

Table 6.2: Microarray samples
Samples used in microarray, separated by model batches. Colours denote array groups.

Time	Treatment	Model batch number 180817	80917	220917	280917	N=
0	Control	x				1
3	Control	x	x	x	x	4
3	SA83	x	x	x	x	4
3	SE12		x	x	x	3
3	SA29	x	x	x	x	4
3	SC27	x	x	x	x	4
3	A/E 1:1	x	x		x	3
3	A/E 3:1	x		x	x	3
3	C/E 1:1	x	x	x		3
3	C/E 3:1		x	x	x	3
24	Control	x		x	x	3
24	SA83	x		x	x	3
24	SE12	x		x	x	3
24	SA29					0
24	SC27	x		x	x	3
24	A/E 1:1	x		x	x	3
24	A/E 3:1	x		x	x	3
24	C/E 1:1	x		x	x	3
24	C/E 3:1	x		x	x	3

Table 6.3: Reason for sample exclusion from microarray

Batch number	Sample	Reasoning
180817	SE12 3hr	Low yield and specificity
	C/E 3:1 3hr	Limited models in batch, colonisation not performed
	SA29 24hr	Low yield
080917	Control 0hr	Limited array space
	A/E 3:1 3hr	Limited array space, but removal ensured n=3 for other colonisations
	All 24hr samples	Control sample had low yield and specificity, therefore samples would lack normalisation
220917	Control 0hr	Limited array space
	A/E 1:1 3hr	Low yield
	SA29 24hr	Low yield and specificity
280917	Control 0hr	Limited array space
	C/E 3:1 3hr	Limited array space
	SA29 24hr	Low yield and specificity

6.2.1.2 Normalisation and probe filtering of microarray data

Microarray data was analysed using GeneSpring Version 14.9 (Agilent). GeneSpring uses quality measures calculated by the microarray feature extraction software, such as signal saturation and signal uniformity, to flag the data from each probe. The qualify measure, as indicated by flags, reflects the reliability of each result and can be filtered accordingly by GeneSpring. The flag analysis was set up to attribute 'absent' if the entity was not detected or was below background. Additionally, probes were flagged as compromised if the entity was not uniform or was saturated, resulting in exclusion.

Principal component analysis (PCA) (**Figure 6.1**) of all the samples identified an outlier, visible in the bottom left corner of the graph, corresponding to C/E 1:1 (See **Table 6.1** for sample nomenclature) at 3hrs of batch 220917. During the experiment, it was noted that this sample had failed hybridisation because of a leaking gasket. Therefore, the sample was removed from further analysis. Additionally, the sample of A/E 1:1 at 3hrs of batch 180817 did not pass quality control, based on the automatically generated quality control report; it was consequently excluded. The sample was shown to fail a number of evaluation metric statistics including the "Maximum average, plus 1 standard deviation, of the spike-in probes below the linear concentration range" (denoted as "DetectionLimit") and the "Standard deviation of the background-subtracted signals of all inlier negative controls" (denoted as "gNegCtrlSDevBGSubSig").

Transcript expression data was normalised to the time relevant control of each individual batch, to reduce variability between batches and array groups.

Within the GeneSpring software, the term "entity" describes a measureable feature within the microarray analysis. The system employed here evaluated 58341 entities. After filtering the entity list based on flags (therefore discounting both not detected and compromised flags), and the inclusion criteria that the probe was identified in all the replicates for at least one of the 18 treatments, 21899 entities were characterised.

After sample exclusion, normalisation and filtering, as described above, PCA was undertaken (**Figure 6.2**). The graph shows some clustering on component 2 based on batch (**Figure 6.2a**), which suggests a batch to batch effect. Component 1 demonstrated a striking clustering which emphasised clustering of samples due to time of colonisation.

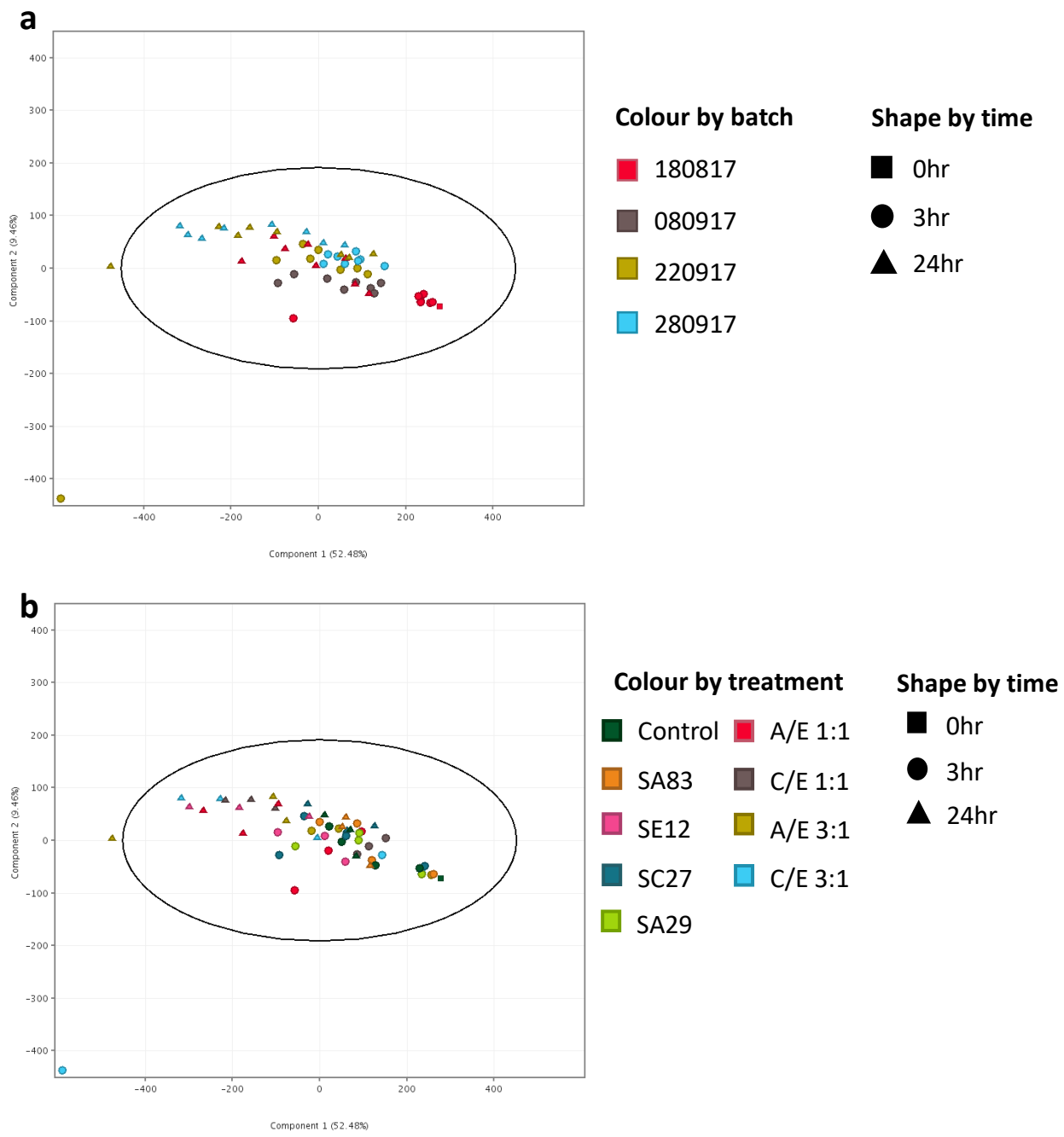

Figure 6:1: Principal component analysis plots of raw microarray data
2D Principal component analysis (PCA) plots of the raw unfiltered data within a sample, demonstrating variance in data. Each data point represents a single array of a sample. Graphs differ only by colour of each data point, either by batch (**a**) or treatment (**b**) to enable identification of each sample. % of components = percentage of total variance. Outliers shown by T^2 Hotelling Elipse with 95% confidence (black ellipse).

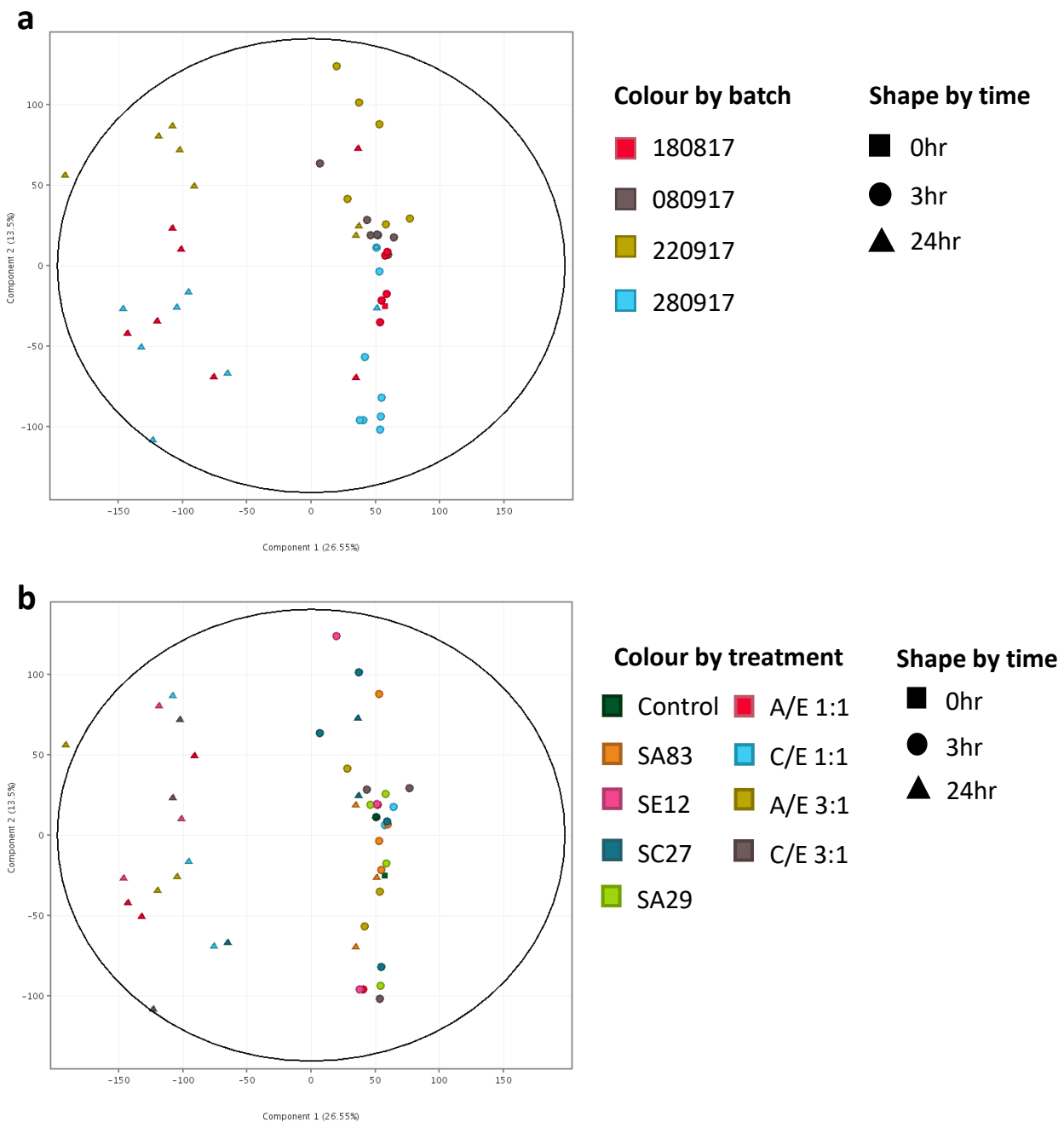

Figure 6:2: Principal component analysis plots of microarray data after sample exclusion, normalisation and entity filtering

2D Principal component analysis (PCA) plots of the variance of the data within a sample after normalisation and flagged based filtering. Each data point represents a single array of a sample. Graphs differ only by colour of each data point, either by batch (**a**) or treatment (**b**) to enable identification of each sample. % of components = percentage of total variance. Outliers shown by T^2 Hotelling Elipse with 95% confidence (black ellipse).

6.2.2 Differential gene expression induced by individual staphylococcal colonisation

6.2.2.1 Clustering analysis of the epidermal response to staphylococcal colonisations.

Hierarchical clustering analysis (GeneSpring) compares variation in gene expression induced by SA, SE or SC colonisation (**Figure 6.3**). The gene expression analysed is derived from staphylococcal colonisations compared against their time relevant control (PBS inoculum). Of all the staphylococci, colonisation of SE induced the greatest change in expression, at both 3hrs and 24hrs.

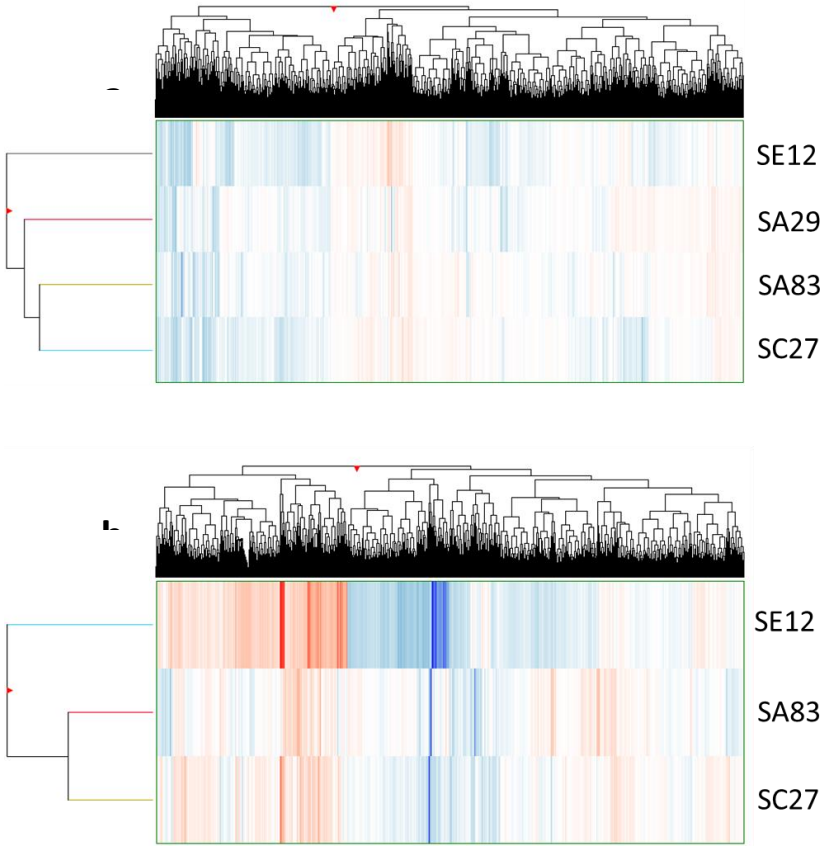

Figure 6:3: Clustering analysis of epidermal response to colonisation of individual microbes
Hierarchical clustering of entities and treatment, performed on the filtered list of 21899 entities, performed separately for 3hrs (**a**) and 24hr (**b**). The y-axis dendrogram demonstrates treatment clustering, whereas the x-axis dendrogram demonstrates entity clustering. The dendrogram branch distance is proportional to variation between the clusters. Colour intensity is proportional to the average change from the control for each entity, red as an increase and blue as a decrease. n = 3/4.

6.2.2.2 Fold change induced by staphylococcal colonisation

To explore significant changes in gene expression of different staphylococcal colonisations, a volcano plot analysis evaluated the change in gene expression compared to the time relevant control for each species (**Figure 6.4**). A significance threshold of P<0.05 assessed a fold change of 1 within the volcano plots. This produces a low stringency analysis that would discover any significant change in gene expression. Multiple test correction (MTC) was also applied to reduce the likelihood of coincidental statistical significance, which is anticipated when analysing such large data sets. Specifically, the Benjamini–Hochberg procedure to control for the false discovery rate (FDR). After MTC, the data similarly shows more prominent induction of gene expression with SE than the other staphylococcal species. This effect was greater at 24hrs than at 3hrs. Examination of SA shows that significant differential gene expression was noted at 3hrs in two entities.

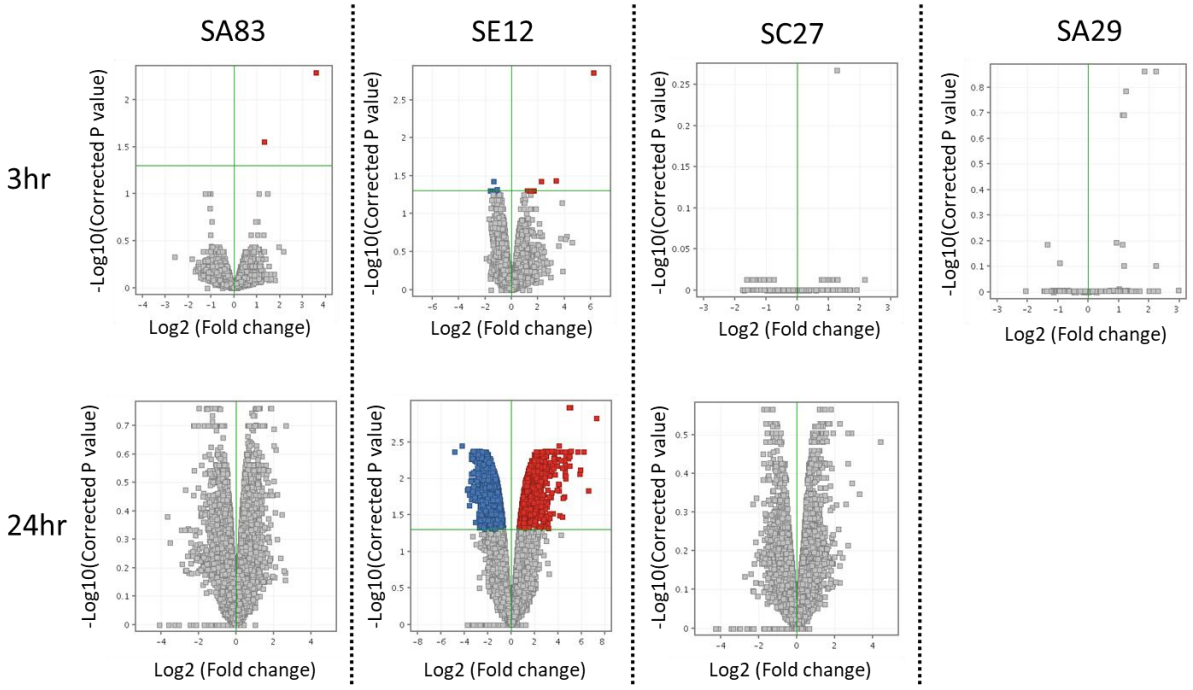

Figure 6:4: Volcano plots of epidermal response to colonisation of individual microbes
Volcano plots of T-tests comparing entities of a treatment against its time relevant control. Each graph displays the results for an individual treatment, comparing Log_2 Fold change against significance of a T-test (P<0.05 using Benjamini Hochberg FDR). Red data points expose significant entities above a FC of 1, whereas blue exposes the significant entities below a FC of 1. n = 3/4

Table 6.4: Number of entities significantly changed from the control after staphylococcal colonisation

Number of entities above thresholds of fold change that are significantly different from the control after colonisation of individual strains of staphylococci. Significance measured by T-test of P<0.05 using Benjamini Hochberg FDR. n = 3/4

Fold Change	SA83		SE12		SC27		SA29
	3hr	24hr	3hr	24hr	3hr	24hr	3hr
1	2	0	19	4228	0	0	0
1.2	2	0	19	4228	0	0	0
1.5	2	0	19	4228	0	0	0
2	2	0	19	3357	0	0	0
3	1	0	6	1406	0	0	0

The minimal or absence of significant entities for SA and SC makes comparison between the different epidermal responses to staphylococci very limited. To further examine the DEGs identified by the volcano analysis incremental fold change thresholds were applied to filter the number of entities based on change in expression (**Table 6.4**). It shows the significant entities are all above 1.5 fold change, which suggests significance is due to high change in expression from the control.

To explore the statistical threshold used in the volcano analysis, the P<0.05 inclusion was removed (**Table 6.5**). This identified many entities in all staphylococcal challenges with variable change in expression, suggesting that low replicate variability was contributing to the low yield of DEGs in the original analysis.

Table 6.5: Number of entities changed from the control after staphylococcal colonisation

Number of entities above thresholds of fold change that are different from the control after colonisation of individual strains of staphylococci. n = 3/4

Fold Change	SA83		SE12		SC27		SA29
	3hr	24hr	3hr	24hr	3hr	24hr	3hr
1	21899	21899	21899	21899	21899	21899	21899
1.2	5655	8105	9097	16519	7608	10050	6561
1.5	1152	2569	2741	10589	1812	3127	1232
2	174	734	622	5246	249	731	127
3	11	143	91	1722	15	114	9

6.2.3 Staphylococcal colonisation induced gene signature

Gene transcription changes show varying kinetics based on the specific pathway signalling properties. However, it is well recognised that these changes can happen rapidly <3 hours. The analysis above had suggested that comparing time points had been limited by replicate variability, which reduced the statistical significance of differences in gene expression. Therefore, although potentially any late gene transcription signals may be reduced, by combining time points thus increasing replicates, it would be possible to increase the power to identify key pathways that were activated early. Therefore, for further analysis the staphylococcal challenges at 3 hour and 24 hour were combined. SA29 was excluded because it lacked samples from 24hrs of colonisation and consequently also had to be excluded further analysis. The top DEGs identified through combined analysis were retrospectively analysed at separate time points, and it was notable that when comparing fold change, there was a strong overlap between the combined time point list of most highly differentially expressed genes and the independent timepoints (see later) which suggests that this approach is valid.

However, this approach assumes genes of interests will be differentially regulated at both 3hrs and 24hrs. Therefore, genes may not be considered significant within the analysis if they are differentially regulated at only one time point or opposingly regulated at the different timepoints.

A 2way ANOVA $p<0.05$ (including Benjamini-Hochberg FDR) compared each timepoint of staphylococcal colonisation against its respective time relevant control, it identified 308 entities for SA83, 4723 for SE12 and 52 for SC27. In support of previous analysis, SE colonisation showed the most striking modulation of gene transcription as compared to SA or SC. Examination of these entity lists within a proportional Venn diagram exposes some overlap with the staphylococcal strains (**Figure 6.5**). However, no common entities were found for all three strains.

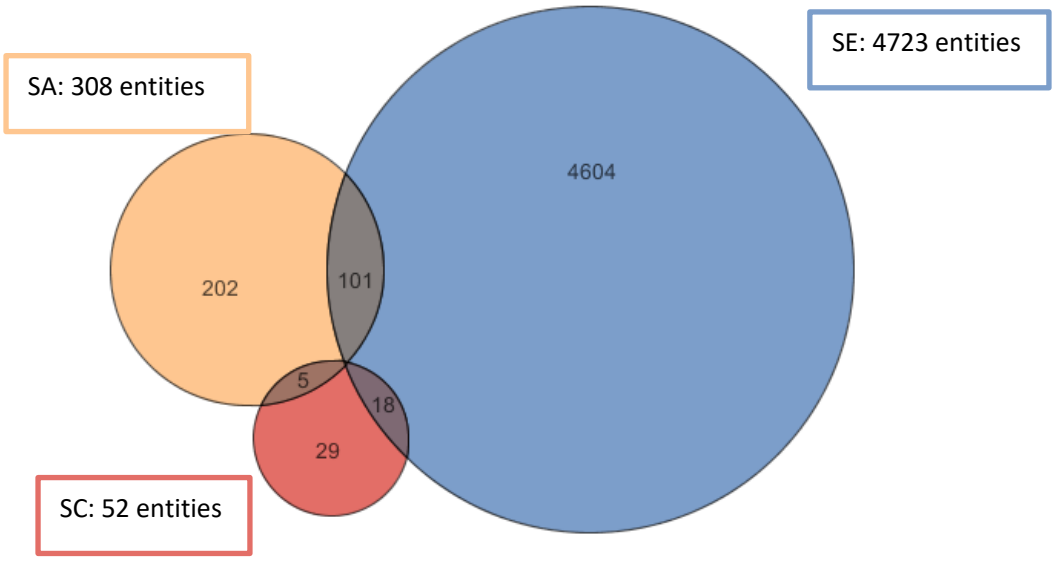

Figure 6:5: Proportional Venn diagram of staphylococcal colonisation induced gene signatures Venn diagram of the entity lists of the gene signatures for the colonisation of SA83, SE12 and SC27. Circle area proportional to the number of entities of each gene signature, labelled in the associated coloured box. Each gene signature generated by 2way ANOVA of individual staphylococci comparing 3hrs and 24hrs against their time relevant control, using P<0.05 with Benjamini Hochberg FDR as MTC.

The ANOVA based analysis generated gene signatures induced by the colonisation of each staphylococcal species, which evaluated differentially expressed genes (DEGs) for 3hrs and 24hrs collectively. These DEGs are therefore part of the epidermal response to the colonisation. Further investigation of the gene signatures examined the DEGs of greatest change from each signature, but also separated 3hrs and 24hrs expression values to assess change at each timepoint. Ranking the DEGs by expression value (Log_2 fold change) (**Table 6.6 - 6.11**) identifies the most expressed genes induced by the staphylococcal colonisation. Comparison of these lists of top DEGs shows that SE12 induced more gene transcription changes globally (**Table 6.8 - 6.9**) than SA83 (**Table 6.6 - 6.7**) or SC27 (**Table 6.10 - 6.11**), which corresponds to previous results.

DEGs identified in the lists of top DEGs at each timepoint, were more likely to feature in the top DEGs at both timepoints. Furthermore, examination of the change in expression of these shared DEGs indicates greater change at 24hrs. SE12 induced the largest overlap of DEGs between 3hrs and 24hrs, with 12 of the 20 DEGs shared between **Table 6.8** and **Table 6.9**. SC27 also shares a large amount of DEGs between **Table 6.10** and **Table 6.11**, with 10 mutual DEGs out of the 20. Alternatively, SA only shares 6 DEGs between Table 6.6 and Table 6.7, which could suggest an alteration in the response to the colonisation between 3hrs and 24hrs.

Between the different staphylococcal species DEGs expression demonstrates minimal overlap. The only mutual DEGs between different staphylococci are IL-17C and IL-23A, which are induced by SA83 and SE12 at both 3hrs and 24hrs.

The notion of IL-17C's importance is also evident from its rank within the DEG lists, and this cytokine has been reported to be important in inflammatory skin disease (Monin et al., 2017). At 3hrs it is the most highly differentially expressed gene (ranked 1st) for both SA (**Table 6.6**) and SE (**Table 6.8**) with expression of 3.57 and 6.24 Log_2 FC respectively. SA also induces IL-17C expression at 24hrs and is one of the most differentially transcribed genes from the control (ranked 3rd) at this timepoint (**Table 6.7**), but the relative expression is reduced at 24 hours (2.21 Log_2 FC). In contrast, SE maintains IL-17C expression at 24hr (**Table 6.9**) to 6.59 Log_2 FC.

IL-23A is essential for differentiation of Th17 cells (Gaffen et al., 2014). High IL-23A expression is induced by SA and SE, with increasing expression for both staphylococci. For SA it is increased from 1.30 to 1.805 Log_2 FC between 3hrs and 24hrs. For SE, IL-23A is increased from 3.36 to 7.27 Log_2 FC.

The genes identified in these lists provide information on the response induced by each species of staphylococcal colonisation on the RHE model. Apart from the IL-17C and IL-23A, SA also upregulates the pro-inflammatory markers uPAR (PLAUR), ADAM8 and versican (VCAN). However, more genes identified within **Table 6.6** and **Table 6.7** indicate an inhibition of epidermal remodelling, demonstrated by the downregulation of LDB2, MXRA5, SYNE1 and PLEC. SA also strongly induces the downregulation of FAM20A at 3hrs (-1.838 Log_2 FC) and 24hrs (-2.705 Log_2 FC), however its role within the skin is undefined and will therefore be considered and reviewed within the discussion.

The response induced by SE colonisation is clearly inflammatory, with more upregulated pro-inflammatory genes than SA (**Table 6.8** and **Table 6.9**). This includes the genes for cytokines such as TNF, CSF2, CSF3, IL-6, IL-20, IL-24; as well as the chemokines CXCL1, CXCL2, CXCL3 and CCL20. However, SE also induces the upregulation of the NF-κB inhibitor TNFAIP3 (also known as A20). This could be an important regulator of inflammation within the response to SE colonisation that needs to be explored within the signal transduction pathways. These pathways relay the communication between the epidermal stimulation and transcription factors generating the response and will be extensively examined in the following chapter of pathway analysis.

Examination of the expression values of the top DEGs for SC colonisation indicates a lesser response induced in comparison to SA or SE (**Table 6.10** and **Table 6.11**), which supports the limited number of DEGs identified (52). Investigating the individual genes of the top DEG lists for SC suggests a minimal response that is less inflammatory.

The main sizeable upregulation at both 3hrs and 24hrs was for the E3 ubiquitin-protein ligase TRIM63, upregulated by 1.035 Log_2 FC (3hrs) and 2.262 Log_2 FC (24hrs). Furthermore, the majority of genes within **Table 6.10** and **Table 6.11** relate to normal cellular processes, such as transcription (RNU2-1, ELF2, CBX3, DDX39A), translation (MRPL39, EIF4ENIF1), signal transduction (DAAM1, BAMBI, TRIB3) and vesicle mediated transport (VPS36, RAB3IP).

Pathway analysis takes into consideration the functional importance of changes in gene expression. It therefore could be more beneficial to understanding the slight changes induced on these normal cellular processes, as well as the larger inflammatory changes induced by SA and SE.

Table 6.6: DEGs of greatest change in the SA gene signature at 3hrs
Top 20 differentially expressed genes of the gene signature generated by colonisation of SA83, sorted by fold change induced at 3hrs. Bold genes indicate presence in top 20 of both 3hrs and 24hrs. Corrected P value: 2way ANOVA of 3hr and 24hr colonisation of SA83 against their time relevant control, using P<0.05 with Benjamini Hochberg FDR as MTC.

Rank at 3hr	Gene Symbol	Description	Corrected P value	Log_2 FC	
				3hr	24hr
1	**IL17C**	**Interleukin 17C**	**0.0035**	**3.570**	**2.211**
2	**FAM20A**	**Family with sequence similarity 20 member A**	**0.0402**	**-1.838**	**-2.705**
3	HBEGF	Heparin-binding EGF-like growth factor	0.002	1.470	0.842
4	**IL23A**	**Interleukin 23, alpha subunit**	**0.0219**	**1.300**	**1.805**
5	KANK4	KN motif and ankyrin repeat domains 4	0.0296	-1.055	-0.715
6	SPRY4	Sprouty homolog 4	0.0368	1.017	0.204
7	RGS5	Regulator of G-protein signaling 5	0.0234	-0.997	-0.211
8	**RABEPK**	**Rab9 effector protein with kelch motifs**	**0.0219**	**-0.931**	**-1.037**
9	DDX60	DEAD (Asp-Glu-Ala-Asp) box polypeptide 60	0.0253	-0.928	-0.280
10	RAP1GAP	RAP1 GTPase activating protein	0.0225	0.877	0.862
11	ERLIN2	ER lipid raft associated 2	0.0415	-0.836	-0.634
12	PLAUR	Plasminogen activator, urokinase receptor	0.0478	0.785	0.982
13	DUSP5	Dual specificity phosphatase 5	0.0397	0.746	0.316
14	**ADAM8**	**ADAM metallopeptidase domain 8**	**0.0225**	**0.723**	**1.294**
15	ERRFI1	ERBB receptor feedback inhibitor 1	0.041	0.695	0.056
16	KLHL3	Kelch-like family member 3	0.0388	-0.679	-0.642
17	GRB7	Growth factor receptor-bound protein 7	0.0433	0.646	0.390
18	NPC1L1	Niemann-Pick C1-Like 1	0.0412	-0.641	-0.970
19	GOLGA8IP	Golgin A8 family, member I, pseudogene	0.0219	-0.633	-0.410
20	**NPL**	**N-acetylneuraminate pyruvate lyase (dihydrodipicolinate synthase)**	**0.0162**	**-0.631**	**-1.547**

Table 6.7: DEGs of greatest change in the SA gene signature at 24hrs

Top 20 differentially expressed genes of the gene signature generated by colonisation of SA83, sorted by fold change induced at 24hrs. Bold genes indicate presence in top 20 of both 3hrs and 24hrs. Corrected P value: 2way ANOVA of 3hr and 24hr colonisation of SA83 against their time relevant control, using P<0.05 with Benjamini Hochberg FDR as MTC.

Rank at 24hr	Gene Symbol	Description	Corrected P value	Log_2 FC 3hr	Log_2 FC 24hr
1	**FAM20A**	**Family with sequence similarity 20 member A**	**0.0402**	**-1.838**	**-2.705**
2	VCAN	Versican	0.0053	0.461	2.667
3	**IL17C**	**Interleukin 17C**	**0.0035**	**3.570**	**2.211**
4	**IL23A**	**Interleukin 23, alpha subunit**	**0.0219**	**1.300**	**1.805**
5	LEP	Leptin	0.0433	-0.199	-1.609
6	**NPL**	**N-acetylneuraminate pyruvate lyase (dihydrodipicolinate synthase)**	**0.0162**	**-0.631**	**-1.547**
7	LDB2	LIM domain binding 2	0.0029	-0.450	-1.502
8	MXRA5	Matrix-remodelling associated 5	0.0175	-0.620	-1.471
9	PDCD6IP	Programmed cell death 6 interacting protein	0.0168	0.248	1.465
10	SLC6A15	Solute carrier family 6 (neutral amino acid transporter), member 15	0.0472	0.345	1.428
11	**ADAM8**	**ADAM metallopeptidase domain 8**	**0.0225**	**0.723**	**1.294**
12	SYNE1	Spectrin repeat containing, nuclear envelope 1	0.0477	0.153	-1.259
13	PLEC	Plectin	0.0328	0.041	-1.189
14	SPRY2	Sprouty homolog 2	0.0432	0.607	1.180
15	WNT4	Wingless-type MMTV integration site family, member 4	0.0399	-0.326	-1.133
16	TMEM200A	Transmembrane protein 200A	0.0273	0.401	1.088
17	HSD17B2	Hydroxysteroid (17-beta) dehydrogenase 2	0.0228	0.255	1.066
18	TM4SF19	Transmembrane 4 L six family member 19	0.0182	0.311	1.059
19	**RABEPK**	**Rab9 effector protein with kelch motifs**	**0.0219**	**-0.931**	**-1.037**
20	FIGNL1	Fidgetin-like 1	0.0225	-0.027	-1.011

Table 6.8: DEGs of greatest change in the SE gene signature at 3hrs

Top 20 differentially expressed genes of the gene signature generated by colonisation of SE12, sorted by fold change induced at 3hrs. Bold genes indicate presence in top 20 of both 3hrs and 24hrs. Corrected P value: 2way ANOVA of 3hr and 24hr colonisation of SE12 against their time relevant control, using P<0.05 with Benjamini Hochberg FDR as MTC.

Rank at 3hr	Gene Symbol	Description	Corrected P value	Log_2 FC 3hr	Log_2 FC 24hr
1	**IL17C**	**Interleukin 17C**	**0.0004**	**6.214**	**6.593**
2	**CXCL3**	**Chemokine (C-X-C motif) ligand 3**	**0.0023**	**4.592**	**5.660**
3	**TNF**	**Tumor necrosis factor**	**0.001**	**4.159**	**6.196**
4	**CXCL2**	**Chemokine (C-X-C motif) ligand 2**	**0.0013**	**4.051**	**5.704**
5	**CCL20**	**Chemokine (C-C motif) ligand 20**	**0.0006**	**3.802**	**5.854**
6	**CSF2**	**Colony stimulating factor 2 (granulocyte-macrophage)**	**0.0007**	**3.578**	**7.269**
7	**IL23A**	**Interleukin 23, alpha subunit p19**	**0.0003**	**3.364**	**5.926**
8	**CXCL1**	**Chemokine (C-X-C motif) ligand 1 (melanoma growth stimulating activity, alpha)**	**0.0065**	**2.738**	**5.021**
9	TNFAIP6	Tumor necrosis factor, alpha-induced protein 6	0.033	2.574	4.251
10	**IL20**	**Interleukin 20**	**0.0015**	**2.429**	**5.015**
11	FMOD	Fibromodulin	0.0155	2.326	1.079
12	CSF3	Colony stimulating factor 3 (granulocyte)	0.0109	2.308	3.187
13	SOCS3	Suppressor of cytokine signaling 3	0.0038	2.291	1.794
14	NFKBIZ	Nuclear factor of kappa light polypeptide gene enhancer in B-cells inhibitor, zeta	0.0003	2.246	1.813
15	**ICAM1**	**Intercellular adhesion molecule 1**	**0.0028**	**2.153**	**4.866**
16	RND1	Rho family GTPase 1	0.0075	2.056	2.717
17	**BIRC3**	**Baculoviral IAP repeat containing 3**	**0.0005**	**2.036**	**4.653**
18	PHGR1	Proline/histidine/glycine-rich 1	0.0325	1.995	0.847
19	TNFAIP3	Tumor necrosis factor, alpha-induced protein 3	0.0007	1.929	4.343
20	**IL6**	**Interleukin 6**	**0.0005**	**1.923**	**4.919**

Table 6.9: DEGs of greatest change in the SE gene signature at 24hrs

Top 20 differentially expressed genes of the gene signature generated by colonisation of SE12, sorted by fold change induced at 24hrs. Bold genes indicate presence in top 20 of both 3hrs and 24hrs. Corrected P value: 2way ANOVA of 3hr and 24hr colonisation of SE12 against their time relevant control, using P<0.05 with Benjamini Hochberg FDR as MTC.

Rank at 24hr	Gene Symbol	Description	Corrected P value	Log_2 FC 3hr	Log_2 FC 24hr
1	**CSF2**	**Colony stimulating factor 2 (granulocyte-macrophage)**	**0.001**	**3.578**	**7.269**
2	**IL17C**	**Interleukin 17C**	**0.000**	**6.214**	**6.593**
3	**TNF**	**Tumor necrosis factor**	**0.001**	**4.159**	**6.196**
4	**IL23A**	**Interleukin 23, alpha subunit p19**	**0.000**	**3.364**	**5.926**
5	**CCL20**	**Chemokine (C-C motif) ligand 20**	**0.001**	**3.802**	**5.854**
6	**CXCL2**	**Chemokine (C-X-C motif) ligand 2**	**0.001**	**4.051**	**5.704**
7	**CXCL3**	**Chemokine (C-X-C motif) ligand 3**	**0.002**	**4.592**	**5.660**
8	ANKRD37	Ankyrin repeat domain 37	0.001	0.789	5.087
9	PTGS2	Prostaglandin-endoperoxide synthase 2 (prostaglandin G/H synthase and cyclooxygenase)	0.001	0.857	5.044
10	**CXCL1**	**Chemokine (C-X-C motif) ligand 1 (melanoma growth stimulating activity, alpha)**	**0.006**	**2.738**	**5.021**
11	**IL20**	**Interleukin 20**	**0.002**	**2.429**	**5.015**
12	IL24	Interleukin 24	0.007	1.237	4.986
13	ANGPTL4	Angiopoietin-like 4	0.001	0.959	4.973
14	**IL6**	**Interleukin 6**	**0.001**	**1.923**	**4.919**
15	**ICAM1**	**Intercellular adhesion molecule 1**	**0.003**	**2.153**	**4.866**
16	TMEM177	Transmembrane protein 177	0.000	-0.496	-4.805
17	IL13RA2	Interleukin 13 receptor, alpha 2	0.002	-0.263	4.687
18	**BIRC3**	**Baculoviral IAP repeat containing 3**	**0.001**	**2.036**	**4.653**
19	G0S2	G0/G1 switch 2	0.020	1.078	4.627
20	EDN2	Endothelin 2	0.001	1.572	4.608

Table 6.10: DEGs of greatest change in the SC gene signature at 3hrs

Top 20 differentially expressed genes of the gene signature generated by colonisation of SC27, sorted by fold change induced at 3hrs. Bold genes indicate presence in top 20 of both 3hrs and 24hrs. Corrected P value: 2way ANOVA of 3hr and 24hr colonisation of SC27 against their time relevant control, using P<0.05 with Benjamini Hochberg FDR as MTC.

Rank at 3hr	Gene Symbol	Description	Corrected P value	Log_2 FC 3hr	Log_2 FC 24hr
1	**TRIM63**	**Tripartite motif containing 63, E3 ubiquitin protein ligase**	**0.042**	**1.035**	**2.262**
2	RNU2-1	RNA, U2 small nuclear 1	0.026	0.843	0.283
3	**SAMD5**	**Sterile alpha motif domain containing 5**	**0.014**	**0.651**	**0.851**
4	CCBL1	Cysteine conjugate-beta lyase, cytoplasmic	0.026	0.530	0.335
5	**TESC**	**Tescalcin**	**0.033**	**0.476**	**1.156**
6	ZFAS1	ZNFX1 antisense RNA 1	0.028	0.345	0.469
7	NLE1	Notchless homolog 1	0.010	0.333	0.145
8	**NDN**	**Necdin, melanoma antigen family member**	**0.025**	**-0.306**	**-1.270**
9	**OAF**	**OAF homolog**	**0.042**	**0.293**	**0.685**
10	DALRD3	DALR anticodon binding domain containing 3	0.010	0.280	0.055
11	RRAS2	Related RAS viral (r-ras) oncogene homolog 2	0.010	0.259	0.432
12	**SLC22A15**	**Solute carrier family 22, member 15**	**0.044**	**0.249**	**0.651**
13	**CPNE8**	**Copine VIII**	**0.044**	**0.240**	**0.702**
14	**EIF4ENIF1**	**Eukaryotic translation initiation factor 4E nuclear import factor 1**	**0.050**	**-0.236**	**-0.799**
15	**ELF2**	**E74-like factor 2 (ets domain transcription factor)**	**0.026**	**0.230**	**0.983**
16	**DAAM1**	**Dishevelled associated activator of morphogenesis 1**	**0.026**	**0.229**	**0.708**
17	SNORD36A	Small nucleolar RNA, C/D box 36A	0.032	0.227	0.564
18	DDX39A	DEAD (Asp-Glu-Ala-Asp) box polypeptide 39A	0.010	0.226	0.472
19	MRPL39	Mitochondrial ribosomal protein L39	0.031	0.226	0.112
20	SLC12A4	Solute carrier family 12 (potassium/chloride transporter), member 4	0.025	0.223	0.442

Table 6.11: DEGs of greatest change in the SC gene signature at 24hrs

Top 20 differentially expressed genes of the gene signature generated by colonisation of SC27, sorted by fold change induced at 24hrs. Bold genes indicate presence in top 20 of both 3hrs and 24hrs. Corrected P value: 2way ANOVA of 3hr and 24hr colonisation of SC27 against their time relevant control, using P<0.05 with Benjamini Hochberg FDR as MTC.

Rank at 24hr	Gene Symbol	Description	Corrected P value	Log_2 FC 3hr	Log_2 FC 24hr
1	**TRIM63**	**Tripartite motif containing 63, E3 ubiquitin protein ligase**	**0.042**	**1.035**	**2.262**
2	AJAP1	Adherens junctions associated protein 1	0.035	-0.053	1.324
3	**NDN**	**Necdin, melanoma antigen (MAGE) family member**	**0.025**	**-0.306**	**-1.270**
4	**TESC**	**Tescalcin**	**0.033**	**0.476**	**1.156**
5	MICAL3	Microtubule associated monooxygenase, calponin and LIM domain containing 3	0.032	0.147	-0.988
6	**ELF2**	**E74-like factor 2 (ets domain transcription factor)**	**0.026**	**0.230**	**0.983**
7	RCCD1	RCC1 domain containing 1	0.025	-0.095	-0.925
8	BAMBI	BMP and activin membrane-bound inhibitor	0.020	0.105	0.920
9	**SAMD5**	**Sterile alpha motif domain containing 5**	**0.014**	**0.651**	**0.851**
10	VPS36	Vacuolar protein sorting 36 homolog	0.011	-0.159	-0.844
11	**EIF4ENIF1**	**Eukaryotic translation initiation factor 4E nuclear import factor 1**	**0.050**	**-0.236**	**-0.799**
12	RAB3IP	RAB3A interacting protein	0.011	0.165	0.751
13	LYPLAL1	Lysophospholipase-like 1	0.025	0.157	-0.718
14	**DAAM1**	**Dishevelled associated activator of morphogenesis 1**	**0.026**	**0.229**	**0.708**
15	**CPNE8**	**Copine VIII**	**0.044**	**0.240**	**0.702**
16	**OAF**	**OAF homolog**	**0.042**	**0.293**	**0.685**
17	ATG4C	Autophagy related 4C, cysteine peptidase	0.035	-0.203	-0.685
18	**SLC22A15**	**Solute carrier family 22, member 15**	**0.044**	**0.249**	**0.651**
19	CBX3	Chromobox homolog 3	0.029	0.173	0.588
20	TRIB3	Tribbles pseudokinase 3	0.025	0.205	0.575

6.2.4 Targeted analysis of inflammatory mediators

Previous analysis of the microarray results used a non-hypothesis driven approach to identify changes in gene expression important to staphylococcal colonisation. However, chapter 5 proposed a number of cytokines, chemokines and growth factors that could be acting as immune modulators and were of interest to study. To examine the gene transcript signal of the protein molecules identified in Chapter 5, the relative gene expression (**Figure 6.6**) of previously identified soluble cytokines and chemokines was examined.

At 3hrs (**Figure 6.6a**) the majority of immune modulators examined show only minimal changes in both gene and protein expression, this included angiogenin, EMMPRIN, IL-22, PDGF-AA or VEGF. However, there are some similar changes in expression of gene and protein, but not by equivalent amounts. This includes increases in CXCL1 induced by SA83, SE12 and SA27; but not SC27. As well as an SE12 induced increase in IL-8.

At 24hrs (**Figure 6.6b**) there is disparity between the change in gene and protein expression induced by the staphylococcal colonisations. This is most evident for the large increases induced by SE12 upon the gene expression of CXCL1, CXCL2, GM-CSF, IL-1α, IL-1β, IL-6 and TNFα; all of which are above 2 Log_2 FC. Whereas, change in protein expression by SE12 for GM-CSF, IL-1α, and TNFα was inferior, with an upregulation of below 1 Log_2 FC. Furthermore, SE12 induces an opposing downregulation of protein expression for CXCL1, CXCL2, IL-1β and IL-6. The divergences in gene and protein expression could suggest these genes are suffering from post transcriptional regulation of protein synthesis.

Additionally, the SA specific increase in sCD14 expression noted in chapter 5 was not reflected in the gene expression. However, there was a relative decrease in gene expression induced by SE12, therefore it could be due to high expression of the control. Alternatively, a single CD14 gene is used to code for sCD14 and membrane bound CD14 (mCD14), thus gene and protein expression may not correspond.

On the other hand, change in gene expression induced by SC27 colonisation is more similar to the change in protein expression, with similar increases in expression of GM-CSF, IL-1α and sIL-4Rα. As well as only minimal gene in other immune modulators.

The change induced by SA83 colonisation also shows disparity between gene and protein, particularly for CXCL1, CXCL2, CXCL5 and IL-1β. However, there are similarities in gene and protein expression of the important pro-inflammatory cytokines TNFα and GM-CSF, indicating the pro-inflammatory nature of the response.

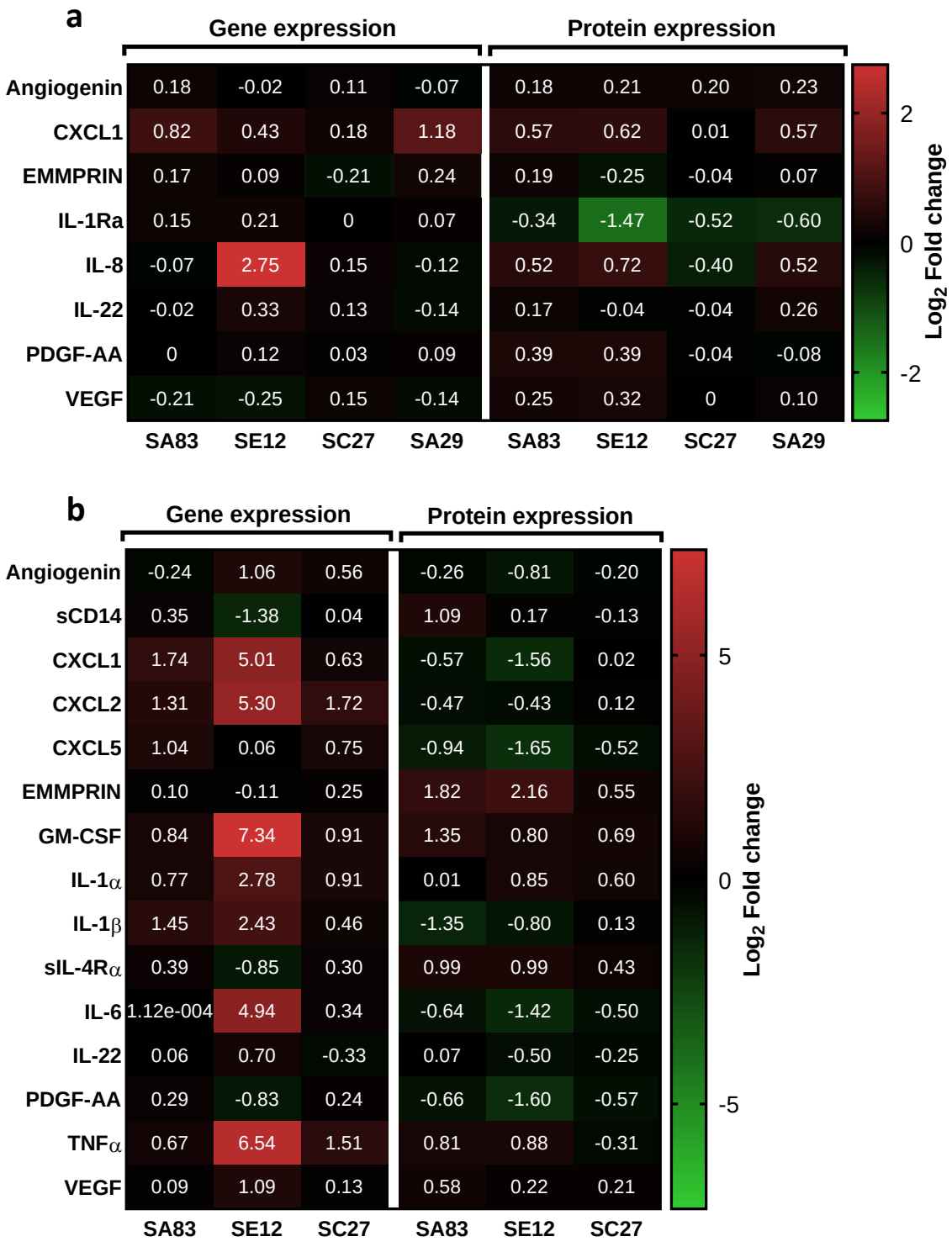

Figure 6:6: Comparison of staphylococcal colonisation induced change in gene and protein expression

Heatmap comparing change in gene expression (microarray) and protein release (luminex) induced by (**a**) 3hrs and (**b**) 24hrs of staphylococcal colonisation. RHE models inoculated with SA83 (8325-4), SE12 (12228), SC27 (27840) and SA29 (29213) at 10^6 CFU in 100 µl PBS. Undernatant harvested for analysis of protein release (n=2) and model lysed for gene expression (n=3/4). Data expressed as mean of Log_2 fold change from time relative control of 100µl PBS.

Analysis of transcripts not measured in the previous assay of protein expression (**Figure 6.7**) demonstrated an upregulation of a number of genes. These pro-inflammatory cytokines and chemokines were upregulated by each staphylococcal colonisation, although SE12 generated the largest increases in expression change. At 3hrs this included CXCL2, GM-CSF, IL-23, pentraxin-3 and TNFα. Furthermore, comparison between SA83 and SA29 indicates very similar changes in expression in each of these noted cytokines and chemokine; apart from IL-23, which was further upregulated by SA83. This could suggests a more similar inflammatory profile between SA strains than other species.

The change in gene expression at 24hrs was similar to 3hrs, with further increases induced by SE12 than by SA83 or SC27. This was most evident in the expression of IL-23, pentraxin-3 and uPAR, but occurs to a lesser extent in the majority of the immune modulators examined.

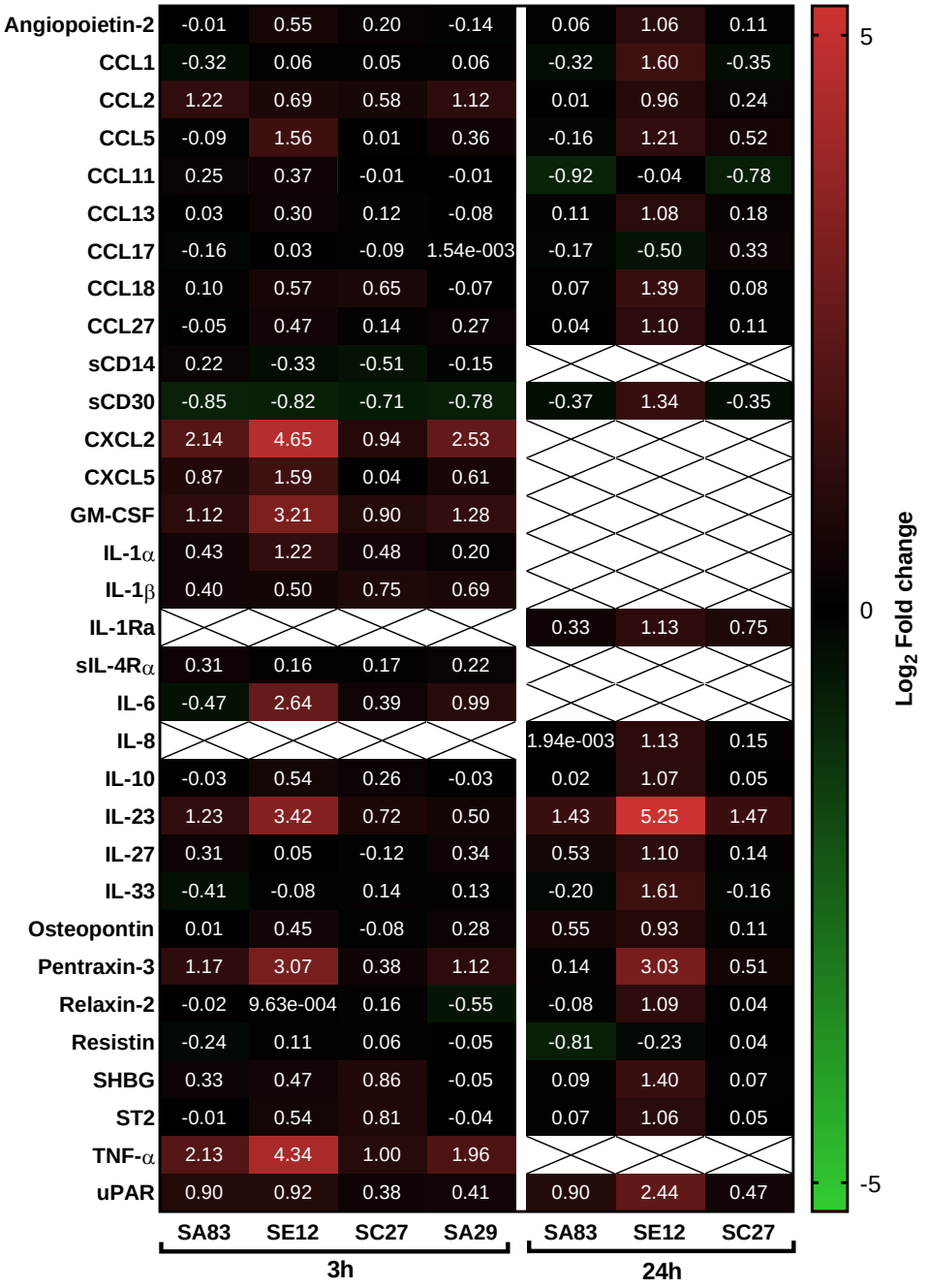

Figure 6:7: Staphylococcal colonisation induced change in gene expression for previously analysed mediators of interest

Heatmap of change in gene expression induced by staphylococcal colonisation for immune mediators that previously exhibited unquantifiable protein release. RHE models inoculated with SA83 (8325-4), SE12 (12228), SC27 (27840) and SA29 (29213) at 10^6 CFU in 100 µl PBS for 3 and 24hrs. Models lysed for gene expression. Data expressed as mean of Log_2 fold change from time relative control of 100µl PBS. (n=3/4). Gaps represent mediators with null results for only one timepoint.

6.2.5 Staphylococcal induced AMP expression

Previous results demonstrated a gradual reduction over time in the colonisation of the epidermal model, when colonised with a high CFU of SA83 (Chapter 4). The data suggested SA83 specific inhibition may be mediated by epidermal synthesis of AMPs. To assess this possibility, expression of epidermal synthesis of AMP transcripts following staphylococcal colonisation were assessed from the microarray data (**Figure 6.8**).

Staphylococcal colonisation showed variable AMP expression between species, as well as between timepoints. Most notable was the upregulation of RNase 7, S100A12, hBD2 and hBD3 by SA83, but corresponding downregulation by SA29, which was not inhibited by the RHE model. These differences occurred at 3hrs of colonisation, which coincides with the steepest rate of change in bacterial CFU (**Figure 4.1**). Examination of these AMPs at 24hrs indicates a reduction in expression induced by SA83 to levels that parallel the 3hr expression of SA29, apart from hBD2. However, the amount of change in expression induced by SA83 at 3hrs is above 0.5 Log_2 FC (equating to 1.42 FC) and therefore is not extensive.

SA83 also upregulates different AMPs at 24hrs, specifically LL-37 and S100A15, which are also upregulated by SE12 and SC27.

SE12 is not inhibited by the RHE model, but does upregulate expression of numerous AMPs. At 3hrs, this includes increases in expression above a 1 Log_2 FC of psoriasin, S100A12, S100A15 and hBD2. At 24hrs, SE12 induces more AMPs upregulated above 1 Log_2 FC, which includes LL-37, angiogenin, S100A8, S100A15, hBD2, hBD3 and hBD4.

At both timepoints the change induced on AMPs expression by SC27 resembles that of SE12, but to a lesser extent for each AMP. This could suggest a similar AMP response, but with less magnitude due to the stagnant colonisation of SC27 that does not proliferate.

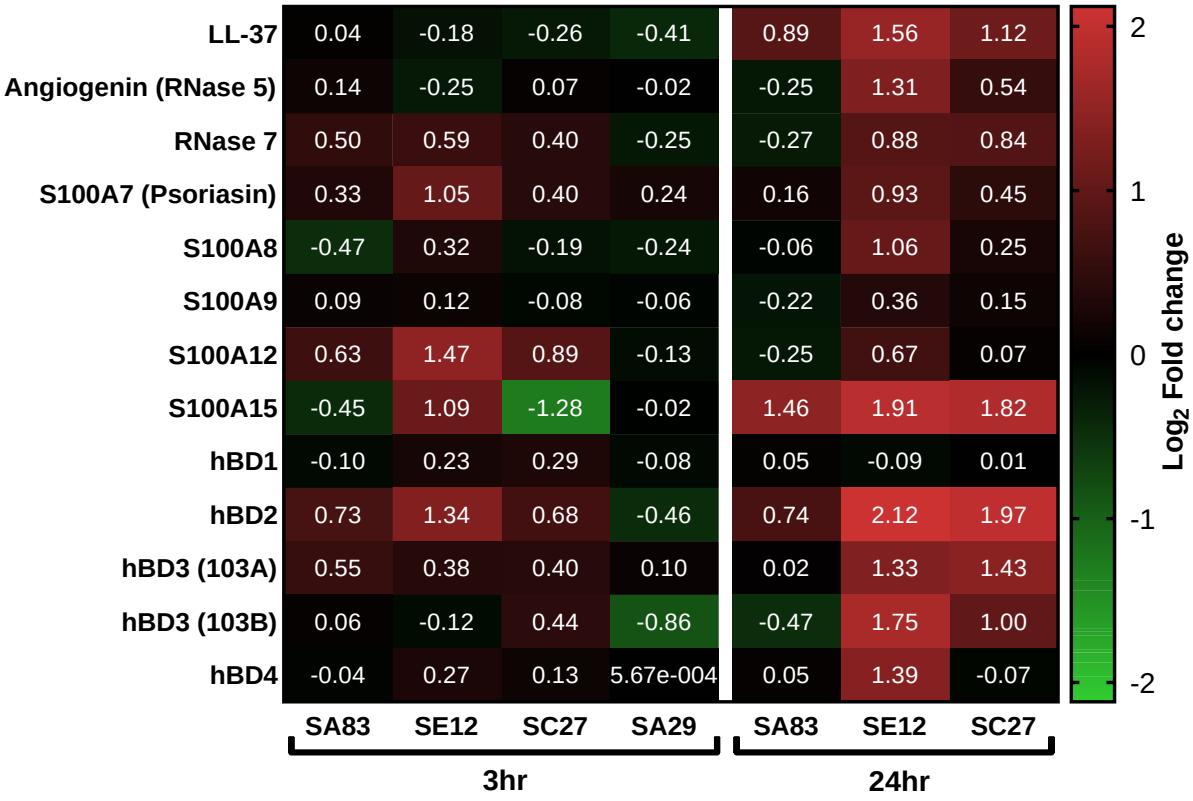

Figure 6:8: Staphylococcal colonisation induced change in gene expression of AMPs
Heatmap of change in gene expression induced by staphylococcal colonisation for various AMPs. RHE models inoculated with SA83 (8325-4), SE12 (12228), SC27 (27840) and SA29 (29213) at 10^6 CFU in 100 µl PBS for 3 and 24hrs. Models lysed for gene expression. Data expressed as mean of Log_2 fold change from time relative control of 100µl PBS. (n=3/4).

6.3 Discussion

This chapter aimed to investigate the outcome on gene expression in the epidermal models following exposure to different staphylococcal species. By employing a non-hypothesis driven approach, the system was designed to identify all key genes involved in the epidermal response and facilitate examination of similarities and differences in expression following exposure to different staphylococci. The microarray system used in this research measured changes in expression of 58341 entities, with 300 biological probes replicated 10 times, as well as 96 ERCC control probes and 10 E1A control probes to provide a statistically robust approach. The ERCC (External RNA Control Consortium) control probes and E1A (Adenovirus E1A gene) control probes provide controls from the spike-in mix that enable internal assessment of the microarrays reliability, as wells as allowing for cross-platform comparisons between major microarray manufacturers (McCall and Irizarry, 2008). Using the classical analysis post normalisation and flag based filtering differentially expressed genes between the control (PBS) and staphylococci exposure were found only for SE at 3 hours and 24 hours. We determined that the problem with the sampling approach was the variability of gene expression within replicates, which resulted in reduced statistical power. To overcome this we combined the 3 hour and 24 hour time points. Whilst this approach succeeded in identifying more DEGs, it assumes that the combination does not introduce bias into the system. Analysis showed that the top DEGs identified from the combined timepoints analysis were also prominent among the maximally differentially expressed genes at the individual time points giving us reassurance that this approach did not significantly bias our analysis against one of the time points.

Global examination of the number of DEGs from the transcriptomic data showed that inoculation with SE induced more changes in gene expression than that identified by SA or SC. Analysis of the hierarchical clustering of transcripts induced by SE also emphasised the strong transcriptional signal with SE, which was increased over time. In considering the implications of these findings, it is important to recognise that the absolute load of bacteria was different for the various pathogen exposures. This is because, as shown in Chapter 4, different staphylococcal species show different patterns of proliferation on RHE models and for SA, at least, the epidermal models were effective inhibitors of the bacteria. It was in light of this understanding of pathogen load that the 3 hour time point was chosen, because it was deemed that this would have been adequate time to induce some transcriptional changes whilst yet also showing limited inhibition of SA. However, the 3 hour time point proved less informative than hoped, and the 24 hour time point appeared to show limited modification by SA or SC. Therefore combining both time points was a pragmatic solution to the analytical problem. However, in retrospect, it would have been ideal to have increased the number or replicates at each time point to facilitate separate analysis.

Examination of DEGs of greatest change for each staphylococcal signature demonstrates a differential response to each colonisation. Investigation of the function of these DEGs provides some understanding of the changes induced during the colonisation, therefore comparison between these functions may provide understanding of how the colonisations differ.

The DEGs of greatest change induced at 3 hours and 24 hours of SA colonisation indicated an inflammatory response, primarily mediated via IL-17C and IL-23A. However upregulation of uPAR, ADAM8 and versican also indicate an inflammatory response. uPAR (urokinase plasminogen activator receptor) is a receptor aiding in migration and recruitment, functioning as a chemoattractant when cleaved from the cell surface. Consequently, it is upregulated in bacterial and viral infections (Rijneveld et al., 2002, Ramos et al., 2015). ADAM8 (a disintegrin and metalloproteinase domain-containing protein 8) is a transmembrane proteases with an undefined function in the skin. However, it is upregulated by TNFα (Schlomann et al., 2000) and strongly correlated with severity of the inflammatory phenotype of asthma and chronic obstructive pulmonary disease (COPD) (Oreo et al., 2014). Versican is an extracellular matrix proteoglycan, involved in adhesion, migration and proliferation. However, it also acts as a regulator of inflammation (Wight et al., 2014). Alternatively, these markers of inflammation could relate to epidermal remodelling via their role in migration, proliferation or recruitment. Inhibition of epidermal remodelling was the other dominant response indicated by the DEGs of greatest change induced by SA colonisation.

SE colonisation induced an upregulation in a large number of inflammatory genes that dominate the response displayed in the lists of greatest changed DEGs. Although this gene expression response is primarily inflammatory, it also includes the inflammatory regulator A20 (TNFAIP3). Furthermore, comparison of gene and protein expression displays disparity in the change induced by SE. Which suggests inflammation is not the only element of the SE induced response.

Colonisation of SC was shown to be the most inconsequential and lacked immune regulators. It mainly displayed small changes to a number of cellular processes, such as signal transduction, transcription, translation and vesicle mediated transport. However, it also showed a larger increase in expression of TRIM63, an E3 ubiquitin-protein ligase, which is involved in enabling protein degradation.

6.3.1 TRIM63

TRIM63 (Tripartite motif containing 63, also known as MURF-1) is the most preeminent differentially expressed gene induced by SC colonisation, which is upregulated at 3hrs and further upregulated after 24hrs. It encodes for an E3 ubiquitin-protein ligase, which is involved in enabling protein degradation. It is most notable for its involvement in myofibrillar protein degradation (Witt et al., 2005) and has even been proposed as a biomarker of muscle damage (Baumert et al., 2018). However it has been notably upregulated in microarray studies of nervirapine induced skin rash (Zhang et al., 2013) and skin pigmentation, including hyperpigmentation (Yin et al., 2015) and UV induced (Choi et al., 2010). Despite none of these elucidating the role of TRIM63 in the skin, it does expose a currently unknown function within the skin. The TRIM protein superfamily contains over 60 members, many of which are E3 ubiquitin ligases and therefore degrade or modulate the function of a substrate (Ozato et al., 2008). Some of these have been shown to regulate immune responses, IFN induction, transcriptional responses and inflammasome activity (Jefferies et al., 2011). Whilst it is different TRIM proteins responsible for these actions the wide variety of functions brings into question the role of TRIM63 within the skin.

6.3.2 Epidermal remodelling

After 24 hours of colonisation SA induces downregulation of LDB2, PLEC, SYNE1 and MXRA5 implying an inhibition of epidermal remodelling. LIM domain binding 2 (LDB2, also known as CLIM1) is a cytoskeletal adaptor protein, which escorts proteins to the cytoskeleton through interaction with α-actinins (Kotaka et al., 2000, Bach, 2000). Plectin (PLEC) acts in organisation by functioning as a cytoskeletal linker protein of microtubules, microfilaments and intermediate filaments. Plectin also links these cytoskeleton components with desmosomes and hemidesmosomes (Wiche, 1998). Spectrin repeat containing, nuclear envelope 1 (SYNE1, also known as enaptin) binds both actin and the nuclear membrane, suggesting involvement with cytoskeleton integration to the nucleoskeleton (Padmakumar et al., 2004). As well as the matrix remodeller MXRA5, which also acts as an anti-inflammatory (Poveda et al., 2017). The downregulation of epidermal remodelling could be induced by SA to inhibit wound repair or induce barrier dysfunction. SA has been shown to inhibit wound repair during infection (Grimble et al., 2001) and has been attributed to staphylococcal eap (extracellular adherence protein) induced inhibition of integrin activity (Athanasopoulos et al., 2006).

Alternatively, dsyregulation of barrier function is an important feature of AD. A certain aspect of barrier dysfunction can be exhibited by low expression of the cytoskeleton coordinator RABGEF1 (RAB guanine nucleotide exchange factor 1). It was shown to be diminished in AD lesional skin, as well as a mouse model of AD, generated by repeated exposure to house dust mite and SEB (staphylococcal enterotoxin B) of SA (Marichal et al., 2016). Additionally, filaggrin deficiency is one of the most investigated genetic predispositions to AD (Zaniboni et al., 2016). This is due to its role in flattening corneocytes during terminal differentiation (Sandilands et al., 2009). This process relies on cytoskeleton rearrangement to bundle keratin filaments during cornification. A necessary arrangement for effectual barrier formation of the stratum corneum. Therefore, dysfunction of cytoskeleton rearrangement by LDB2, PLEC and SYNE1 may also inhibit cornification. Although these genes have not currently been directly associated to AD, their downregulation could be beneficial for generating a more favourable niche for colonisation.

Furthermore, the downregulation of FAM20A was also shown to be a highly ranked DEG in SA colonisation at both 3hrs and 24hrs, with further reduction overtime. Nothing is known about FAM20A's role in the skin. Most functional information on FAM20A is based on its mutation causing a number of different enamel deformities and thus it has been shown to aid in biomineralisation (Zhang et al., 2018). However, FAM20A is a pseudokinase that functions by forming a complex with FAM20C and has been shown to regulate its localisation (Ohyama et al., 2016). A decrease in FAM20A results in poor secretion of FAM20C. FAM20C is more studied and has been shows to be able to phosphorylate a large number of secreted phosphoproteins. Tagliabracci et al. (2015) identified over 100 substrates for FAM20C and thus suggested it has a broad biological role, affecting lipid homeostasis, wound healing, cell migration and adhesion. Therefore, downregulation of FAM20A could be related to impaired epidermal remodelling, which also suggests an unexplored role of FAM20A in the skin.

6.3.3 IL-17 and associated pathways

The main response shown by the differential gene expression induced by SA colonisation was the increase in IL-17C and IL-23, which was also identified in the SE colonisation.

Evaluating the largest changes in gene expression within the SA gene signature shows that colonisation induces a phenotype of downregulated growth and remodelling, but also induces upregulation of inflammatory markers, such as IL-17C, IL-23A and ADAM8 (Zarbock and Rossaint, 2011). The SA gene signature presents as an inflammatory response to the colonisation, with IL-

17C clearly being a considerable factor involved in the response. At 3hrs it is upregulated by 3.57 log2 FC (equating to a fold change of 11.8) and after 24hrs it is upregulated by 2.211

The DEGs of largest change induced by SE appears to show an inflammatory profile of SE at both 3hrs and 24hrs, whilst this includes upregulation of IL-17C and IL-23 it also includes many other proinflammatory markers. For example, at both timepoints SE induces the upregulation and increase of proinflammatory cytokines TNFα, GM-CSF (CSF2), G-CSF (CSF3), IL-20 and IL-6. As well as proinflammatory chemokines CCL20, CXCL1, CXCL2 and CXCL3. Another proinflammatory marker upregulated by SE colonisation was ICAM1, which functions as an endothelial regulator of leukocytes trafficking and has been shown to be critical to lymphocyte homing to the skin. The recruitment of leukocytes occurs due to chemotaxis generated by chemokines, such as the neutrophil chemoattractants CXCL1 (Sawant et al., 2016), CXCL2 (De Filippo et al., 2013) and CXCL3 (Griffith et al., 2014). As well as DC and T cell chemoattractant CCL20 (Schutyser et al., 2003). The IL-6 expression also indicates a shift from a neutrophil response to one conducted by monocytes (McLoughlin et al., 2004). However, chemokines can also have other functionality, such as immunomodulatory and antimicrobial activities. More specifically CXCL1, CXCL2, CXCL3 and CCL20 have antimicrobial activity against a variety of bacteria, including SA (Yang et al., 2003). But in general the increased expression of CXCL1, CXCL2, CXCL3 and CCL20 is characteristic of keratinocytes response to IL-17 (Nograles et al., 2008), suggesting IL-17C is also the major component of the epidermal response to SE colonisation.

The IL-17 response induced by SA and SE is characteristic of a normal epidermal response to bacteria, activating the keratinocyte NLRP inflammasome and the immune system (**Figure 6.9**), which results in the stimulation of antimicrobial defence mechanisms (Speeckaert et al., 2016). Inflammasomes are assembled in the cytosol by stimulated PRRs to produce multiprotein complexes, which activate inflammatory caspase cascades to generate a cytokines and chemokine response (Broz and Dixit, 2016). This includes a number of cytokines and chemokines upregulated by SE, such as CXCL1, CXCL2, CXCL3 and CCL20. IL-17C is an epithelial specific isoform of IL-17 that acts in an autocrine manner to regulate an epithelial immune response (Ramirez-Carrozzi et al., 2011).

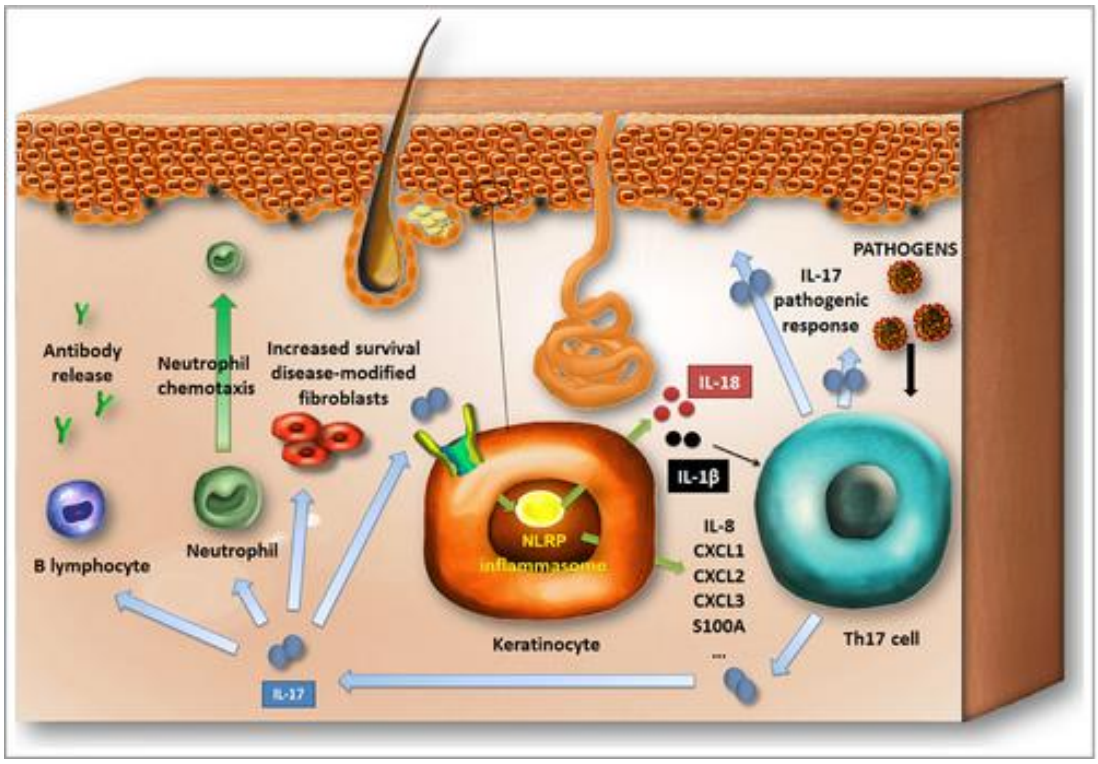

Figure 6:9: Cutaneous interleukin-17 response to pathogens
Pathogenic induced effect of IL-17 on keratinocytes and immune cells in the skin, showing the keratinocyte cytokine and chemokine response generated by NLRP inflammasome. (Speeckaert et al., 2016)

IL-23 is an important aspect of the IL-17 response, functioning to differentiate naïve $CD4^+$ T cells into Th17 cells with the aid of IL-6 and TGF-β, but also inducing the production of inflammatory cytokines facilitating the inflammatory response (Iwakura and Ishigame, 2006). For example, the IL-23 induced expression of TNFα and IL-1β from macrophages and DCs (Cua et al., 2003).

Similar microarray analysis of SA and SE colonisation was performed by Holland et al. (2009) but with differing results. They show 24hrs of SA colonisation to induce a more inflammatory profile with upregulation of IL-17, IL-23, TNFα, GM-CSF, IL-8, IL-1α and IL-1β. As well as AMPs such as hBD4, S100A12 and S100A15. However, SA was not inhibited by their full thickness skin model and therefore corresponds to the colonisation of SA29, which was shown to be more inflammatory in chapter 5. Alternatively and opposing to results of this research, 24hrs of SE colonisation by Holland et al. (2009) only induced a change in a few genes, which included the downregulation of AMPs such as hBD3, hBD4, psoriasin (S100A7), S100A12 and S100A15. The only corresponding change in gene expression of SE was an increase in pentraxin-3 that was similarly generated in this research. Pentraxin-3 is a soluble PRR that acts as an acute phase response protein to aid in the phagocytosis of bacteria, but also has other situational roles in inflammation (Mantovani et al., 2008).

6.3.4 Inflammatory regulation

SE colonisation also upregulated the NF-κB inhibitor A20 (TNFAIP3). The extent of this upregulation and incorporation into the lists of most changed DEGs suggests regulation of inflammation was also a meaningful aspect of the response. A20 inhibits TRAF6, a pathway mediator of the IL-1R/TLR4 activation of NF-κB, which is a major proinflammatory transcription factor (Shembade et al., 2010). Upregulation of A20 therefore negatively regulates inflammation. Furthermore, downregulation of A20 in the epidermis is associated to the inflammatory skin diseases AD and psoriasis. This was identified in transcriptomic analysis of diseased skin and verified by an increased susceptibility to both disease like phenotypes in epidermis-specific A20 knockout mice (Devos et al., 2018). The negative regulation of A20 opposes the remaining pro-inflammatory response induced by SE, it could therefore suggest the formation of a negative feedback loop (Mouton-Liger et al., 2018); limiting the response to SE colonisation.

6.3.5 Differing gene and protein expression

Analysis of inflammatory markers that compared staphylococcal induced change in gene and protein expression showed disparity between increases in mRNA and the actual protein release by the epidermal model. This was particularly notable for the change induced by SE colonisation, which at 24hrs demonstrated high increases in mRNA expression for important inflammatory cytokines and chemokines; such as TNFα, GM-CSF, IL-1α, IL-1β, IL-6 CXCL1 and CXCL2. The change in protein release of these cytokines and chemokines was shown to be either a slight increase (TNFα, GM-CSF, IL-1α) or a decrease (IL-1β, IL-6, CXCL1, CXCL2) from the control. This disparity could suggest inhibition of a cellular process between transcription generating the increase in mRNA and the extracellular release of the protein. The inhibition could be occurring during translation, post-translational modification, protein folding or during transport along the secretory pathway. Current analysis of the top DEGs of the staphylococcal induced gene signatures did not allude to changes involving these cellular processes. However, gene expression analysis that considers functional involvement along signalling pathways may be more insightful in regards to revealing changes to these cellular processes.

6.3.6 AMP expression

Analysis of the transcriptomic data also enabled study of the staphylococcal induced change to specific genes. Therefore, staphylococcal induced changes to AMP expression was analysed. This aimed to investigate the hypothesis that AMP expression is differentially regulated by the different strains, which is based on the quantification of colonisation of chapter 4. The results showed a difference in expression of a number of AMPs between SA83 and SA29, which were the two differentially regulated strains of SA. Whilst these differences were not large or significant, the combination of different AMPs may have resulted in a larger impact to inhibit SA growth (Midorikawa et al., 2003). SE12 and SC27 also showed increased expression of numerous AMPs, but were not inhibited when investigated in chapter 4. This could suggest resistance of the staphylococci to the AMPs, as previously discussed in chapter 4. Alternatively, there could be disparity between the gene expression and the protein release, similarly to the inflammatory markers discussed above. Consequently, further determination of the AMP induced affects from staphylococcal colonisation would require study of the AMPs released into the undernatant by the RHE model.

Overall this analysis demonstrated differing proinflammatory responses to SA and SE colonisation, but both are distinguished by IL-17. It also demonstrated a minimal response to SC colonisation. To further examine these responses and how they differ, the signalling pathways causing them will be investigated to assess how they are provoked and regulated.

Chapter 7: Chapter 7: pathway analysis

7.1 Introduction

The previous chapter analysed the epidermal response to staphylococcal colonisation by characterising the DEGs significant to each species. Whilst identification of DEGs induced by exposure of skin to pathogens can describe the specific molecular changes that arise within the epidermis from colonisation, these lists are challenging to assimilate to better understand the cellular process that are responding to pathogens. To better understand the interaction of epidermal keratinocyte cellular machinery in sensing and responding to skin bacteria, pathway analysis was undertaken.

Pathway analysis is a broad term to describe analysis of a gene expression database to highlight correlated changes in defined sets of genes within canonical or pre-defined pathways. This is based on the knowledge of the pathway and indicates how these expression changes impact the functional responses. It therefore requires data input of the gene list, the expression data and curated knowledge about cellular pathways. There are many different systems of analysis possible, most of which can be grouped into over-representation analysis, functional class scoring or pathway topology (Khatri et al., 2012). Here, over-representation analysis was undertaken with Ingenuity Pathway Analysis (IPA) software (QIAGEN). IPA determines associations between each gene of the dataset to the different pathways and then calculates their significance. The proportion of significant genes of a specific pathway are compared to all the significantly associated genes that are not associated to that specific pathway (Cirillo et al., 2017). This provides a statistical measure (P-value calculated by right-tailed Fisher's exact test) of the overlap between genes associated to the pathway against the remaining dataset. Each pathway identified in the IPA software, is considered a network of associated genes connected by the known relationships of the curated knowledge. IPA aims to identify relationships, mechanisms, functions, and pathways relevant to the dataset using the curated knowledge of the ingenuity knowledge base (Kramer et al., 2014).

To further characterise the epidermal response to staphylococcal colonisation, this chapter aims to use pathway analysis to explore the most activated or inhibited pathways in epidermal models following colonisation with skin pathogens and relate these to biological function. The data will be used to cross-compare biological responses to pathogens and the behaviour of pathogens and immune signalling modelled in previous chapters.

7.2 Results

7.2.1 Pathway analysis

The initial step in pathway analysis requires the selection of genes for analysis. By reducing the threshold for differential expression cut-off, thereby increasing the number of genes in the analysis, the data set will be broader and more comprehensive, but the power to distinguish activated from unaffected signalling pathways will be reduced. Thus, the stringency of gene selection impacts the reliability of the results.

The transcript lists included for analysis were collated from all differentially expressed genes from each pathogen exposure model to construct a comprehensive list. Analysis of such a combined list was undertaken so that all gene transcripts significantly changed in expression by any of the studied staphylococci, would be analysed across the studied staphylococcus genus. The combined transcript list together with relevant expression data was imported into IPA from both time points: 3hrs and 24hrs. This derivation of entity lists is summarised in the flow diagram **Figure 7.1**. To increase the stringency of the entity lists, a 1.2 fold cut off was applied that excludes results between 1.2 and -1.2 fold change. This reduced the transcript signals analysed from 4959 to 1013-4830 per experiment as described in **Figure 7.1.** Therefore genes of minimal expression change were excluded, to balance noise versus signal. This also forms lists within the recommended boundary (500-5000) of IPA's core analysis.

Analysis of the refined entity lists showed that there was considerable overlap between genes which were upregulated or downregulated in response to different staphylococci (**Figure 7.2**). At 3hrs the same 385 (188 up + 197 down) genes were differentially expressed by all three pathogens, which represents a large proportion of all genes modified by each pathogen (38% SA; 23% SC; 18% SE). The overlap between the list of genes up or down regulated by both SA and SC was greater than that seen when comparing SC and SE (70% vs 55% respectively). At 24 hours, 777 genes were up (471) or down (306) regulated in the same way overall by all three pathogens (representing 58% SA; 16% SE; 28% SC of all genes modified). However, at this later timepoint the differences induced by the staphylococci were far fewer. The total number of genes regulated by both SA and SE remained stable, but SC became much more similar to SE and the binary 'off or on' transcriptomic signal from SC was almost perfectly replicated in the signals identified in SE (SE 97% similar vs SA 72% similar to SC). However, the gene signature from SE was overall broader than SC and even broader as compared to SA, where 45% of the SE gene signature was distinct from SC, in comparison to 80% of the SE signature which was distinct from SA.

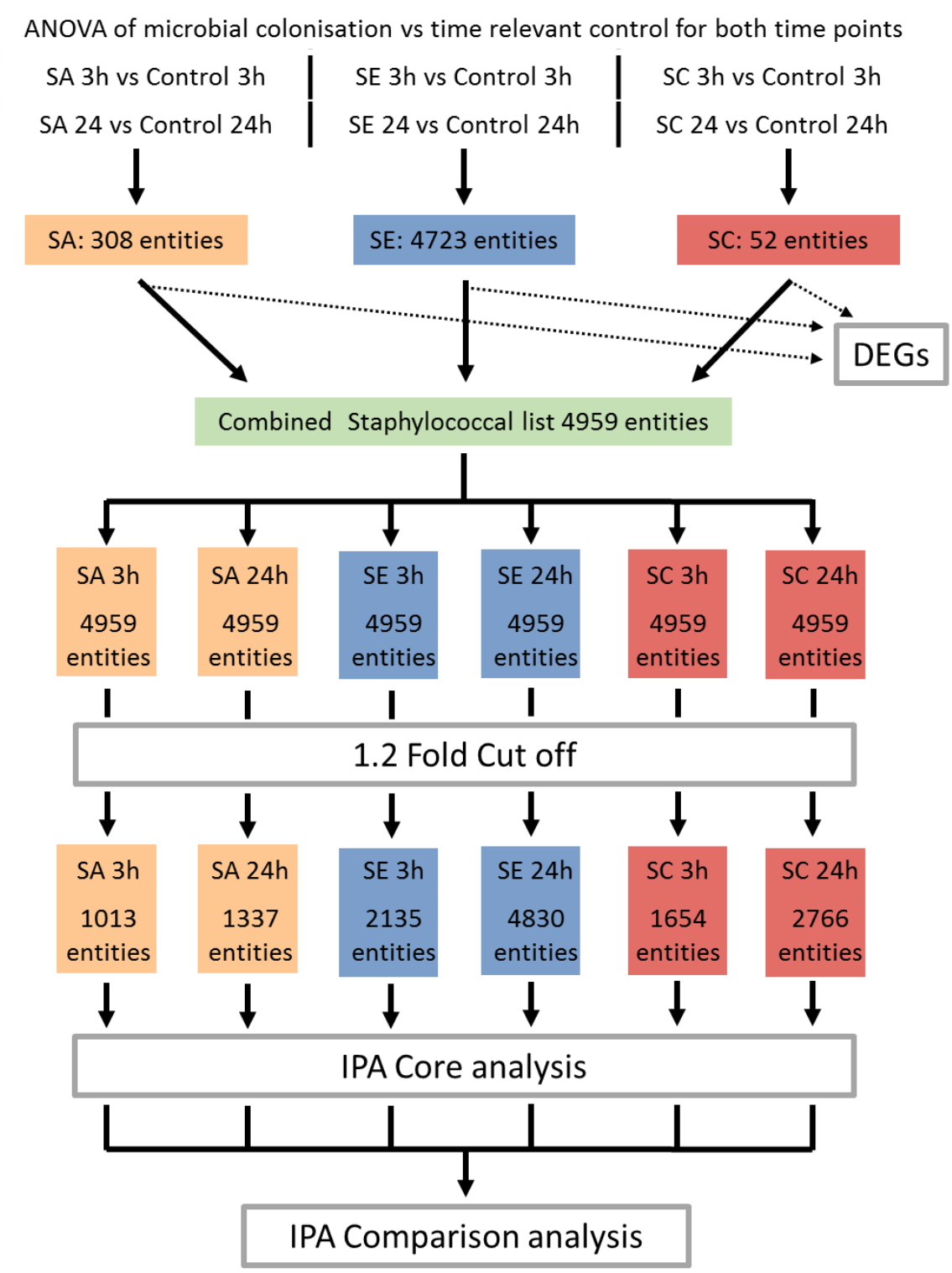

Figure 7:1: Flow diagram of staphylococcal entity lists for pathway analysis
Flow diagram summarising the derivation of the entities lists used in IPA. Displaying the separate lists used for SA (8325-4), SE (12228) and SC (27840); at 3 and 24hrs. Displaying the refinement of each entity list generated by the 1.2 fold change cut off, the core analysis per individual treatment and the merger of lists in the comparison analysis.

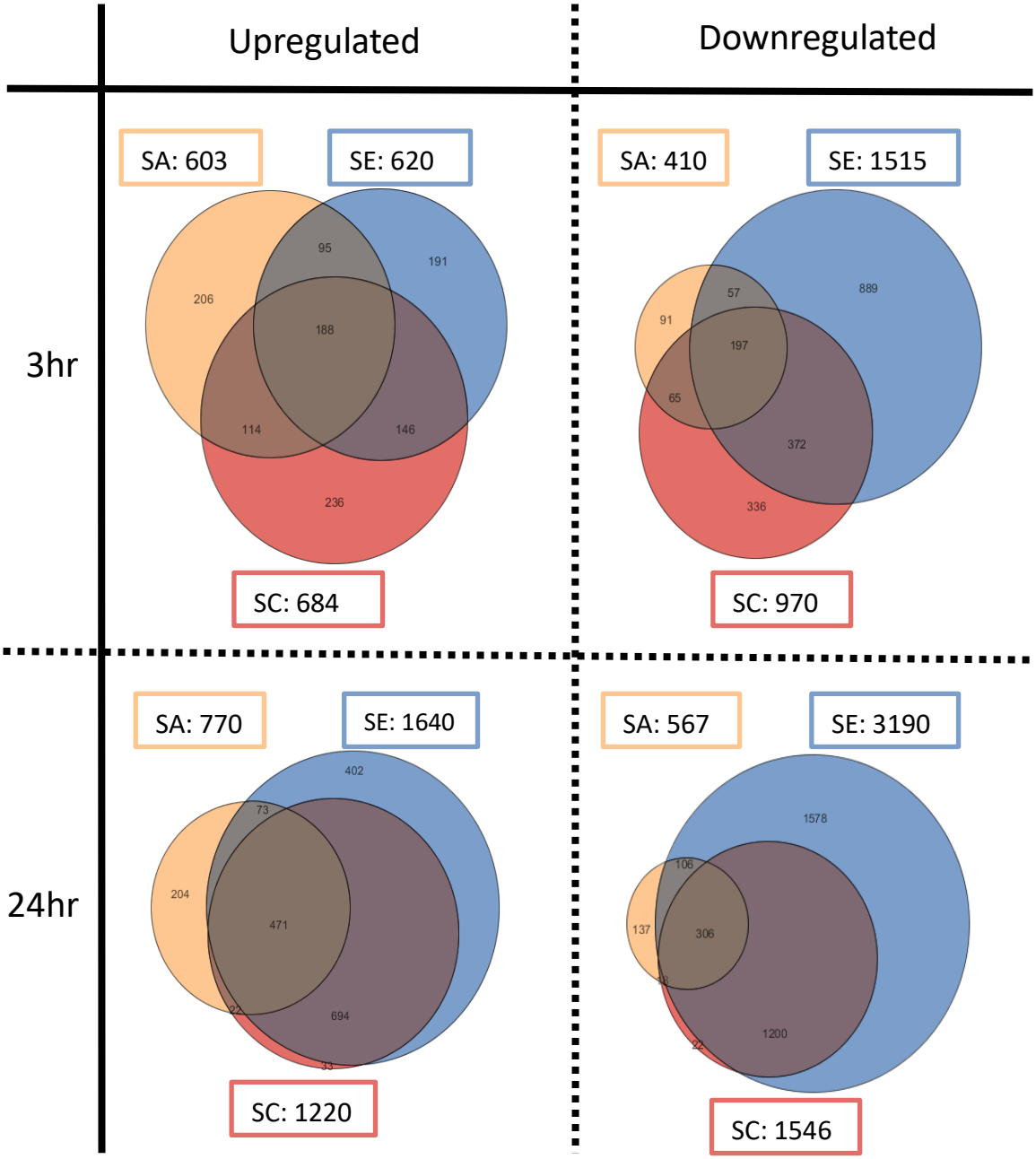

Figure 7:2: Proportional Venn diagrams of combined entity lists of staphylococcal signatures upregulated and downregulated after 1.2 fold change cut off

Venn diagrams of the combined staphylococcal entity list refined by the 1.2 fold cut off for each colonisation. Each venn diagram compares SA (8325-4), SE (12228) and SC (27840), with circles of proportional area to the number of entities of each list and labelled with the corresponding entity number in the associated coloured box. Separate diagrams compare upregulation (above 1.2 fold change) and downregulation (below -1.2 fold change) at 3 and 24hrs.

The imported dataset of genes and associated fold change expression was run through core analysis and then comparison analysis, as shown in **Figure 7.1**. The core analysis uses curated knowledge from the ingenuity® knowledge base to identify pathways, relationships, mechanisms and functions within a dataset. The ingenuity® knowledge base is derived from primary literature, as well as public and third-party databases to provide knowledge from millions of individually modelled relationships between proteins, genes, complexes, cells, tissues and diseases. These relationships are curated and manually reviewed for accuracy within context of the original publication. Therefore, the curated knowledge base provides organised and annotated networks of functional and biological interactions. The core analysis uses the curated knowledge to generate a prediction of activation for different pathways associated to the changes in expression caused by each staphylococcal colonisation. It also enables the prediction of upstream and downstream regulators within these pathways. It is possible to overlay the expression values from the dataset onto the canonical pathway maps, visually showing where the differentially expressed genes are located. As a result is it possible to identify the impact the differentially expressed genes are having within the pathway. Furthermore, it is possible to add the predictions onto the pathway map, to show what the curated knowledge is suggesting from the imported data.

As part of the core analysis IPA generates two statistical values associated to each pathway, the P-value and Z-score:

- P-value: a statistical test gauging the overlap of molecules of the dataset in the pathway in comparison to the whole dataset; therefore evaluating the likelihood of the overlap of genes being random. The smaller the P-value, the less likely the association is coincidental. Calculated by a Right-Tailed Fishers Exact Test.
- Z-score: A statistical measure of the correlation between relationship direction and gene expression, which can be used to predict pathway activation or inhibition. It is weighted by the relationship depicted in the curated knowledge base, the observed gene expression of the dataset. It is therefore weakened by conflictions that occur between them. Statistically, a Z-score of >2 is considered significantly activated and a Z-score of <-2 is considered significantly inhibited.

The comparison analysis is then performed to juxtapose the different staphylococcal colonisations, comparing the predicted pathway activation from the core analysis. This is based on each pathways Z-score.

7.2.2 Staphylococcal induced pathway activation

The comparison analysis was initially used to examine the most activated or inhibited pathways induced by staphylococcal colonisation. Using the cumulative Z-score's of each treatment it was possible to rank the pathways based on activation or inhibition. The top 10 most activated/inhibited pathways (**Figure 7.3**) included a number of inflammatory pathways recognised to be important in the cutaneous response to bacteria, such as Acute Phase Response Signalling, IL-1 Signalling and Toll-like Receptor (TLR) Signalling. Acute phase response is associated to the non-specific induction of inflammation via production of proinflammatory cytokines and can be induced by infection, tissue injury, stress, trauma and immune disorder (Gruys et al., 2005). Similarly, IL-1 Signalling induces proinflammatory cytokine production via activation by the IL-1 family of cytokines, including proinflammatory IL-1α and IL-1β (Dinarello, 2018). This overlaps with the TLR Signalling pathway that is part of the PAMP activation of PRRs signalling to sense bacteria and generate an appropriate response for defence (Kawasaki and Kawai, 2014). Activation of TLRs and IL-1 receptors require the intracellular TIR (Toll/interleukin-1 receptor) domain for recruitment of MyD88 to generate proinflammatory and/or antimicrobial defences (Cohen, 2014).

The activation of the pathways identified (**Figure 7.3a**) suggest induction of an overall inflammatory phenotype for the different staphylococcal species. However different species seem to show differential induction of the inflammatory regulators and these signals change with time length of pathogen exposure.

The Z-scores show that SA induces prominent activation of 8/10 pathways at both 3hrs and 24hrs, with 6 pathways significantly activated at 3hrs and 7 at 24hrs. The majority of these pathways are inflammatory in nature, therefore suggesting an inflammatory phenotype is induced rapidly and maintained with colonisation. Whereas at 24hrs SE induces much lower non-significant activation in the inflammatory pathways, Suggesting SE induces a less inflammatory phenotype than SA or SC.

The heatmap of Z-scores also suggests a delayed response is induced by SC colonisation, as the lower non-significant activation of inflammatory pathways displayed at 3hrs are increased to significant activation at 24hrs.

The significance of these pathways independent of activation or inhibition is presented as a P-value (**Figure 7.3b**), which is based on the overlap of genes of the dataset within the pathway, against the whole dataset. An insignificant P-value leads to uncertainty in the confidence of the Z-score. For example, at 3hrs the majority of the most activated/inhibited pathways are insignificant

in P-value for SE, which suggests SE induces less change in genes that are specifically involved in these pathways. Therefore, making the corresponding Z-scores unreliable. Conversely, the P-values are all significant for SA, providing more confidence in the importance of these pathways to SA colonisation and verifying the reliability of their Z-score.

a

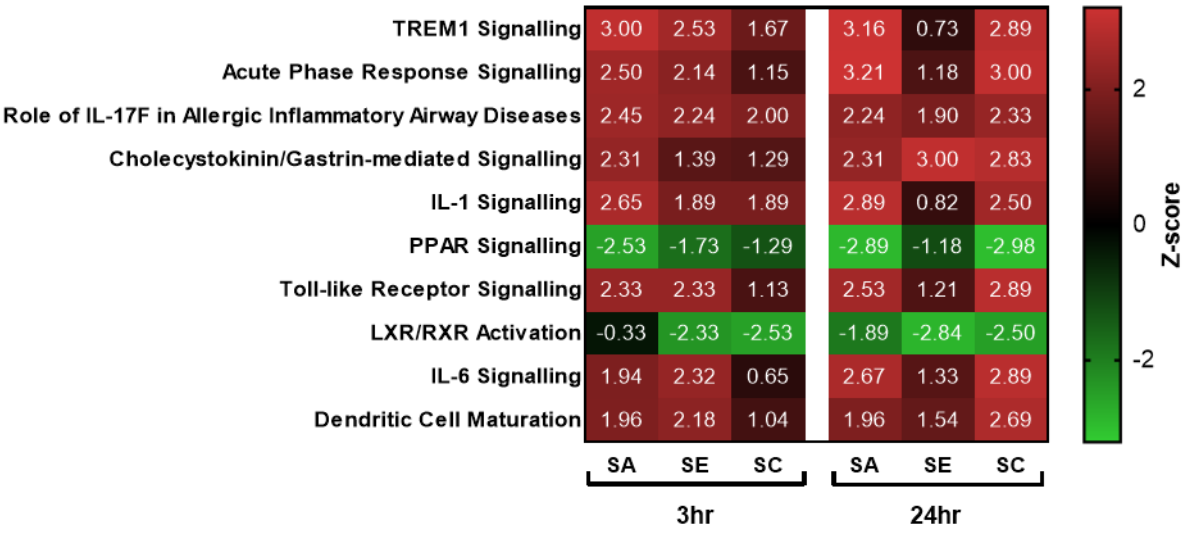

b

Pathway	3hr			24hr		
	SA	SE	SC	SA	SE	SC
TREM1 Signalling	***	ns	*	**	ns	ns
Acute Phase Response Signalling	**	ns	**	*	ns	*
Role of IL-17F in Allergic Inflammatory Airway Diseases	***	ns	ns	ns	*	***
Cholecystokinin/Gastrin-mediated Signalling	***	*	***	**	*	**
IL-1 Signalling	*	ns	ns	**	**	**
PPAR Signalling	**	ns	***	**	**	**
Toll-like Receptor Signalling	****	*	ns	***	**	***
LXR/RXR Activation	*	ns	**	ns	ns	ns
IL-6 Signalling	***	ns	****	**	***	****
Dendritic Cell Maturation	****	ns	***	***	*	**

Figure 7:3: Most activated/inhibited pathways induced by staphylococcal colonisation
Top 10 most cumulatively activated or inhibited pathways predicted to be induced by (8325-4), SE (12228) and SC (27840) colonisation at 3hrs and 24hrs. Heatmap (**a**) displays Z-scores as a measure of pathway activation or inhibition, with activation above 2 and inhibition below -2 considered significant. Table (**b**) displays pathway significance based on gene overlap, therefore irrespective of regulation. Calculated by Fishers Exact Test. * P>0.05, ** P>0.01, *** P>0.001, **** P>0.0001, ns: not significant.

7.2.3 Differential pathway regulation of SA and SE

The previous analysis (**Figure 7.3**) identified the top pathways activated or inhibited by staphylococci in comparison to the control unchallenged epidermal model. However, in view of their known differences in biology, where SE is a commensal and both SA and SC have an association with inflammation, to better understand the differences in epidermal response, it is appropriate to analyse the top differentially regulated pathways at a pathogen to pathogen basis.

Comparisons of SA versus SE (**Figure 7.4 - 7.5**) and SC versus SE (**Figure 7.6 - 7.7**) was undertaken for both 3hrs and 24hrs to determine the difference in Z-score (ΔZ-score). Thus, ranking the pathways by ΔZ exposes the most differentially regulated pathways between the two staphylococcal challenges. With this approach, positive ΔZ aims to reflect SA or SC pathway activation and SE pathway inhibition, and vice versa. It is important to note that a high ΔZ does not necessarily reflect contrasting directions of regulation of expression, as can be seen with B Cell receptor Signalling with SA and SE at 3 hours (**Figure 7.4a**).

Inspection of the SA upregulated pathways Gα12/13 Signalling, Thrombin Signalling, Sirtuin Signalling Pathway, NGF (Nerve growth factor) Signalling and B Cell Receptor Signalling, is notable because of the overlapping biological function for these processes which induce NF-κB Signalling. Furthermore, the SA down regulated pathways PPAR (Peroxisome proliferator-activated receptor) Signalling, PPARα/RXRα Activation and RhoGDI Signalling all suppress NF-κB Signalling. These data suggest that keratinocyte sensing of staphylococci is highly tuned to SA (as opposed to SE) and is mediated via TLR molecules (e.g. TLR2) on the cell surface which are critical for NF-κB Signalling and cytokine induction (Kollisch et al., 2005).

Overall, it seems there is an important role of NF-κB Signalling within the epidermal response to staphylococcal colonisation.

However, at 3hrs only the Sirtuin Signalling Pathway showed statistical significance for both SA and SE, and also differential direction of regulation between SA and SE (**Figure 7.4a,b**), suggesting that this may be a critical distinguishing regulator for the cellular response to SA and SE.

a

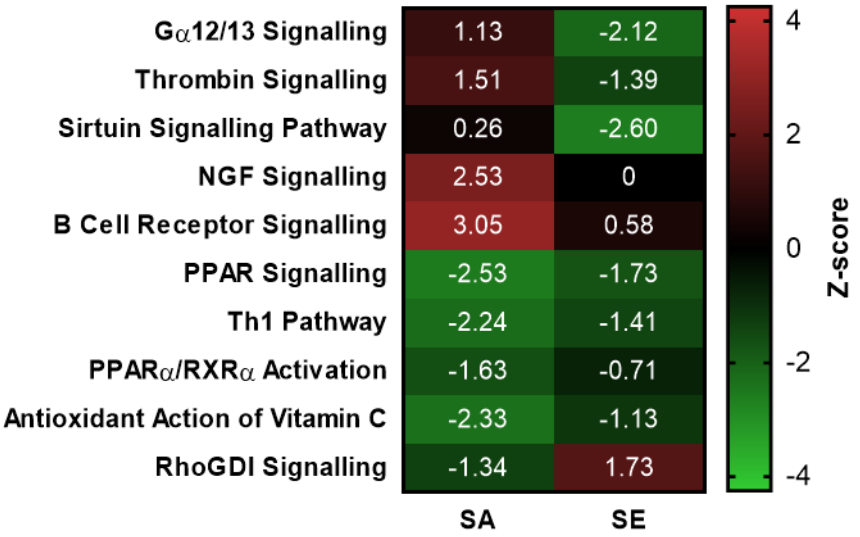

b

Pathway	SA	SE
Gα12/13 Signalling	*	ns
Thrombin Signalling	*	ns
Sirtuin Signalling Pathway	**	*
NGF Signalling	**	ns
B Cell Receptor Signalling	**	ns
PPAR Signalling	**	ns
Th1 Pathway	ns	ns
PPARα/RXRα Activation	*	ns
Antioxidant Action of Vitamin C	***	ns
RhoGDI Signalling	ns	ns

Figure 7:4: Differential pathway activation/inhibition of SA and SE at 3hrs of colonisation
Pathways differentially regulated by 3hrs of SA (8325-4) or SE (12228) colonisation. Exposing the 5 most differentially activated and 5 most differentially inhibited pathways for SA versus SE. Heatmap (**a**) shows Z-scores for these pathways; with activation above 2 and inhibition below -2 considered significant. Table (**b**) displays pathway significance based on gene overlap, therefore irrespective of its regulation. Calculated by Fishers Exact Test. * P>0.05, ** P>0.01, *** P>0.001, **** P>0.0001, ns: not significant.

NGF Signalling, PPAR Signalling, Antioxidant Action of Vitamin C and RhoGDI Signalling pathways were in the top 10 ΔZ pathways at both 3hrs and 24hrs, suggesting a strong role in mediating differential regulation of SA and SE. Of these, RhoGDI Signalling, demonstrated counter regulation by SA versus SE (inhibition with SA) and ΔZ is higher at 24hrs (**Figure 7.5a**). However, significance testing failed to meet the required threshold at either time point for both pathogens (**Figure 7.4b, 7.5b**). This lends some uncertainty to the importance of RhoGDI Signalling in keratinocyte staphylococcal responses.

Only 4/10 pathways studied reached statistical significance for SA, whereas 8/10 achieved this for SE (**Figure 7.5b**). Of these only NF-κB Signalling and PPAR Signalling were significantly different with both pathogens. For NF-κB Signalling, SA induces significant activation, whereas SE induces inhibition. Additionally, as discussed earlier, a number of pathways which induce NF-κB Signalling (Death Receptor Signalling and NGF Signalling) are activated by SA at 3hrs and also at 24hrs. Similarly pathways which inhibit NF-κB Signalling (PPAR Signalling, Antioxidant Action of Vitamin C, Sumoylation Pathway and RhoGDI Signalling) are inhibited by SA at 3hrs and also at 24hrs and vice versa by SE.

NF-κB Signalling and PPAR Signalling reached statistical significance with both pathogens, and will be further discussed later. However, only NF-κB Signalling showed differential direction of regulation with SA and SE, suggesting that it is a key pathway separating keratinocyte biological responses between SA and SE.

a

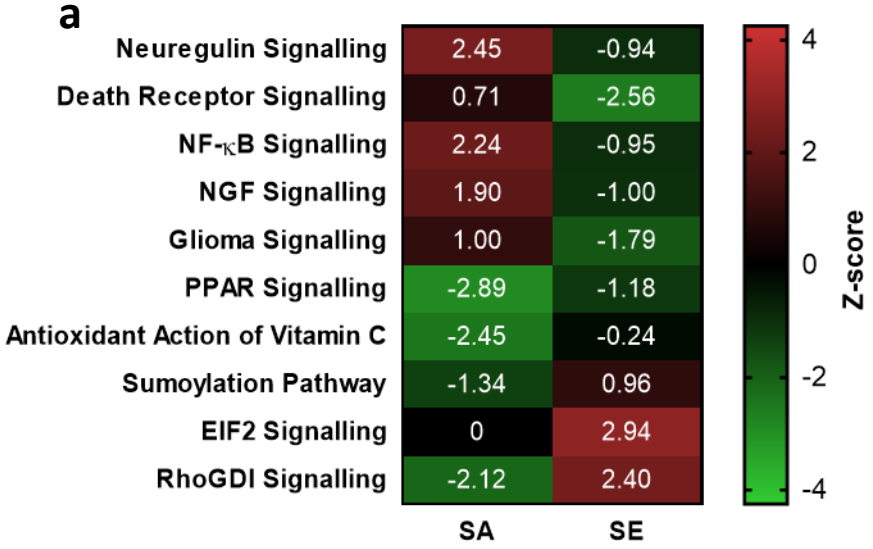

b

Pathway	SA	SE
Neuregulin Signalling	ns	*
Death Receptor Signalling	ns	***
NF-κB Signalling	***	*
NGF Signalling	ns	***
Glioma Signalling	*	ns
PPAR Signalling	**	**
Antioxidant Action of Vitamin C	*	ns
Sumoylation Pathway	ns	***
EIF2 Signalling	ns	****
RhoGDI Signalling	ns	*

Figure 7:5: Differential pathway activation/inhibition of SA and SE at 24hrs of colonisation
Pathways differentially regulated by 24hrs of SA (8325-4) or SE (12228) colonisation. Exposing the 5 most differentially activated and 5 most differentially inhibited pathways for SA versus SE. Heatmap (**a**) shows Z-scores for these pathways; with activation above 2 and inhibition below -2 considered significant. Table (**b**) displays pathway significance based on gene overlap, therefore irrespective of its regulation. Calculated by Fishers Exact Test. * P>0.05, ** P>0.01, *** P>0.001, **** P>0.0001, ns: not significant.

7.2.4 Differential pathway regulation of SC and SE

The top 10 ΔZ pathways activated or inhibited at 3hrs following SC or SE colonisation are shown in **Figure 7.6**. Out of the 10 pathways, 5 showed ΔZ differential direction of regulation between SE and SC. It is also interesting to note that the Sirtuin Signalling Pathway was modified by SE (downregulate) vs SC (upregulate), as with SA vs SE described above. However, all of these differentially regulated pathways failed significance testing, thereby limiting the inference for their role in regulating differences between SC and SE (**Figure 7.6b**). In fact, only TWEAK showed to be significantly down regulated by pathogens (SE>SC), and it is of note that this pathway is directly linked to NF-κB as a non-canonical signalling pathway (Sun, 2011)

a

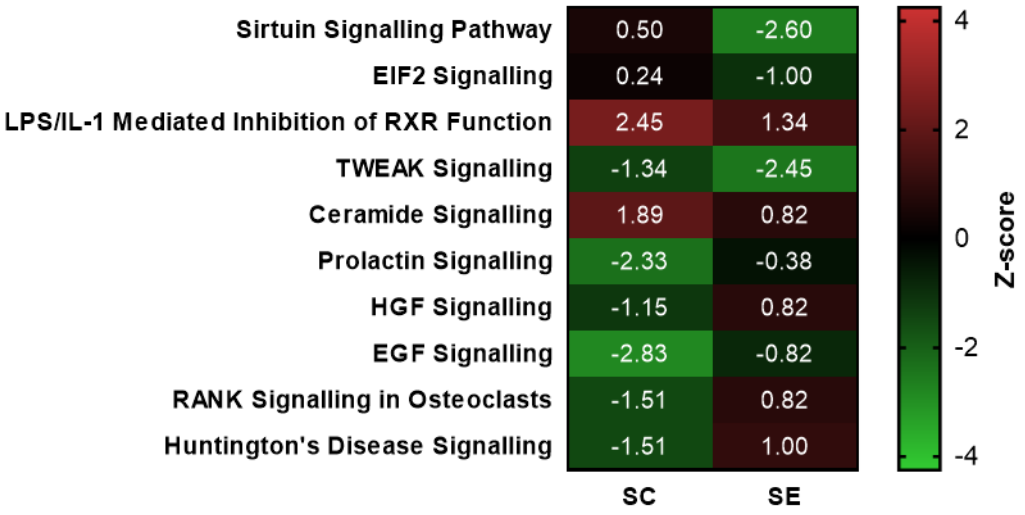

b

Pathway	SC	SE
Sirtuin Signalling Pathway	ns	*
EIF2 Signalling	***	ns
LPS/IL-1 Mediated Inhibition of RXR Function	*	ns
TWEAK Signalling	*	*
Ceramide Signalling	ns	ns
Prolactin Signalling	*	ns
HGF Signalling	**	ns
EGF Signalling	*	ns
RANK Signalling in Osteoclasts	**	ns
Huntington's Disease Signalling	*	ns

Figure 7:6: Differential pathway activation/inhibition of SC and SE at 3hrs of colonisation
Pathways differentially regulated by 3hrs of SC (27840) or SE (12228) colonisation. Exposing the 5 most differentially activated and 5 most differentially inhibited pathways for SA versus SE. Heatmap (**a**) shows Z-scores for these pathways; with activation above 2 and inhibition below -2 considered significant. Table (**b**) displays pathway significance based on gene overlap, therefore irrespective of its regulation. Calculated by Fishers Exact Test. * P>0.05, ** P>0.01, *** P>0.001, **** P>0.0001, ns: not significant.

At 24hrs the comparison of SC versus SE showed 5/10 pathways regulated in a different direction with the two microbes (**Figure 7.7a**). Yet of all the pathways identified at 3 hours, only RANK Signalling was also in the top 10 ΔZ pathways at 24 hours. At 3hrs SC induces inhibition and SE induces activation, whereas at 24hrs SC induces activation and SE induces inhibition. This may suggest that for analysis of the difference between SE and SC, the interaction with the epidermis is quite different at 3 hours than at 24 hours.

Of the counter regulated pathways, only NGF Signalling and p53 Signalling achieved the significance testing threshold for both SE and SC (**Figure 7.7b**). PPAR Signalling also demonstrated statistical significance, but was inhibited (SC>SE) by both organisms. This similar finding to SA, underlines the importance of PPAR in regulating skin microbial sensing, and the link with inhibition of NF-κB of this pathway as discussed above, suggests that SC may utilise similar strategies to modify host responses as identified with SA above.

Comparison of the top pathways of SC versus SE with SA versus SE at 24hrs (**Figure 7.5** and **Figure 7.7**) shows similar activation of NGF Signalling, and the inhibition of PPAR Signalling, Antioxidant Action of Vitamin C and RhoGDI Signalling. Yet, SA induces stronger changes on these pathways than SC (except PPAR signalling), which implies that epidermal sensing may be more highly tuned to detect SA.

a

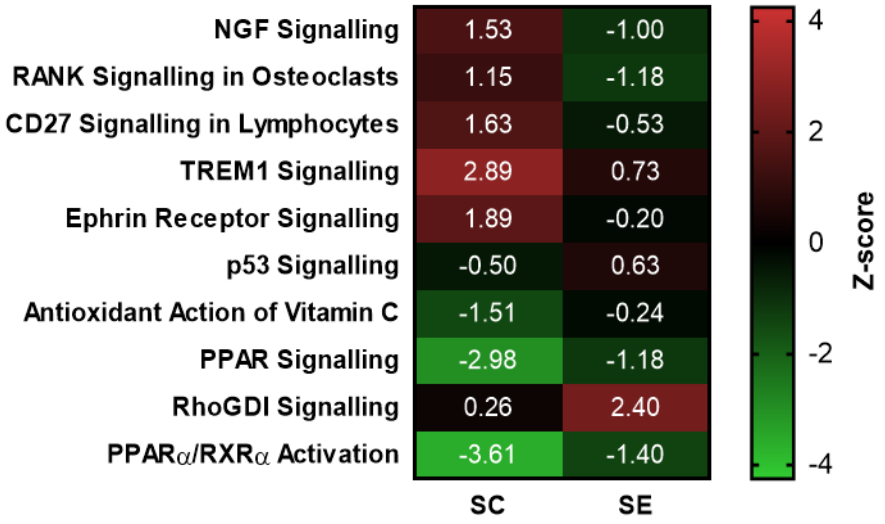

b

Pathway	SC	SE
NGF Signalling	**	***
RANK Signalling in Osteoclasts	ns	**
CD27 Signalling in Lymphocytes	ns	**
TREM1 Signalling	ns	ns
Ephrin Receptor Signalling	*	ns
p53 Signalling	**	***
Antioxidant Action of Vitamin C	*	ns
PPAR Signalling	**	**
RhoGDI Signalling	ns	*
PPARα/RXRα Activation	ns	ns

Figure 7:7: Differential pathway activation/inhibition of SC and SE at 24hrs of colonisation
Pathways differentially regulated by 24hrs of SC (27840) or SE (12228) colonisation. Exposing the 5 most differentially activated and 5 most differentially inhibited pathways for SA versus SE. Heatmap (**a**) shows Z-scores for these pathways; with activation above 2 and inhibition below -2 considered significant. Table (**b**) displays pathway significance based on gene overlap, therefore irrespective of its regulation. Calculated by Fishers Exact Test. * P>0.05, ** P>0.01, *** P>0.001, **** P>0.0001, ns: not significant.

7.2.5 Differential inflammatory response to Staphylococcal colonisation

Previously, the analysis has taken a non-hypothesis driven approach to examining the most significant differences in regulation of epidermal responses by staphylococci by analysing the most differentially expressed genes over control experiments or in comparison to other bacteria. However, the hypothesis outlined in this thesis is that, the key differences in potential to mediate inflammatory skin disease (or not) by the species of staphylococci is dependent upon the induction or otherwise of inflammatory signalling from keratinocytes. Therefore, it is appropriate also to examine the gene expression of relevant inflammatory mediators that were stimulating the inflammatory signalling pathways within the previous pathway analysis (**Figure 7.8**).

At 3 hours, differential direction of gene expression between SA83 and SE was noted in CCL5, and IL-6 only, but these were not seen with SA29, where only IL-36γ was oppositely regulated (**Figure 7.8**). At 24 hours, the CCL5 counter-regulation was maintained, whereas IL-6 inhibition by SA was reduced to very low levels, such that direct counter-regulation could no longer be observed, and instead VEGF-A was counter-regulated. For SE versus SC, opposite regulation was noted for BMP2 at 3 hours, but this was absent at 24 hours where all of the inflammatory signature was in the same direction. However, with regard ΔFold change, it was notable that SE generally induced a greater increase in gene expression across the inflammatory signature, most marked in CXCL1, CXCL3, GM-CSF, IL-23p19, IL-36γ, IL-6, PGF and TNFα.

IL-36γ has been shown to induce keratinocyte AMP expression (Johnston et al., 2011) as well as be induced by the AMP LL-37 (Li et al., 2014). This may suggest a mechanism whereby SE resistant to AMP inhibition, could induce a less tolerant environment for other competing staphylococci as has been shown by their induction of hBD3 via AhR signalling (Rademacher et al., 2018), and also hBD2 (Simanski et al., 2018)

CXCL1 and CXCL3 are both chemoattractants functioning through chemokine receptor CXCR2, which is expressed on the surface of neutrophils, monocytes, DCs, and mast cell precursors (Sokol and Luster, 2015). Thus, both CXCL1 and CXCL3 act to recruit immune cells to the site of inflammation. Similarly, GM-CSF acts to recruit monocytes, DCs and lymphocytes, but also enhances their role in inflammation, such as inducing maturation of DCs and polarising T cells (Shi et al., 2006). This suggests an important role of the adaptive immune system in the response induced by SE colonisation.

IL-23p19, more commonly known as IL-23 subunit alpha (IL-23A), is one of two subunits (p40 being the other) that comprise the proinflammatory cytokine IL-23. IL-23 has a prominent role in stimulating Th17 differentiation, proliferation and proinflammatory cytokine release (Floss et al.,

2015). Therefore suggesting the adaptive response to staphylococci is favoured towards an IL-17 response, as indicated in chapter 6.

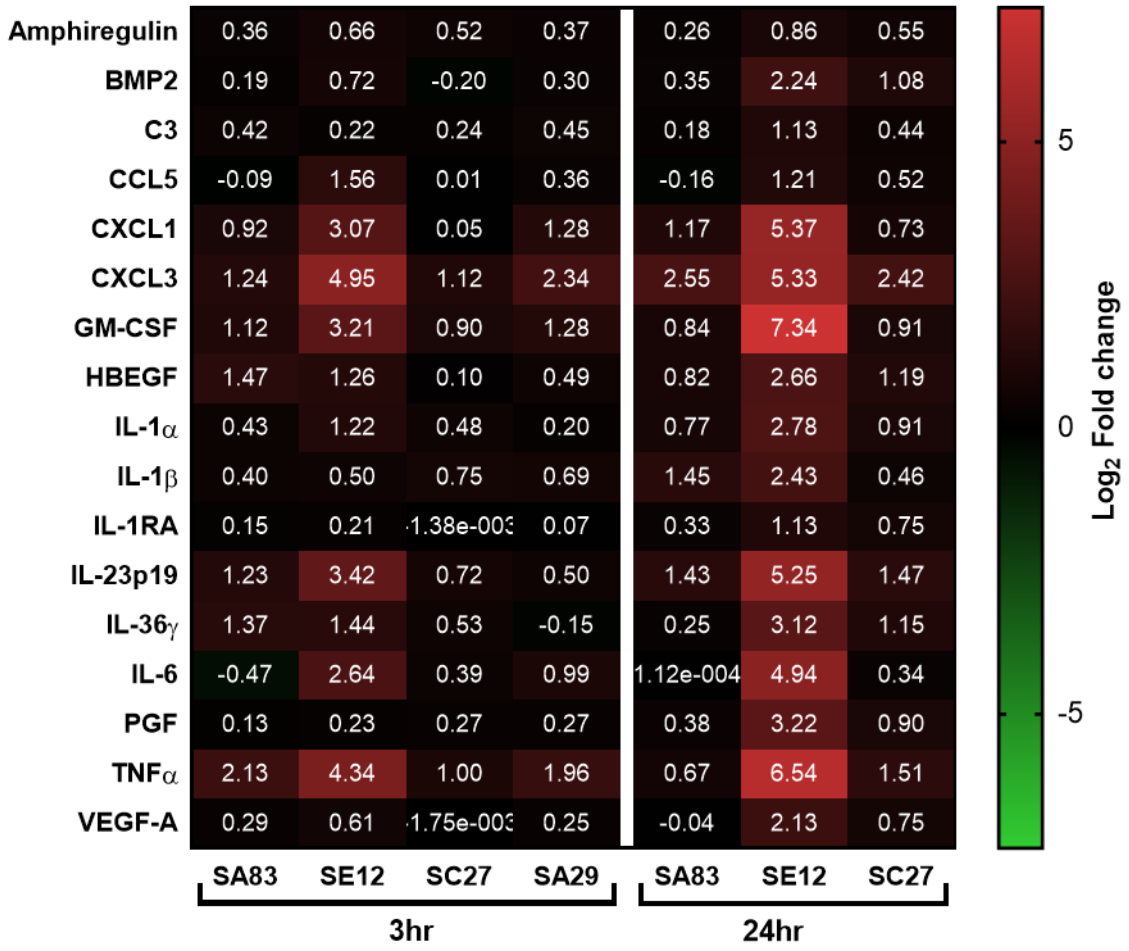

Figure 7:8: Differential gene expression of immune mediators associated to activated pathways induced by staphylococcal colonisation

Heatmap of change in gene expression induced by colonisation of SA83 (8325-4), SE12 (12228), SC27 (27840) and SA29 (29213), after 3hrs or 24hrs. Genes analysed are cytokines, chemokines and growth factors from activated inflammatory pathways, measured by microarray. Data expressed as mean of Log_2 fold change from time relative control of PBS (n=3/4).

7.2.6 Differential regulation of NF-κB signalling by staphylococcal species

The NF- κB transcription factor is an important regulator of inflammation that is involved in a large number of the pathways studied in this analysis. This includes a number of the inflammatory pathways noted when analysing the most activated/inhibited pathways (**Figure 7.3**) and also the inflammatory mediators studied in **Figure 7.8**.

The importance of NF-κB Signalling within the epidermal response was also elucidated from analysing the most divergently regulated pathways between SA and SE, at both timepoints. Furthermore, the NF-κB Signalling pathway was shown to be statistically different between SA and SE at 24hrs (**Figure 7.5a**). Thus justifying greater investigation of the specific NF-κB Signalling pathway and the difference between the induced effects of SA and SE upon it.

a

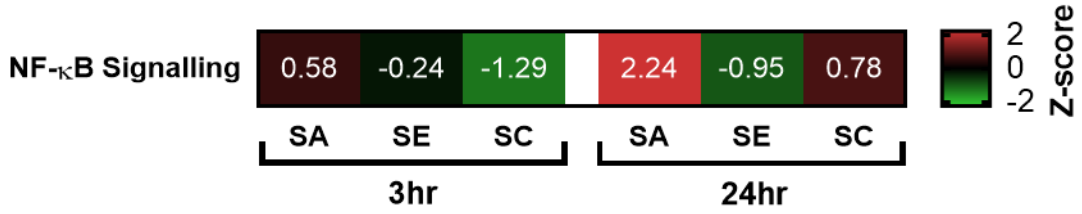

b

	3hr			24hr		
Pathway	SA	SE	SC	SA	SE	SC
NF-κB Signalling	*	ns	ns	***	*	*

Figure 7:9: Pathway analysis of NF-κB Signalling
Activation or inhibition of NF-κB Signalling induced by (8325-4), SE (12228) and SC (27840) colonisation at 3hrs and 24hrs. Heatmap (**a**) displays Z-scores as a measure of pathway regulation with activation above 2 and inhibition below -2 considered significant. Table (**b**) displays pathway significance based on gene overlap, therefore irrespective of the regulation. Calculated by Fishers Exact Test. * P>0.05, ** P>0.01, *** P>0.001, **** P>0.0001, ns: not significant.

Analysis of the Z-scores for NF-κB Signalling shows SA induced pathway activation and SE induced pathway inhibition at both time points, with greater difference in gene expression at 24hrs (**Figure 7.9a**). At 24hrs this pathway met the threshold for statistical significance of gene overlap (P-value) across all pathogens. Interestingly, SC showed a heterogeneous regulation of NF-κB with inhibition at 3hrs and induction at 24hrs albeit to a lesser degree than SA.

To investigate the inhibition of the NF-κB Signalling pathway specifically induced by SE it will be examined in greater detail. Analysis of the Ingenuity pathway map overlays the experimental induction of gene expression onto the known regulatory pathway for any of the staphylococcal challenges (**Figure 7.10**). This identifies the key molecules interrogated by Ingenuity to derive the modulation of the signalling pathway and provides a visual assessment of the breadth of involvement in the pathway by altered gene expression mediated by Staphylococci as well as specific check point regulation mediated by key molecules.

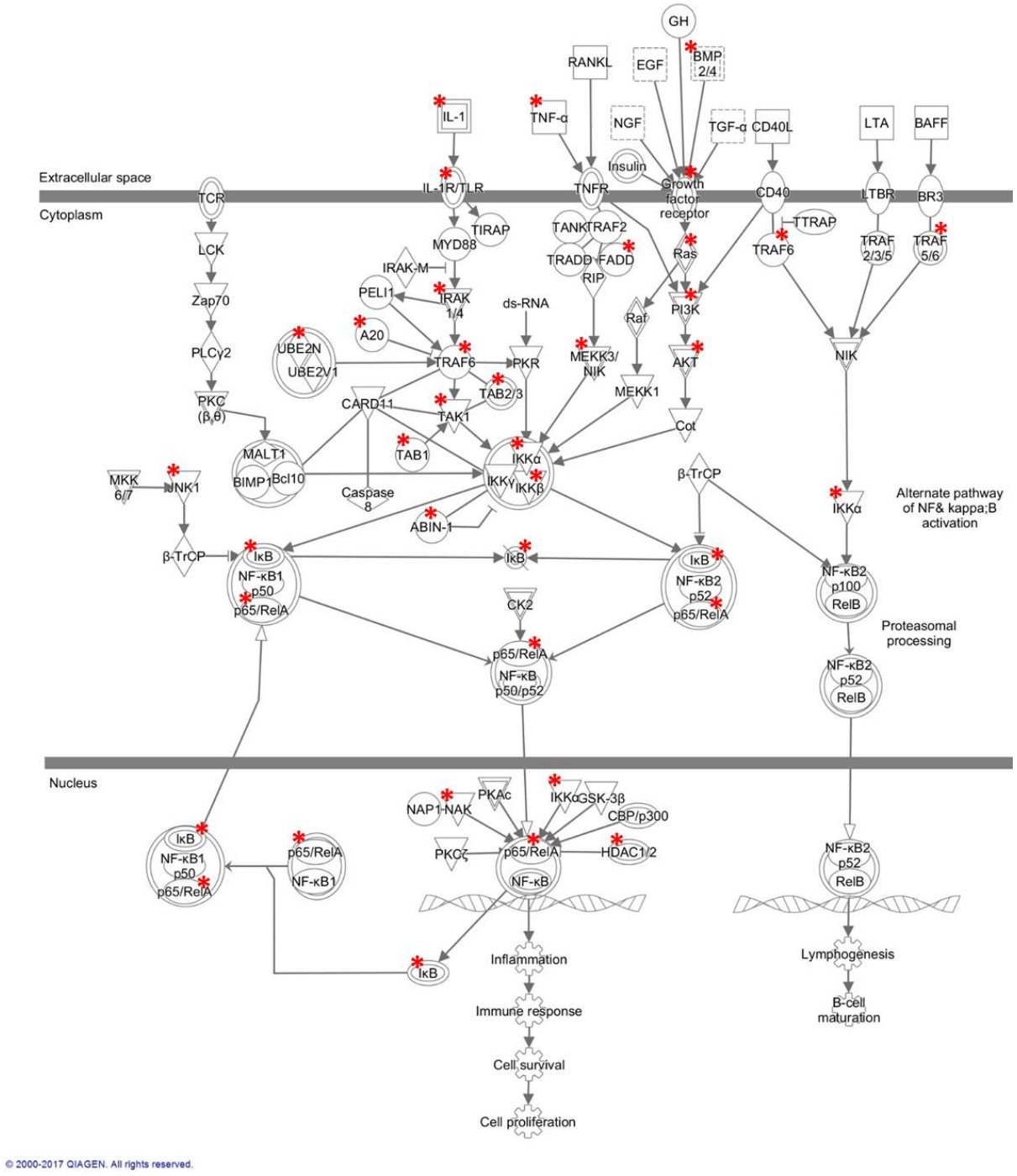

Figure 7:10: NF-κB Signalling pathway map
Network associated to NF-κB Signalling pathway from IPA. Red * indicates gene differentially expressed by at least one of the staphylococcal colonisations.

The pathway map shows the central role of the IKK (IκB kinase) complex for NF-κB's activation. The IKK complex, composed of IKKα, IKKβ and IKKγ subunits (shown centrally in **Figure 7.10**), phosphorylates inhibitors of NF-κB, thereby rendering them inactive (Hinz and Scheidereit, 2014). These inhibitors of NF-κB are members of the IκB family, comprised of IκBα, IκBβ, IκBε and IκBγ, which bind NF-κB subunits to inhibit there dimerization. Therefore, phosphorylation of IκB by the IKK complex, which leads to ubiquitination and degradation of IκB, enables NF-κB activation through dimerization of the NF-κB subunits: RelA/p65, c-Rel, P105/50, p100 and RelB (Christian et al., 2016).

The pathway map also shows the signalling pathways that induce IKK complex activation and the activatory signals initiating them. This included: IL-1, TNFα, and BMP2/4 (**Figure 7.10**); each will be considered in greater detail.

IL-1 pathway (including IL-1α, IL-1β and IL-36γ) activation of the IKK complex is summarised by the flow diagram in (**Figure 7.11**), with the corresponding gene expression data. The data support the activation of this pathway most prominently by SE at both time points but more so at 24hrs and corresponds to data previously shown in **Figure 7.8**. Downstream of the IL-1 pathway, a number of signal mediators are downregulated by 24hrs of SE colonisation, including IRAK1, UBE2N, TAB1 and TAK1. However, importantly SE also induces the upregulation of the TRAF6 inhibitor A20, which occurs at both 3hrs and 24hrs. As a TRAF6 inhibitor, A20 acts as a brake on the IL-1:IKK activation pathway, showing that SE induces negative regulation through decreased activation of the IKK complex.

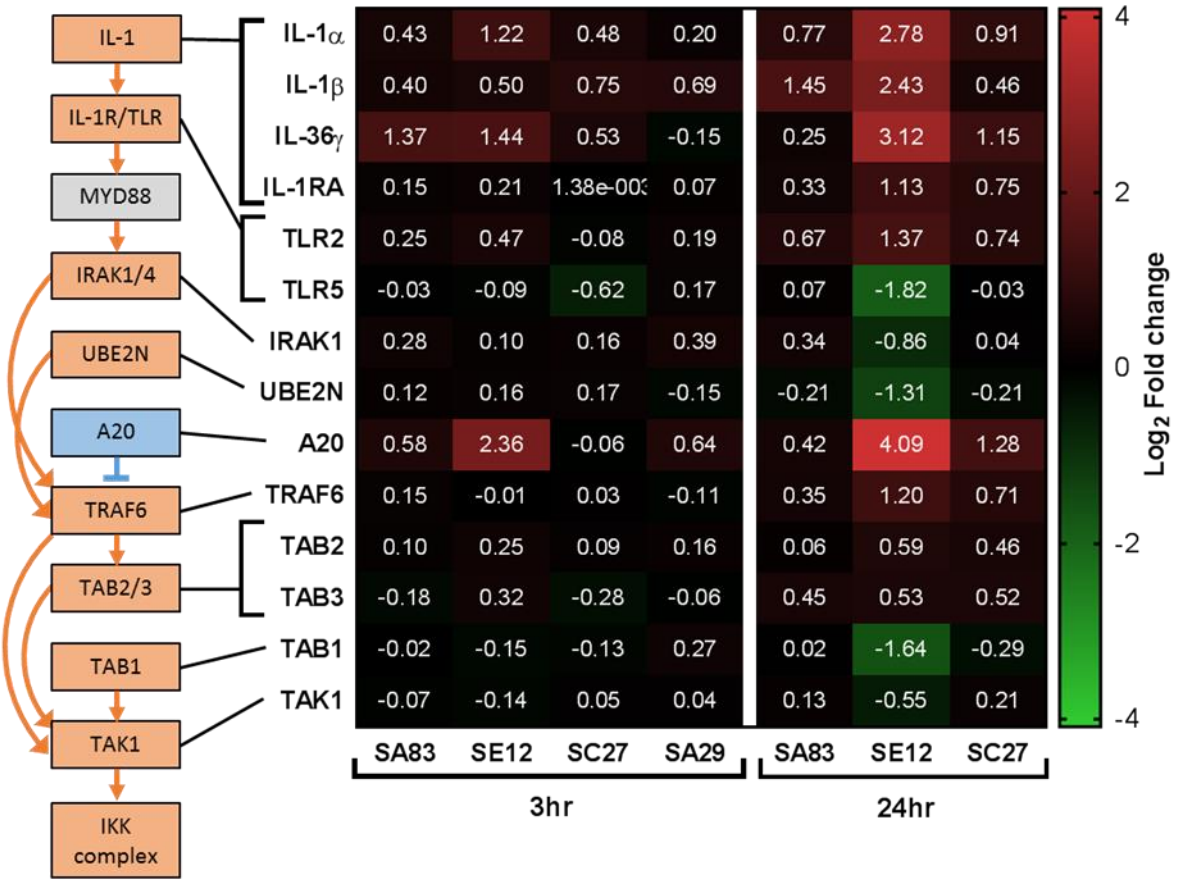

Figure 7:11: IL-1 activation of the IKK complex
Analysis of IL-1 induced activation of the IKK complex, displayed in flow diagram linked to associated genes within a heatmap. Heatmap shows change in gene expression induced by colonisation of SA83 (8325-4), SE12 (12228), SC27 (27840) and SA29 (29213); after 3hrs or 24hrs. Gene expression measured by microarray and expressed as mean of Log_2 fold change from time relative control of PBS (n=3/4).
Flow diagram: Orange - signal transduction; Blue - inhibition; Grey - transcript not included in analysis (See **Figure 7.1**).

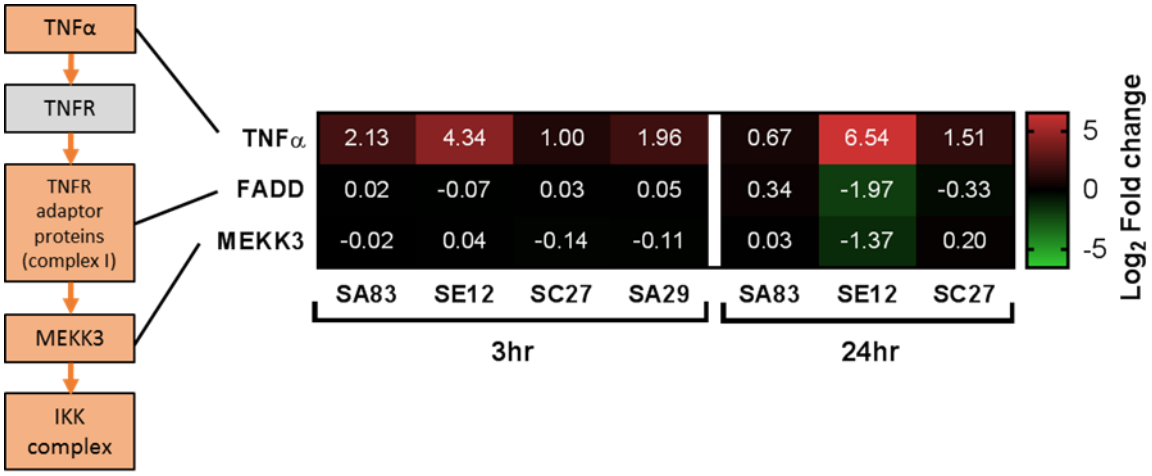

Figure 7:12: TNFα activation of the IKK complex
Analysis of TNFα induced activation of the IKK complex, displayed in flow diagram linked to associated genes within a heatmap. Heatmap shows change in gene expression induced by colonisation of SA83 (8325-4), SE12 (12228), SC27 (27840) and SA29 (29213); after 3hrs or 24hrs. Gene expression measured by microarray and expressed as mean of Log_2 fold change from time relative control of PBS (n=3/4).
Flow diagram: Orange - signal transduction; Blue - inhibition; Grey - transcript not included in analysis (See **Figure 7.1**).

Similar SE induced inhibition is demonstrated along the TNFα induced activation route of the IKK complex. Although, SE upregulation of TNFα is prominent, both FADD and MEKK3 (also known as MAP3K3) are downregulated by 24hrs of SE colonisation thereby resulting in an overall inhibition of IKK activation (**Figure 7.12**).

The third route of IKK complex activation by BMP2/4 also shows SE induced upregulation of the signal molecule (BMP2), but dominant inhibition of signalling molecules in the pathway to IKK activation (**Figure 7.13**), specifically by downregulation of the PI3K complex and AKT. The regulation of PI3K and AKT is of further importance, as they can be induced to activation by TNFα via TNFR (F**igure 7.10**)

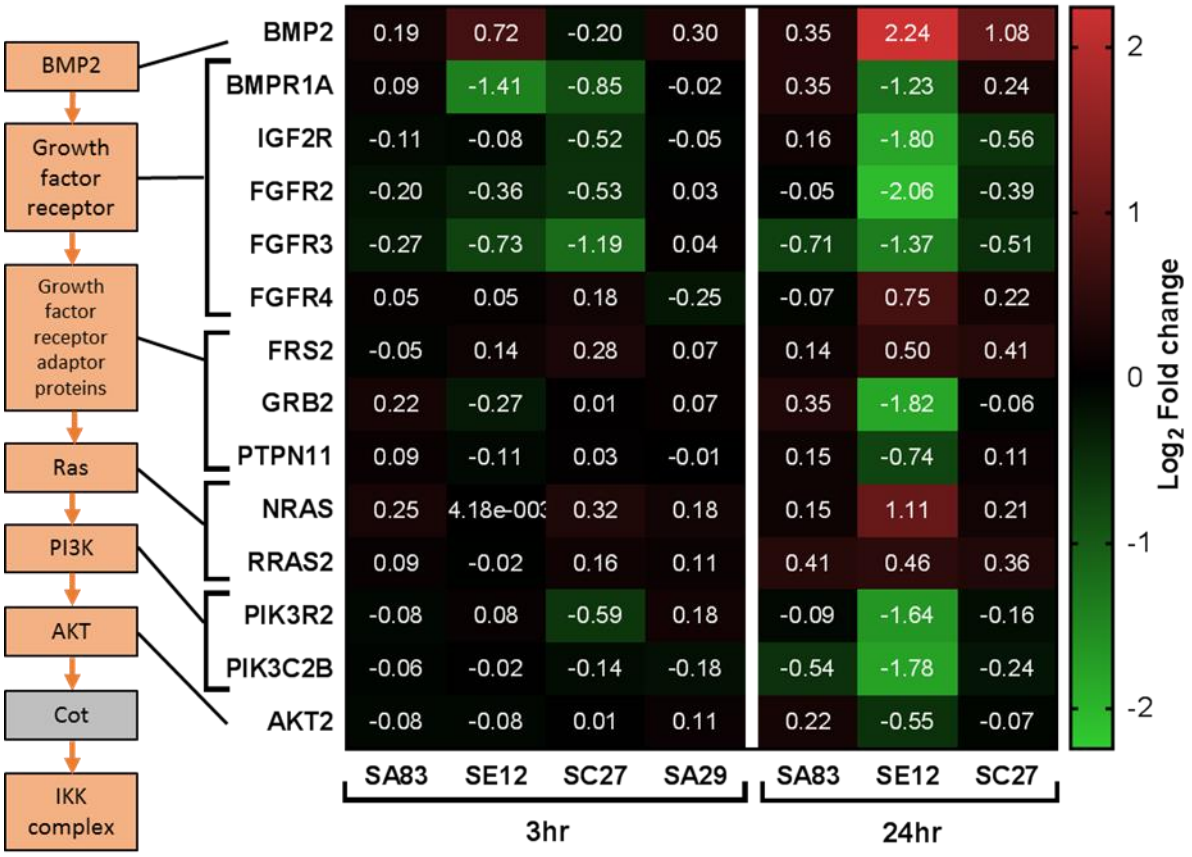

Figure 7:13: BMP2/4 activation of the IKK complex
Analysis of BMP2/4 induced activation of the IKK complex, displayed in flow diagram linked to associated genes within a heatmap. Heatmap shows change in gene expression induced by colonisation of SA83 (8325-4), SE12 (12228), SC27 (27840) and SA29 (29213); after 3hrs or 24hrs. Gene expression measured by microarray and expressed as mean of Log_2 fold change from time relative control of PBS (n=3/4).
Flow diagram: Orange - signal transduction; Blue - inhibition; Grey - transcript not included in analysis (See **Figure 7.1**).

Therefore, the key signalling pathways regulating IKK complex activation are all inhibited by SE, which suggests a contribution to the negative effect on NF-κB activation. Indeed, negative regulation is of NF-κB by SE at 24hrs is shown not only by the downregulation of the IKKα and IKKβ subunits, but also by an upregulation of the IKK complex inhibitor ABIN-1 (**Figure 7.14**). Furthermore SE induces upregulation of the NF-κB inhibitors IκBα and IκBε at both 3hrs and 24hrs.

Of the five NF-κB subunits only p65 (also known as RelA) was incorporated into a gene signature and consequently the pathway analysis, therefore the other four showed no significant change in

expression. SE induces a slight increase in p65, but the tightly regulated nature of NF-κB (Christian et al., 2016) by the IKK complex and IκB, as displayed in this analysis, indicates the increase is most likely inconsequential.

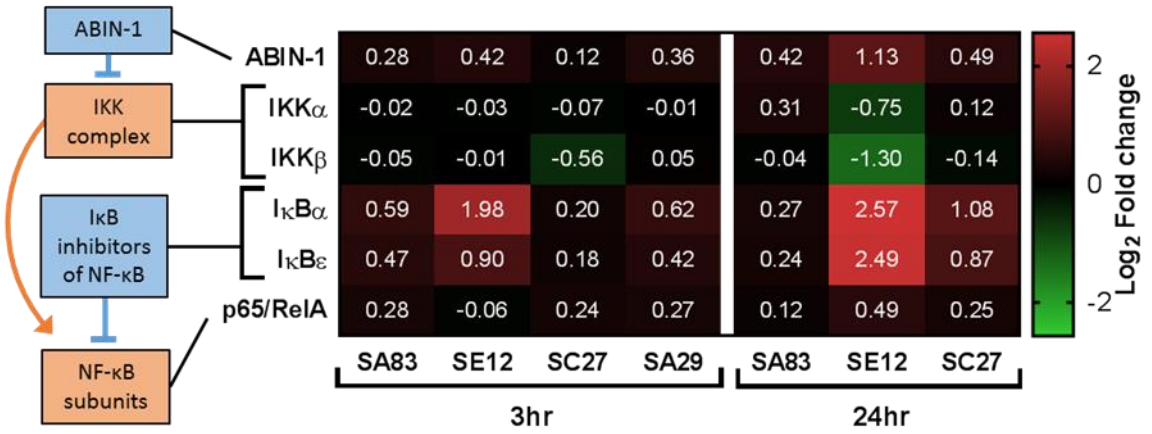

Figure 7:14: IKK complex activation of NF-κB
Analysis of the IKK complex activation of NF-κB, displayed in flow diagram linked to associated genes within a heatmap. Heatmap shows change in gene expression induced by colonisation of SA83 (8325-4), SE12 (12228), SC27 (27840) and SA29 (29213); after 3hrs or 24hrs. Gene expression measured by microarray and expressed as mean of Log_2 fold change from time relative control of PBS (n=3/4).
Flow diagram: Orange - signal transduction; Blue - inhibition; Grey - transcript not included in analysis (See **Figure 7.1**).

The role of the molecules described above as part of the NF-κB Signalling pathway are not restricted to this pathway alone. Therefore to examine activation of which other pathways may give rise or contribute the NF-κB signalling signature, a comprehensive analysis of the Ingenuity profiles of these molecules was undertaken (**Table 7.1**). This showed the wide importance of SE inhibition of these molecules towards an effect on many different cellular pathways.

Table 7.1: NF-κB signalling within other pathways

Table denoting the incorporation of genes associated to NF-κB signalling within other pathways. These pathways were previously studied for differential regulation or highest activation/inhibition.

		IκBα	IκBε	IKKα	IKKβ	p65/RelA
Most activation/inhibtion	TREM1 Signalling					x
	Acute Phase Response Signalling	x	x	x	x	x
	Role of IL-17F in Allergic Inflammatory Airway Diseases					x
	Cholecystokinin/Gastrin-mediated Signaling					
	IL-1 Signalling	x	x	x	x	x
	PPAR Signalling	x	x	x	x	x
	Toll-like Receptor Signalling	x		x	x	x
	LXR/RXR Activation					x
	IL-6 Signalling	x	x	x	x	x
	Dendritic Cell Maturation	x	x	x	x	x
SA v SE 3h	Gα12/13 Signalling	x	x	x	x	x
	Thrombin Signalling				x	x
	Sirtuin Signalling Pathway					x
	NGF Signalling			x	x	x
	B Cell Receptor Signalling	x	x	x	x	x
	PPAR Signalling	x	x	x	x	x
	Th1 Pathway					
	PPARα/RXRα Activation	x	x	x	x	x
	Antioxidant Action of Vitamin C	x	x	x	x	x
	RhoGDI Signalling					
SA v SE 24h	Neuregulin Signalling					
	Death Receptor Signalling	x	x	x	x	x
	NF-κB Signalling	x	x	x	x	x
	NGF Signalling			x	x	x
	Glioma Signalling					
	PPAR Signalling	x	x	x	x	x
	Antioxidant Action of Vitamin C	x	x	x	x	x
	Sumoylation Pathway	x				
	EIF2 Signalling					
	RhoGDI Signalling					
SC v SE 3h	Sirtuin Signalling Pathway					x
	EIF2 Signalling					
	LPS/IL-1 Mediated Inhibition of RXR Function					
	TWEAK Signalling	x	x	x	x	x
	Ceramide Signalling					x
	Prolactin Signalling					
	HGF Signalling					
	EGF Signalling					
	RANK Signalling in Osteoclasts	x	x	x	x	x
	Huntington's Disease Signalling					
SC v SE 24h	NGF Signalling			x	x	x
	RANK Signalling in Osteoclasts	x	x	x	x	x
	CD27 Signalling in Lymphocytes	x	x	x	x	x
	TREM1 Signalling					x
	Ephrin Receptor Signalling					
	p53 Signalling					
	Antioxidant Action of Vitamin C	x	x	x	x	x
	PPAR Signalling	x	x	x	x	x
	RhoGDI Signalling					
	PPARα/RXRα Activation	x	x	x	x	x

7.2.7 Differential regulation of eIF2 signalling by staphylococcal colonisation

Data presented in Chapter 6 showed some disparity between the mRNA expression and the protein released. This suggested possible inhibition of translation, post-translational modification, protein folding or transport along the secretory pathway. Therefore, pathways associated to these post transcriptional regulatory steps were examined. EIF2 Signalling pathway is recognised as key in regulating translation of mRNA. This requires heterotrimeric formation of the eIF2 (Eukaryotic initiation factor 2) protein complex from the α, β and γ subunits to initiate translation (Beilsten-Edmands et al., 2015). Thus making the pathway interesting to explore in greater detail.

The EIF2 Signalling pathway was identified in the differential analysis of SA and SE at 24hrs (**Figure 7.5**), as well as SC and SE at 3hrs (**Figure 7.6**), but failed to reach the threshold for statistical significance. However, at 24hrs SE and SC both significantly activated the pathway (**Figure 7.15**) and had highly significant gene overlap; with SE and SC reaching P-values of $P=1.78x10^{-16}$ and $2.48x10^{-16}$ respectively. Whereas SA did not appear to modulate the EIF2 Signalling pathway.

a

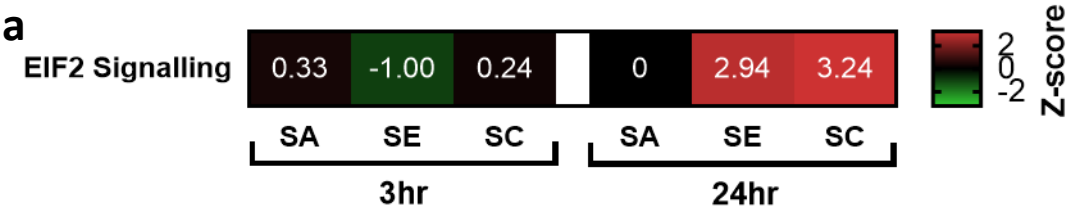

b

Pathway	3hr SA	3hr SE	3hr SC	24hr SA	24hr SE	24hr SC
EIF2 Signalling	ns	ns	***	ns	****	****

Figure 7:15: Pathway analysis of EIF2 Signalling
Activation or inhibition of EIF2 Signalling induced by SA (8325-4), SE (12228) and SC (27840) colonisation at 3hrs and 24hrs. Heatmap (**a**) displays Z-scores as a measure of pathway regulation, with activation above 2 and inhibition below -2 considered significant. Table (**b**) displays pathway significance based on gene overlap, therefore irrespective of the regulation. Calculated by Fishers Exact Test. * P>0.05, ** P>0.01, *** P>0.001, **** P>0.0001, ns: not significant.

The network associated to the EIF2 Signalling pathway can be divided into two sections that share activation by the eIF2 complex; the eIF2 induced integrated stress response (ISR) and the initiation of translation. ISR is cellular stress induced response common to all eurkaryotic cells. Various different stress stimuli can inhibit the formation of eIF2 via phosphorylation of the eIF2α subunit, which results in repression of translation, with exception of specific mRNAs using an alternative translation mechanism not reliant on 43S formation. These mRNAs contain short uORFs (upstream Open Reading Frames) in their 5' untranslated region (Pakos-Zebrucka et al., 2016). Translation of these mRNAs is Key to the response and induces translation of transcription factors such as activating transcription factor 4 (ATF4), which regulates the ISRs outcome based on the stress inducing stimuli (Dey et al., 2010). This outcome can vary between proinflammatory cytokine production, re-establishment of homeostasis, autophagy or apoptosis (Pakos-Zebrucka et al., 2016).

Examination of the eIF2 induced ISR section of the EIF2 Signalling pathway at 24hrs of colonisation shows that SE (**Figure 7.16**) and SC (**Figure 7.17**) induced increased mRNA expression of ATF4. SE appears to induce a larger increase in ATF4, however the pathway also shows decreases in other components of the pathway such as the transcription factor SREBP1 and apoptosis inhibitor XIAP. Overall these data suggest a differential ISR is induced by SE and SC.

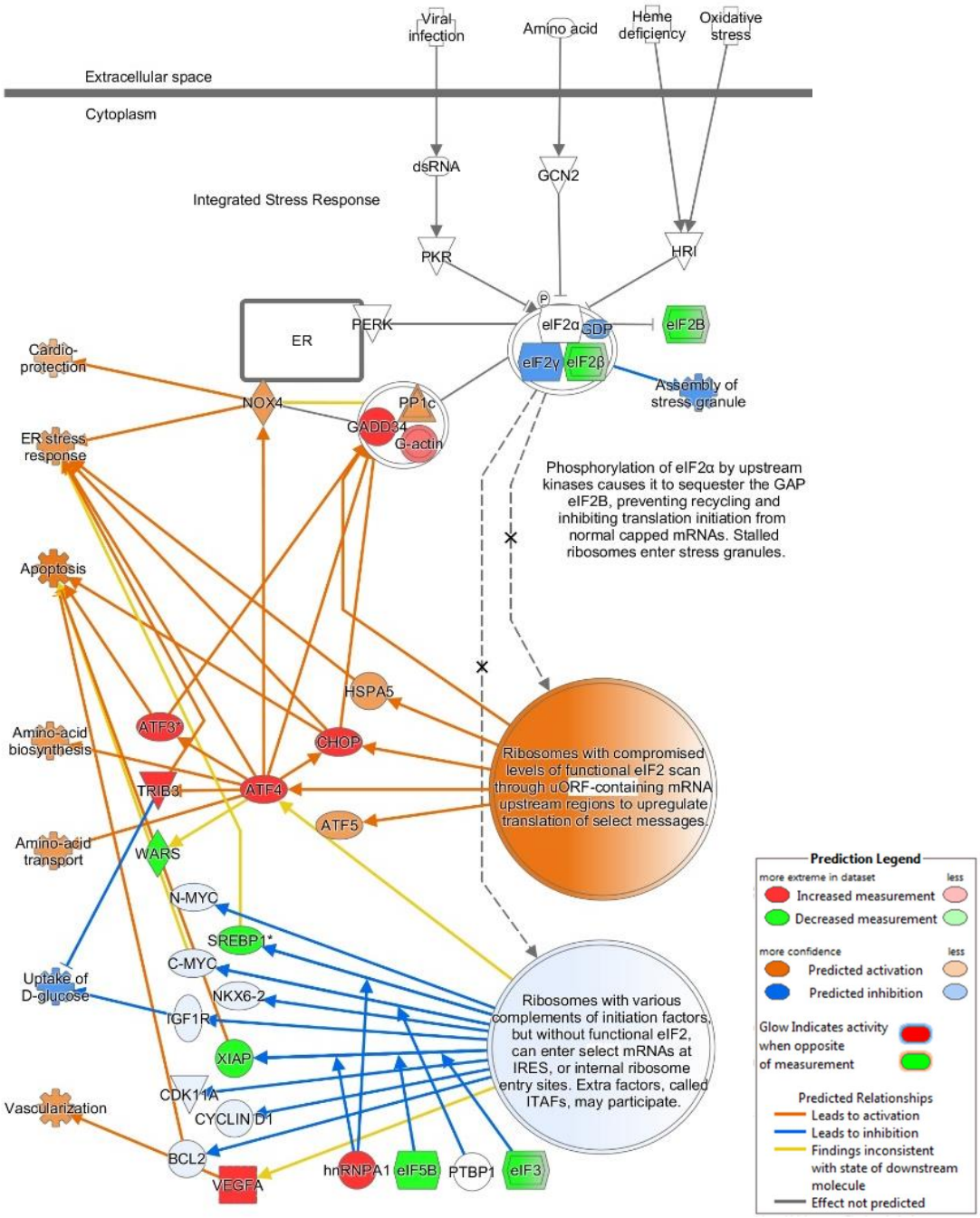

Figure 7:16: Predicted pathway regulation of the eIF2 induced integrated stress response by SE
Section of the canonical pathway for EIF2 Signalling displaying eIF2 induction of the integrated stress response. The pathway map is overlaid with expression data of fold change induced by 24hrs of SE (12228) colonisation and predictions based on the IPA core analysis of the colonisation.

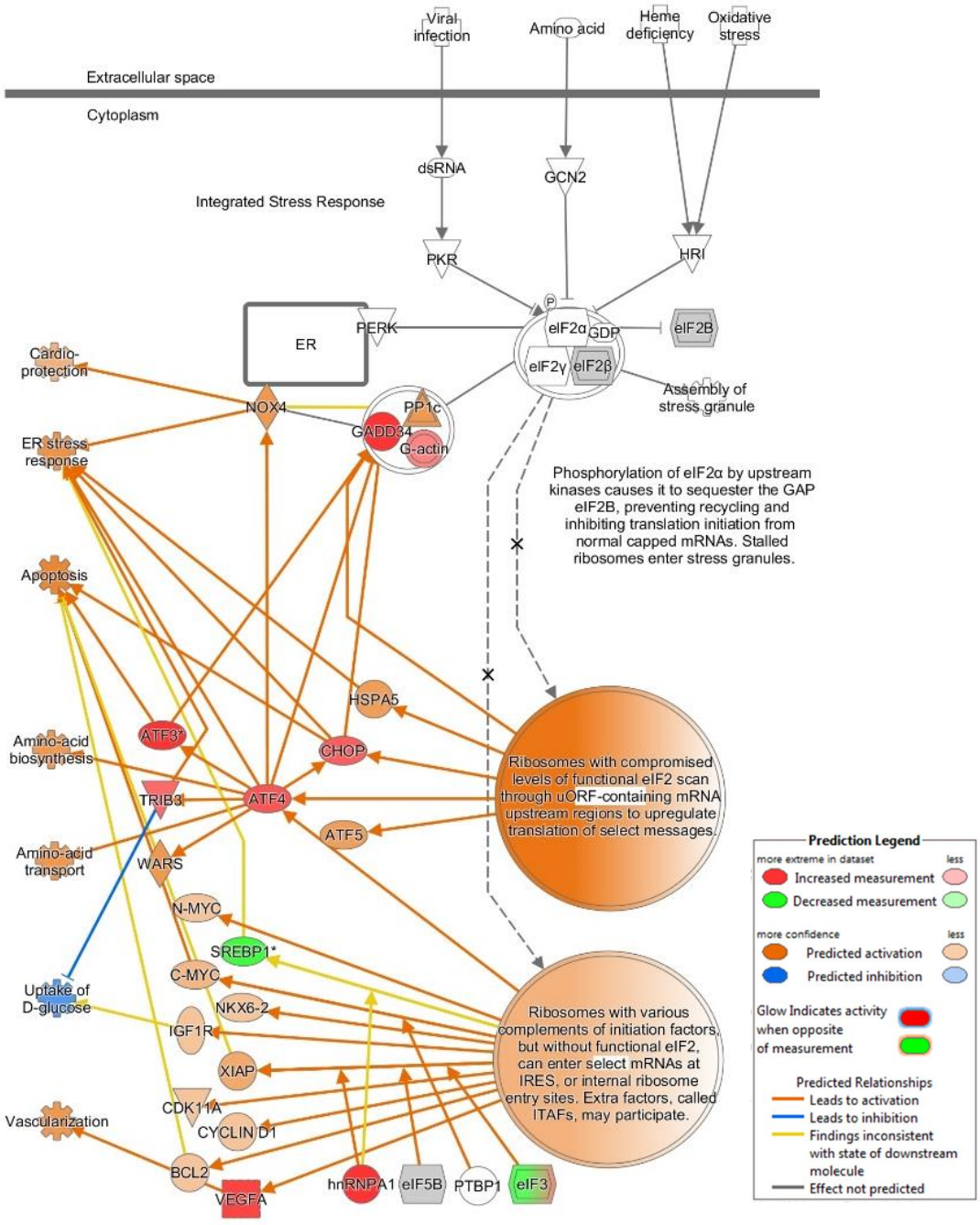

Figure 7:17: Predicted pathway regulation of the eIF2 induced integrated stress response by SC
Section of the canonical pathway for EIF2 Signalling displaying eIF2 induction of the integrated stress response. The pathway map is overlaid with expression data of fold change induced by 24hrs of SC (27840) colonisation and predictions based on the IPA core analysis of the colonisation.

The other section of the EIF2 signalling pathway is the initiation of translation, which involves delivering the initial tRNA start codon (methionyl-tRNA) to the 40S ribosomal subunit leading to the formation of the 43S pre-initiation complex (Sokabe and Fraser, 2014). This is regulated by eIF2B (Jennings et al., 2017), a guanosine nucleoside exchange factor that exchanges GDP for GTP on eIF2 enabling the attachment of met-tRNA (Beilsten-Edmands et al., 2015). Thus forming the ternary complex of eIF2:GTP:Met-tRNA$_i$. Other initiation factors include eIF1, eIF1A, eIF3, eIF4A, eIF4E, eIF4G, eIF5 and eIF5B. They all aid in the initiation of translation but are not as crucial for the initiation, except for eIF5. eIF5 acts as a regulator of translation by hydrolysing eIF2's GTP into GDP, but only when bound to the ternary complex at AUG codons (Pavitt, 2018).

Analysis of the initiation of translation section of the EIF2 signalling pathway at 24hrs shows SE colonisation induces a large downregulation of eIF2B, the key regulator of initiation (**Figure 7.18**). Furthermore, SE colonisation induces downregulation of the initiation factors eIF1A, eIF3, eIF4E and eIF5B; as well as the β subunit of the eIF2 heterotrimer. Overall, such down-regulation would suggest that SE inhibits cellular translation widely in a non-selective manner. Conversely, 24hrs of SC colonisation does not alter expression of eIF2B, although the core analysis predicts a slight downregulation (**Figure 7.19**). Whilst the expression data overlaid on the pathway map shows some minor downregulation the initiation factors eIF1A, eIF3 and eIF4E the core analysis predicts it is not enough to inhibit translation.

Although, when considering the whole EIF2 signalling pathway it is important to note that phosphorylation of eIF2α inhibits eIF2B function and induces translation in a 40S independent manner making the ISR activation the dominant response (Pavitt, 2018). However, this does not account for the SE induced downregulation of eIF2B.

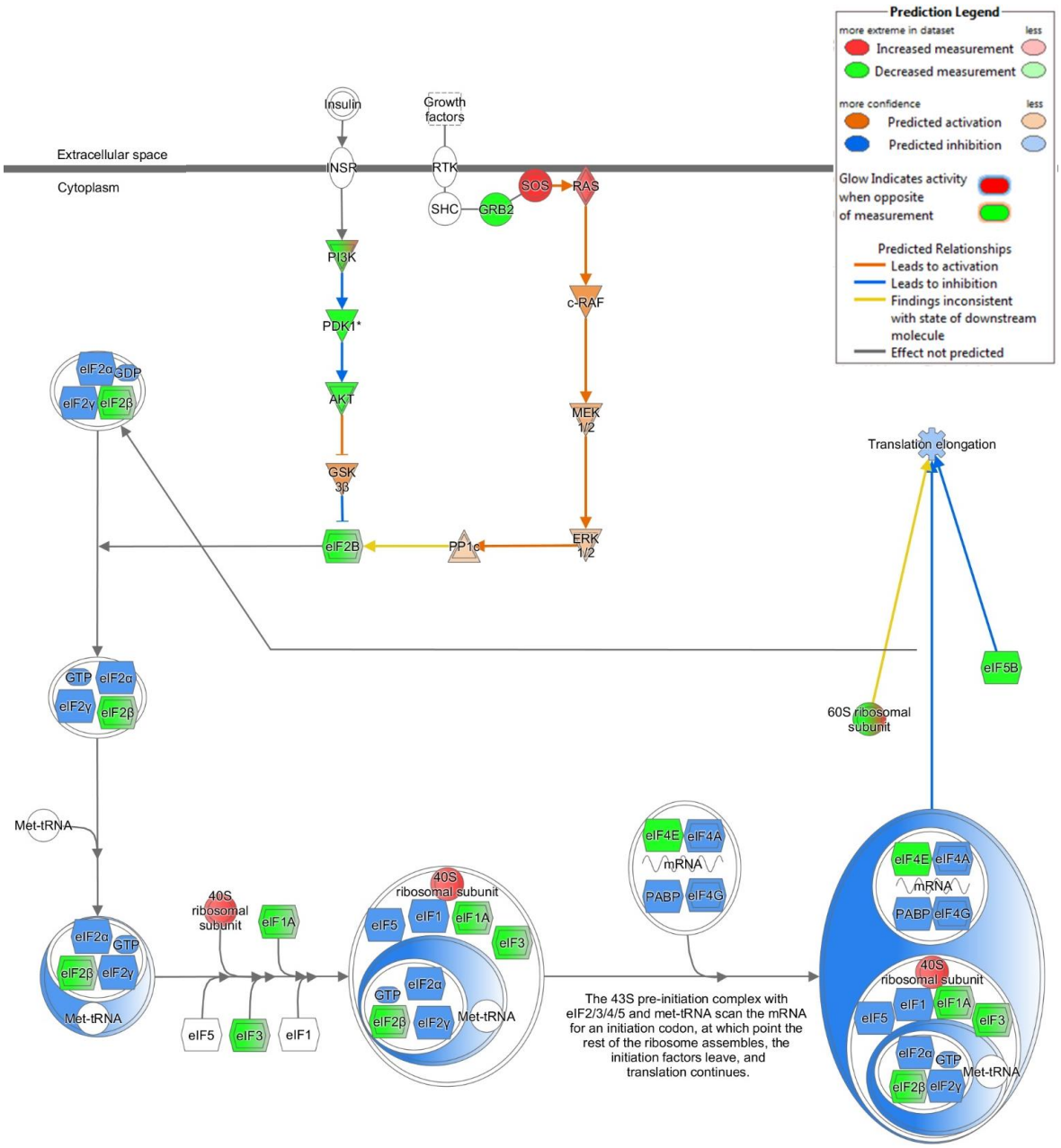

Figure 7:18: Predicted pathway regulation of eIF2 translation initiation by SE
Section of the canonical pathway for EIF2 Signalling displaying the initiation of translation by eIF2. The pathway map is overlaid with expression data of fold change induced by 24hrs of SE (12228) colonisation and predictions based on the IPA core analysis of the colonisation.

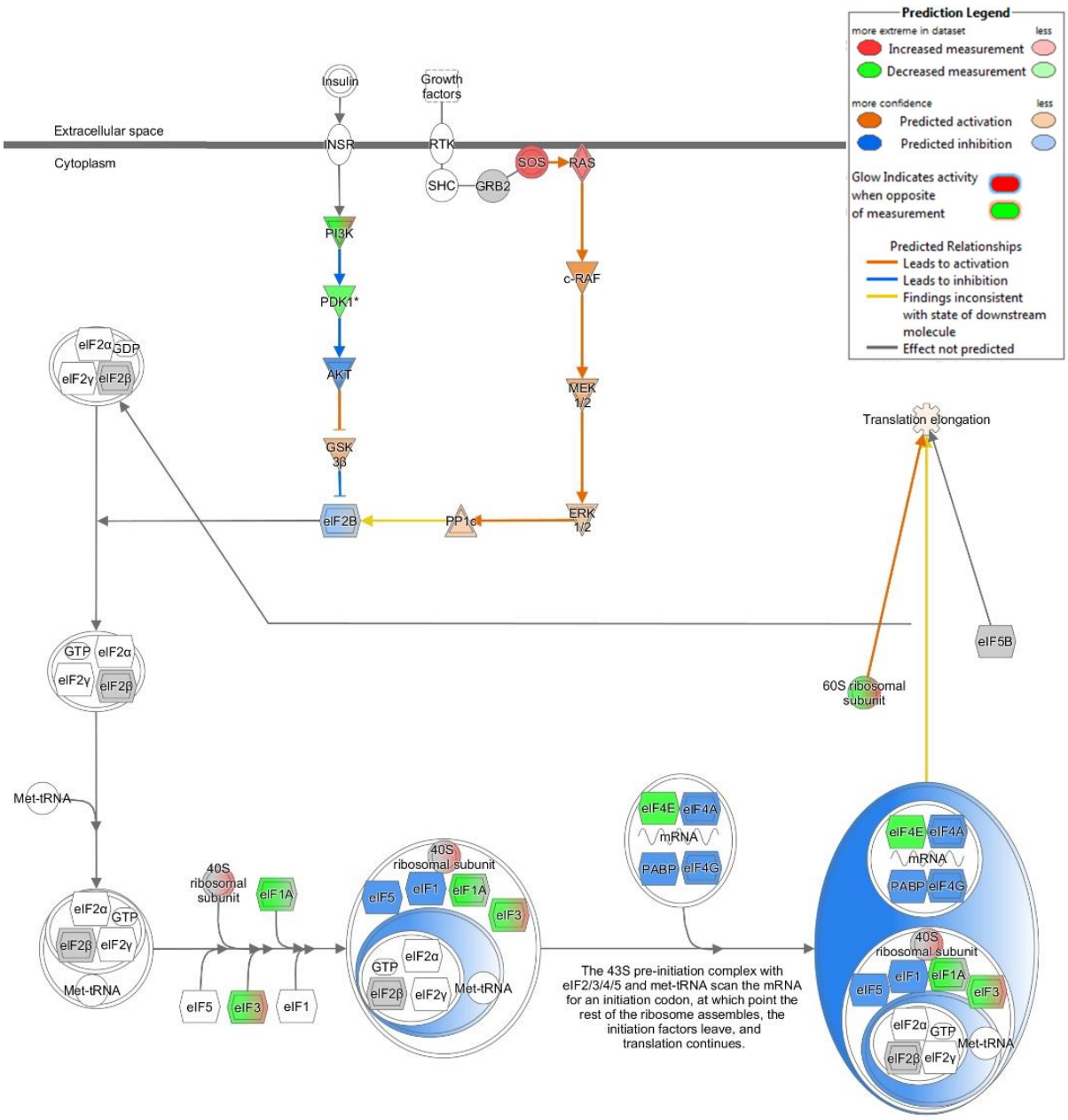

Figure 7:19: Predicted pathway regulation of eIF2 translation initiation by SC
Section of the canonical pathway for EIF2 Signalling displaying the initiation of translation by eIF2. The pathway map is overlaid with expression data of fold change induced by 24hrs of SC (27840) colonisation and predictions based on the IPA core analysis of the colonisation.

7.3 Discussion

In Chapter 6, the data presented showed distinct gene expression responses induced by SA, SE and SC. Here these gene expression data have been analysed by their known role in signalling pathways. Pathway analysis enables a more functional and mechanistic perspective on the characterisation of the epidermal response.

Analysis of the top 10 differentially expressed pathways by staphylococci revealed that the epidermal model responded in a predictable manner with induction of acute phase response, IL-1 signalling and Toll-like receptor signalling at both 3 hrs and 24hrs. However, this analysis did not facilitate the exploration of differences in the gene regulation by the pathogens, so instead Ingenuity pathway analysis of gene expression was compared across the staphylococci. The results of the pathway analysis highlighted Sirtuin Signalling, PPAR Signalling, NF-κB Signalling and TWEAK Signalling to be of interest.

7.3.1 Sirtuin Signalling

The cellular role of sirtuins is complex, but fundamentally they are a family of enzymes (Sirt1-Sirt7) that regulate transcription factors. Functionally sirtuins are involved in a wide range of cellular processes including inflammation, cell cycle, DNA repair, proliferation and apoptosis. Each of the sirtuin proteins have different targets and thus elicit different effects, but function via histone deactylase (HDAC) and/or adenosine diphosphate riboosyltransferase (ADPRT) activity (Yamamoto et al., 2007, Serravallo et al., 2013). HDACs regulate acetylation of proteins (especially histones), which is an epigenetic mechanism to regulate gene expression (Keppler and Archer, 2008). The ADPRT functionality of sirtuin can also affect transcriptional regulation but has also been shown to be important for intracellular signalling, proliferation, DNA repair and differentiation.

Sirtuins involvement in inflammation is complex and has been shown to differentially modulate immune activation and suppression based on the specific function (Chen et al., 2015). For example, SIRT1 suppresses NF-κB induced pro-inflammatory cytokine production in macrophages (Yoshizaki et al., 2010), whilst also enhancing macrophage phagocytosis via deacetylation of activator protein-1 (AP-1). This suppression of AP-1 reduces COX-2 expression, in turn reducing prostaglandin E_2 (PGE_2), an important inhibitor of phagocytosis (Zhang et al., 2010). Furthermore, inhibition of HDAC activity has shown to inhibit phagocytic clearance of SA and *E.coli* (Mombelli et al., 2011). Therefore in this context SE induced inhibition of sirtuins would be highly beneficial for its survival.

Although sirtuins effect different aspects of cellular signalling their impact on immune function is also situational regarding the immune cell type. **Figure 7.20** summarises effects on immune functioning that HDAC inhibitors can cause in different immune cells, which could reflect effects induced by the inhibition of SE. Regarding the epidermis, SIRT1 was shown to aid in the recruitment of macrophages and neutrophils, as well as the production of pro-inflammatory cytokines. This was demonstrated using an epidermal specific SIRT1 deficient mouse model (Qiang et al., 2017). This suggests a favourable environment is induced by SE's inhibition of sirtuin signalling.

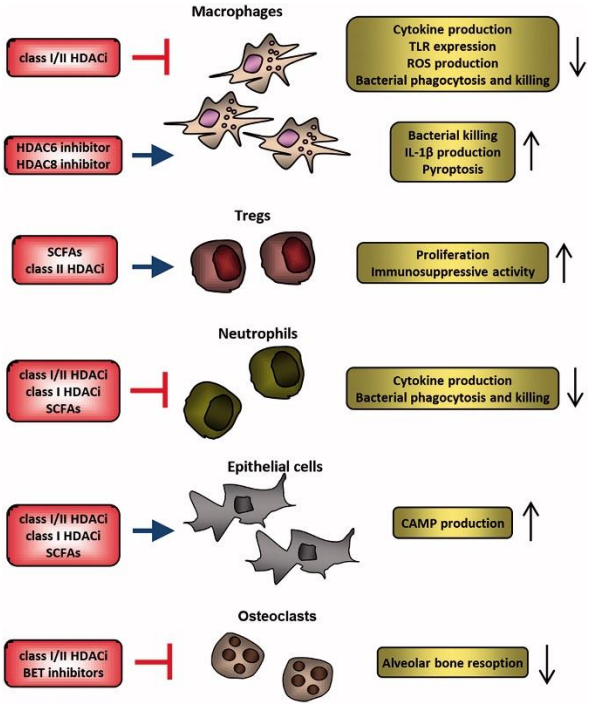

Figure 7:20: Anti-inflammatory effects of HDAC inhibitors in different immune cell types
Figure duplicated from a review bacterial regulation of histone deacetylases (Grabiec and Potempa, 2018) and summarises effects of different HDACs inhibitors. Class I/II HDAC inhibitors suppress macrophage inflammatory and phagocytosis, however inhibitors of HDAC6 and HDAC8 enhance bacterial clearance. SCFAs (Short chain fatty acids) and class II HDAC inhibitors activate Tregs to provide an immunosuppressive response. Class I/II HDAC inhibitors and SCFAs inhibit antimicrobial neutrophil response and induce an increase in cationic AMP (CAMP) expression. Class I/II HDAC inhibitors and BET protein inhibitors suppress osteoclast function

Although inhibition of SIRT1 has been shown to induce an anti-inflammatory effect other work has shown pathogens can induce HDACs to generate favourable conditions for their infection. Whilst the bacterial modulation of the histone deactylase system is not specific to sirtuins it has been show to include SIRT2 (Grabiec and Potempa, 2018). For example, *Listeria monocytogenes* infection induces the SIRT2 mediated deacylation of H3K18. The resultant transcriptional modulation causes downregulation of transcriptional regulators, which includes immune response regulators. This pivotal role of SIRT2 in aiding the infection was confirmed in both *in vivo* and *in vitro* (Eskandarian et al., 2013). Therefore, it seems that overall regulation of inflammatory processes is mediated by precise regulation of different components of the sirtuin pathway.

Whilst the effect of SE on sirtuin signalling has not previously been studied, the inhibition demonstrated in this work could indicate another mechanism in which SE is able to regulate cutaneous inflammatory responses.

7.3.2 PPAR Signalling

At 24hrs the PPAR signalling pathway was significantly inhibited by SA and was inhibited by SE to a lesser extent, albeit lacking significance. PPAR signalling is a mechanism of transcription regulation relying on peroxisome proliferator-activated receptors (PPARs), which are nuclear receptors that function as lipid-dependent transcription factors. The three members of the PPAR family (PPARα, PPARβ/δ and PPARγ) have differing but overlapping expression within different tissues, which depends on the tissue functionality. For example PPARα's main role is in homeostatic energy regulation and activates fatty acid catabolism, thus is highly expressed in brown adipose tissue, kidney, liver, heart and intestine (Mandard et al., 2004, Michalik et al., 2006). PPARα also has major anti-inflammatory effects achieved by transrepression, the ligand dependant antagonistic inhibition of transcription factors such as NF-κB (Ricote and Glass, 2007). Furthermore, PPARα can also induce the upregulation of IκB to inhibit NF-κB (Delerive et al., 2002), and the upregultion of soluble IL-1Ra an inhibitor of IL-1 stimulation (Stienstra et al., 2007). PPARα's anti-inflammatory effects have also been demonstrated in the skin (Dubrac and Schmuth, 2011).

All three PPAR isotypes are expressed in the skin, but PPARβ/δ is predominant and also functions as a metabolic regulator. It therefore also has an important role in gut, brain, adipose tissue and placenta. In the skin PPARβ/δ has been shown important for proliferation, differentiation, wound repair; controlling these via regulation of energy homeostasis (Michalik et al., 2006). However, it also has some anti-inflammatory effects. A mouse model deficiency in PPARβ/δ was shown to have increases in epidermal thickness, differentiation and inflammation (Man et al., 2008). These models were also shown to have a delayed response to wound repair, which overall demonstrates the role of epidermal PPARs in dampening cutaneous inflammation and aiding reepithelialisation (Michalik and Wahli, 2006). It has been suggested that PPARα is the dominant isotype regarding the suppression of inflammation (Michalik and Wahli, 2007) and has been shown to be downregulated in lesional sites of AD (Staumont-Salle et al., 2008). However the downregulation of PPARα is not specific to the Th2 response associated to AD, instead it occurs during general skin inflammation (Dubrac and Schmuth, 2011). Therefore the significant SA induced inhibition of PPAR signalling is not specific to the SA colonisation, but a symptom of the inflammatory profile demonstrated by other activated pathways.

7.3.3 TWEAK signalling

TWEAK signalling was also identified as a pathway differentially regulated, but in the comparison of SC versus SE. At 3hrs TWEAK signalling was inhibited by both SC and SE, however the inhibition was larger and significant only for SE. The protein TWEAK (TNF related weak inducer of apoptosis, also known as tumour necrosis factor ligand superfamily member 12) is a cytokine able to modulate inflammation to induce apoptosis through NF-κB (Chicheportiche et al., 1997, Winkles, 2008). Furthermore, it has been shown to be highly expressed in AD lesional skin (Zimmermann et al., 2011). However our results do not relate to the regulation induced by SA, only the inhibition demonstrated by SE, which is generated by inhibition of NF-κB**.**

7.3.4 NF-κB Signalling

The prominent finding within this chapter of research was the differential regulation of NF-κB signalling by SA and SE. The results showed significant activation of the NF-κB signalling pathway by SA and inhibition by SE. Furthermore analysis of pathways differentially regulated by SA and SE identified a large number of pathways that involved NF-κB as a transcription factor, therefore showing it has a wide impact in the differential response. Additionally, more in depth analysis of the signal transduction of NF-κB showed the inhibition induced by SE was performed by inhibiting both the mediation of the signal, as well as direct inhibition of the dimerization of NF-κB subunits that would enable its function.

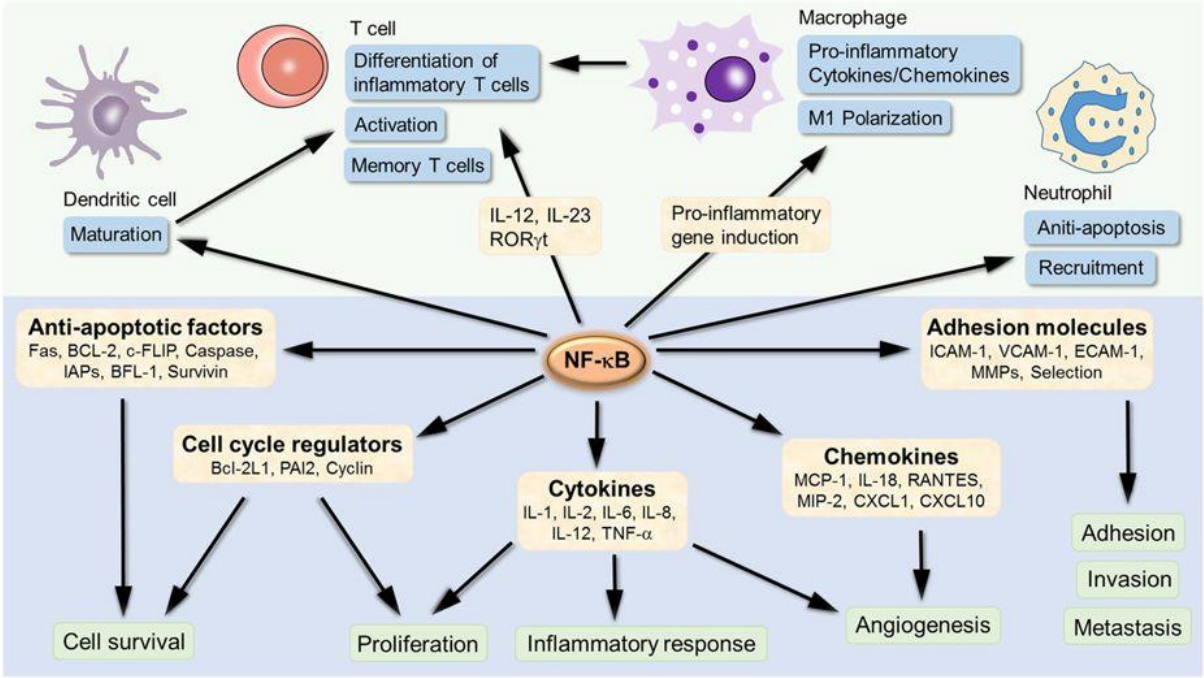

Figure 7:21: Genes transcribed by NF-κB and the resultant effects
Summary of genes produced by NF-κB and the cellular processes effected by the products of it. Figure duplicated from Liu et al. (2017).

NF-κB performs a central role in the mediation of inflammation, transcribing a number pro-inflammatory cytokines, chemokines and adhesion molecules. These can impact a variety of cellular processes such as proliferation, angiogenesis, adhesion and cell survival (**Figure 7.21**).

Activation of NF-κB is primarily caused by the degradation of the IκB inhibitors of NF-κB, as discussed during exploration of the canonical pathway. Stimulation of this pathway can be induced via a variety of stimuli, such as the stimulation of cytokine receptors, PRRs or TNF receptor superfamily members. Thus, NF-κB activation by the staphylococcal colonisation could be due to a staphylococcal PAMPs, such as LTA or peptidoglycan stimulation of TLR2 (Schwandner et al., 1999), Peptidoglycan stimulation of NOD2 (Roth et al., 2014) or the SpA (staphylococcal protein A) stimulation of TNFR1 (Gomez et al., 2006). Alternatively, pro-inflammatory cytokines, such as TNFα, IL-1α and IL-1β could also be inducing the activation of NF-κB, which would result in a positive feedback loop.

NF-κB's regulation of inflammation has previously been demonstrated in the epidermis via a number of mouse models. IκBα knockout mice exhibited widespread dermatitis, with increased expression of TNFα, IL-1α and IL-1β (Klement et al., 1996). Mice with Keratinocyte specific overpression of IKKβ also induced an inflammatory phenotype of the epidermis, mologphorolgically characterised by lichenification (Page et al., 2010). NF-κB is also associated to a number of inflammatory skin diseases including both AD and psoriasis. Topical NF-κB decoy oligodeoxynucleotides and NF-κB inhibitors have reduced AD like physiological symptoms and progression in NC/Nga mice, which act as AD like mouse models(Nakamura et al., 2002). The inhibitor was further shown to causes suppression of epidermal cytokines and B cell produced IgE (Tanaka et al., 2007).

Although the effects of NF-κB are proinflammatory, complete ablation of the NF-κB pathway also results in inflammation, suggesting a role of NF-κB in epidermal homeostasis (Pasparakis, 2009). Epidermis specific IKKβ (of the IKK complex) knockout mice generate severe skin inflammation (Pasparakis et al., 2002). The inflammation manifests as increased IL-1β (localised to the epidermis) and TNFα (localised to the dermis) expression, immune cell infiltration (macrophages, granulocytes and $CD4^+$ T cells) and epidermal hyperplasia. Suggesting complete ablation of IKKβ disrupts the highly regulated balance of NF-κB, which causes inflammation, however it also resulted keratinocyte apoptosis and mouse death within 10 days. Similarly, epidermal specific TAK1 knockout mice, which abolish the IL-1/TLR activation of the IKK complex result in TNF dependent skin inflammation and apoptosis (Omori et al., 2008). The complete ablation of NF-κB results in severe inflammatory effects which coincide with apoptosis, this response is not reflected in the gene expression data or pathway analysis. Therefore, inhibition of NF-κB induced

by SE colonisation is more likely a controlled negative regulation, demonstrated by the upregulation of inhibitors along the pathway, such as A20, ABIN-1, IκBα and IκBε.

A20 was revealed in the pathway analysis as a regulator of signalling within the NF-κB pathway, however it was also identified as one of the most differentially expressed genes of the gene signature of SE colonisation. A20 is a zinc finger protein with two ubiquitin modification domains, functioning as both E3 ligase and deubiquitating enzyme (Wertz et al., 2004). The ligase activity polyubiquitates RIP1, targeting it for proteasomal degradation. RIP1 acts as signalling mediator of the TNFR1 induced apoptotic pathway. Therefore, polyubiquitation of RIP1 by A20 inhibits apoptosis (He and Ting, 2002). Alternatively, A20 inhibits TRAF6 via deubiquitination of Ubc13, which is required for TRAF6 activation (Shembade et al., 2010). TRAF6 is a key mediator of the IL-1/TLR activation of NF-κB. Thus A20 acts as negative regulator of NF-κB function (Cooper et al., 1996, Sohn et al., 2016).

The importance of A20 in regulating both NF-κB and apoptosis is demonstrated by an association to numerous immune diseases. Single-nucleotide polymorphisms of A20's gene, TNFAIP3, generates a susceptibility to systemic lupus erythematosus (Graham et al., 2008), rheumatoid arthritis (Shimane et al., 2010) and psoriasis (Tejasvi et al., 2012). Furthermore, significant downregulation of TNFAIP3 has been exhibited in microarray analysis of patient AD and psoriatic skin (Devos et al., 2018).

TLR mediated NF-κB activation is an innate response to cellular recognition of bacteria, thus inhibition by A20 would reduce the inflammatory response, enabling colonisation or infection to persist. Therefore, upregulation of A20 by SE colonisation would be highly beneficial and has been recently substantiated by Simanski et al. (2018). Human primary keratinocytes stimulated by SE induced upregulation of TNFAIP3. Additionally, silencing A20 with siRNA generated increased NF-κB activity and expression of IL-1β and hBD2 (Simanski et al., 2018). Evidence of A20's role in regulating tolerance to commensals has also been demonstrated in the intestine. Mice with an A20 knockout specific to intestinal epithelial cells (enterocytes) treated to induce TNFα had increased susceptibility to commensal bacteria, which resulted in severe inflammation (Vereecke et al., 2010). Correspondingly, A20 was shown to mediate tolerance to LPS in enterocytes and A20 expression correlated with bacterial load (Wang et al., 2009a), indicating an important function in regulating commensal colonisation.

7.3.5 eIF2 signalling

Comparison of changes induced in gene and protein expression suggested a discrepancy between what it transcripted into mRNA and the proteins translated from it. Prompting the exploration of

pathways associated to regulation of translation. Differential pathway analysis between SA and SE at 24hrs indicated a significant activation of EIF2 signalling by SE, but lacked the gene overlap to disclose the SA induced pathway regulation. Further analysis of Z-scores and P-values showed similar activation induced by SC at 24hrs of colonisation. As well as extremely significant P-values induced by SE ($P=1.78x10^{-16}$) and SC ($P=2.48x10^{-16}$) at 24hrs, due to high gene overlap within the EIF2 signalling pathway network. Breakdown of this network revealed two separate parts of the pathway, the ISR (integrated stress response) and the initiation of translation.

Analysis of the SE and SC induced gene expression modulating the ISR demonstrated an activation by both staphylococcal colonisations. However, there were differences between SE and SC in activation of transcription factors within the ISR. Stimulation of ISR can occur via amino acid deprivation, viral infection, heme deprivation or ER stress (Pakos-Zebrucka et al., 2016). However, bacteria have been shown to indirectly activate the ISR from generating cellular stresses during infection (Rodrigues et al., 2018). Yet, it has also been postulated that the increased ER activity needed to generate an inflammatory response could generate ER stress, which could activate the ISR (van 't Wout et al., 2014). The resultant response of the ISR is dependent on the stimulation, varying the activation of different transcription factors to resolve the trauma, returning the cell to homeostasis. Alternatively, if the stress stimulation is excessive the ISR induces apoptosis. However, without more information of the specific form of stress activating the ISR by SE or SC the differences between or resultant response cannot be elucidated. A principal mechanism of the ISR is the phosphorylation of eIF2α that provokes it, this phosphorylation prevents eIF2 complex formation, repressing translation. This mechanism allows the cell to specifically focus on responding to the trauma.

The initiation of translation by eIF2 was shown to be inhibited by SE through downregulation of multiple eIF2 signalling mediators, including the key regulatory, eIF2B. However, despite the important role of eIF2B within regulation of translation little is known on how bacteria could induce this response. The inhibition of translation is separate to the ISR, which is known to inhibit eIF2B function. However, diseases caused by eIF2B mutations have the potential to cause chronic or heightened ISRs (Pavitt, 2018), which could suggest an exacerbated response.

The differential pathway analysis showed NF-κB signalling enhanced by SA could provide evidence as to why this organism might be more associated with inflammatory skin disease. Additionally, inhibition of NF-κB by SE could account for the non-inflammatory status of skin colonised by SE.

The most cumulatively activated or inhibited pathways included the acute phase response, Toll-like receptor (TLR) signalling, IL-1 signalling and IL-6 signalling. The acute phase response is the rapid initiation of the immune system towards PRRs and other danger signals, which is mediated though the stimulation of TLRs. TLR2 is the main TLR homolog known to be stimulated by LTA of SA (Schwandner et al., 1999, Fournier and Philpott, 2005). The resulting immune response includes the production of IL-1α, IL-1β and IL-6 (Mattsson et al., 1993). This route of stimulation by SA is usually regarded as bacterial invasion rather than colonisation. However, it is important to note that bacterial load of SA83 measured (Chapter 3, 4) was dramatically reduced over 24 hrs, presumably by the induction of TLR2, which functions extracellularly and therefore would not be expected to cause inhibition of internalised SA.

TREM1 (Triggering receptor expressed on myeloid cells 1) signalling pathway was found to be the highest cumulatively activated pathway across all three pathogens at 3 and 24 hours. Although, statistical significance was only reached for SA (3, 24hrs) and SC (3hrs), TREM1 signalling amplifies proinflammatory signals from DAMPs and PAMPs to promote host defence through cytokine production (Yang et al., 2015). Whilst the precise ligand of TREM1 has not been fully elucidated, activation has been shown to be induced by a range of bacterial stimuli and it has been suggested that it might recognise multiple epitopes (Roe et al., 2014). However, the role of TREM1 in mediating inflammation is not clear cut (Roe et al., 2014) and has been supported in human psoriasis studies (Hyder et al., 2013) and AD (Suarez-Farinas et al., 2015), but brought into question in mouse models (Drager et al., 2017). Therefore, whilst its function is not perfectly clear it could prove to be important for skin sensing of staphylococci.

The analysis performed within this chapter is unbiased by the cell type in which it was performed in, consequently certain pathways were shown to be activated that are not necessarily associated to the skin. This included the role of IL-17F in Allergic Inflammatory Airway Disease, which shows similar activation across all of the colonisations in **Figure 7.8**, but lack of association to the skin stopped further investigation. Within asthma, a common allergic inflammatory airway disease, IL-17F expression corresponds to the disease severity (Al-Ramli et al., 2009, Ota et al., 2014). The pathway involves IL-17F stimulation to induce the upregulation of inflammatory cytokines and chemokines, including CXCL1, GM-CSF, IL-1β, IL-6 and IL-8. However IL-17F expression is specific to immune cells, such as Th17 cells, natural killer cells, neutrophils and γδ T cells (Pappu et al., 2011). Keratinocytes express the IL-17C isotype instead, which was shown to be highly expressed by SA and SE at both timepoints in chapter 6. However, it is not comparable as the immune response induced by IL-17 is specific to the family member and the site of interaction (Jin and Dong, 2013). Therefore the induced cytokine and chemokine response causing the activation of this pathway is unlikely specific to an IL-17 response. Alternatively, it is part of a boarder

inflammatory phenotype induced by the staphylococci that overlaps into the Role of IL-17F in Allergic Inflammatory Airway Disease pathway.

Despite chapter 6 demonstrating high expression of IL-17C it was not associated to any of the pathways studied within the pathway analysis, which highlights the limitations of using curated knowledge databases. IL-17C is far less characterised than other IL-17 family members, such as IL-17A, IL-17F and IL-17E. These isotypes are expressed by various immune cells and have been far more extensively studied (Pappu et al., 2011).

The results also show an increase in TNFα production by SA (3hrs), SE (3hrs and 24hrs) and SC (24hrs), which is a major pro-inflammatory cytokine involved in many inflammatory pathways; including acute phase response, TLR signalling, IL-1 signalling and IL-6 signalling. It has been shown that TNFα can elicit a keratinocyte response without cellular entry (Aufiero et al., 2007). Suggesting colonisation can induce inflammatory effects on the skin. This brings into question, why do SA not regularly induce inflammation, but only during dysbiosis. However, by colonising the epidermal model with a single strain of high loads of staphylococci, it could be argued that this emulates dysbiosis rather than a normal colonisation. Therefore, it would be of interest to study the difference between the individual SA colonisation and SA within a mixed community colonisation.

Overall the pathway analysis enabled an investigation of the signal transduction generating the epidermal response to the different staphylococcal colonisations. It also applied functional information to known relationships within different networks of signalling, which was based on the extensive curated knowledge database of IPA. Initial analysis studied the most activated pathways common to all staphylococcal colonisations and noted the majority were involved in the inflammatory response. Comparison between the activation of these pathways suggested SA to be more inflammatory overall. Whereas, SE showed a reduced inflammatory profile after 24 hours and SC showed a minimal response that increased in inflammation over 24 hours.

Further analysis aimed to find differences between the signalling responses of the different staphylococcal colonisations. Thus, it calculated the most differentially activated or inhibited pathways between SA versus SE and SC versus SE. This analysis identified a number of significant pathways of interest, most notably NF-κB, which was activated by SA and inhibited by SE. Examination of the NF-κB signalling pathway indicated a highly controlled negative regulation of the pathway, rather than a direct bacterial inhibition. Furthermore, NF-κB was shown to have a

transcriptional role in a large number of pathways identified within this analysis, suggesting an influential and important role in the entire differential response to colonisation.

Chapter 8: Discussion

The intention of this research was to investigate the interaction between the skin and different staphylococcal species to examine how differences in their colonisation may contribute to regulation of skin tolerance or inflammation. The investigation began with the development of an epidermal model to act as a suitable platform to study staphylococcal colonisation. Initially quantification and proliferation curves of different staphylococcal colonisations were explored, followed by examination of the epidermal response to the colonisation.

The research presented in this thesis is based on development of an epidermal model that was optimised as an in house iteration of the RHE model. The optimisation produced a physiologically relevant model of the epidermis that could be grown in large batches to be used as a platform to study staphylococcal colonisation. Initial evaluation of the model demonstrated differential regulation of staphylococcus species colonisation, which was not specific to fully differentiated epidermis and not detected on keratinocyte monolayers thus indicating species specific modulation of the staphylococci by the epidermal model. Further examination of the colonised model demonstrated that it could also be utilised to model cross-talk between the structural epidermal cells (keratinocytes) and immune cells, as shown by the an immune response induced by soluble factors from the RHE model. These factors were shown to be sufficient to regulate the adaptive immune system through study of the induced activation of MoDCs.

8.1 Staphylococcus aureus

Initial quantification of the colonisation of SA indicated a differential regulation by the epidermis in a strain specific manner. Colonisation of SA 8325-4 and SA 29213 was similar over 3 hours. After which, until 24 hours, SA 29213 was able to further proliferate, whereas SA 8325-4 numbers were gradually inhibited. The strain specific inhibitory effect was verified in an *ex vivo* model using full thickness human skin, which also demonstrated the inhibitory factors were soluble in nature. Later analysis using microarray data indicated a differential mRNA expression of AMPs at 3hrs. Specifically, SA 8325-4 upregulated RNase 7, S100A12, hBD2 and hBD3, but SA 29213 induced no change in expression or downregulated these AMPs. Such inhibition of proliferation is likely to be caused by expression of AMPs, but further work would be required to prove precise mechanism regulating SA proliferation within this model. However, hBD3 would be a prime candidate as previous reports have documented that it may inhibit SA in a species specific manner (Kisich et al.,

2007, Midorikawa et al., 2003, Zanger et al., 2010, Zanger et al., 2011). The differential AMP response by strains of SA could suggest a tightly regulated system for interaction employed by the epidermal model. Another possibility would be a difference in SA virulence factors. Both SA strains have commonly been used as reference strains, acting as controls for investigating other SA isolates (Muller et al., 2016, Qiu et al., 2010, Moore and Lindsay, 2001, Peacock et al., 2000). However, SA 29213 is regarded as a more cytotoxic strain (Krut et al., 2003), whereas SA 8325-4 is considered less virulent due to a number of mutations. This includes disruption of the virulence factor PSMα3, and deletion of genes *rsbU* and *tcaR* (O'Neill, 2010).

The epidermal inflammatory response induced by SA colonisation was shown in changes induced in mRNA expression and protein release. Analysis of proteins released by the epidermal model indicated a continued inflammatory response over 24 hours, by further increased change in inflammatory mediators. This included increased production of common proinflammatory cytokines TNFα and GM-CSF, as well as increases in soluble receptor sIL-4Rα and co-receptor sCD14; denoting an acute phase response to bacterial PAMPs (pathogen associated molecular patterns). These increases were similarly induced by both strains of SA, but SA 29213 also increased production of IL-1α and IL-1β. Later analysis of gene expression within the activated inflammatory signalling pathways (Chapter 7) highlighted IL-36γ as an important inflammatory cytokine, but also demonstrated a 1.37 $\log_2$ fold change increase specific to SA 8325-4 after 3 hours of colonisation. IL-1α, IL-1β and IL-36γ are all proinflammatory mediators belonging to the IL-1 family, they stimulate the IL-1/TLR signalling pathway mediating microbial defence through production of pro-inflammatory cytokines, chemokines and AMPs (Cohen, 2014). These signalling pathways were also shown to be highly activated in the pathway analysis by increased expression of the IL-1 cytokines. However, the association of IL-36γ to increased AMP expression in keratinocytes (Johnston et al., 2011) could suggest critical importance in regulation of the differential colonisation by SA 8325-4 and SA 29213.

Transcriptomic analysis of the SA (8325-4) colonisation indicated an IL-17 inflammatory phenotype (increased in mRNA expression of IL-17C and IL-23A). The IL-17 mediation of inflammation occurs through the production of cytokines via NF-κB and the activation of the inflammasome (Speeckaert et al., 2016). IL-17 is also essential in host defence against cutaneous SA infection, as demonstrated in mice with a γδ T cell deficiency and consequent IL-17 impairment that have increased inflammation and bacterial load (Cho et al., 2010). Further evidence is demonstrated by a hyper-IgE syndrome caused by a STAT3 deficiency, which results in a decreased Th17 cell population and consequently leads to recurrent SA infections (Vogel et al., 2015). More specifically, UV-killed SA can induce PBMC IL-17 production in a toxin dependant

manner. SEA, SEB and SEC were all shown to be more potent at IL-17 induction than TSST-1 (Islander et al., 2010).

The pathway analysis of the transcriptomic data also exhibited the inflammatory nature of the SA colonisation, with activation of pathways associated to IL-1 signalling, TLR signalling, acute phase response and TREM1 signalling. More in depth analysis of activated pathways indicated prominent involvement of the NF-κB signalling pathway, which would correspond to the effects induced by IL-17 and IL-1 that both induce a proinflammatory response through the transcription factor NF-κB.

The transcriptomic analysis of SA colonisation also suggested the suppression of epidermal remodelling, via the downregulation of genes associated to cytoskeleton rearrangement (LDB2) and matrix remodelling (MXRA5); as well as a cytoskeleton component (PLEC) and an actin binding protein (SYNE1). However, pathway analysis did not expose any pathways related to cytoskeleton rearrangement or epidermal remodelling that were significantly activated or inhibited. Whilst suppression of epidermal remodelling could be beneficial to generating a niche for SA, it could also be detrimental to SA survival and invasion. Transcriptomic analysis of a cow's udder infection model showed SA infection caused activation of pathways associated to cytoskeletal rearrangements, including: RhoA Signalling, Actin Cytoskeleton Signalling and Regulation of Actin-based Motility by Rho (Gunther et al., 2017). This was suggested to be associated to SA internalisation, therefore inhibition of this rearrangement could stop internalisation.

8.2 Staphylococcus epidermidis

Epidermal colonisation of SE was shown to be highly proliferative, which emulates the skin's preference towards SE colonisation. However, SE also induced a prominent transcriptomic inflammatory response as shown by analysis of protein release, changes in mRNA expression, and the network analysis from transcriptomic data.

Epidermal protein release in response to SE colonisation showed increased TNFα, GM-CSF, IL-1α and IL-4Rα; with comparable increases to SA colonisation. Transcriptomic analysis showed increased mRNA expression of proinflammatory cytokines and chemokines including IL-17C, IL-23A, TNFα, GM-CSF, G-CSF, IL-20, IL-6, CXCL1, CXCL2 CXCL3 and CCL20; additionally highlighting a number of them as the most differentially expressed genes of significance. These inflammatory mediators showed a response characterised by IL-17 and stimulation of IL-1 and TLR signalling,

similar to SA colonisation. Neonatal skin SE has been shown to mediate immune tolerance in a murine model (Scharschmidt et al., 2015). Therefore, the inflammatory transcriptome noted by SE here may serve to be important for induction of tolerance in the human model (Chapter 3). Indeed, it has previously been suggested that TLR induced inflammation by SE colonisation may be important for induction of an antimicrobial response to defend against other pathogens (Lai et al., 2010).

The inflammatory mediators mentioned above increased in mRNA expression between 3 hours and 24 hours, suggesting an elevated inflammatory response, corresponding to the increased colonisation during the time course. However in contrast, pathway analysis indicated a reduction in inflammation between 3 hours and 24 hours. This reduction was inhibition of pathways such as TLR signalling, IL-1 signalling, acute phase response, TREM1 signalling, IL-6 signalling and DC maturation. Further analysis associated it to inhibition of NF-κB signalling, which was shown to be controlled negative regulation via upregulation of inhibitors of its signalling pathway. This included A20 (TNFAIP3), which was also highlighted as one of the most differentially expressed genes of significance in the transcriptomic analysis. However, despite this inhibition, inflammatory effects were demonstrated at 24 hours in both protein and mRNA expression. Indeed, tolerance induction was ongoing after 24 hours, which would recommend the study of later colonisation time points. The negative regulation of inflammation could be part of limiting the inflammatory response to induce tolerance.

The transciptomic analysis of SE colonisation also indicated an inhibition of translation via the inhibition of eIF2 dependent initiation. However, this is inconsistent with protein expression analysis that showed increased release of a number of inflammatory mediators. Therefore, it is not possible to elucidate the effects of the inhibition of the eIF2 signalling future investigation. eIF2B was shown to be key in regulating the initiation of translation and SE induced downregulation of its mRNA expression. ISRIB (Integrated stress response inhibitor) was recently shown to be an eIF2B activator that inhibited the ISR (Sidrauski et al., 2015), another aspect of eIF2 signalling pathway shown to be activated by SE colonisation. Therefore, if ISRIB could modulate the epidermal response to SE colonisation it may demonstrate the role of the ISR or deficiency of eIF2B.

8.3 Staphylococcus capitis

SC was able to colonise the epidermal model and was maintained over the 24 hours of study, but did not proliferate. This difference in colonisation to both SA and SE, could be due to an

unfavourable environment, for instance the lack of specific nutrients required for proliferation. This corresponds to the specific nature of SC's epidermal niche, which is around sebaceous glands of the scalp (Kloos and Schleifer, 1975).

The response induced by SC colonisation was minimal in comparison to SA or SE, whilst this was primarily evident in the transciptomic analysis, it also demonstrated in the epidermal protein analysis. SC induced only slight changes to the release of proinflammatory cytokines and chemokines, with minor increases to GM-CSF, IL-1α and sIL-4Rα after 24hrs of colonisation. Transciptomic analysis only identified 52 differentially expressed genes of significance and examination of the most differentially expressed of these did not indicate any inflammation. Instead revealing only slight increases in normal cellular processes.

Conversely, pathway analysis of the transcriptomic data did indicate an inflammatory response, via activation of TLR Signalling, IL-1 Signalling, Acute Phase Response, IL-6 Signalling and DC Maturation. At 3hrs the pathway activation was slight and insignificant, however by 24 hours of colonisation, many pathways were significantly activated; including each of the inflammatory pathways previously noted. This suggests a gradual or delayed inflammatory response, which would require a later timepoint of colonisation to fully elucidate.

Due to the experimental set up, the data from 3 and 24hrs were combined to test for the statistically significantly differentially expressed genes. Although this provided a greater statistical power, the down side is that individual responses unique to 3 hours or 24 hours would be disadvantaged in reaching top DEG status from a combined list.

8.4 Summary

Colonisation of SA and SE induced similar IL-17 responses on the epidermis that were mediated by different proinflammatory cytokines and chemokines. Both SA and SE induced significant expression of IL-17C and IL-23A. The IL-17C indicates the epidermis can drive an IL-17 response without Th17 cells present, but the IL-23 shows Th17 polarisation would occur if recruited. The recruitment and activation of the adaptive immune system was demonstrated by chemokine and GM-CSF expression, as well as DC activation. Both SA and SE induced this communication between epidermis and immune cells, but SE exhibited a more prominent response towards the adaptive immune system, thought to be instigating neonatal tolerance as demonstrated *in vivo* (Scharschmidt et al., 2015).

The IL-17 response was induced through a number of pathways including TLR Signalling and IL-1 Signalling but cumulated in the activation of NF-κB to enhance host defence. This caused inhibition of SA colonisation, most likely through production of IL-36γ, which can regulate AMP production. However, the response towards SE colonisation eventually caused negative regulation of NF-κB through downregulation of pathway mediators, as well as upregulation of NF-κB inhibitors, such as A20.

The minimal response induced by SC colonisation suggested a delayed inflammatory response, which would be induced through pathways such as TLR Signalling and IL-1 Signalling, similarly to SA and SE. However, analysis of lengthened colonisation periods would be required for further examination.

8.5 Future work

This research highlighted important differences in keratinocyte sensing of different staphylococcal species. These differences were shown at a cellular, protein and molecular level. However, due to the nature of the approaches taken, direct pathway / molecule cross-referencing between the models and systems utilised was challenging. To consolidate the transcriptomic data, confirmation of key differences in target gene transcription (e.g. IKK complex pathway, eIF2) with qPCR is planned. Furthermore, exploration of the cellular system for confirmation of protein expression with bead array or Western blot is required. Having demonstrated the observed differential pathway regulation, it would be important to demonstrate functional relevance of these pathways. The group has successfully undertaken knock downs in other keratinocyte models. With this in mind various knock-down approaches are planned for IKK complex and EIF2 signalling pathway to determine the impact on dendritic cell activation.

There are various further control analyses that would be important to consider in the attempt to fully characterise the epidermal response to staphylococci. These include challenging the described systems with many other strains of staphylococci. To address this, a large collection of clinical isolates have been gathered (n=100).

Of course, *in vivo*, the skin microbiome exists as a complex mixture of bacteria. Therefore, it is possible that direct interaction between bacterial species could also play an important role in regulating cutaneous inflammation. To study this, the characterisation of mixed microbial colonisations is underway to assess how these staphylococci would differentially modulate the

epidermal response when in a community. Thus taking into account the inter-strain competition typical of the microbiome, which may elucidate differences important in dysbiosis.

Additionally, further examination of the bacteria primed cross-talk between the epidermis and adaptive cutaneous immune system will be examined using similar model systems through analysis of bacteria primed skin models regulation of DC:T cell priming with subsequent T cell phenotypic analysis. This work will be important to understand how microbe – skin interactions may modify immune responses throughout a tissue or potentially in a systemic manner.

References

AKDIS, M., PALOMARES, O., VAN DE VEEN, W., VAN SPLUNTER, M. & AKDIS, C. A. 2012. TH17 and TH22 cells: a confusion of antimicrobial response with tissue inflammation versus protection. *J Allergy Clin Immunol,* 129**,** 1438-49; quiz1450-1.

AL-RAMLI, W., PRÉFONTAINE, D., CHOUIALI, F., MARTIN, J. G., OLIVENSTEIN, R., LEMIÈRE, C. & HAMID, Q. 2009. Th17-associated cytokines (IL-17A and IL-17F) in severe asthma. *Journal of Allergy and Clinical Immunology,* 123**,** 1185-1187.

ALIAHMADI, E., GRAMLICH, R., GRUTZKAU, A., HITZLER, M., KRUGER, M., BAUMGRASS, R., SCHREINER, M., WITTIG, B., WANNER, R. & PEISER, M. 2009. TLR2-activated human langerhans cells promote Th17 polarization via IL-1beta, TGF-beta and IL-23. *Eur J Immunol,* 39**,** 1221-30.

ANDREWS, A. L., HOLLOWAY, J. W., HOLGATE, S. T. & DAVIES, D. E. 2006. IL-4 Receptor Is an Important Modulator of IL-4 and IL-13 Receptor Binding: Implications for the Development of Therapeutic Targets. *The Journal of Immunology,* 176**,** 7456-7461.

ARDERN-JONES, M. R., BLACK, A. P., BATEMAN, E. A. & OGG, G. S. 2007. Bacterial superantigen facilitates epithelial presentation of allergen to T helper 2 cells. *Proc Natl Acad Sci U S A,* 104**,** 5557-62.

ARIAS, M. A., REY NORES, J. E., VITA, N., STELTER, F., BORYSIEWICZ, L. K., FERRARA, P. & LABETA, M. O. 2000. Cutting Edge: Human B Cell Function Is Regulated by Interaction with Soluble CD14: Opposite Effects on IgG1 and IgE Production. *The Journal of Immunology,* 164**,** 3480-3486.

ARIOTTI, S., BELTMAN, J. B., CHODACZEK, G., HOEKSTRA, M. E., VAN BEEK, A. E., GOMEZ-EERLAND, R., RITSMA, L., VAN RHEENEN, J., MAREE, A. F., ZAL, T., DE BOER, R. J., HAANEN, J. B. & SCHUMACHER, T. N. 2012. Tissue-resident memory CD8+ T cells continuously patrol skin epithelia to quickly recognize local antigen. *Proc Natl Acad Sci U S A,* 109**,** 19739-44.

ARRECUBIETA, C., LEE, M. H., MACEY, A., FOSTER, T. J. & LOWY, F. D. 2007. SdrF, a Staphylococcus epidermidis surface protein, binds type I collagen. *J Biol Chem,* 282**,** 18767-76.

ASKARIAN, F., AJAYI, C., HANSSEN, A. M., VAN SORGE, N. M., PETTERSEN, I., DIEP, D. B., SOLLID, J. U. & JOHANNESSEN, M. 2016. The interaction between Staphylococcus aureus SdrD and desmoglein 1 is important for adhesion to host cells. *Sci Rep,* 6**,** 22134.

ATHANASOPOULOS, A. N., ECONOMOPOULOU, M., ORLOVA, V. V., SOBKE, A., SCHNEIDER, D., WEBER, H., AUGUSTIN, H. G., EMING, S. A., SCHUBERT, U., LINN, T., NAWROTH, P. P., HUSSAIN, M., HAMMES, H.-P., HERRMANN, M., PREISSNER, K. T. & CHAVAKIS, T. 2006. The extracellular adherence protein (Eap) of *Staphylococcus aureus* inhibits wound healing by interfering with host defense and repair mechanisms. *Blood,* 107**,** 2720.

AUFIERO, B., GUO, M., YOUNG, C., DUANMU, Z., TALWAR, H., LEE, H. K. & MURAKAWA, G. J. 2007. Staphylococcus aureus induces the expression of tumor necrosis factor-α in primary human keratinocytes. *International Journal of Dermatology,* 46**,** 687-694.

BACH, I. 2000. The LIM domain: regulation by association. *Mechanisms of Development,* 91**,** 5-17.

BÆK, K. T., FREES, D., RENZONI, A., BARRAS, C., RODRIGUEZ, N., MANZANO, C. & KELLEY, W. L. 2013. Genetic Variation in the Staphylococcus aureus 8325 Strain Lineage Revealed by Whole-Genome Sequencing. *PLoS ONE,* 8**,** e77122.

BAKER, B. S. 2006. The role of microorganisms in atopic dermatitis. *Clin Exp Immunol,* 144**,** 1-9.

BANERJEE, G., DAMODARAN, A., DEVI, N., DHARMALINGAM, K. & RAMAN, G. 2004. Role of Keratinocytes in Antigen Presentation and Polarization of Human T Lymphocytes. *Scandinavian Journal of Immunology,* 59**,** 385-394.

BARATIN, M., FORAY, C., DEMARIA, O., HABBEDDINE, M., POLLET, E., MAURIZIO, J., VERTHUY, C., DAVANTURE, S., AZUKIZAWA, H., FLORES-LANGARICA, A., DALOD, M. & LAWRENCE, T. 2015. Homeostatic NF-kappaB Signaling in Steady-State Migratory Dendritic Cells Regulates Immune Homeostasis and Tolerance. *Immunity,* 42**,** 627-39.

BARBU, E. M., GANESH, V. K., GURUSIDDAPPA, S., MACKENZIE, R. C., FOSTER, T. J., SUDHOF, T. C. & HOOK, M. 2010. beta-Neurexin is a ligand for the Staphylococcus aureus MSCRAMM SdrC. *PLoS Pathog,* 6**,** e1000726.

BARNARD, E., SHI, B., KANG, D., CRAFT, N. & LI, H. 2016. The balance of metagenomic elements shapes the skin microbiome in acne and health. *Sci Rep,* 6**,** 39491.

BAS, S., GAUTHIER, B. R., SPENATO, U., STINGELIN, S. & GABAY, C. 2004. CD14 Is an Acute-Phase Protein. *The Journal of Immunology,* 172**,** 4470-4479.

BAUMERT, P., CONSORTIUM, G. R., LAKE, M. J., DRUST, B., STEWART, C. E. & ERSKINE, R. M. 2018. TRIM63 (MuRF-1) gene polymorphism is associated with biomarkers of exercise-induced muscle damage. *Physiological Genomics,* 50**,** 142-143.

BECKER, K., HEILMANN, C. & PETERS, G. 2014. Coagulase-negative staphylococci. *Clin Microbiol Rev,* 27**,** 870-926.

BEILSTEN-EDMANDS, V., GORDIYENKO, Y., KUNG, J. C., MOHAMMED, S., SCHMIDT, C. & ROBINSON, C. V. 2015. eIF2 interactions with initiator tRNA and eIF2B are regulated by post-translational modifications and conformational dynamics. *Cell Discov,* 1**,** 15020.

BELL, E., EHRLICH, H. P., BUTTLE, D. J. & NAKATSUJI, T. 1981. Living tissue formed in vitro and accepted as skin-equivalent tissue of full thickness. *Science,* 211**,** 1052.

BENDELAC, A., SAVAGE, P. B. & TEYTON, L. 2007. The biology of NKT cells. *Annu Rev Immunol,* 25**,** 297-336.

BERGERS, L., REIJNDERS, C. M. A., VAN DEN BROEK, L. J., SPIEKSTRA, S. W., DE GRUIJL, T. D., WEIJERS, E. M. & GIBBS, S. 2016. Immune-competent human skin disease models. *Drug Discov Today,* 21**,** 1479-1488.

BERROTH, A., KUHNL, J., KURSCHAT, N., SCHWARZ, A., STAB, F., SCHWARZ, T., WENCK, H., FOLSTER-HOLST, R. & NEUFANG, G. 2013. Role of fibroblasts in the pathogenesis of atopic dermatitis. *J Allergy Clin Immunol,* 131**,** 1547-54.

BERTOLERO, F., KAIGHN, M. E., CAMALIER, R. F. & SAFFIOTTI, U. 1986. Effects of serum and serum-derived factors on growth and differentiation of mouse keratinocytes. *In Vitro Cellular & Developmental Biology,* 22**,** 423-428.

BIEN, J., SOKOLOVA, O. & BOZKO, P. 2011. Characterization of Virulence Factors of Staphylococcus aureus: Novel Function of Known Virulence Factors That Are Implicated in Activation of Airway Epithelial Proinflammatory Response. *J Pathog,* 2011**,** 601905.

BIKLE, D. D., XIE, Z. & TU, C. L. 2012. Calcium regulation of keratinocyte differentiation. *Expert Rev Endocrinol Metab,* 7**,** 461-472.

BISWAS, R., VOGGU, L., SIMON, U. K., HENTSCHEL, P., THUMM, G. & GOTZ, F. 2006. Activity of the major staphylococcal autolysin Atl. *FEMS Microbiol Lett,* 259**,** 260-8.

BLACK, A. P., ARDERN-JONES, M. R., KASPROWICZ, V., BOWNESS, P., JONES, L., BAILEY, A. S. & OGG, G. S. 2007. Human keratinocyte induction of rapid effector function in antigen-specific memory CD4+ and CD8+ T cells. *Eur J Immunol,* 37**,** 1485-93.

BLONSKA, M., SHAMBHARKAR, P. B., KOBAYASHI, M., ZHANG, D., SAKURAI, H., SU, B. & LIN, X. 2005. TAK1 is recruited to the tumor necrosis factor-alpha (TNF-alpha) receptor 1 complex in a receptor-interacting protein (RIP)-dependent manner and cooperates with MEKK3 leading to NF-kappaB activation. *J Biol Chem,* 280**,** 43056-63.

BOUKAMP, P., PETRUSSEVSKA, R. T., BREITKREUTZ, D., HORNUNG, J., MARKHAM, A. & FUSENIG, N. E. 1988. Normal keratinization in a spontaneously immortalized aneuploid human keratinocyte cell line. *The Journal of Cell Biology,* 106**,** 761-771.

BOWCOCK, A. M., SHANNON, W., DU, F., DUNCAN, J., CAO, K., AFTERGUT, K., CATIER, J., FERNANDEZ-VINA, M. A. & MENTER, A. 2001. Insights into psoriasis and other inflammatory diseases from large-scale gene expression studies. *Human Molecular Genetics,* 10**,** 1793-1805.

BOWDEN, M. G., CHEN, W., SINGVALL, J., XU, Y., PEACOCK, S. J., VALTULINA, V., SPEZIALE, P. & HOOK, M. 2005. Identification and preliminary characterization of cell-wall-anchored proteins of Staphylococcus epidermidis. *Microbiology,* 151**,** 1453-64.

BOYCE, S. T. & HAM, R. G. 1983. Calcium-Regulated Differentiation of Normal Human Epidermal Keratinocytes in Chemically Defined Clonal Culture and Serum-Free Serial Culture. *J Investig Dermatol,* 81**,** 33s-40s.

BOYLE, J. 2008. Molecular biology of the cell, 5th edition by B. Alberts, A. Johnson, J. Lewis, M. Raff, K. Roberts, and P. Walter. *Biochemistry and Molecular Biology Education,* 36**,** 317-318.

BRAFF, M. H., DI NARDO, A. & GALLO, R. L. 2005. Keratinocytes store the antimicrobial peptide cathelicidin in lamellar bodies. *J Invest Dermatol,* 124**,** 394-400.

BRANDT, E. B. & SIVAPRASAD, U. 2011. Th2 Cytokines and Atopic Dermatitis. *Journal of clinical & cellular immunology,* 2**,** 110.

BRAVERMAN, I. M. 1989. Ultrastructure and Organization of the Cutaneous Microvasculature in Normal and Pathologic States. *Journal of Investigative Dermatology,* 93**,** S2-S9.

BREED, R. S., MURRAY, E. G. D. & N.R, S. 1957. Bergey's Manual of Determinative Bacteriology (7th ed.). *American Journal of Public Health and the Nations Health,* 54**,** 544-544.

BROWN, A. F., LEECH, J. M., ROGERS, T. R. & MCLOUGHLIN, R. M. 2014. Staphylococcus aureus Colonization: Modulation of Host Immune Response and Impact on Human Vaccine Design. *Front Immunol,* 4**,** 507.

BROZ, P. & DIXIT, V. M. 2016. Inflammasomes: mechanism of assembly, regulation and signalling. *Nat Rev Immunol,* 16**,** 407-20.

BRUNNER, P. M., GUTTMAN-YASSKY, E. & LEUNG, D. Y. 2017. The immunology of atopic dermatitis and its reversibility with broad-spectrum and targeted therapies. *J Allergy Clin Immunol,* 139**,** S65-S76.

BUCHBINDER, E. I. & DESAI, A. 2016. CTLA-4 and PD-1 Pathways: Similarities, Differences, and Implications of Their Inhibition. *Am J Clin Oncol,* 39**,** 98-106.

BUKOWSKI, M., WLADYKA, B. & DUBIN, G. 2010. Exfoliative toxins of Staphylococcus aureus. *Toxins (Basel),* 2**,** 1148-65.

BUMGARNER, R. 2013. Overview of DNA microarrays: types, applications, and their future. *Curr Protoc Mol Biol,* Chapter 22**,** Unit 22 1.

BUR, S., PREISSNER KT FAU - HERRMANN, M., HERRMANN M FAU - BISCHOFF, M. & BISCHOFF, M. 2013. The Staphylococcus aureus extracellular adherence protein promotes bacterial internalization by keratinocytes independent of fibronectin-binding proteins. *journal of investigative dermatology,* 133**,** 2004-12.

BURIAN, M., WOLZ, C. & GOERKE, C. 2010. Regulatory adaptation of Staphylococcus aureus during nasal colonization of humans. *PLoS One,* 5**,** e10040.

BURKE, F. M., MCCORMACK, N., RINDI, S., SPEZIALE, P. & FOSTER, T. J. 2010. Fibronectin-binding protein B variation in Staphylococcus aureus. *BMC Microbiology,* 10**,** 160.

CAMERON, D. R., JIANG, J. H., HASSAN, K. A., ELBOURNE, L. D., TUCK, K. L., PAULSEN, I. T. & PELEG, A. Y. 2015. Insights on virulence from the complete genome of Staphylococcus capitis. *Front Microbiol,* 6**,** 980.

CARLSON, M. W., ALT-HOLLAND, A., EGLES, C. & GARLICK, J. A. 2008. Three-dimensional tissue models of normal and diseased skin. *Curr Protoc Cell Biol,* Chapter 19**,** Unit 19 9.

CARNEIRO, C. R., POSTOL, E., NOMIZO, R., REIS, L. F. & BRENTANI, R. R. 2004. Identification of enolase as a laminin-binding protein on the surface of Staphylococcus aureus. *Microbes Infect,* 6**,** 604-8.

CARSON, K. C., BARTLETT, J. G., TAN, T. J. & RILEY, T. V. 2007. In Vitro susceptibility of methicillin-resistant Staphylococcus aureus and methicillin-susceptible Staphylococcus aureus to a new antimicrobial, copper silicate. *Antimicrob Agents Chemother,* 51**,** 4505-7.

CHAVAKIS, T., WIECHMANN, K., PREISSNER, K. T. & HERRMANN, M. 2005. Staphylococcus aureus interactions with the endothelium: the role of bacterial "secretable expanded repertoire adhesive molecules" (SERAM) in disturbing host defense systems. *Thromb Haemost,* 94**,** 278-85.

CHEN, X., LU, Y., ZHANG, Z., WANG, J., YANG, H. & LIU, G. 2015. Intercellular interplay between Sirt1 signalling and cell metabolism in immune cell biology. *Immunology,* 145**,** 455-67.

CHEUNG, G. Y., WANG, R., KHAN, B. A., STURDEVANT, D. E. & OTTO, M. 2011. Role of the accessory gene regulator agr in community-associated methicillin-resistant Staphylococcus aureus pathogenesis. *Infect Immun,* 79**,** 1927-35.

CHICHEPORTICHE, Y., BOURDON, P. R., XU, H., HSU, Y.-M., SCOTT, H., HESSION, C., GARCIA, I. & BROWNING, J. L. 1997. TWEAK, a New Secreted Ligand in the Tumor Necrosis Factor Family That Weakly Induces Apoptosis. *Journal of Biological Chemistry,* 272**,** 32401-32410.

CHIRICOZZI, A., NOGRALES, K. E., JOHNSON-HUANG, L. M., FUENTES-DUCULAN, J., CARDINALE, I., BONIFACIO, K. M., GULATI, N., MITSUI, H., GUTTMAN-YASSKY, E., SUAREZ-FARINAS, M. &

KRUEGER, J. G. 2014. IL-17 induces an expanded range of downstream genes in reconstituted human epidermis model. *PLoS One,* 9**,** e90284.

CHO, J. S., PIETRAS, E. M., GARCIA, N. C., RAMOS, R. I., FARZAM, D. M., MONROE, H. R., MAGORIEN, J. E., BLAUVELT, A., KOLLS, J. K., CHEUNG, A. L., CHENG, G., MODLIN, R. L. & MILLER, L. S. 2010. IL-17 is essential for host defense against cutaneous Staphylococcus aureus infection in mice. *J Clin Invest,* 120**,** 1762-73.

CHO, S. H., STRICKLAND, I., TOMKINSON, A., FEHRINGER, A. P., GELFAND, E. W. & LEUNG, D. Y. 2001. Preferential binding of Staphylococcus aureus to skin sites of Th2-mediated inflammation in a murine model. *J Invest Dermatol,* 116**,** 658-63.

CHOI, W., MIYAMURA, Y., WOLBER, R., SMUDA, C., REINHOLD, W., LIU, H., KOLBE, L. & HEARING, V. J. 2010. Regulation of human skin pigmentation in situ by repetitive UV exposure: molecular characterization of responses to UVA and/or UVB. *J Invest Dermatol,* 130**,** 1685-96.

CHOY, D. F., HSU, D. K., SESHASAYEE, D., FUNG, M. A., MODRUSAN, Z., MARTIN, F., LIU, F. T. & ARRON, J. R. 2012. Comparative transcriptomic analyses of atopic dermatitis and psoriasis reveal shared neutrophilic inflammation. *J Allergy Clin Immunol,* 130**,** 1335-43 e5.

CHRISTIAN, F., SMITH, E. L. & CARMODY, R. J. 2016. The Regulation of NF-kappaB Subunits by Phosphorylation. *Cells,* 5.

CIRILLO, E., PARNELL, L. D. & EVELO, C. T. 2017. A Review of Pathway-Based Analysis Tools That Visualize Genetic Variants. *Front Genet,* 8**,** 174.

CLARK, R. A., CHONG, B., MIRCHANDANI, N., BRINSTER, N. K., YAMANAKA, K. I., DOWGIERT, R. K. & KUPPER, T. S. 2006. The Vast Majority of CLA+ T Cells Are Resident in Normal Skin. *The Journal of Immunology,* 176**,** 4431-4439.

CLARKE, S. R., HARRIS, L. G., RICHARDS, R. G. & FOSTER, S. J. 2002. Analysis of Ebh, a 1.1-megadalton cell wall-associated fibronectin-binding protein of Staphylococcus aureus. *Infect Immun,* 70.

CLARKE, S. R., WILTSHIRE, M. D. & FOSTER, S. J. 2004. IsdA of Staphylococcus aureus is a broad spectrum, iron-regulated adhesin. *Mol Microbiol,* 51**,** 1509-19.

COGEN, A. L., YAMASAKI, K., SANCHEZ, K. M., DORSCHNER, R. A., LAI, Y., MACLEOD, D. T., TORPEY, J. W., OTTO, M., NIZET, V., KIM, J. E. & GALLO, R. L. 2010. Selective antimicrobial action is provided by phenol-soluble modulins derived from Staphylococcus epidermidis, a normal resident of the skin. *J Invest Dermatol,* 130**,** 192-200.

COHEN, P. 2014. The TLR and IL-1 signalling network at a glance. *Journal of cell science,* 127**,** 2383-2390.

COLE, C., KROBOTH, K., SCHURCH, N. J., SANDILANDS, A., SHERSTNEV, A., O'REGAN, G. M., WATSON, R. M., MCLEAN, W. H., BARTON, G. J., IRVINE, A. D. & BROWN, S. J. 2014. Filaggrin-stratified transcriptomic analysis of pediatric skin identifies mechanistic pathways in patients with atopic dermatitis. *J Allergy Clin Immunol,* 134**,** 82-91.

CONE, L. A., SONTZ, E. M., WILSON, J. W. & MITRUKA, S. N. 2005. Staphylococcus capitis endocarditis due to a transvenous endocardial pacemaker infection: case report and review of Staphylococcus capitis endocarditis. *Int J Infect Dis,* 9**,** 335-9.

COOPER, J. T., STROKA, D. M., BROSTJAN, C., PALMETSHOFER, A., BACH, F. H. & FERRAN, C. 1996. A20 Blocks Endothelial Cell Activation through a NF-κB-dependent Mechanism. *Journal of Biological Chemistry,* 271**,** 18068-18073.

CORTHAY, A. 2009. How do regulatory T cells work? *Scand J Immunol,* 70**,** 326-36.

CRAMTON, S. E., GERKE, C., SCHNELL, N. F., NICHOLS, W. W. & GÖTZ, F. 1999. The intercellular adhesion (ica) locus is present in Staphylococcus aureus and is required for biofilm formation. *Infection and immunity,* 67**,** 5427-5433.

CREECH, C. B., AL-ZUBEIDI, D. N. & FRITZ, S. A. 2015. Prevention of Recurrent Staphylococcal Skin Infections. *Infect Dis Clin North Am,* 29**,** 429-64.

CREECH, C. B., JOHNSON, B. G., ALSENTZER, A. R., HOHENBOKEN, M., EDWARDS, K. M. & TALBOT, T. R. 2009. Vaccination as infection control: a pilot study to determine the impact of Staphylococcus aureus vaccination on nasal carriage. *Vaccine,* 28.

CUA, D. J., SHERLOCK, J., CHEN, Y., MURPHY, C. A., JOYCE, B., SEYMOUR, B., LUCIAN, L., TO, W., KWAN, S., CHURAKOVA, T., ZURAWSKI, S., WIEKOWSKI, M., LIRA, S. A., GORMAN, D., KASTELEIN, R. A. & SEDGWICK, J. D. 2003. Interleukin-23 rather than interleukin-12 is the critical cytokine for autoimmune inflammation of the brain. *Nature,* 421**,** 744.

CUMMINGS, R. J., BARBET, G., BONGERS, G., HARTMANN, B. M., GETTLER, K., MUNIZ, L., FURTADO, G. C., CHO, J., LIRA, S. A. & BLANDER, J. M. 2016. Different tissue phagocytes sample apoptotic cells to direct distinct homeostasis programs. *Nature,* 539**,** 565-569.

DANSO, M. O., VAN DRONGELEN, V., MULDER, A., VAN ESCH, J., SCOTT, H., VAN SMEDEN, J., EL GHALBZOURI, A. & BOUWSTRA, J. A. 2014. TNF-[alpha] and Th2 Cytokines Induce Atopic Dermatitis-Like Features on Epidermal Differentiation Proteins and Stratum Corneum Lipids in Human Skin Equivalents. *J Invest Dermatol,* 134**,** 1941-1950.

DARLENSKI, R., *KAZANDJIEVA, J.* & *TSANKOV, N.* 2011. SKIN BARRIER FUNCTION: MORPHOLOGICAL BASIS AND REGULATORY MECHANISMS. *Journal of Clinical medicine,* 4**,** 36-45.

DAVIS, S. L., GURUSIDDAPPA, S., MCCREA, K. W., PERKINS, S. & HOOK, M. 2001. SdrG, a fibrinogen-binding bacterial adhesin of the microbial surface components recognizing adhesive matrix molecules subfamily from Staphylococcus epidermidis, targets the thrombin cleavage site in the Bbeta chain. *J Biol Chem,* 276**,** 27799-805.

DE BUEGER, M., BAKKER A FAU - GOULMY, E. & GOULMY, E. 1993. Human keratinocytes activate primed major and minor histocompatibility antigen specific Th cells in vitro. *Transpl Immunol,* 1**,** 52-59.

DE FILIPPO, K., DUDECK, A., HASENBERG, M., NYE, E., VAN ROOIJEN, N., HARTMANN, K., GUNZER, M., ROERS, A. & HOGG, N. 2013. Mast cell and macrophage chemokines CXCL1/CXCL2 control the early stage of neutrophil recruitment during tissue inflammation. *Blood,* 121**,** 4930-7.

DE VUYST, E., SALMON, M., EVRARD, C., LAMBERT DE ROUVROIT, C. & POUMAY, Y. 2017. Atopic Dermatitis Studies through In Vitro Models. *Front Med (Lausanne),* 4**,** 119.

DELERIVE, P., DE BOSSCHER, K., VANDEN BERGHE, W., FRUCHART, J.-C., HAEGEMAN, G. & STAELS, B. 2002. DNA Binding-Independent Induction of IκBα Gene Transcription by PPARα. *Molecular Endocrinology,* 16**,** 1029-1039.

DEN HEIJER, C. D. J., VAN BIJNEN, E. M. E., PAGET, W. J., PRINGLE, M., GOOSSENS, H., BRUGGEMAN, C. A., SCHELLEVIS, F. G. & STOBBERINGH, E. E. 2013. Prevalence and resistance of commensal Staphylococcus aureus, including meticillin-resistant S aureus, in nine European countries: a cross-sectional study. *The Lancet Infectious Diseases,* 13**,** 409-415.

DEVOS, M., MOGILENKO, D. A., FLEURY, S., GILBERT, B., BECQUART, C., QUEMENER, S., DEHONDT, H., TOUGAARD, P., STAELS, B., BACHERT, C., VANDENABEELE, P., VAN LOO, G., STAUMONT-SALLE, D., DECLERCQ, W. & DOMBROWICZ, D. 2018. Keratinocyte Expression of A20/TNFAIP3 Controls Skin Inflammation Associated with Atopic Dermatitis and Psoriasis. *J Invest Dermatol*.

DEY, S., BAIRD, T. D., ZHOU, D., PALAM, L. R., SPANDAU, D. F. & WEK, R. C. 2010. Both transcriptional regulation and translational control of ATF4 are central to the integrated stress response. *J Biol Chem,* 285**,** 33165-74.

DI PAOLO, N. C. & SHAYAKHMETOV, D. M. 2016. Interleukin 1alpha and the inflammatory process. *Nat Immunol,* 17**,** 906-13.

DILIOGLOU, S., CRUSE, J. M. & LEWIS, R. E. 2003. Function of CD80 and CD86 on monocyte- and stem cell-derived dendritic cells. *Experimental and Molecular Pathology,* 75**,** 217-227.

DINARELLO, C. A. 2018. Overview of the IL-1 family in innate inflammation and acquired immunity. *Immunol Rev,* 281**,** 8-27.

DOTTERUD, L. K., WILSGAARD, T., VORLAND, L. H. & FALK, E. S. 2016. The effect of UVB radiation on skin microbiota in patients with atopic dermatitis and healthy controls. *International Journal of Circumpolar Health,* 67**,** 254-260.

DOWNER, R., ROCHE, F., PARK, P. W., MECHAM, R. P. & FOSTER, T. J. 2002. The elastin-binding protein of Staphylococcus aureus (EbpS) is expressed at the cell surface as an integral membrane protein and not as a cell wall-associated protein. *J Biol Chem,* 277.

DRAGER, S., KALIES, K., SIDRONIO, T. B., WITTE, M., LUDWIG, R. J. & BIEBER, K. 2017. Increased TREM-1 expression in inflamed skin has no functional impact on the pathogenesis of cutaneous disorders. *J Dermatol Sci,* 88**,** 152-155.

DRAKE, D. R., BROGDEN, K. A., DAWSON, D. V. & WERTZ, P. W. 2008. Thematic review series: skin lipids. Antimicrobial lipids at the skin surface. *J Lipid Res,* 49**,** 4-11.

DUBRAC, S. & SCHMUTH, M. 2011. PPAR-alpha in cutaneous inflammation. *Dermatoendocrinol,* 3**,** 23-6.

DUMONT, A. L., NYGAARD, T. K., WATKINS, R. L., SMITH, A., KOZHAYA, L., KREISWIRTH, B. N., SHOPSIN, B., UNUTMAZ, D., VOYICH, J. M. & TORRES, V. J. 2011. Characterization of a new cytotoxin that contributes to Staphylococcus aureus pathogenesis. *Mol Microbiol,* 79**,** 814-25.

ECKHART, L., LIPPENS, S., TSCHACHLER, E. & DECLERCQ, W. 2013. Cell death by cornification. *Biochimica et Biophysica Acta (BBA) - Molecular Cell Research,* 1833**,** 3471-3480.

EDWARDS, A. M., POTTER, U., MEENAN, N. A. G., POTTS, J. R. & MASSEY, R. C. 2011. *Staphylococcus aureus* Keratinocyte Invasion Is Dependent upon Multiple High-Affinity Fibronectin-Binding Repeats within FnBPA. *PLoS ONE,* 6**,** e18899.

EGAWA, G. & KABASHIMA, K. 2018. Barrier dysfunction in the skin allergy. *Allergol Int,* 67**,** 3-11.

EGAWA, G., WENINGER, W. & GINHOUX, F. 2015. Pathogenesis of atopic dermatitis: A short review. *Cogent Biology,* 1.

EIDSMO, L. & MARTINI, E. 2018. Human Langerhans Cells with Pro-inflammatory Features Relocate within Psoriasis Lesions. *Front Immunol,* 9**,** 300.

EL GHALBZOURI, A., SIAMARI R FAU - WILLEMZE, R., WILLEMZE R FAU - PONEC, M. & PONEC, M. 2008. Leiden reconstructed human epidermal model as a tool for the evaluation of the skin corrosion and irritation potential according to the ECVAM guidelines. *Toxicology in Vitro,* 22**,** 1311-20.

ELIAS, P. M., GRUBER, R., CRUMRINE, D., MENON, G., WILLIAMS, M. L., WAKEFIELD, J. S., HOLLERAN, W. M. & UCHIDA, Y. 2014. Formation and functions of the corneocyte lipid envelope (CLE). *Biochim Biophys Acta,* 1841**,** 314-8.

ELLINGHAUS, D., BAURECHT, H., ESPARZA-GORDILLO, J., RODRIGUEZ, E., MATANOVIC, A., MARENHOLZ, I., HUBNER, N., SCHAARSCHMIDT, H., NOVAK, N., MICHEL, S., MAINTZ, L., WERFEL, T., MEYER-HOFFERT, U., HOTZE, M., PROKISCH, H., HEIM, K., HERDER, C., HIROTA, T., TAMARI, M., KUBO, M., TAKAHASHI, A., NAKAMURA, Y., TSOI, L. C., STUART, P., ELDER, J. T., SUN, L., ZUO, X., YANG, S., ZHANG, X., HOFFMANN, P., NOTHEN, M. M., FOLSTER-HOLST, R., WINKELMANN, J., ILLIG, T., BOEHM, B. O., DUERR, R. H., BUNING, C., BRAND, S., GLAS, J., MCALEER, M. A., FAHY, C. M., KABESCH, M., BROWN, S., MCLEAN, W. H., IRVINE, A. D., SCHREIBER, S., LEE, Y. A., FRANKE, A. & WEIDINGER, S. 2013. High-density genotyping study identifies four new susceptibility loci for atopic dermatitis. *Nat Genet,* 45**,** 808-12.

ERIKSEN, N. H., ESPERSEN, F., ROSDAHL, V. T. & JENSEN, K. 1995. Carriage of Staphylococcus aureus among 104 healthy persons during a 19-month period. *Epidemiology and infection,* 115**,** 51-60.

ERMERTCAN, A. T., ÖZTÜRK, F. & GÜNDÜZ, K. 2011. Toll-like receptors and skin. *Journal of the European Academy of Dermatology and Venereology,* 25**,** 997-1006.

ESKANDARIAN, H. A., IMPENS, F., NAHORI, M. A., SOUBIGOU, G., COPPEE, J. Y., COSSART, P. & HAMON, M. A. 2013. A role for SIRT2-dependent histone H3K18 deacetylation in bacterial infection. *Science,* 341**,** 1238858.

EWALD, D. A., NODA, S., OLIVA, M., LITMAN, T., NAKAJIMA, S., LI, X., XU, H., WORKMAN, C. T., SCHEIPERS, P., SVITACHEVA, N., LABUDA, T., KRUEGER, J. G., SUAREZ-FARINAS, M., KABASHIMA, K. & GUTTMAN-YASSKY, E. 2017. Major differences between human atopic dermatitis and murine models, as determined by using global transcriptomic profiling. *J Allergy Clin Immunol,* 139**,** 562-571.

FANG, Y., GONG, S. J., XU, Y. H., HAMBLY, B. D. & BAO, S. 2007. Impaired cutaneous wound healing in granulocyte/macrophage colony-stimulating factor knockout mice. *Br J Dermatol,* 157**,** 458-65.

FEINGOLD, K. R. 2012. Lamellar bodies: the key to cutaneous barrier function. *J Invest Dermatol,* 132**,** 1951-3.

FEINGOLD, K. R. & ELIAS, P. M. 2014. Role of lipids in the formation and maintenance of the cutaneous permeability barrier. *Biochimica et Biophysica Acta (BBA) - Molecular and Cell Biology of Lipids,* 1841**,** 280-294.

FENTEM, J. H. & BOTHAM, P. A. 2002. ECVAM's activities in validating alternative tests for skin corrosion and irritation. *Alternatives to Laboratory Animals,* 30**,** 61-7.

FEUILLIE, C., FORMOSA-DAGUE, C., HAYS, L. M. C., VERVAECK, O., DERCLAYE, S., BRENNAN, M. P., FOSTER, T. J., GEOGHEGAN, J. A. & DUFRÊNE, Y. F. 2017. Molecular interactions and inhibition of the staphylococcal biofilm-forming protein SdrC. *Proceedings of the National Academy of Sciences,* 114**,** 3738-3743.

FLOSS, D. M., SCHRODER, J., FRANKE, M. & SCHELLER, J. 2015. Insights into IL-23 biology: From structure to function. *Cytokine Growth Factor Rev,* 26**,** 569-78.

FOSTER, T. J., GEOGHEGAN, J. A., GANESH, V. K. & HOOK, M. 2014. Adhesion, invasion and evasion: the many functions of the surface proteins of Staphylococcus aureus. *Nat Rev Microbiol,* 12**,** 49-62.

FOURNIER, B. & PHILPOTT, D. J. 2005. Recognition of Staphylococcus aureus by the innate immune system. *Clin Microbiol Rev,* 18**,** 521-40.

FRANKART, A., MALAISSE, J., DE VUYST, E., MINNER, F., DE ROUVROIT, C. L. & POUMAY, Y. 2012. Epidermal morphogenesis during progressive in vitro 3D reconstruction at the air–liquid interface. *Experimental Dermatology,* 21**,** 871-875.

FREDRICKS , D. N., FIEDLER , T. L. & MARRAZZO , J. M. 2005. Molecular Identification of Bacteria Associated with Bacterial Vaginosis. *New England Journal of Medicine,* 353**,** 1899-1911.

GAFFEN, S. L., JAIN, R., GARG, A. V. & CUA, D. J. 2014. The IL-23-IL-17 immune axis: from mechanisms to therapeutic testing. *Nat Rev Immunol,* 14**,** 585-600.

GALLO, R. L. & NAKATSUJI, T. 2011. Microbial symbiosis with the innate immune defense system of the skin. *J Invest Dermatol,* 131**,** 1974-80.

GAZEL, A., RAMPHAL, P., ROSDY, M., DE WEVER, B., TORNIER, C., HOSEIN, N., LEE, B., TOMIC-CANIC, M. & BLUMENBERG, M. 2003. Transcriptional profiling of epidermal keratinocytes: comparison of genes expressed in skin, cultured keratinocytes, and reconstituted epidermis, using large DNA microarrays. *J Invest Dermatol,* 121**,** 1459-68.

GEOGHEGAN, J. A., IRVINE, A. D. & FOSTER, T. J. 2018. Staphylococcus aureus and Atopic Dermatitis: A Complex and Evolving Relationship. *Trends Microbiol,* 26**,** 484-497.

GHASEMIAN, A., NAJAR PEERAYEH, S., BAKHSHI, B. & MIRZAEE, M. 2015. The Microbial Surface Components Recognizing Adhesive Matrix Molecules (MSCRAMMs) Genes among Clinical Isolates of Staphylococcus aureus from Hospitalized Children. *Iranian journal of pathology,* 10**,** 258-264.

GIROLOMONI, G. & PASTORE, S. 2001. The role of keratinocytes in the pathogenesis of atopic dermatitis. *Journal of the American Academy of Dermatology,* 45**,** S25-S28.

GOMEZ, M. I., O'SEAGHDHA, M., MAGARGEE, M., FOSTER, T. J. & PRINCE, A. S. 2006. Staphylococcus aureus protein A activates TNFR1 signaling through conserved IgG binding domains. *J Biol Chem,* 281**,** 20190-6.

GONG, J. Q., LIN L FAU - LIN, T., LIN T FAU - HAO, F., HAO F FAU - ZENG, F. Q., ZENG FQ FAU - BI, Z. G., BI ZG FAU - YI, D., YI D FAU - ZHAO, B. & ZHAO, B. 2006. Skin colonization by Staphylococcus aureus in patients with eczema and atopic dermatitis and relevant combined topical therapy: a double-blind multicentre randomized controlled trial. *British Journal of Dermatology,* 155**,** 680-687.

GRABIEC, A. M. & POTEMPA, J. 2018. Epigenetic regulation in bacterial infections: targeting histone deacetylases. *Crit Rev Microbiol,* 44**,** 336-350.

GRAHAM, R. R., COTSAPAS, C., DAVIES, L., HACKETT, R., LESSARD, C. J., LEON, J. M., BURTT, N. P., GUIDUCCI, C., PARKIN, M., GATES, C., PLENGE, R. M., BEHRENS, T. W., WITHER, J. E., RIOUX, J. D., FORTIN, P. R., GRAHAM, D. C., WONG, A. K., VYSE, T. J., DALY, M. J., ALTSHULER, D., MOSER, K. L. & GAFFNEY, P. M. 2008. Genetic variants near TNFAIP3 on 6q23 are associated with systemic lupus erythematosus. *Nat Genet,* 40**,** 1059-61.

GRICE, E. A., KONG, H. H., CONLAN, S., DEMING, C. B., DAVIS, J., YOUNG, A. C., PROGRAM, N. C. S., BOUFFARD, G. G., BLAKESLEY, R. W., MURRAY, P. R., GREEN, E. D., TURNER, M. L. & SEGRE, J. A. 2009. Topographical and temporal diversity of the human skin microbiome. *Science,* 324**,** 1190-2.

GRICE, E. A. & SEGRE, J. A. 2011. The skin microbiome. *Nat Rev Microbiol,* 9**,** 244-53.

GRIFFITH, J. W., SOKOL, C. L. & LUSTER, A. D. 2014. Chemokines and chemokine receptors: positioning cells for host defense and immunity. *Annu Rev Immunol,* 32**,** 659-702.

GRIMBLE, S. A., MAGEE, T. R. & GALLAND, R. B. 2001. Methicillin resistant Staphylococcus aureus in patients undergoing major amputation. *Eur J Vasc Endovasc Surg,* 22**,** 215-8.

GRUYS, E., TOUSSAINT, M. J., NIEWOLD, T. A. & KOOPMANS, S. J. 2005. Acute phase reaction and acute phase proteins. *J Zhejiang Univ Sci B,* 6**,** 1045-56.

GUDJONSSON, J. E., DING, J., JOHNSTON, A., TEJASVI, T., GUZMAN, A. M., NAIR, R. P., VOORHEES, J. J., ABECASIS, G. R. & ELDER, J. T. 2010. Assessment of the psoriatic transcriptome in a large sample: additional regulated genes and comparisons with in vitro models. *J Invest Dermatol,* 130**,** 1829-40.

GUNTHER, J., PETZL, W., BAUER, I., PONSUKSILI, S., ZERBE, H., SCHUBERTH, H. J., BRUNNER, R. M. & SEYFERT, H. M. 2017. Differentiating Staphylococcus aureus from Escherichia coli mastitis: S. aureus triggers unbalanced immune-dampening and host cell invasion immediately after udder infection. *Sci Rep,* 7**,** 4811.

GUO, H., CALLAWAY, J. B. & TING, J. P. 2015. Inflammasomes: mechanism of action, role in disease, and therapeutics. *Nat Med,* 21**,** 677-87.

HAGGAR, A., EHRNFELT, C., HOLGERSSON, J. & FLOCK, J. I. 2004. The extracellular adherence protein from Staphylococcus aureus inhibits neutrophil binding to endothelial cells. *Infect Immun,* 72**,** 6164-7.

HANEL, K. H., CORNELISSEN, C., LUSCHER, B. & BARON, J. M. 2013. Cytokines and the skin barrier. *Int J Mol Sci,* 14**,** 6720-45.

HANIFFA, M., GUNAWAN, M. & JARDINE, L. 2015. Human skin dendritic cells in health and disease. *J Dermatol Sci,* 77**,** 85-92.

HANSSEN, A. M., KINDLUND, B., STENKLEV, N. C., FURBERG, A. S., FISMEN, S., OLSEN, R. S., JOHANNESSEN, M. & SOLLID, J. U. 2017. Localization of Staphylococcus aureus in tissue from the nasal vestibule in healthy carriers. *BMC Microbiol,* 17**,** 89.

HARDER, J., SCHRODER, J. M. & GLASER, R. 2013. The skin surface as antimicrobial barrier: present concepts and future outlooks. *Exp Dermatol,* 22**,** 1-5.

HATAKEYAMA, M., FUKUNAGA, A., WASHIO, K., TAGUCHI, K., ODA, Y., OGURA, K. & NISHIGORI, C. 2017. Anti-Inflammatory Role of Langerhans Cells and Apoptotic Keratinocytes in Ultraviolet-B-Induced Cutaneous Inflammation. *J Immunol,* 199**,** 2937-2947.

HATANO, Y., TERASHI, H., ARAKAWA, S. & KATAGIRI, K. 2005. Interleukin-4 suppresses the enhancement of ceramide synthesis and cutaneous permeability barrier functions induced by tumor necrosis factor-alpha and interferon-gamma in human epidermis. *J Invest Dermatol,* 124**,** 786-92.

HE, K. L. & TING, A. T. 2002. A20 Inhibits Tumor Necrosis Factor (TNF) Alpha-Induced Apoptosis by Disrupting Recruitment of TRADD and RIP to the TNF Receptor 1 Complex in Jurkat T Cells. *Molecular and Cellular Biology,* 22**,** 6034-6045.

HEATH, W. R. & CARBONE, F. R. 2009. Dendritic cell subsets in primary and secondary T cell responses at body surfaces. *Nat Immunol,* 10**,** 1237-44.

HEDLEY, S. J., LAYTON, C., HEATON, M., CHAKRABARTY, K. H., DAWSON, R. A., GAWKRODGER, D. J. & NEIL, S. M. 2002. Fibroblasts Play a Regulatory Role in the Control of Pigmentation in Reconstructed Human Skin from Skin Types I and II. *Pigment Cell Research,* 15**,** 49-56.

HENDERSON, W. R., CHI, E. Y. & MALISZEWSKI, C. R. 2000. Soluble IL-4 Receptor Inhibits Airway Inflammation Following Allergen Challenge in a Mouse Model of Asthma. *The Journal of Immunology,* 164**,** 1086-1095.

HERBERT, S., ZIEBANDT, A. K., OHLSEN, K., SCHAFER, T., HECKER, M., ALBRECHT, D., NOVICK, R. & GOTZ, F. 2010. Repair of global regulators in Staphylococcus aureus 8325 and comparative analysis with other clinical isolates. *Infect Immun,* 78**,** 2877-89.

HIGAKI, S., MOROHASHI, M., YAMAGISHI, T. & HASEGAWA, Y. 1999. Comparative study of staphylococci from the skin of atopic dermatitis patients and from healthy subjects. *International Journal of Dermatology,* 38**,** 265-269.

HINZ, M. & SCHEIDEREIT, C. 2014. The IkappaB kinase complex in NF-kappaB regulation and beyond. *EMBO Rep,* 15**,** 46-61.

HOEFFEL, G., WANG, Y., GRETER, M., SEE, P., TEO, P., MALLERET, B., LEBOEUF, M., LOW, D., OLLER, G., ALMEIDA, F., CHOY, S. H., GRISOTTO, M., RENIA, L., CONWAY, S. J., STANLEY, E. R., CHAN, J. K., NG, L. G., SAMOKHVALOV, I. M., MERAD, M. & GINHOUX, F. 2012. Adult Langerhans cells derive predominantly from embryonic fetal liver monocytes with a minor contribution of yolk sac-derived macrophages. *J Exp Med,* 209**,** 1167-81.

HOLLAND, D. B., BOJAR, R. A., FARRAR, M. D. & HOLLAND, K. T. 2009. Differential innate immune responses of a living skin equivalent model colonized by Staphylococcus epidermidis or Staphylococcus aureus. *FEMS Microbiol Lett,* 290**,** 149-55.

HOLLAND, D. B., BOJAR, R. A., JEREMY, A. H., INGHAM, E. & HOLLAND, K. T. 2008. Microbial colonization of an in vitro model of a tissue engineered human skin equivalent--a novel approach. *FEMS Microbiol Lett,* 279**,** 110-5.

HOWELL, M. D., BOGUNIEWICZ, M., PASTORE, S., NOVAK, N., BIEBER, T., GIROLOMONI, G. & LEUNG, D. Y. 2006a. Mechanism of HBD-3 deficiency in atopic dermatitis. *Clin Immunol,* 121**,** 332-8.

HOWELL, M. D., GALLO, R. L., BOGUNIEWICZ, M., JONES, J. F., WONG, C., STREIB, J. E. & LEUNG, D. Y. 2006b. Cytokine milieu of atopic dermatitis skin subverts the innate immune response to vaccinia virus. *Immunity,* 24**,** 341-8.

HOWELL, M. D., KIM, B. E., GAO, P., GRANT, A. V., BOGUNIEWICZ, M., DEBENEDETTO, A., SCHNEIDER, L., BECK, L. A., BARNES, K. C. & LEUNG, D. Y. 2007. Cytokine modulation of atopic dermatitis filaggrin skin expression. *J Allergy Clin Immunol,* 120**,** 150-5.

HOWELL, M. D., KIM, B. E., GAO, P., GRANT, A. V., BOGUNIEWICZ, M., DEBENEDETTO, A., SCHNEIDER, L., BECK, L. A., BARNES, K. C. & LEUNG, D. Y. 2009. Cytokine modulation of atopic dermatitis filaggrin skin expression. *J Allergy Clin Immunol,* 124**,** R7-R12.

HRUZ, P., ZINKERNAGEL, A. S., JENIKOVA, G., BOTWIN, G. J., HUGOT, J. P., KARIN, M., NIZET, V. & ECKMANN, L. 2009. NOD2 contributes to cutaneous defense against Staphylococcus aureus through alpha-toxin-dependent innate immune activation. *Proc Natl Acad Sci U S A,* 106**,** 12873-8.

HUBO, M., TRINSCHEK, B., KRYCZANOWSKY, F., TUETTENBERG, A., STEINBRINK, K. & JONULEIT, H. 2013. Costimulatory molecules on immunogenic versus tolerogenic human dendritic cells. *Front Immunol,* 4**,** 82.

HUMAN MICROBIOME PROJECT, C. 2012. Structure, function and diversity of the healthy human microbiome. *Nature,* 486**,** 207-14.

HYDER, L. A., GONZALEZ, J., HARDEN, J. L., JOHNSON-HUANG, L. M., ZABA, L. C., PIERSON, K. C., EUNGDAMRONG, N. J., LENTINI, T., GULATI, N., FUENTES-DUCULAN, J., SUAREZ-FARINAS, M. & LOWES, M. A. 2013. TREM-1 as a potential therapeutic target in psoriasis. *J Invest Dermatol,* 133**,** 1742-51.

IQBAL, Z., SELEEM, M. N., HUSSAIN, H. I., HUANG, L., HAO, H. & YUAN, Z. 2016. Comparative virulence studies and transcriptome analysis of Staphylococcus aureus strains isolated from animals. *Sci Rep,* 6**,** 35442.

ISHIDA-YAMAMOTO, A. & IGAWA, S. 2015. The biology and regulation of corneodesmosomes. *Cell Tissue Res,* 360**,** 477-82.

ISLANDER, U., ANDERSSON, A., LINDBERG, E., ADLERBERTH, I., WOLD, A. E. & RUDIN, A. 2010. Superantigenic Staphylococcus aureus stimulates production of interleukin-17 from memory but not naive T cells. *Infect Immun,* 78**,** 381-6.

IWAKURA, Y. & ISHIGAME, H. 2006. The IL-23/IL-17 axis in inflammation. *Journal of Clinical Investigation,* 116**,** 1218-1222.

IWASE, T., UEHARA, Y., SHINJI, H., TAJIMA, A., SEO, H., TAKADA, K., AGATA, T. & MIZUNOE, Y. 2010. Staphylococcus epidermidis Esp inhibits Staphylococcus aureus biofilm formation and nasal colonization. *Nature,* 465**,** 346-9.

JAMESON, J. & HAVRAN, W. L. 2007. Skin γδ T-cell functions in homeostasis and wound healing. *Immunological Reviews,* 215**,** 114-122.

JEFFERIES, C., WYNNE, C. & HIGGS, R. 2011. Antiviral TRIMs: friend or foe in autoimmune and autoinflammatory disease? *Nat Rev Immunol,* 11**,** 617-25.

JENKINS, A., DIEP BA FAU - MAI, T. T., MAI, T. T., VO, N. H., WARRENER, P., SUZICH, J., STOVER, C. K. & SELLMAN, B. R. 2015. Differential expression and roles of Staphylococcus aureus virulence determinants during colonization and disease. *American Society for Microbiology,* 6**,** e02272-14.

JENNINGS, M. D., KERSHAW, C. J., ADOMAVICIUS, T. & PAVITT, G. D. 2017. Fail-safe control of translation initiation by dissociation of eIF2alpha phosphorylated ternary complexes. *Elife,* 6.

JENSEN, L. E. 2010. Targeting the IL-1 family members in skin inflammation. *Current opinion in investigational drugs (London, England : 2000),* 11**,** 1211-1220.

JIN, W. & DONG, C. 2013. IL-17 cytokines in immunity and inflammation. *Emerg Microbes Infect,* 2**,** e60.

JO, E. K., KIM, J. K., SHIN, D. M. & SASAKAWA, C. 2016. Molecular mechanisms regulating NLRP3 inflammasome activation. *Cell Mol Immunol,* 13**,** 148-59.

JOHNSTON, A., XING, X., GUZMAN, A. M., RIBLETT, M., LOYD, C. M., WARD, N. L., WOHN, C., PRENS, E. P., WANG, F., MAIER, L. E., KANG, S., VOORHEES, J. J., ELDER, J. T. & GUDJONSSON, J. E. 2011. IL-1F5, -F6, -F8, and -F9: a novel IL-1 family signaling system that is active in psoriasis and promotes keratinocyte antimicrobial peptide expression. *J Immunol,* 186**,** 2613-22.

KABASHIMA, K., HONDA, T., GINHOUX, F. & EGAWA, G. 2019. The immunological anatomy of the skin. *Nat Rev Immunol,* 19**,** 19-30.

KAEMPFER, R., POPUGAILO, A., LEVY, R., ARAD, G., HILLMAN, D. & ROTFOGEL, Z. 2017. Bacterial superantigen toxins induce a lethal cytokine storm by enhancing B7-2/CD28 costimulatory receptor engagement, a critical immune checkpoint. *Receptors & clinical investigation,* 4**,** e1500.

KAESLER, S., VOLZ, T., SKABYTSKA, Y., KOBERLE, M., HEIN, U., CHEN, K. M., GUENOVA, E., WOLBING, F., ROCKEN, M. & BIEDERMANN, T. 2014. Toll-like receptor 2 ligands promote chronic atopic dermatitis through IL-4-mediated suppression of IL-10. *J Allergy Clin Immunol,* 134**,** 92-9.

KAMSTEEG, M., BERGERS, M., DE BOER, R., ZEEUWEN, P. L., HATO, S. V., SCHALKWIJK, J. & TJABRINGA, G. S. 2011. Type 2 helper T-cell cytokines induce morphologic and molecular characteristics of atopic dermatitis in human skin equivalent. *Am J Pathol,* 178**,** 2091-9.

KANG, J. Y., NAN, X., JIN, M. S., YOUN, S. J., RYU, Y. H., MAH, S., HAN, S. H., LEE, H., PAIK, S. G. & LEE, J. O. 2009. Recognition of lipopeptide patterns by Toll-like receptor 2-Toll-like receptor 6 heterodimer. *Immunity,* 31**,** 873-84.

KAWASAKI, H., NAGAO, K., KUBO, A., HATA, T., SHIMIZU, A., MIZUNO, H., YAMADA, T. & AMAGAI, M. 2012. Altered stratum corneum barrier and enhanced percutaneous immune responses in filaggrin-null mice. *J Allergy Clin Immunol,* 129**,** 1538-46 e6.

KAWASAKI, T. & KAWAI, T. 2014. Toll-like receptor signaling pathways. *Front Immunol,* 5**,** 461.

KEPPLER, B. R. & ARCHER, T. K. 2008. Chromatin-modifying enzymes as therapeutic targets--Part 1. *Expert Opin Ther Targets,* 12**,** 1301-12.

KHATRI, P., SIROTA, M. & BUTTE, A. J. 2012. Ten years of pathway analysis: current approaches and outstanding challenges. *PLoS Comput Biol,* 8**,** e1002375.

KIM, B., LEE, Y., KIM, E., KWAK, A., RYOO, S., BAE, S. H., AZAM, T., KIM, S. & DINARELLO, C. A. 2013. The Interleukin-1alpha Precursor is Biologically Active and is Likely a Key Alarmin in the IL-1 Family of Cytokines. *Front Immunol,* 4**,** 391.

KIM, B. E., LEUNG, D. Y. M., BOGUNIEWICZ, M. & HOWELL, M. D. 2008. Loricrin and involucrin expression is down-regulated by Th2 cytokines through STAT-6. *Clinical immunology (Orlando, Fla.),* 126**,** 332-337.

KIM, J. Y., JEONG, M. S., PARK, M. K., LEE, M. K. & SEO, S. J. 2014. Time-dependent progression from the acute to chronic phases in atopic dermatitis induced by epicutaneous allergen stimulation in NC/Nga mice. *Exp Dermatol,* 23**,** 53-7.

KIM, Y. K., SHIN, J. S. & NAHM, M. H. 2016. NOD-Like Receptors in Infection, Immunity, and Diseases. *Yonsei Med J,* 57**,** 5-14.

KISICH, K. O., HOWELL, M. D., BOGUNIEWICZ, M., HEIZER, H. R., WATSON, N. U. & LEUNG, D. Y. 2007. The constitutive capacity of human keratinocytes to kill Staphylococcus aureus is dependent on beta-defensin 3. *J Invest Dermatol,* 127**,** 2368-80.

KITAMURA, A., TAKATA, R., AIZAWA, S., WATANABE, H. & WADA, T. 2018. A murine model of atopic dermatitis can be generated by painting the dorsal skin with hapten twice 14 days apart. *Sci Rep,* 8**,** 5988.

KLEMENT, J. F., RICE, N. R., CAR, B. D., ABBONDANZO, S. J., POWERS, G. D., BHATT, P. H., CHEN, C. H., ROSEN, C. A. & STEWART, C. L. 1996. IkappaBalpha deficiency results in a sustained NF-kappaB response and severe widespread dermatitis in mice. *Molecular and cellular biology,* 16**,** 2341-2349.

KLICZNIK, M. M., SZENES-NAGY, A. B., CAMPBELL, D. J. & GRATZ, I. K. 2018. Taking the lead - how keratinocytes orchestrate skin T cell immunity. *Immunol Lett,* 200**,** 43-51.

KLOOS, W. E. & MUSSELWHITE, M. S. 1975. Distribution and Persistence of Staphylococcus and Micrococcus Species and Other Aerobic Bacteria on Human Skin. *Applied Microbiology,* 30**,** 381-395.

KLOOS, W. E. & SCHLEIFER, K. H. 1975. Isolation and Characterization of Staphylococci from Human Skin II. Descriptions of Four New Species: Staphylococcus warneri, Staphylococcus capitis, Staphylococcus hominis, and Staphylococcus simulans. *International Journal of Systematic Bacteriology,* 25**,** 62-79.

KO, Y. P., LIANG, X., SMITH, C. W., DEGEN, J. L. & HOOK, M. 2011. Binding of Efb from Staphylococcus aureus to fibrinogen blocks neutrophil adherence. *J Biol Chem,* 286**,** 9865-74.

KOBAYASHI, S. D. & DELEO, F. R. 2013. Staphylococcus aureus protein A promotes immune suppression. *MBio,* 4**,** e00764-13.

KOBAYASHI, T., GLATZ, M., HORIUCHI, K., KAWASAKI, H., AKIYAMA, H., KAPLAN, D. H., KONG, H. H., AMAGAI, M. & NAGAO, K. 2015. Dysbiosis and Staphylococcus aureus Colonization Drives Inflammation in Atopic Dermatitis. *Immunity,* 42**,** 756-66.

KOLLISCH, G., KALALI, B. N., VOELCKER, V., WALLICH, R., BEHRENDT, H., RING, J., BAUER, S., JAKOB, T., MEMPEL, M. & OLLERT, M. 2005. Various members of the Toll-like receptor family contribute to the innate immune response of human epidermal keratinocytes. *Immunology,* 114**,** 531-41.

KONG, H. H., OH, J., DEMING, C., CONLAN, S., GRICE, E. A., BEATSON, M. A., NOMICOS, E., POLLEY, E. C., KOMAROW, H. D., PROGRAM, N. C. S., MURRAY, P. R., TURNER, M. L. & SEGRE, J. A. 2012. Temporal shifts in the skin microbiome associated with disease flares and treatment in children with atopic dermatitis. *Genome Res,* 22**,** 850-9.

KOSE, K. N., XIE, J.-F., CARNES, D. L. & GRAVES, D. T. 1996. Pro-inflammatory cytokines downregulate platelet derived growth factor-α receptor gene expression in human osteoblastic cells. *Journal of Cellular Physiology,* 166**,** 188-197.

KOTAKA, M., KOSTIN, S., NGAI, S.-M., CHAN, K.-K., LAU, Y.-M., LEE, S. M. Y., LI, H.-Y., NG, E. K. O., SCHAPER, J., TSUI, S. K. W., FUNG, K.-P., LEE, C.-Y. & WAYE, M. M. Y. 2000. Interaction of hCLIM1, an enigma family protein, with α-actinin 2. *Journal of Cellular Biochemistry,* 78**,** 558-565.

KOTEN, B., SIMANSKI, M., GLASER, R., PODSCHUN, R., SCHRODER, J. M. & HARDER, J. 2009. RNase 7 contributes to the cutaneous defense against Enterococcus faecium. *PLoS One,* 4**,** e6424.

KRAMER, A., GREEN, J., POLLARD, J., JR. & TUGENDREICH, S. 2014. Causal analysis approaches in Ingenuity Pathway Analysis. *Bioinformatics,* 30**,** 523-30.

KRIEG, T. & AUMAILLEY, M. 2011. The extracellular matrix of the dermis: flexible structures with dynamic functions. *Exp Dermatol,* 20**,** 689-95.

KRUT, O., UTERMOHLEN, O., SCHLOSSHERR, X. & KRONKE, M. 2003. Strain-Specific Association of Cytotoxic Activity and Virulence of Clinical Staphylococcus aureus Isolates. *Infection and Immunity,* 71**,** 2716-2723.

KUMAGAI, A., KUBO, T., KAWATA, K., KAMEKURA, R., YAMASHITA, K., JITSUKAWA, S., NAGAYA, T., SUMIKAWA, Y., HIMI, T., YAMASHITA, T. & ICHIMIYA, S. 2017. Keratinocytes in atopic dermatitis express abundant DeltaNp73 regulating thymic stromal lymphopoietin production via NF-kappaB. *J Dermatol Sci,* 88**,** 175-183.

KUSUNOKI, T., WRIGHT, S. D., INOUE, Y., MIYANOMAE, T., YOSHIDA, Y. & YONEDA, K. 1998. Serum levels of soluble CD14 in allergic inflammation. *Allergology International,* 47**,** 271-278.

LABOREL-PRENERON, E., BIANCHI, P., BORALEVI, F., LEHOURS, P., FRAYSSE, F., MORICE-PICARD, F., SUGAI, M., SATO'O, Y., BADIOU, C., LINA, G., SCHMITT, A. M., REDOULES, D., CASAS, C. & DAVRINCHE, C. 2015. Effects of the Staphylococcus aureus and Staphylococcus epidermidis Secretomes Isolated from the Skin Microbiota of Atopic Children on CD4+ T Cell Activation. *PLoS One,* 10**,** e0141067.

LAI, Y., COGEN, A. L., RADEK, K. A., PARK, H. J., MACLEOD, D. T., LEICHTLE, A., RYAN, A. F., DI NARDO, A. & GALLO, R. L. 2010. Activation of TLR2 by a small molecule produced by Staphylococcus epidermidis increases antimicrobial defense against bacterial skin infections. *J Invest Dermatol,* 130**,** 2211-21.

LAI, Y., DI NARDO, A., NAKATSUJI, T., LEICHTLE, A., YANG, Y., COGEN, A. L., WU, Z. R., HOOPER, L. V., SCHMIDT, R. R., VON AULOCK, S., RADEK, K. A., HUANG, C. M., RYAN, A. F. & GALLO, R. L. 2009. Commensal bacteria regulate Toll-like receptor 3-dependent inflammation after skin injury. *Nat Med,* 15**,** 1377-82.

LE, K. Y. & OTTO, M. 2015. Quorum-sensing regulation in staphylococci-an overview. *Front Microbiol,* 6**,** 1174.

LE, K. Y., PARK, M. D. & OTTO, M. 2018. Immune Evasion Mechanisms of Staphylococcus epidermidis Biofilm Infection. *Front Microbiol,* 9**,** 359.

LEE, S. E. & LEE, S. H. 2018. Skin Barrier and Calcium. *Ann Dermatol,* 30**,** 265-275.

LEE, S. H., JEONG, S. K. & AHN, S. K. 2006. An Update of the Defensive Barrier Function of Skin. *Yonsei Medical Journal,* 47**,** 293-306.

LEE, S. H., KIM, K. W., MIN, K. M., KIM, K. W., CHANG, S. I. & KIM, J. C. 2014. Angiogenin reduces immune inflammation via inhibition of TANK-binding kinase 1 expression in human corneal fibroblast cells. *Mediators Inflamm,* 2014**,** 861435.

LENORMAND, C., SPIEGELHALTER, C., CINQUIN, B., BARDIN, S., BAUSINGER, H., ANGENIEUX, C., ECKLY, A., PROAMER, F., WALL, D., LICH, B., TOURNE, S., HANAU, D., SCHWAB, Y., SALAMERO, J. & DE LA SALLE, H. 2013. Birbeck granule-like "organized smooth

endoplasmic reticulum" resulting from the expression of a cytoplasmic YFP-tagged langerin. *PLoS One,* 8**,** e60813.

LI, J. G., DU, Y. M., YAN, Z. D., YAN, J., ZHUANSUN, Y. X., CHEN, R., ZHANG, W., FENG, S. L. & RAN, P. X. 2016. CD80 and CD86 knockdown in dendritic cells regulates Th1/Th2 cytokine production in asthmatic mice. *Exp Ther Med,* 11**,** 878-884.

LI, M., CHA, D. J., LAI, Y., VILLARUZ, A. E., STURDEVANT, D. E. & OTTO, M. 2007a. The antimicrobial peptide-sensing system aps of Staphylococcus aureus. *Mol Microbiol,* 66**,** 1136-47.

LI, M., LAI, Y., VILLARUZ, A. E., CHA, D. J., STURDEVANT, D. E. & OTTO, M. 2007b. Gram-positive three-component antimicrobial peptide-sensing system. *Proc Natl Acad Sci U S A,* 104**,** 9469-74.

LI, N., YAMASAKI, K., SAITO, R., FUKUSHI-TAKAHASHI, S., SHIMADA-OMORI, R., ASANO, M. & AIBA, S. 2014. Alarmin function of cathelicidin antimicrobial peptide LL37 through IL-36gamma induction in human epidermal keratinocytes. *J Immunol,* 193**,** 5140-8.

LIPPENS, S., DENECKER, G., OVAERE, P., VANDENABEELE, P. & DECLERCQ, W. 2005. Death penalty for keratinocytes: apoptosis versus cornification. *Cell Death Differ,* 12 Suppl 2**,** 1497-508.

LIU, T., ZHANG, L., JOO, D. & SUN, S. C. 2017. NF-kappaB signaling in inflammation. *Signal Transduct Target Ther,* 2.

LIU, Y., AMES, B., GOROVITS, E., PRATER, B. D., SYRIBEYS, P., VERNACHIO, J. H. & PATTI, J. M. 2004. SdrX, a serine-aspartate repeat protein expressed by Staphylococcus capitis with collagen VI binding activity. *Infect Immun,* 72**,** 6237-44.

LLOYD-JONES, K. L., KELLY, M. M. & KUBES, P. 2008. Varying Importance of Soluble and Membrane CD14 in Endothelial Detection of Lipopolysaccharide. *The Journal of Immunology,* 181**,** 1446-1453.

LOO, Y. M. & GALE, M., JR. 2011. Immune signaling by RIG-I-like receptors. *Immunity,* 34**,** 680-92.

LOWE, R., SHIRLEY, N., BLEACKLEY, M., DOLAN, S. & SHAFEE, T. 2017. Transcriptomics technologies. *PLoS Comput Biol,* 13**,** e1005457.

LOWY , F. D. 1998. Staphylococcus aureus Infections. *New England Journal of Medicine,* 339**,** 520-532.

LUNDELL, A. C., ADLERBERTH, I., LINDBERG, E., KARLSSON, H., EKBERG, S., ÅBERG, N., SAALMAN, R., HOCK, B., STEINKASSERER, A., HESSELMAR, B., WOLD, A. E. & RUDIN, A. 2006. Increased levels of circulating soluble CD14 but not CD83 in infants are associated with early intestinal colonization with Staphylococcus aureus. *Clinical & Experimental Allergy,* 37**,** 62-71.

LUTZ, M. B. 2016. Induction of CD4(+) Regulatory and Polarized Effector/helper T Cells by Dendritic Cells. *Immune Netw,* 16**,** 13-25.

LUTZ, M. B., STROBL, H., SCHULER, G. & ROMANI, N. 2017. GM-CSF Monocyte-Derived Cells and Langerhans Cells As Part of the Dendritic Cell Family. *Front Immunol,* 8**,** 1388.

MACLEA, K. & M TRACHTENBERG, A. 2017. *Complete Genome Sequence of Staphylococcus epidermidis ATCC 12228 Chromosome and Plasmids, Generated by Long-Read Sequencing*.

MADHUSOODANAN, J., SEO, K. S., REMORTEL, B., PARK, J. Y., HWANG, S. Y., FOX, L. K., PARK, Y. H., DEOBALD, C. F., WANG, D., LIU, S., DAUGHERTY, S. C., GILL, A. L., BOHACH, G. A. & GILL, S.

R. 2011. An Enterotoxin-Bearing Pathogenicity Island in Staphylococcus epidermidis. *J Bacteriol,* 193**,** 1854-62.

MALISSEN, B., TAMOUTOUNOUR, S. & HENRI, S. 2014. The origins and functions of dendritic cells and macrophages in the skin. *Nat Rev Immunol,* 14**,** 417-28.

MAN, M. Q., BARISH, G. D., SCHMUTH, M., CRUMRINE, D., BARAK, Y., CHANG, S., JIANG, Y., EVANS, R. M., ELIAS, P. M. & FEINGOLD, K. R. 2008. Deficiency of PPARbeta/delta in the epidermis results in defective cutaneous permeability barrier homeostasis and increased inflammation. *J Invest Dermatol,* 128**,** 370-7.

MANDARD, S., MULLER, M. & KERSTEN, S. 2004. Peroxisome proliferator-activated receptor alpha target genes. *Cell Mol Life Sci,* 61**,** 393-416.

MANICHANH, C., RIGOTTIER-GOIS, L., BONNAUD, E., GLOUX, K., PELLETIER, E., FRANGEUL, L., NALIN, R., JARRIN, C., CHARDON, P., MARTEAU, P., ROCA, J. & DORE, J. 2006. Reduced diversity of faecal microbiota in Crohn's disease revealed by a metagenomic approach. *Gut,* 55**,** 205-11.

MANTOVANI, A., GARLANDA, C., DONI, A. & BOTTAZZI, B. 2008. Pentraxins in innate immunity: from C-reactive protein to the long pentraxin PTX3. *J Clin Immunol,* 28**,** 1-13.

MARICHAL, T., GAUDENZIO, N., EL ABBAS, S., SIBILANO, R., ZUREK, O., STARKL, P., REBER, L. L., PIROTTIN, D., KIM, J., CHAMBON, P., ROERS, A., ANTOINE, N., KAWAKAMI, Y., KAWAKAMI, T., BUREAU, F., TAM, S. Y., TSAI, M. & GALLI, S. J. 2016. Guanine nucleotide exchange factor RABGEF1 regulates keratinocyte-intrinsic signaling to maintain skin homeostasis. *J Clin Invest,* 126**,** 4497-4515.

MARSHALL, A., CELENTANO, A., CIRILLO, N., MCCULLOUGH, M. & PORTER, S. 2017. Tissue-specific regulation of CXCL9/10/11 chemokines in keratinocytes: Implications for oral inflammatory disease. *PLoS One,* 12**,** e0172821.

MARTEL, B. C., LOVATO, P., BÄUMER, W. & OLIVRY, T. 2017. Translational Animal Models of Atopic Dermatitis for Preclinical Studies. 90**,** 389-402.

MATHES, S. H., RUFFNER, H. & GRAF-HAUSNER, U. 2014. The use of skin models in drug development. *Advanced Drug Delivery Reviews,* 69–70**,** 81-102.

MATSUI, K., MORI, A. & IKEDA, R. 2015. Langerhans cell-like dendritic cells stimulated with an adjuvant direct the development of Th1 and Th2 cells in vivo. *Clin Exp Immunol,* 182**,** 101-7.

MATTHEWS, K. R., ROBERSON, J., GILLESPIE, B. E., LUTHER, D. A. & OLIVER, S. P. 1997. Identification and Differentiation of Coagulase-Negative Staphylococcus aureus by Polymerase Chain Reaction. *Journal of Food Protection,* 60**,** 686-688.

MATTSSON, E., VERHAGE, L., ROLLOF, J., FLEER, A., VERHOEF, J. & VAN DIJK, H. 1993. *Peptidoglycan and teichoic acid from Staphylococcus epidermidis stimulate human monocytes to release tumour necrosis factor-alpha, interleukin-1beta, and interleukin-6*.

MC DERMOTT, R., ZIYLAN, U., SPEHNER, D., BAUSINGER, H., LIPSKER, D., MOMMAAS, M., CAZENAVE, J. P., RAPOSO, G., GOUD, B., DE LA SALLE, H., SALAMERO, J. & HANAU, D. 2002. Birbeck granules are subdomains of endosomal recycling compartment in human epidermal Langerhans cells, which form where Langerin accumulates. *Mol Biol Cell,* 13**,** 317-35.

MCALEESE, F. M., WALSH, E. J., SIEPRAWSKA, M., POTEMPA, J. & FOSTER, T. J. 2001. Loss of clumping factor B fibrinogen binding activity by Staphylococcus aureus involves cessation of transcription, shedding and cleavage by metalloprotease. *J Biol Chem,* 276**,** 29969-78.

MCCALL, M. N. & IRIZARRY, R. A. 2008. Consolidated strategy for the analysis of microarray spike-in data. *Nucleic Acids Res,* 36**,** e108.

MCLOUGHLIN, R. M., HURST, S. M., NOWELL, M. A., HARRIS, D. A., HORIUCHI, S., MORGAN, L. W., WILKINSON, T. S., YAMAMOTO, N., TOPLEY, N. & JONES, S. A. 2004. Differential Regulation of Neutrophil-Activating Chemokines by IL-6 and Its Soluble Receptor Isoforms. *The Journal of Immunology,* 172**,** 5676-5683.

MEE, J. B., JOHNSON, C. M., MORAR, N., BURSLEM, F. & GROVES, R. W. 2007. The psoriatic transcriptome closely resembles that induced by interleukin-1 in cultured keratinocytes: dominance of innate immune responses in psoriasis. *Am J Pathol,* 171**,** 32-42.

MEISTER, M., TOUNSI, A., GAFFAL, E., BALD, T., PAPATRIANTAFYLLOU, M., LUDWIG, J., POUGIALIS, G., BESTVATER, F., KLOTZ, L., MOLDENHAUER, G., TUTING, T., HAMMERLING, G. J., ARNOLD, B. & OELERT, T. 2015. Self-Antigen Presentation by Keratinocytes in the Inflamed Adult Skin Modulates T-Cell Auto-Reactivity. *J Invest Dermatol,* 135**,** 1996-2004.

MEMPEL, M., SCHNOPP, C., HOJKA, M., FESQ, H., WEIDINGER, S., SCHALLER, M., KORTING, H. C., RING, J. & ABECK, D. 2002. Invasion of human keratinocytes by Staphylococcus aureus and intracellular bacterial persistence represent haemolysin-independent virulence mechanisms that are followed by features of necrotic and apoptotic keratinocyte cell death. *British Journal of Dermatology,* 146**,** 943-951.

MENON, G. K., CLEARY, G. W. & LANE, M. E. 2012. The structure and function of the stratum corneum. *Int J Pharm,* 435**,** 3-9.

MICHALIK, L., AUWERX, J., BERGER, J. P., CHATTERJEE, V. K., GLASS, C. K., GONZALEZ, F. J., GRIMALDI, P. A., KADOWAKI, T., LAZAR, M. A., O'RAHILLY, S., PALMER, C. N., PLUTZKY, J., REDDY, J. K., SPIEGELMAN, B. M., STAELS, B. & WAHLI, W. 2006. International Union of Pharmacology. LXI. Peroxisome proliferator-activated receptors. *Pharmacol Rev,* 58**,** 726-41.

MICHALIK, L. & WAHLI, W. 2006. Involvement of PPAR nuclear receptors in tissue injury and wound repair. *J Clin Invest,* 116**,** 598-606.

MICHALIK, L. & WAHLI, W. 2007. Peroxisome proliferator-activated receptors (PPARs) in skin health, repair and disease. *Biochim Biophys Acta,* 1771**,** 991-8.

MIDORIKAWA, K., OUHARA, K., KOMATSUZAWA, H., KAWAI, T., YAMADA, S., FUJIWARA, T., YAMAZAKI, K., SAYAMA, K., TAUBMAN, M. A., KURIHARA, H., HASHIMOTO, K. & SUGAI, M. 2003. Staphylococcus aureus Susceptibility to Innate Antimicrobial Peptides, -Defensins and CAP18, Expressed by Human Keratinocytes. *Infection and Immunity,* 71**,** 3730-3739.

MILDNER, M., JIN, J., ECKHART, L., KEZIC, S., GRUBER, F., BARRESI, C., STREMNITZER, C., BUCHBERGER, M., MLITZ, V., BALLAUN, C., STERNICZKY, B., FODINGER, D. & TSCHACHLER, E. 2010. Knockdown of filaggrin impairs diffusion barrier function and increases UV sensitivity in a human skin model. *J Invest Dermatol,* 130**,** 2286-94.

MILSTONE, L. M. 2004. Epidermal desquamation. *Journal of Dermatological Science,* 36**,** 131-140.

MOMBELLI, M., LUGRIN, J., RUBINO, I., CHANSON, A. L., GIDDEY, M., CALANDRA, T. & ROGER, T. 2011. Histone deacetylase inhibitors impair antibacterial defenses of macrophages. *J Infect Dis,* 204**,** 1367-74.

MONIN, L., GUDJONSSON, J. E., CHILDS, E. E., AMATYA, N., XING, X., VERMA, A. H., COLEMAN, B. M., GARG, A. V., KILLEEN, M., MATHERS, A., WARD, N. L. & GAFFEN, S. L. 2017. MCPIP1/Regnase-1 Restricts IL-17A- and IL-17C-Dependent Skin Inflammation. *J Immunol,* 198**,** 767-775.

MONTES-TORRES, A., LLAMAS-VELASCO, M., PEREZ-PLAZA, A., SOLANO-LOPEZ, G. & SANCHEZ-PEREZ, J. 2015. Biological Treatments in Atopic Dermatitis. *J Clin Med,* 4**,** 593-613.

MOORE, P. C. & LINDSAY, J. A. 2001. Genetic variation among hospital isolates of methicillin-sensitive Staphylococcus aureus: evidence for horizontal transfer of virulence genes. *J Clin Microbiol,* 39**,** 2760-7.

MOUTON-LIGER, F., ROSAZZA, T., SEPULVEDA-DIAZ, J., IEANG, A., HASSOUN, S. M., CLAIRE, E., MANGONE, G., BRICE, A., MICHEL, P. P., CORVOL, J. C. & CORTI, O. 2018. Parkin deficiency modulates NLRP3 inflammasome activation by attenuating an A20-dependent negative feedback loop. *Glia*.

MULCAHY, M. E., GEOGHEGAN, J. A., MONK, I. R., O'KEEFFE, K. M., WALSH, E. J., FOSTER, T. J. & MCLOUGHLIN, R. M. 2012. Nasal colonisation by Staphylococcus aureus depends upon clumping factor B binding to the squamous epithelial cell envelope protein loricrin. *PLoS Pathog,* 8**,** e1003092.

MULLER, A., SEINIGE, D., JANSEN, W., KLEIN, G., EHRICHT, R., MONECKE, S. & KEHRENBERG, C. 2016. Variety of Antimicrobial Resistances and Virulence Factors in Staphylococcus aureus Isolates from Meat Products Legally and Illegally Introduced to Germany. *PLoS One,* 11**,** e0167864.

NAKAMURA, H., AOKI, M., TAMAI, K., OISHI, M., OGIHARA, T., KANEDA, Y. & MORISHITA, R. 2002. Prevention and regression of atopic dermatitis by ointment containing NF-kB decoy oligodeoxynucleotides in NC/Nga atopic mouse model. *Gene Ther,* 9**,** 1221-9.

NAMBU, A. & NAKAE, S. 2010. IL-1 and Allergy. *Allergol Int,* 59**,** 125-35.

NEDOSZYTKO, B., SOKOLOWSKA-WOJDYLO, M., RUCKEMANN-DZIURDZINSKA, K., ROSZKIEWICZ, J. & NOWICKI, R. J. 2014. Chemokines and cytokines network in the pathogenesis of the inflammatory skin diseases: atopic dermatitis, psoriasis and skin mastocytosis. *Postepy Dermatol Alergol,* 31**,** 84-91.

NESTLE, F. O., DI MEGLIO, P., QIN, J.-Z. & NICKOLOFF, B. J. 2009. Skin immune sentinels in health and disease. *Nature reviews. Immunology,* 9**,** 679-691.

NETZLAFF, F., LEHR, C. M., WERTZ, P. W. & SCHAEFER, U. F. 2005. The human epidermis models EpiSkin®, SkinEthic® and EpiDerm®: An evaluation of morphology and their suitability for testing phototoxicity, irritancy, corrosivity, and substance transport. *European Journal of Pharmaceutics and Biopharmaceutics,* 60**,** 167-178.

NGUYEN, T. H., PARK, M. D. & OTTO, M. 2017. Host Response to Staphylococcus epidermidis Colonization and Infections. *Front Cell Infect Microbiol,* 7**,** 90.

NICKOLOFF, B. J. & TURKA, L. A. 1994. Immunological functions of non-professional antigen-presenting cells: new insights from studies of T-cell interactions with keratinocytes.

NIEBUHR, M., BAUMERT, K. & WERFEL, T. 2010. TLR-2-mediated cytokine and chemokine secretion in human keratinocytes. *Exp Dermatol,* 19**,** 873-7.

NILSSON, M., FRYKBERG, L., FLOCK, J. I., PEI, L., LINDBERG, M. & GUSS, B. 1998. A fibrinogen-binding protein of Staphylococcus epidermidis. *Infection and immunity,* 66**,** 2666-2673.

NISHIFUJI, K. & YOON, J. S. 2013. The stratum corneum: the rampart of the mammalian body. *Veterinary Dermatology,* 24**,** 60-e16.

NOCKHER, W. A., WIGAND, R., SCHOEPPE, W. & SCHERBERICH, J. E. 1994. Elevated levels of soluble CD14 in serum of patients with systemic lupus erythematosus. *Clinical and experimental immunology,* 96**,** 15-19.

NOGRALES, K. E., ZABA, L. C., GUTTMAN-YASSKY, E., FUENTES-DUCULAN, J., SUAREZ-FARINAS, M., CARDINALE, I., KHATCHERIAN, A., GONZALEZ, J., PIERSON, K. C., WHITE, T. R., PENSABENE, C., COATS, I., NOVITSKAYA, I., LOWES, M. A. & KRUEGER, J. G. 2008. Th17 cytokines interleukin (IL)-17 and IL-22 modulate distinct inflammatory and keratinocyte-response pathways. *Br J Dermatol,* 159**,** 1092-102.

NOMURA, I., GOLEVA, E., HOWELL, M. D., HAMID, Q. A., ONG, P. Y., HALL, C. F., DARST, M. A., GAO, B., BOGUNIEWICZ, M., TRAVERS, J. B. & LEUNG, D. Y. M. 2003. Cytokine Milieu of Atopic Dermatitis, as Compared to Psoriasis, Skin Prevents Induction of Innate Immune Response Genes. *The Journal of Immunology,* 171**,** 3262-3269.

NOORE, J., NOORE, A. & LI, B. 2013. Cationic antimicrobial peptide LL-37 is effective against both extra- and intracellular Staphylococcus aureus. *Antimicrob Agents Chemother,* 57**,** 1283-90.

NORES, J. E. R., BENSUSSAN, A., VITA, N., STELTER, F., ARIAS, M. A., JONES, M., LEFORT, S., BORYSIEWICZ, L. K., FERRARA, P. & LABÉTA, M. O. 1999. Soluble CD14 acts as a negative regulator of human T cell activation and function. *European Journal of Immunology,* 29**,** 265-276.

NOWROUZIAN, F. L., DAUWALDER, O., MEUGNIER, H., BES, M., ETIENNE, J., VANDENESCH, F., LINDBERG, E., HESSELMAR, B., SAALMAN, R., STRANNEGARD, I. L., ABERG, N., ADLERBERTH, I., WOLD, A. E. & LINA, G. 2011. Adhesin and superantigen genes and the capacity of Staphylococcus aureus to colonize the infantile gut. *J Infect Dis,* 204**,** 714-21.

O'NEILL, A. J. 2010. Staphylococcus aureus SH1000 and 8325-4: comparative genome sequences of key laboratory strains in staphylococcal research. *Lett Appl Microbiol,* 51**,** 358-61.

O'REGAN, G. M., SANDILANDS, A., MCLEAN, W. H. & IRVINE, A. D. 2008. Filaggrin in atopic dermatitis. *J Allergy Clin Immunol,* 122**,** 689-93.

OHYAMA, Y., LIN, J. H., GOVITVATTANA, N., LIN, I. P., VENKITAPATHI, S., ALAMOUDI, A., HUSEIN, D., AN, C., HOTTA, H., KAKU, M. & MOCHIDA, Y. 2016. FAM20A binds to and regulates FAM20C localization. *Sci Rep,* 6**,** 27784.

OLARU, F. & JENSEN, L. E. 2010. Staphylococcus aureus stimulates neutrophil targeting chemokine expression in keratinocytes through an autocrine IL-1alpha signaling loop. *J Invest Dermatol,* 130**,** 1866-76.

OMORI, E., MORIOKA, S., MATSUMOTO, K. & NINOMIYA-TSUJI, J. 2008. TAK1 regulates reactive oxygen species and cell death in keratinocytes, which is essential for skin integrity. *J Biol Chem,* 283**,** 26161-8.

OREN, A., GANZ, T., LIU, L. & MEERLOO, T. 2003. In human epidermis, β-defensin 2 is packaged in lamellar bodies. *Experimental and Molecular Pathology,* 74**,** 180-182.

OREO, K. M., GIBSON, P. G., SIMPSON, J. L., WOOD, L. G., MCDONALD, V. M. & BAINES, K. J. 2014. Sputum ADAM8 expression is increased in severe asthma and COPD. *Clin Exp Allergy,* 44**,** 342-52.

OTA, K., KAWAGUCHI, M., MATSUKURA, S., KUROKAWA, M., KOKUBU, F., FUJITA, J., MORISHIMA, Y., HUANG, S. K., ISHII, Y., SATOH, H. & HIZAWA, N. 2014. Potential involvement of IL-17F in asthma. *J Immunol Res,* 2014**,** 602846.

OTTO, M. 2009. Staphylococcus epidermidis--the 'accidental' pathogen. *Nat Rev Microbiol,* 7**,** 555-67.

OTTO, M. 2010. Staphylococcus colonization of the skin and antimicrobial peptides. *Expert Rev Dermatol,* 5**,** 183-195.

OTTO, M. 2012. Molecular basis of Staphylococcus epidermidis infections. *Semin Immunopathol,* 34**,** 201-14.

OTTO, M. 2014. Phenol-soluble modulins. *Int J Med Microbiol,* 304**,** 164-9.

OTTO, M. 2017. Staphylococcus epidermidis: a major player in bacterial sepsis? *Future microbiology,* 12**,** 1031-1033.

OTTO, M., SÜßMUTH, R., VUONG, C., JUNG, G. & GÖTZ, F. 1999. Inhibition of virulence factor expression in Staphylococcus aureus by the Staphylococcus epidermidis agr pheromone and derivatives. *FEBS Letters,* 450**,** 257-262.

OU, L. S., GOLEVA, E., HALL, C. & LEUNG, D. Y. 2004. T regulatory cells in atopic dermatitis and subversion of their activity by superantigens. *J Allergy Clin Immunol,* 113**,** 756-63.

OUWEHAND, K., SPIEKSTRA, S. W., WAAIJMAN, T., SCHEPER, R. J., DE GRUIJL, T. D. & GIBBS, S. 2011. Technical advance: Langerhans cells derived from a human cell line in a full-thickness skin equivalent undergo allergen-induced maturation and migration. *J Leukoc Biol,* 90**,** 1027-33.

OZATO, K., SHIN, D. M., CHANG, T. H. & MORSE, H. C., 3RD 2008. TRIM family proteins and their emerging roles in innate immunity. *Nat Rev Immunol,* 8**,** 849-60.

PADMAKUMAR, V. C., ABRAHAM, S., BRAUNE, S., NOEGEL, A. A., TUNGGAL, B., KARAKESISOGLOU, I. & KORENBAUM, E. 2004. Enaptin, a giant actin-binding protein, is an element of the nuclear membrane and the actin cytoskeleton. *Exp Cell Res,* 295**,** 330-9.

PAGE, A., NAVARRO, M., GARIN, M., PEREZ, P., CASANOVA, M. L., MORENO, R., JORCANO, J. L., CASCALLANA, J. L., BRAVO, A. & RAMIREZ, A. 2010. IKKbeta leads to an inflammatory skin disease resembling interface dermatitis. *J Invest Dermatol,* 130**,** 1598-610.

PAKOS-ZEBRUCKA, K., KORYGA, I., MNICH, K., LJUJIC, M., SAMALI, A. & GORMAN, A. M. 2016. The integrated stress response. *EMBO Rep,* 17**,** 1374-1395.

PALMA, M., HAGGAR, A. & FLOCK, J. I. 1999. Adherence of Staphylococcus aureus is enhanced by an endogenous secreted protein with broad binding activity. *Journal of bacteriology,* 181**,** 2840-2845.

PAPPAS, A. 2009. Epidermal surface lipids. *Dermato-endocrinology,* 1**,** 72-76.

PAPPU, R., RAMIREZ-CARROZZI, V. & SAMBANDAM, A. 2011. The interleukin-17 cytokine family: critical players in host defence and inflammatory diseases. *Immunology,* 134**,** 8-16.

PARK, W. B., KIM, S. H., KANG, C. I., CHO, J. H., BANG, J. W., PARK, K. W., LEE, Y. S., KIM, N. J., OH, M. D., KIM, H. B. & CHOE, K. W. 2007. In vitro ability of Staphylococcus aureus isolates from bacteraemic patients with and without metastatic complications to invade vascular endothelial cells. *J Med Microbiol,* 56**,** 1290-5.

PASPARAKIS, M. 2009. Regulation of tissue homeostasis by NF-kappaB signalling: implications for inflammatory diseases. *Nat Rev Immunol,* 9**,** 778-88.

PASPARAKIS, M., COURTOIS, G., HAFNER, M., SCHMIDT-SUPPRIAN, M., NENCI, A., TOKSOY, A., KRAMPERT, M., GOEBELER, M., GILLITZER, R., ISRAEL, A., KRIEG, T., RAJEWSKY, K. & HAASE, I. 2002. TNF-mediated inflammatory skin disease in mice with epidermis-specific deletion of IKK2. *Nature,* 417**,** 861.

PASPARAKIS, M., HAASE, I. & NESTLE, F. O. 2014. Mechanisms regulating skin immunity and inflammation. *Nat Rev Immunol,* 14**,** 289-301.

PASTAR, I., STOJADINOVIC, O., YIN, N. C., RAMIREZ, H., NUSBAUM, A. G., SAWAYA, A., PATEL, S. B., KHALID, L., ISSEROFF, R. R. & TOMIC-CANIC, M. 2014. Epithelialization in Wound Healing: A Comprehensive Review. *Adv Wound Care (New Rochelle),* 3**,** 445-464.

PASTORE, S., FANALES-BELASIO, E., ALBANESI, C., CHINNI, L. M., GIANNETTI, A. & GIROLOMONI, G. 1997. Granulocyte macrophage colony-stimulating factor is overproduced by keratinocytes in atopic dermatitis. Implications for sustained dendritic cell activation in the skin. *Journal of Clinical Investigation,* 99**,** 3009-3017.

PATTI, J. M., BREMELL, T., KRAJEWSKA-PIETRASIK, D., ABDELNOUR, A., TARKOWSKI, A., RYDÉN, C. & HÖÖK, M. 1994. The Staphylococcus aureus collagen adhesin is a virulence determinant in experimental septic arthritis. *Infection and immunity,* 62**,** 152-161.

PAVITT, G. D. 2018. Regulation of translation initiation factor eIF2B at the hub of the integrated stress response. *Wiley Interdiscip Rev RNA,* 9**,** e1491.

PEACOCK, S. J., DAY, N. P., THOMAS, M. G., BERENDT, A. R. & FOSTER, T. J. 2000. Clinical isolates of Staphylococcus aureus exhibit diversity in fnb genes and adhesion to human fibronectin. *J Infect,* 41**,** 23-31.

PENG, W. & NOVAK, N. 2015. Pathogenesis of atopic dermatitis. *Clin Exp Allergy,* 45**,** 566-74.

PESCHEL, A., JACK, R. W., OTTO, M., COLLINS, L. V., STAUBITZ, P., NICHOLSON, G., KALBACHER, H., NIEUWENHUIZEN, W. F., JUNG, G., TARKOWSKI, A., VAN KESSEL, K. P. M. & VAN STRIJP, J. A. G. 2001. Staphylococcus aureus Resistance to Human Defensins and Evasion of Neutrophil Killing via the Novel Virulence Factor Mprf Is Based on Modification of Membrane Lipids with l-Lysine. *The Journal of Experimental Medicine,* 193**,** 1067-1076.

PESCHEL, A. & OTTO, M. 2013. Phenol-soluble modulins and staphylococcal infection. *Nat Rev Microbiol,* 11**,** 667-73.

PESCHEL, A., OTTO, M., JACK, R. W., KALBACHER, H., JUNG, G. & GÖTZ, F. 1999. Inactivation of the dlt Operon inStaphylococcus aureus Confers Sensitivity to Defensins, Protegrins, and Other Antimicrobial Peptides. *Journal of Biological Chemistry,* 274**,** 8405-8410.

PESCHEL, A. & SAHL, H. G. 2006. The co-evolution of host cationic antimicrobial peptides and microbial resistance. *Nat Rev Microbiol,* 4**,** 529-36.

POLAK, M. E., THIRDBOROUGH, S. M., UNG, C. Y., ELLIOTT, T., HEALY, E., FREEMAN, T. C. & ARDERN-JONES, M. R. 2014. Distinct molecular signature of human skin Langerhans cells denotes critical differences in cutaneous dendritic cell immune regulation. *J Invest Dermatol,* 134**,** 695-703.

POPOV, L., KOVALSKI, J., GRANDI, G., BAGNOLI, F. & AMIEVA, M. R. 2014. Three-dimensional human skin models to understand Staphylococcus aureus skin colonization and infection. *Frontiers in Immunology,* 5.

POVEDA, J., SANZ, A. B., FERNANDEZ-FERNANDEZ, B., CARRASCO, S., RUIZ-ORTEGA, M., CANNATA-ORTIZ, P., ORTIZ, A. & SANCHEZ-NINO, M. D. 2017. MXRA5 is a TGF-beta1-regulated human protein with anti-inflammatory and anti-fibrotic properties. *J Cell Mol Med,* 21**,** 154-164.

PUNNONEN, J., YSSEL, H. & DE VRIES, J. 1997. The relative contribution of IL-4 and IL-13 to human IgE synthesis induced by activated CD4+ or CD8+ T cells. *Journal of Allergy and Clinical Immunology,* 100**,** 792-801.

QIANG, L., SAMPLE, A., LIU, H., WU, X. & HE, Y. Y. 2017. Epidermal SIRT1 regulates inflammation, cell migration, and wound healing. *Sci Rep,* 7**,** 14110.

QIN, J.-Z., CHATURVEDI, V., DENNING, M. F., CHOUBEY, D., DIAZ, M. O. & NICKOLOFF, B. J. 1999. Role of NF-κB in the Apoptotic-resistant Phenotype of Keratinocytes. *Journal of Biological Chemistry,* 274**,** 37957-37964.

QIU, J., FENG, H., LU, J., XIANG, H., WANG, D., DONG, J., WANG, J., WANG, X., LIU, J. & DENG, X. 2010. Eugenol reduces the expression of virulence-related exoproteins in Staphylococcus aureus. *Appl Environ Microbiol,* 76**,** 5846-51.

RADEMACHER, F., SIMANSKI, M., HESSE, B., DOMBROWSKY, G., VENT, N., GLASER, R. & HARDER, J. 2018. Staphylococcus epidermidis Activates Aryl Hydrocarbon Receptor Signaling in Human Keratinocytes: Implications for Cutaneous Defense. *J Innate Immun***,** 1-11.

RAMIREZ-CARROZZI, V., SAMBANDAM, A., LUIS, E., LIN, Z., JEET, S., LESCH, J., HACKNEY, J., KIM, J., ZHOU, M., LAI, J., MODRUSAN, Z., SAI, T., LEE, W., XU, M., CAPLAZI, P., DIEHL, L., DE VOSS, J., BALAZS, M., GONZALEZ, L., JR., SINGH, H., OUYANG, W. & PAPPU, R. 2011. IL-17C regulates the innate immune function of epithelial cells in an autocrine manner. *Nat Immunol,* 12**,** 1159-66.

RAMOS, M., LAO, Y., EGUILUZ, C., DEL VAL, M. & MARTINEZ, I. 2015. Urokinase receptor-deficient mice mount an innate immune response to and clarify respiratory viruses as efficiently as wild-type mice. *Virulence,* 6**,** 710-5.

RICOTE, M. & GLASS, C. K. 2007. PPARs and molecular mechanisms of transrepression. *Biochimica et biophysica acta,* 1771**,** 926-935.

RIEG, S., KAASCH, A. J., WEHRLE, J., HOFMANN, S. C., SZYMANIAK-VITS, M., SABOROWSKI, V., JONAS, D., KALBACHER, H., SEIFERT, H. & KERN, W. V. 2011. Susceptibility of clinical Staphylococcus aureus isolates to innate defense antimicrobial peptides. *Microbes Infect,* 13**,** 761-5.

RIJNEVELD, A. W., LEVI, M., FLORQUIN, S., SPEELMAN, P., CARMELIET, P. & VAN DER POLL, T. 2002. Urokinase Receptor Is Necessary for Adequate Host Defense Against Pneumococcal Pneumonia. *The Journal of Immunology,* 168**,** 3507.

RINNERTHALER, M., STREUBEL, M. K., BISCHOF, J. & RICHTER, K. 2015. Skin aging, gene expression and calcium. *Exp Gerontol,* 68**,** 59-65.

RODRIGUES, L., GRACA, R. S. F. & CARNEIRO, L. A. M. 2018. Integrated Stress Responses to Bacterial Pathogenesis Patterns. *Front Immunol,* 9**,** 1306.

ROE, K., GIBOT, S. & VERMA, S. 2014. Triggering receptor expressed on myeloid cells-1 (TREM-1): a new player in antiviral immunity? *Front Microbiol,* 5**,** 627.

ROMANI, N., CLAUSEN, B. E. & STOITZNER, P. 2010. Langerhans cells and more: langerin-expressing dendritic cell subsets in the skin. *Immunol Rev,* 234**,** 120-41.

ROSDY, M. & CLAUSS, L.-C. 1990. Terminal Epidermal Differentiation of Human Keratinocytes Grown in Chemically Defined Medium on Inert Filter Substrates at the Air-Liquid Interface. *J Investig Dermatol,* 95**,** 409-414.

ROTH, S. A., SIMANSKI, M., RADEMACHER, F., SCHRODER, L. & HARDER, J. 2014. The pattern recognition receptor NOD2 mediates Staphylococcus aureus-induced IL-17C expression in keratinocytes. *J Invest Dermatol,* 134**,** 374-380.

ROUAUD-TINGUELY, P., BOUDIER, D., MARCHAND, L., BARRUCHE, V., BORDES, S., COPPIN, H., ROTH, M. P. & CLOSS, B. 2015. From the morphological to the transcriptomic characterization of a compromised three-dimensional in vitro model mimicking atopic dermatitis. *Br J Dermatol,* 173**,** 1006-14.

SANDILANDS, A., SUTHERLAND, C., IRVINE, A. D. & MCLEAN, W. H. I. 2009. Filaggrin in the frontline: role in skin barrier function and disease. *Journal of cell science,* 122**,** 1285-1294.

SAWADA, E., YOSHIDA, N., SUGIURA, A. & IMOKAWA, G. 2012. Th1 cytokines accentuate but Th2 cytokines attenuate ceramide production in the stratum corneum of human epidermal equivalents: an implication for the disrupted barrier mechanism in atopic dermatitis. *J Dermatol Sci,* 68**,** 25-35.

SAWAMURA, D., GOTO, M., SHIBAKI, A., AKIYAMA, M., MCMILLAN, J. R., ABIKO, Y. & SHIMIZU, H. 2005. Beta defensin-3 engineered epidermis shows highly protective effect for bacterial infection. *Gene Ther,* 12**,** 857-861.

SAWANT, K. V., POLURI, K. M., DUTTA, A. K., SEPURU, K. M., TROSHKINA, A., GAROFALO, R. P. & RAJARATHNAM, K. 2016. Chemokine CXCL1 mediated neutrophil recruitment: Role of glycosaminoglycan interactions. *Sci Rep,* 6**,** 33123.

SCHARSCHMIDT, T. C. 2017. Establishing Tolerance to Commensal Skin Bacteria: Timing Is Everything. *Dermatol Clin,* 35**,** 1-9.

SCHARSCHMIDT, T. C., VASQUEZ, K. S., TRUONG, H. A., GEARTY, S. V., PAULI, M. L., NOSBAUM, A., GRATZ, I. K., OTTO, M., MOON, J. J., LIESE, J., ABBAS, A. K., FISCHBACH, M. A. & ROSENBLUM, M. D. 2015. A Wave of Regulatory T Cells into Neonatal Skin Mediates Tolerance to Commensal Microbes. *Immunity,* 43**,** 1011-21.

SCHLITZER, A., MCGOVERN, N. & GINHOUX, F. 2015. Dendritic cells and monocyte-derived cells: Two complementary and integrated functional systems. *Semin Cell Dev Biol,* 41**,** 9-22.

SCHLOMANN, U., RATHKE-HARTLIEB, S., YAMAMOTO, S., JOCKUSCH, H. & BARTSCH, J. W. 2000. Tumor Necrosis Factor α Induces a Metalloprotease-Disintegrin, ADAM8 (CD 156): Implications for Neuron–Glia Interactions during Neurodegeneration. *The Journal of Neuroscience,* 20**,** 7964.

SCHMIDT, S. V., NINO-CASTRO, A. C. & SCHULTZE, J. L. 2012. Regulatory dendritic cells: there is more than just immune activation. *Front Immunol,* 3**,** 274.

SCHOOP, V. M., MIRANCEA, N. & FUSENIG, N. E. 1999. Epidermal organization and differentiation of HaCaT keratinocytes in organotypic coculture with human dermal fibroblasts. *J Invest Dermatol,* 112**,** 343-53.

SCHUTYSER, E., STRUYF, S. & VAN DAMME, J. 2003. The CC chemokine CCL20 and its receptor CCR6. *Cytokine & Growth Factor Reviews,* 14**,** 409-426.

SCHWANDNER, R., DZIARSKI, R., WESCHE, H., ROTHE, M. & KIRSCHNING, C. J. 1999. Peptidoglycan- and Lipoteichoic Acid-induced Cell Activation Is Mediated by Toll-like Receptor 2. *Journal of Biological Chemistry,* 274**,** 17406-17409.

SEILIE, E. S. & BUBECK WARDENBURG, J. 2017. Staphylococcus aureus pore-forming toxins: The interface of pathogen and host complexity. *Semin Cell Dev Biol,* 72**,** 101-116.

SEJVAR, J. J. 2013. Neuroinfections (What Do I Do Now?). *Emerging Infectious Diseases,* 19**,** 1553-1553.

SENESCHAL, J., CLARK, R. A., GEHAD, A., BAECHER-ALLAN, C. M. & KUPPER, T. S. 2012. Human epidermal Langerhans cells maintain immune homeostasis in skin by activating skin resident regulatory T cells. *Immunity,* 36**,** 873-84.

SEO, M. D., KANG, T. J., LEE, C. H., LEE, A. Y. & NOH, M. 2012. HaCaT Keratinocytes and Primary Epidermal Keratinocytes Have Different Transcriptional Profiles of Cornified Envelope-Associated Genes to T Helper Cell Cytokines. *Biomol Ther (Seoul),* 20**,** 171-6.

SERRAVALLO, M., JAGDEO, J., GLICK, S. A., SIEGEL, D. M. & BRODY, N. I. 2013. Sirtuins in dermatology: applications for future research and therapeutics. *Arch Dermatol Res,* 305**,** 269-82.

SERRE, G., MILS, V., HAFTEK, M., VINCENT, C., CROUTE, F., REANO, A., OUHAYOUN, J.-P., BETTINGER, S. & SOLEIHAVOUP, J.-P. 1991. Identification of Late Differentiation Antigens of Human Cornified Epithelia, Expressed in Re-Organized Desmosomes and Bound to Cross-Linked Envelope. *J Investig Dermatol,* 97**,** 1061-1072.

SHARMA, D. & KANNEGANTI, T. D. 2016. The cell biology of inflammasomes: Mechanisms of inflammasome activation and regulation. *J Cell Biol,* 213**,** 617-29.

SHARP, J. A., ECHAGUE, C. G., HAIR, P. S., WARD, M. D., NYALWIDHE, J. O., GEOGHEGAN, J. A., FOSTER, T. J. & CUNNION, K. M. 2012. Staphylococcus aureus surface protein SdrE binds complement regulator factor H as an immune evasion tactic. *PLoS One,* 7**,** e38407.

SHEMBADE, N., MA, A. & HARHAJ, E. W. 2010. Inhibition of NF-kappaB signaling by A20 through disruption of ubiquitin enzyme complexes. *Science,* 327**,** 1135-9.

SHI, Y., LIU, C. H., ROBERTS, A. I., DAS, J., XU, G., REN, G., ZHANG, Y., ZHANG, L., YUAN, Z. R., TAN, H. S., DAS, G. & DEVADAS, S. 2006. Granulocyte-macrophage colony-stimulating factor (GM-CSF) and T-cell responses: what we do and don't know. *Cell Res,* 16**,** 126-33.

SHIH, V. F., TSUI, R., CALDWELL, A. & HOFFMANN, A. 2011. A single NFkappaB system for both canonical and non-canonical signaling. *Cell Res,* 21**,** 86-102.

SHIMANE, K., KOCHI, Y., HORITA, T., IKARI, K., AMANO, H., HIRAKATA, M., OKAMOTO, A., YAMADA, R., MYOUZEN, K., SUZUKI, A., KUBO, M., ATSUMI, T., KOIKE, T., TAKASAKI, Y., MOMOHARA, S., YAMANAKA, H., NAKAMURA, Y. & YAMAMOTO, K. 2010. The association of a nonsynonymous single-nucleotide polymorphism in TNFAIP3 with systemic lupus erythematosus and rheumatoid arthritis in the Japanese population. *Arthritis Rheum,* 62**,** 574-9.

SHINJI, H., YOSIZAWA, Y., TAJIMA, A., IWASE, T., SUGIMOTO, S., SEKI, K. & MIZUNOE, Y. 2011. Role of fibronectin-binding proteins A and B in in vitro cellular infections and in vivo septic infections by Staphylococcus aureus. *Infect Immun,* 79**,** 2215-23.

SIDRAUSKI, C., TSAI, J. C., KAMPMANN, M., HEARN, B. R., VEDANTHAM, P., JAISHANKAR, P., SOKABE, M., MENDEZ, A. S., NEWTON, B. W., TANG, E. L., VERSCHUEREN, E., JOHNSON, J.

R., KROGAN, N. J., FRASER, C. S., WEISSMAN, J. S., RENSLO, A. R. & WALTER, P. 2015. Pharmacological dimerization and activation of the exchange factor eIF2B antagonizes the integrated stress response. *Elife,* 4**,** e07314.

SIGGERS, T., CHANG, A. B., TEIXEIRA, A., WONG, D., WILLIAMS, K. J., AHMED, B., RAGOUSSIS, J., UDALOVA, I. A., SMALE, S. T. & BULYK, M. L. 2011. Principles of dimer-specific gene regulation revealed by a comprehensive characterization of NF-kappaB family DNA binding. *Nat Immunol,* 13**,** 95-102.

SILVERBERG, J. I. & HANIFIN, J. M. 2013. Adult eczema prevalence and associations with asthma and other health and demographic factors: a US population-based study. *J Allergy Clin Immunol,* 132**,** 1132-8.

SIMANSKI, M., DRESSEL, S., GLASER, R. & HARDER, J. 2010. RNase 7 protects healthy skin from Staphylococcus aureus colonization. *J Invest Dermatol,* 130**,** 2836-8.

SIMANSKI, M., ERKENS, A. S., RADEMACHER, F. & HARDER, J. 2018. Staphylococcus epidermidis-induced Interleukin-1 Beta and Human Beta-defensin-2 Expression in Human Keratinocytes is Regulated by the Host Molecule A20 (TNFAIP3). *Acta Derm Venereol*.

SIMANSKI, M., RADEMACHER, F., SCHRODER, L., GLASER, R. & HARDER, J. 2016. The Inflammasome and the Epidermal Growth Factor Receptor (EGFR) Are Involved in the Staphylococcus aureus-Mediated Induction of IL-1alpha and IL-1beta in Human Keratinocytes. *PLoS One,* 11**,** e0147118.

SOGE, O. O., MESCHKE, J. S., NO, D. B. & ROBERTS, M. C. 2009. Characterization of methicillin-resistant Staphylococcus aureus and methicillin-resistant coagulase-negative Staphylococcus spp. isolated from US West Coast public marine beaches. *J Antimicrob Chemother,* 64**,** 1148-55.

SOHN, K. C., BACK, S. J., CHOI, D. K., SHIN, J. M., KIM, S. J., IM, M., LEE, Y., SEO, Y. J., YOON, T. J., LEE, Y. H., LEE, J. H. & KIM, C. D. 2016. The inhibitory effect of A20 on the inflammatory reaction of epidermal keratinocytes. *Int J Mol Med,* 37**,** 1099-104.

SOKABE, M. & FRASER, C. S. 2014. Human eukaryotic initiation factor 2 (eIF2)-GTP-Met-tRNAi ternary complex and eIF3 stabilize the 43 S preinitiation complex. *J Biol Chem,* 289**,** 31827-36.

SOKOL, C. L. & LUSTER, A. D. 2015. The chemokine system in innate immunity. *Cold Spring Harb Perspect Biol,* 7.

SPAULDING, A. R., SALGADO-PABON, W., KOHLER, P. L., HORSWILL, A. R., LEUNG, D. Y. & SCHLIEVERT, P. M. 2013. Staphylococcal and streptococcal superantigen exotoxins. *Clin Microbiol Rev,* 26**,** 422-47.

SPEECKAERT, R., LAMBERT, J., GRINE, L., VAN GELE, M., DE SCHEPPER, S. & VAN GEEL, N. 2016. The many faces of interleukin-17 in inflammatory skin diseases. *Br J Dermatol,* 175**,** 892-901.

STARK, H. J., BOEHNKE K FAU - MIRANCEA, N., MIRANCEA N FAU - WILLHAUCK, M. J., WILLHAUCK MJ FAU - PAVESIO, A., PAVESIO A FAU - FUSENIG, N. E., FUSENIG NE FAU - BOUKAMP, P. & BOUKAMP, P. 2006. Epidermal homeostasis in long-term scaffold-enforced skin equivalents. *Journal of Investigative Dermatology Symposium Proceedings,* 11**,** 93-105.

STAUMONT-SALLE, D., ABBOUD, G., BRENUCHON, C., KANDA, A., ROUMIER, T., LAVOGIEZ, C., FLEURY, S., REMY, P., PAPIN, J. P., BERTRAND-MICHEL, J., TERCE, F., STAELS, B., DELAPORTE, E., CAPRON, M. & DOMBROWICZ, D. 2008. Peroxisome proliferator-activated

receptor alpha regulates skin inflammation and humoral response in atopic dermatitis. *J Allergy Clin Immunol,* 121**,** 962-8 e6.

STIENSTRA, R., MANDARD, S., TAN, N. S., WAHLI, W., TRAUTWEIN, C., RICHARDSON, T. A., LICHTENAUER-KALIGIS, E., KERSTEN, S. & MULLER, M. 2007. The Interleukin-1 receptor antagonist is a direct target gene of PPARalpha in liver. *J Hepatol,* 46**,** 869-77.

STRANDT, H., PINHEIRO, D. F., KAPLAN, D. H., WIRTH, D., GRATZ, I. K., HAMMERL, P., THALHAMER, J. & STOECKLINGER, A. 2017. Neoantigen Expression in Steady-State Langerhans Cells Induces CTL Tolerance. *J Immunol,* 199**,** 1626-1634.

STROBER, W. 2004. Epithelial cells pay a Toll for protection. *Nat Med,* 10**,** 898-900.

SUAREZ-FARINAS, M., UNGAR, B., CORREA DA ROSA, J., EWALD, D. A., ROZENBLIT, M., GONZALEZ, J., XU, H., ZHENG, X., PENG, X., ESTRADA, Y. D., DILLON, S. R., KRUEGER, J. G. & GUTTMAN-YASSKY, E. 2015. RNA sequencing atopic dermatitis transcriptome profiling provides insights into novel disease mechanisms with potential therapeutic implications. *J Allergy Clin Immunol,* 135**,** 1218-27.

SUGIURA, H., EBISE, H., TAZAWA, T., TANAKA, K., SUGIURA, Y., UEHARA, M., KIKUCHI, K. & KIMURA, T. 2005. Large-scale DNA microarray analysis of atopic skin lesions shows overexpression of an epidermal differentiation gene cluster in the alternative pathway and lack of protective gene expression in the cornified envelope. *Br J Dermatol,* 152**,** 146-9.

SUMIGRAY, K. D. & LECHLER, T. 2015. Cell adhesion in epidermal development and barrier formation. *Curr Top Dev Biol,* 112**,** 383-414.

SUMIKAWA, Y., ASADA, H., HOSHINO, K., AZUKIZAWA, H., KATAYAMA, I., AKIRA, S. & ITAMI, S. 2006. Induction of beta-defensin 3 in keratinocytes stimulated by bacterial lipopeptides through toll-like receptor 2. *Microbes Infect,* 8**,** 1513-21.

SUMMERFIELD, V. L. 2015. *Characterisation of keratinocyte-derived epidermal signals in the initiation of contact hypersensitivity to chemicals.*

SUN, R., CELLI, A., CRUMRINE, D., HUPE, M., ADAME, L. C., PENNYPACKER, S. D., PARK, K., UCHIDA, Y., FEINGOLD, K. R., ELIAS, P. M., ILIC, D. & MAURO, T. M. 2015. Lowered humidity produces human epidermal equivalents with enhanced barrier properties. *Tissue Eng Part C Methods,* 21**,** 15-22.

SUN, S. C. 2011. Non-canonical NF-kappaB signaling pathway. *Cell Res,* 21**,** 71-85.

SUN, S. C. 2017. The non-canonical NF-kappaB pathway in immunity and inflammation. *Nat Rev Immunol,* 17**,** 545-558.

SWAIN, S. L. 1995. T-Cell Subsets: Who does the polarizing? *Current Biology,* 5**,** 849-851.

TAGLIABRACCI, V. S., WILEY, S. E., GUO, X., KINCH, L. N., DURRANT, E., WEN, J., XIAO, J., CUI, J., NGUYEN, K. B., ENGEL, J. L., COON, J. J., GRISHIN, N., PINNA, L. A., PAGLIARINI, D. J. & DIXON, J. E. 2015. A Single Kinase Generates the Majority of the Secreted Phosphoproteome. *Cell,* 161**,** 1619-32.

TANAKA, A., MUTO, S., JUNG, K., ITAI, A. & MATSUDA, H. 2007. Topical application with a new NF-kappaB inhibitor improves atopic dermatitis in NC/NgaTnd mice. *J Invest Dermatol,* 127**,** 855-63.

TEJASVI, T., STUART, P. E., CHANDRAN, V., VOORHEES, J. J., GLADMAN, D. D., RAHMAN, P., ELDER, J. T. & NAIR, R. P. 2012. TNFAIP3 gene polymorphisms are associated with response to TNF blockade in psoriasis. *J Invest Dermatol,* 132**,** 593-600.

TEVELL, S., HELLMARK, B., NILSDOTTER-AUGUSTINSSON, A. & SODERQUIST, B. 2017. Staphylococcus capitis isolated from prosthetic joint infections. *Eur J Clin Microbiol Infect Dis,* 36**,** 115-122.

THAKOERSING, V. S., VAN SMEDEN, J., MULDER, A. A., VREEKEN, R. J., EL GHALBZOURI, A. & BOUWSTRA, J. A. 2013. Increased presence of monounsaturated fatty acids in the stratum corneum of human skin equivalents. *J Invest Dermatol,* 133**,** 59-67.

THEOCHARIS, A. D., SKANDALIS, S. S., GIALELI, C. & KARAMANOS, N. K. 2016. Extracellular matrix structure. *Adv Drug Deliv Rev,* 97**,** 4-27.

TIAN, S., KRUEGER, J. G., LI, K., JABBARI, A., BRODMERKEL, C., LOWES, M. A. & SUAREZ-FARINAS, M. 2012. Meta-analysis derived (MAD) transcriptome of psoriasis defines the "core" pathogenesis of disease. *PLoS One,* 7**,** e44274.

TILL, A., ROSENSTIEL, P., BRAUTIGAM, K., SINA, C., JACOBS, G., OBERG, H. H., SEEGERT, D., CHAKRABORTY, T. & SCHREIBER, S. 2008. A role for membrane-bound CD147 in NOD2-mediated recognition of bacterial cytoinvasion. *J Cell Sci,* 121**,** 487-95.

TLASKALOVA-HOGENOVA, H., STEPANKOVA, R., HUDCOVIC, T., TUCKOVA, L., CUKROWSKA, B., LODINOVA-ZADNIKOVA, R., KOZAKOVA, H., ROSSMANN, P., BARTOVA, J., SOKOL, D., FUNDA, D. P., BOROVSKA, D., REHAKOVA, Z., SINKORA, J., HOFMAN, J., DRASTICH, P. & KOKESOVA, A. 2004. Commensal bacteria (normal microflora), mucosal immunity and chronic inflammatory and autoimmune diseases. *Immunol Lett,* 93**,** 97-108.

TOEBAK, M. J., GIBBS, S., BRUYNZEEL, D. P., SCHEPER, R. J. & RUSTEMEYER, T. 2009. Dendritic cells: biology of the skin. *Contact Dermatitis,* 60**,** 2-20.

TONG, S. Y., DAVIS, J. S., EICHENBERGER, E., HOLLAND, T. L. & FOWLER, V. G., JR. 2015. Staphylococcus aureus infections: epidemiology, pathophysiology, clinical manifestations, and management. *Clin Microbiol Rev,* 28**,** 603-61.

TOTTE, J. E., VAN DER FELTZ, W. T., HENNEKAM, M., VAN BELKUM, A., VAN ZUUREN, E. J. & PASMANS, S. G. 2016. Prevalence and odds of Staphylococcus aureus carriage in atopic dermatitis: a systematic review and meta-analysis. *Br J Dermatol,* 175**,** 687-95.

TRIVEDI, S., UHLEMANN, A. C., HERMAN-BAUSIER, P., SULLIVAN, S. B., SOWASH, M. G., FLORES, E. Y., KHAN, S. D., DUFRENE, Y. F. & LOWY, F. D. 2017. The Surface Protein SdrF Mediates Staphylococcus epidermidis Adherence to Keratin. *J Infect Dis,* 215**,** 1846-1854.

TUCHSCHERR, L., BISCHOFF, M., LATTAR, S. M., NOTO LLANA, M., PFORTNER, H., NIEMANN, S., GERACI, J., VAN DE VYVER, H., FRAUNHOLZ, M. J., CHEUNG, A. L., HERRMANN, M., VOLKER, U., SORDELLI, D. O., PETERS, G. & LOFFLER, B. 2015. Sigma Factor SigB Is Crucial to Mediate Staphylococcus aureus Adaptation during Chronic Infections. *PLoS Pathog,* 11**,** e1004870.

VALLADEAU, J., RAVEL, O., DEZUTTER-DAMBUYANT, C., MOORE, K., KLEIJMEER, M., LIU, Y., DUVERT-FRANCES, V., VINCENT, C., SCHMITT, D., DAVOUST, J., CAUX, C., LEBECQUE, S. & SAELAND, S. 2000. Langerin, a Novel C-Type Lectin Specific to Langerhans Cells, Is an Endocytic Receptor that Induces the Formation of Birbeck Granules. *Immunity,* 12**,** 71-81.

VAN 'T WOUT, E. F., HIEMSTRA, P. S. & MARCINIAK, S. J. 2014. The integrated stress response in lung disease. *Am J Respir Cell Mol Biol,* 50**,** 1005-9.

VAN BELKUM, A., VERKAIK, N. J., DE VOGEL, C. P., BOELENS, H. A., VERVEER, J., NOUWEN, J. L., VERBRUGH, H. A. & WERTHEIM, H. F. 2009. Reclassification of Staphylococcus aureus nasal carriage types. *J Infect Dis,* 199**,** 1820-6.

VAN DER ZWET, W. C., DEBETS-OSSENKOPP, Y. J., REINDERS, E., KAPI, M., SAVELKOUL, P. H. M., VAN ELBURG, R. M., HIRAMATSU, K. & VANDENBROUCKE-GRAULS, C. M. J. E. 2002. Nosocomial Spread of a Staphylococcus capitis Strain with Heteroresistance to Vancomycin in a Neonatal Intensive Care Unit. *Journal of Clinical Microbiology,* 40**,** 2520-2525.

VANDENESCH, F., LINA, G. & HENRY, T. 2012. Staphylococcus aureus hemolysins, bi-component leukocidins, and cytolytic peptides: a redundant arsenal of membrane-damaging virulence factors? *Front Cell Infect Microbiol,* 2**,** 12.

VEREECKE, L., SZE, M., MC GUIRE, C., ROGIERS, B., CHU, Y., SCHMIDT-SUPPRIAN, M., PASPARAKIS, M., BEYAERT, R. & VAN LOO, G. 2010. Enterocyte-specific A20 deficiency sensitizes to tumor necrosis factor-induced toxicity and experimental colitis. *J Exp Med,* 207**,** 1513-23.

VITRY, P., VALOTTEAU, C., FEUILLIE, C., BERNARD, S., ALSTEENS, D., GEOGHEGAN, J. A. & DUFRENE, Y. F. 2017. Force-Induced Strengthening of the Interaction between Staphylococcus aureus Clumping Factor B and Loricrin. *MBio,* 8.

VOGEL, R. 2009. Alternatives to the use of animals in safety testing as required by the EU-Cosmetics Directive 2009. *Altex,* 26**,** 223-6.

VOGEL, T. P., MILNER, J. D. & COOPER, M. A. 2015. The Ying and Yang of STAT3 in Human Disease. *J Clin Immunol,* 35**,** 615-23.

VUONG, C. & OTTO, M. 2002. Staphylococcus epidermidis infections. *Microbes and Infection,* 4**,** 481-489.

WAN, Y. Y. & FLAVELL, R. A. 2009. How diverse--CD4 effector T cells and their functions. *J Mol Cell Biol,* 1**,** 20-36.

WANG, B., MCHUGH, B. J., QURESHI, A., CAMPOPIANO, D. J., CLARKE, D. J., FITZGERALD, J. R., DORIN, J. R., WELLER, R. & DAVIDSON, D. J. 2017. IL-1beta-Induced Protection of Keratinocytes against Staphylococcus aureus-Secreted Proteases Is Mediated by Human beta-Defensin 2. *J Invest Dermatol,* 137**,** 95-105.

WANG, G. 2014. Human antimicrobial peptides and proteins. *Pharmaceuticals (Basel),* 7**,** 545-94.

WANG, J., OUYANG, Y., GUNER, Y., FORD, H. R. & GRISHIN, A. V. 2009a. Ubiquitin-editing enzyme A20 promotes tolerance to lipopolysaccharide in enterocytes. *J Immunol,* 183**,** 1384-92.

WANG, L., CLAVAUD, C., BAR-HEN, A., CUI, M., GAO, J., LIU, Y., LIU, C., SHIBAGAKI, N., GUENICHE, A., JOURDAIN, R., LAN, K., ZHANG, C., ALTMEYER, R. & BRETON, L. 2015. Characterization of the major bacterial-fungal populations colonizing dandruff scalps in Shanghai, China, shows microbial disequilibrium. *Exp Dermatol,* 24**,** 398-400.

WANG, R., BRAUGHTON, K. R., KRETSCHMER, D., BACH, T. H., QUECK, S. Y., LI, M., KENNEDY, A. D., DORWARD, D. W., KLEBANOFF, S. J., PESCHEL, A., DELEO, F. R. & OTTO, M. 2007. Identification of novel cytolytic peptides as key virulence determinants for community-associated MRSA. *Nat Med,* 13**,** 1510-4.

WANG, X., GE, J., LIU, B., HU, Y. & YANG, M. 2013. Structures of SdrD from Staphylococcus aureus reveal the molecular mechanism of how the cell surface receptors recognize their ligands. *Protein Cell,* 4**,** 277-85.

WANG, X. P., SCHUNCK, M., KALLEN, K. J., NEUMANN, C., TRAUTWEIN, C., ROSE-JOHN, S. & PROKSCH, E. 2004. The interleukin-6 cytokine system regulates epidermal permeability barrier homeostasis. *J Invest Dermatol,* 123**,** 124-31.

WANG, Z., GERSTEIN, M. & SNYDER, M. 2009b. RNA-Seq: a revolutionary tool for transcriptomics. *Nat Rev Genet,* 10**,** 57-63.

WEIDINGER, S., O'SULLIVAN, M., ILLIG, T., BAURECHT, H., DEPNER, M., RODRIGUEZ, E., RUETHER, A., KLOPP, N., VOGELBERG, C., WEILAND, S. K., MCLEAN, W. H., VON MUTIUS, E., IRVINE, A. D. & KABESCH, M. 2008. Filaggrin mutations, atopic eczema, hay fever, and asthma in children. *J Allergy Clin Immunol,* 121**,** 1203-1209 e1.

WERFEL, T., ALLAM, J. P., BIEDERMANN, T., EYERICH, K., GILLES, S., GUTTMAN-YASSKY, E., HOETZENECKER, W., KNOL, E., SIMON, H. U., WOLLENBERG, A., BIEBER, T., LAUENER, R., SCHMID-GRENDELMEIER, P., TRAIDL-HOFFMANN, C. & AKDIS, C. A. 2016. Cellular and molecular immunologic mechanisms in patients with atopic dermatitis. *J Allergy Clin Immunol,* 138**,** 336-49.

WERTHEIM, H. F. L., MELLES, D. C., VOS, M. C., VAN LEEUWEN, W., VAN BELKUM, A., VERBRUGH, H. A. & NOUWEN, J. L. 2005. The role of nasal carriage in Staphylococcus aureus infections. *The Lancet Infectious Diseases,* 5**,** 751-762.

WERTHEIM, H. F. L., VOS, M. C., OTT, A., VAN BELKUM, A., VOSS, A., KLUYTMANS, J. A. J. W., VAN KEULEN, P. H. J., VANDENBROUCKE-GRAULS, C. M. J. E., MEESTER, M. H. M. & VERBRUGH, H. A. 2004. Risk and outcome of nosocomial Staphylococcus aureus bacteraemia in nasal carriers versus non-carriers. *The Lancet,* 364**,** 703-705.

WERTZ, I. E., O'ROURKE, K. M., ZHOU, H., EBY, M., ARAVIND, L., SESHAGIRI, S., WU, P., WIESMANN, C., BAKER, R., BOONE, D. L., MA, A., KOONIN, E. V. & DIXIT, V. M. 2004. De-ubiquitination and ubiquitin ligase domains of A20 downregulate NF-κB signalling. *Nature,* 430**,** 694.

WEST, H. C. & BENNETT, C. L. 2017. Redefining the Role of Langerhans Cells As Immune Regulators within the Skin. *Front Immunol,* 8**,** 1941.

WICHE, G. 1998. Role of plectin in cytoskeleton organization and dynamics. *Journal of Cell Science,* 111**,** 2477.

WICKETT, R. R. & VISSCHER, M. O. 2006. Structure and function of the epidermal barrier. *American Journal of Infection Control,* 34**,** S98-S110.

WIGHT, T. N., KANG, I. & MERRILEES, M. J. 2014. Versican and the control of inflammation. *Matrix Biol,* 35**,** 152-61.

WIKRAMANAYAKE, T. C., STOJADINOVIC, O. & TOMIC-CANIC, M. 2014. Epidermal Differentiation in Barrier Maintenance and Wound Healing. *Adv Wound Care (New Rochelle),* 3**,** 272-280.

WILLIAMS, R. E. O. 1963. HEALTHY CARRIAGE OF STAPHYLOCOCCUS AUREUS: ITS PREVALENCE AND IMPORTANCE. *Bacteriological Reviews,* 27**,** 56-71.

WINKLES, J. A. 2008. The TWEAK-Fn14 cytokine-receptor axis: discovery, biology and therapeutic targeting. *Nat Rev Drug Discov,* 7**,** 411-25.

WITT, S. H., GRANZIER, H., WITT, C. C. & LABEIT, S. 2005. MURF-1 and MURF-2 target a specific subset of myofibrillar proteins redundantly: towards understanding MURF-dependent muscle ubiquitination. *J Mol Biol,* 350**,** 713-22.

XIANG, H., FENG, Y., WANG, J., LIU, B., CHEN, Y., LIU, L., DENG, X. & YANG, M. 2012. Crystal structures reveal the multi-ligand binding mechanism of Staphylococcus aureus ClfB. *PLoS Pathog,* 8**,** e1002751.

YAMAMOTO, H., SCHOONJANS, K. & AUWERX, J. 2007. Sirtuin functions in health and disease. *Mol Endocrinol,* 21**,** 1745-55.

YANEZ, D. A., LACHER, R. K., VIDYARTHI, A. & COLEGIO, O. R. 2017. The role of macrophages in skin homeostasis. *Pflugers Arch,* 469**,** 455-463.

YANG, C., CHEN, B., ZHAO, J., LIN, L., HAN, L., PAN, S., FU, L., JIN, M., CHEN, H. & ZHANG, A. 2015. TREM-1 signaling promotes host defense during the early stage of infection with highly pathogenic Streptococcus suis. *Infect Immun,* 83**,** 3293-301.

YANG, D., CHEN, Q., HOOVER, D. M., STALEY, P., TUCKER, K. D., LUBKOWSKI, J. & OPPENHEIM, J. J. 2003. Many chemokines including CCL20/MIP-3α display antimicrobial activity. *Journal of Leukocyte Biology,* 74**,** 448-455.

YAZDI, A. S., ROCKEN, M. & GHORESCHI, K. 2016. Cutaneous immunology: basics and new concepts. *Semin Immunopathol,* 38**,** 3-10.

YIN, L., COELHO, S. G., VALENCIA, J. C., EBSEN, D., MAHNS, A., SMUDA, C., MILLER, S. A., BEER, J. Z., KOLBE, L. & HEARING, V. J. 2015. Identification of Genes Expressed in Hyperpigmented Skin Using Meta-Analysis of Microarray Data Sets. *J Invest Dermatol,* 135**,** 2455-2463.

YOSHIZAKI, T., SCHENK, S., IMAMURA, T., BABENDURE, J. L., SONODA, N., BAE, E. J., OH, D. Y., LU, M., MILNE, J. C., WESTPHAL, C., BANDYOPADHYAY, G. & OLEFSKY, J. M. 2010. SIRT1 inhibits inflammatory pathways in macrophages and modulates insulin sensitivity. *American Journal of Physiology - Endocrinology and Metabolism,* 298**,** E419-E428.

YU, S., NAKASHIMA, N., XU, B. H., MATSUDA, T., IZUMIHARA, A., SUNAHARA, N., NAKAMURA, T., TSUKANO, M. & MATSUYAMA, T. 1998. Pathological significance of elevated soluble CD14 production in rheumatoid arthritis: in the presence of soluble CD14, lipopolysaccharides at low concentrations activate RA synovial fibroblasts. *Rheumatol Int,* 17**,** 237-43.

ZANGER, P., HOLZER, J., SCHLEUCHER, R., SCHERBAUM, H., SCHITTEK, B. & GABRYSCH, S. 2010. Severity of Staphylococcus aureus infection of the skin is associated with inducibility of human beta-defensin 3 but not human beta-defensin 2. *Infect Immun,* 78**,** 3112-7.

ZANGER, P., NURJADI, D., VATH, B. & KREMSNER, P. G. 2011. Persistent nasal carriage of Staphylococcus aureus is associated with deficient induction of human beta-defensin 3 after sterile wounding of healthy skin in vivo. *Infect Immun,* 79**,** 2658-62.

ZANIBONI, M. C., SAMORANO, L. P., ORFALI, R. L. & AOKI, V. 2016. Skin barrier in atopic dermatitis: beyond filaggrin. *An Bras Dermatol,* 91**,** 472-8.

ZARBOCK, A. & ROSSAINT, J. 2011. Regulating inflammation: ADAM8--a new player in the game. *Eur J Immunol,* 41**,** 3419-22.

ZHANG, H., ZHU, Q., CUI, J., WANG, Y., CHEN, M. J., GUO, X., TAGLIABRACCI, V. S., DIXON, J. E. & XIAO, J. 2018. Structure and evolution of the Fam20 kinases. *Nat Commun,* 9**,** 1218.

ZHANG, R., CHEN, H. Z., LIU, J. J., JIA, Y. Y., ZHANG, Z. Q., YANG, R. F., ZHANG, Y., XU, J., WEI, Y. S., LIU, D. P. & LIANG, C. C. 2010. SIRT1 suppresses activator protein-1 transcriptional activity and cyclooxygenase-2 expression in macrophages. *J Biol Chem,* 285**,** 7097-110.

ZHANG, X., SHARMA, A. M. & UETRECHT, J. 2013. Identification of danger signals in nevirapine-induced skin rash. *Chem Res Toxicol,* 26**,** 1378-83.

ZIMMERMANN, M., KORECK, A., MEYER, N., BASINSKI, T., MEILER, F., SIMONE, B., WOEHRL, S., MORITZ, K., EIWEGGER, T., SCHMID-GRENDELMEIER, P., KEMENY, L. & AKDIS, C. A. 2011. TNF-like weak inducer of apoptosis (TWEAK) and TNF-alpha cooperate in the induction of keratinocyte apoptosis. *J Allergy Clin Immunol,* 127**,** 200-7, 207 e1-10.